

Copolymerization of Acrylonitrile and Sodium *p*-Styrenesulfonate in Dimethyl Sulfoxide Solution

Z. IZUMI, H. KIUCHI, M. WATANABE, and H. UCHIYAMA, *Central Research Laboratories, Toyo Rayon Company, Otsu, Japan*

Synopsis

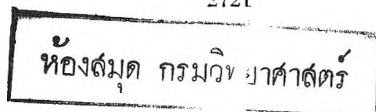
The copolymerization of acrylonitrile (AN) with sodium *p*-styrenesulfonate (SSS) in dimethyl sulfoxide solution has been investigated. Monomer reactivity ratios at 45°C., for AN and SSS are found to be $r_1 = 0.15 \pm 0.02$, $r_2 = 0.55 \pm 0.03$. From these data Price Q and e values for SSS of 0.44 and -0.38 , respectively, are calculated. The values are found to be different from those in aqueous solutions, which may be attributed to the different electron distributions in all solvents. Initial rates of copolymerization at 45°C. with azobisisobutyronitrile as initiator were determined over the entire range of composition from pure AN to pure SSS. It was found that there is a slight rise in copolymerization rates in the range of 90–95 mole-% SSS in the monomer feed; this is attributed to the coexistence of liquids of different optical density. Homopolymerization of AN and SSS in dimethyl sulfoxide was also investigated and $\delta = (k_t^{1/2}/k_p)$ for AN and SSS found to be 6.55 (mole-sec./l.)^{1/2} and 2.46 (mole-sec./l.)^{1/2}, respectively. From these values the cross-termination constant φ is calculated to be 6.5.

INTRODUCTION

The reactivity ratios and the rates of copolymerization of acrylonitrile (AN) and sodium *p*-styrenesulfonate (SSS) in aqueous solution were reported previously,¹ and in that study it was shown that the kinetic behavior of AN and SSS during copolymerization was markedly dependent on the pH of the reaction medium. It was generally believed that the reactivity ratios in copolymerization were unaffected by the reaction medium, except in the case of acidic and basic water-soluble monomers in aqueous solutions of different pH or in the case of heterogeneous copolymerization.² As the ionized and unionized forms of the monomer exhibit different reactivities in aqueous solution, the acidic and basic monomers may have different reactivities in organic solvent. In this report the authors present the reactivity ratios and rates of copolymerization of AN and SSS in dimethyl sulfoxide (DMSO) solution which gives a homogeneous system for the most part, as in aqueous solutions. The kinetic behavior of AN and SSS during copolymerization in organic solvent has been found to be greatly different from the cases in aqueous solution.

In an investigation of the rates of copolymerization, the ratio of the termination and propagation rate constants, $\delta (= k_t^{1/2}/k_p)$ is required, so that the determination of these quantities for the two monomers is also given in this report.

2721



19 มี.ค. 2508

EXPERIMENTAL

Materials

SSS was prepared from phenyl ethyl alcohol as a starting material by the method of Wiley³ and purified by recrystallizing twice from 90% ethanol. The purity of this monomer was determined to be 98.5% by bromine addition method. AN (supplied by Nitto Chemical Co.) was dried with calcium chloride and then twice distilled under nitrogen. The middle fraction having a refractive index of 1.3914 at 20°C. was used; the absolute purity was ascertained by gas chromatography. Azobisisobutyronitrile (AIBN), supplied by Otsuka Chemical Co., was purified with anhydrous methanol. The recrystallized product was refrigerated to minimize thermal decomposition. DMSO (supplied by Crown Zellerbach Co.) was dried by shaking with sodium carbonate for at least 24 hr. The dried DMSO was twice distilled in a closed system under 3 mm. pressure. The fraction boiling in the range $49.7 \pm 0.2^\circ\text{C}$. was collected. This procedure gives a product whose refractive index was 1.4783 at 20°C.; the absolute purity was ascertained by gas chromatography.

Copolymerization Technique

The experimental methods employed were identical with those described previously.¹ The polymerization was carried out in the dark under 10^{-4} mm. Hg pressure. Rates of copolymerization were obtained from the observed rates of volume contraction in a dilatometer, and the total mole fraction α consumed in the reaction is obtained from eq. (1):¹

$$\alpha = (1000/V)(Ah/[M_1] + [M_2])(R + 1/\Delta_1R + \Delta_2) \quad (1)$$

where h is the observed change in the height of the liquid in a dilatometer capillary at time t , A is the cross-sectional area of the capillary, V is the volume of the dilatometer bulb, $[M_1]$ and $[M_2]$ are the initial concentrations of AN and SSS monomer, respectively, in the feed in moles/liter, Δ_1 and Δ_2 are the changes in volume caused by complete polymerization of 1 mole of the respective monomers to the polymers, and R is the molar ratio of AN/SSS in the initial copolymer. The numerical values used here at 45°C. are $V = 8.99 \text{ cm.}^3$, $[M_1] + [M_2] = 1.0 \text{ mole/l.}$, $\Delta_1 = 20.52 \text{ cm.}^3/\text{mole}$, $\Delta_2 = 11.42 \text{ cm.}^3/\text{mole}$, and $A = 5.291 \times 10^{-3} \text{ cm.}^2$. The equation obtained by substituting the values described above is:

$$\alpha = [0.588(R+1)/(20.52R+11.42)]h \quad (2)$$

where R is the molar ratio AN/SSS in the initial copolymer. Initial rates of copolymerization were obtained from tangents to the curve of α against t at low conversion.

Degree of Polymerization

The degrees of polymerization of polyacrylonitrile were calculated by Onyon's equation⁴ for the relation between intrinsic viscosity in dimethylformamide at 25.0°C. and molecular weight.

The degree of polymerization p of sodium *p*-polystyrene-sulfonate were calculated from Kato's equation⁵

$$[\eta] = 5.75 \times 10^{-4}p \quad (3)$$

where $[\eta]$ is the intrinsic viscosity determined in 0.5*N* aqueous solution of sodium chloride at 25.0°C.

RESULTS AND DISCUSSION

Monomer Reactivity Ratios

The data for calculating monomer reactivity ratios are listed in Table I. Monomer reactivity ratios were determined graphically by the method of Mayo and Lewis.⁶ The intersections coincide fairly well, and from these intercepts were obtained the values r_1 (AN) = 0.15 ± 0.02, r_2 (SSS) = 0.55 ± 0.03. From these reactivity ratios and the Q and e values for AN ($Q_1 = 0.44$, $e_1 = 1.2$), Price⁷ Q and e for SSS are calculated Q_2 (SSS) = 0.44, e_2 (SSS) = -0.38. Table II compares the values in different homogeneous solutions, in DMSO, and in aqueous solution at pH 3 and pH 7. From Table II, it is concluded that the resonance stabilization of the SSS radical decreases and the polar value of SSS tends to be more electropositive in organic solvents, and therefore SSS becomes less reactive. Plots of the mole per cent SSS in the copolymer (m_2) against that in the monomer

TABLE I
Copolymerization of AN and SSS^a

SSS in the monomer feed M_2 , mole-%	Monomer reacted, wt.-%	SSS in the copolymer m_2 , mole-%
1.0	5.89	6.0
2.0	6.88	10.9
5.0	8.10	23.1
10.0	7.15	32.2
50.0	11.9	55.1
90.0	6.80	85.3
95.0	5.85	90.8

^a Copolymerization conditions: 1.00 mole/l. monomer, 0.03 mole/l. AIBN initiator, 45°C.

TABLE II
Copolymerization Parameters for AN and SSS
in Different Solvents at 45°C.

Copolymerization medium	r_1 (AN)	r_2 (SSS)	Q_2 (SSS)	e_2 (SSS)
Aqueous solution, pH 3	0.10	1.20	0.76	-0.26
Aqueous solution, pH 7	0.05	1.40	1.24	-0.43
Dimethyl sulfoxide solution	0.15	0.55	0.44	-0.38

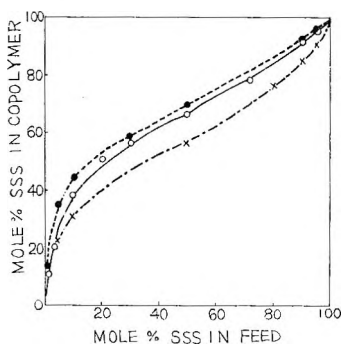


Fig. 1. Plot of mole-% SSS(m_2) in the copolymer against mole-% SSS(M_2) in the monomer feed: in aqueous solution at pH 3 (O) experimental points: (—) calculated for $r_1 = 0.10$ and $r_2 = 1.20$; at pH 7 (●) experimental points: (---) calculated for $r_1 = 0.05$ and $r_2 = 1.40$; in DMSO (X) experimental points: (· · · ·) calculated for $r_1 = 0.15$ and $r_2 = 0.55$.

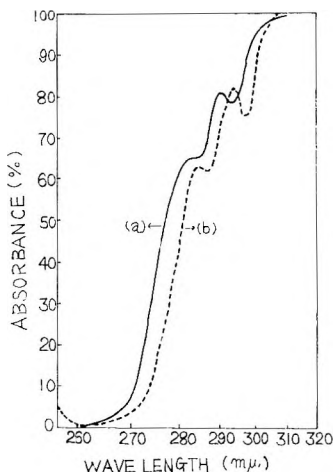


Fig. 2. Ultraviolet absorption spectra of (a) SSS in aqueous solution at pH 7 and (b) SSS in dimethylsulfoxide solution.

feed (M_2) are shown in Figure 1. The results obtained above are the first which showed that the electrolytic monomer has different reactivities in organic solvent. The different reactivities of SSS in aqueous solution at pH 3 and pH 7 and in DMSO may be attributed to the different electron distributions in SSS which are caused by SO_3H , SO_3^- , and $-\text{SO}_3^- \dots \text{Na}^+$ respectively. This explanation may be supported by ultraviolet absorption spectra of SSS in H_2O and in DMSO (Fig. 2).

Copolymerization Rates

The initial rates of copolymerization R_p at 45°C . in the presence of 3×10^{-2} mole/l. of AIBN as the initiator are given in Table III and Figure 3.

TABLE III
 Initial Rate of Copolymerization of AN and SSS^a

SSS in monomer feed M_2 , mole-%	Rate of copolymerization $R_p \times 10^5$, mole/l.-sec.
0	2.17
1.0	2.85
2.0	3.25
5.0	3.57
10.0	3.89
20.0	4.65
50.0	5.25
80.0	6.16
90.0	6.69
95.0	6.13
100.0	4.62

^a Copolymerization conditions: 1.00 mole/l. monomer, 0.03 mole/l. AIBN initiator, 45°C.

In Figure 3, a fairly sharp rise at 90 mole-% SSS in the monomer feed is noticeable. In our experiments the existence of a fairly sharp rise in the copolymerization rate may be due to a physical effect rather than a chemical effect. At 90 mole-% SSS in the monomer feed, the polymerization mixture appears to be translucent. Microscopic observation of this mixture shows coexistence of liquids of different optical density; this mixture

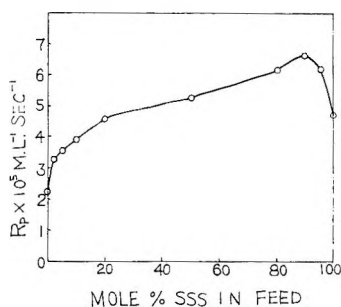


Fig. 3. Plot of initial rate of copolymerization R_p , against mole-% SSS in the monomer feed.

becomes homogeneous when the temperature decreases under 30°C. Therefore it is suggested that the copolymerization at 90 mole-% SSS in the monomer feed occurs in a heterogeneous system where the polymer is precipitated but highly swollen. The slight increase in the rate of copolymerization at 90 mole-% SSS in the monomer feed may be attributed to this effect. In the case of pure SSS, the polymer may be more highly swollen than in the case of copolymer and the effect of heterogeneity on the polymerization of SSS may be less than that on the copolymerization;

(this may be supported by the square-root dependence of rate on initiator concentration.

Cross-Termination Constant φ

The copolymerization rates obtained above were also calculated from the known kinetic parameters of the two monomers and an assumed value of the cross-termination constant φ by means of the copolymerization rate equation:⁸

$$R_p = \frac{R_i^{1/2}(r_A[A]^2 + 2[A][B] + r_B[B]^2)}{(r_A^2\delta_A^2[A]^2 + 2\varphi r_A r_B \delta_A \delta_B [A][B] + r_B^2\delta_B^2[B]^2)^{1/2}} \quad (4)$$

where $R_i = 2k_{df}[I]$ is the rate of initiation, $\varphi = k_{t_{AB}}/(k_{t_{AA}}k_{t_{BB}})^{1/2}$, $[I]$ is the initiator concentration, and the other terms are defined as given by Walling. For obtaining values in this case, δ_A and δ_B must be derived from studies of the polymerization of the individual monomers. It has been shown that eqs. (5) and (6) are derived in catalyzed homogeneous polymerization:

$$\begin{aligned} R_p &= \frac{k_p}{[k_{td} - (k_{tc}/2)]^{1/2}} \left[\frac{k_{td} + (k_{tc}/2)}{k_{td} + k_{tc}} \right]^{1/2} (2k_{df})^{1/2} [I]^{1/2} [M] \\ &= \delta^{-1} \left(\frac{1+x}{2} \right)^{1/2} R_i^{1/2} [M] \end{aligned} \quad (5)$$

$$\begin{aligned} \frac{1}{P} &= \left[\frac{k_{td} + (k_{tc}/2)}{k_p^2} \right] \frac{R_p}{[M]^2} + C_m \\ &= \delta^2(R_p/[M]^2) + c_m \end{aligned}$$

For the evaluation of rate of initiation R_i from eq. (5), it should be ascertained whether the termination occurs by disproportionation or combination of two radicals. In the case of AN, termination by combination may be more probable; this has been confirmed by several authors.^{9,10} In the case of SSS, there are no data available concerning the mechanism of termination, but as styrene has been confirmed to terminate by combination,¹¹ SSS may be deduced to terminate by the same mechanism from the similarity of the structure with styrene. By using eqs. (4) and (5), δ , R_i , and f for each monomer were evaluated.

Evaluation of $\delta = k_i^{1/2}/k_p$ for AN

The effect of initiator concentration on polymerization rate at 45°C. is shown in Figure 4 by a plot of $\log R_p$ against $\log [I]$. Experimental points in Figure 4 are well represented by a straight line of slope $1/2$, indicating a one-half-order dependence of rate on initiator concentration. The results of the molecular weight studies are given in Table IV, and the plot of $1/P_n$ against rate is shown in Figure 5. From Figure 5, the values for δ_{AN} can be derived as 6.55 (mole-sec./l.)^{1/2} from eq. (6). Hence, from eq. (5), the

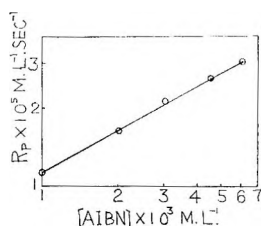


Fig. 4. Dependence of rate of polymerization of AN on initiator concentration at 45°C.

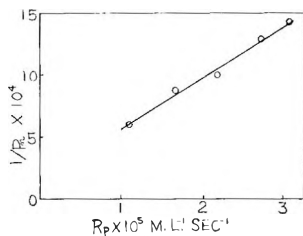


Fig. 5. Plot of the reciprocal degree of polymerization against rate of polymerization of AN.

rate of initiation of AN may be calculated as 4.04×10^{-8} mole/l.-sec. at the concentration of 0.03 mole/l. AIBN at 45°C. As the velocity constant for decomposition of AIBN at 45°C. is¹² 1.07×10^{-6} sec.⁻¹, the efficiency of initiator may be calculated as 0.629.

TABLE IV
Homopolymerization of AN in DMSO^a

Initiator concentration, mole/l.	Reaction rate $R_p \times 10^5$, mole/l.-sec.	Degree of polymerization P_n
0.01	1.11	1632
0.02	1.64	1125
0.03	2.17	999
0.045	2.69	772
0.06	3.03	740

^a Polymerization conditions: 1.00 mole/l. AN, AIBN initiator, $45.00 \pm 0.02^\circ\text{C}$.

Evaluation of $\delta = k_t^{1/2}/k_p$ for SSS

The effect of initiator concentration on polymerization rate at 45°C. is shown in Figure 6. During the homopolymerization of SSS, a translucent viscous phase is produced at the bottom of a dilatometer bulb, and it may not belong to usual homogeneous polymerization. However, experimental points in Figure 6 are well represented by a straight line of slope $1/2$, and polymerization does not seem to occur in many particles as common heterogeneous polymerization; thus this system may be treated as a homogeneous polymerization system. The results of the molecular weight

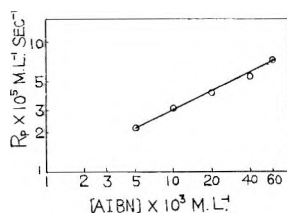


Fig. 6. Dependence of rate of polymerization of SSS on Initiator concentration at 45°C.

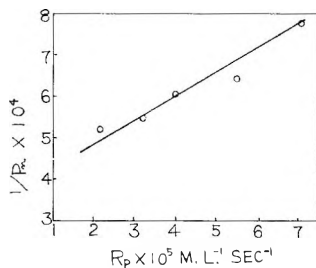


Fig. 7. Plot of the reciprocal degree of polymerization against rate of polymerization of SSS.

determinations are shown in Table V, and $1/P_n$ is plotted as a function of the rate of polymerization in Figure 7. The plot of $1/P_n$ against R_p satisfies eq. (6) for $(\delta/[M])^2 = 2.46$, $\delta = 2.46$ (mole-sec./l.)^{1/2}.

TABLE V
Homopolymerization of SSS in DMSO^a

Initiator concentration, mole/l.	Reaction rate $R_p \times 10^5$, mole/l.-sec.	Degree of polymerization P_n
0.005	2.15	1910
0.01	3.20	1844
0.02	4.02	1652
0.04	5.50	1565
0.06	7.10	1288

^a Polymerization conditions: 1.00 mole/l. SSS, AIBN initiator, 45.00 ± 0.02°C.

From these results the values of R_i and f are calculated to be 2.86×10^{-8} mole/l.-sec. and 0.444, respectively.

Evaluation of Cross-Termination Constant φ

As shown above, the catalyst has different efficiencies of chain starting in pure monomers AN and SSS, respectively. Although it is desirable to determine R_i experimentally, a linear interpolation for monomer mixtures is adopted in this experiment. This appears to hold approximately for AIBN.^{13,14} By substituting the values obtained above into eq. (4), φ

factors for each composition of the feed were calculated as shown in Table VI. From Table VI, the value of φ is found to be 6.5, except in the range of high SSS content, where abnormal polymerization occurs. The high values of φ , indicating the preference for cross-termination in this system, coincide with the alternating tendency in the propagation reaction which is shown by the low value of $r_1r_2 = 0.0825$.

TABLE VI
Cross-Termination Constant x for Copolymerization of AN and SSS in
Dimethyl Sulfoxide Solution at 45°C.

SSS in the monomer feed M_2 , mole-%	x
2	6.7
5	6.4
10	6.9
20	6.3
50	7.5
80	6.0
90	5.3
95	8.3

The authors wish to express their sincere gratitude to Dr. Kobayashi, our Director of Research, for his help and permission to publish the results.

References

1. Izumi, Z., H. Kiuchi, and M. Watanabe, *J. Polymer Sci.*, **A1**, 705 (1963).
2. Alfrey, T., Jr., J. J. Bohrer, and H. Mark, *Copolymerization*, Interscience, New York, 1952, p. 111.
3. Wiley, R. H., N. R. Smith, and C. C. Kettner, *J. Am. Chem. Soc.*, **76**, 720 (1954).
4. Onyon, P. F., *J. Polymer Sci.*, **22**, 13 (1956).
5. Kato, M., T. Nakagawa, and H. Akamatsu, *Bull. Chem. Soc. Japan*, **33**, 322 (1960).
6. Mayo, F. R., and F. M. Lewis, *J. Am. Chem. Soc.*, **66**, 1594 (1944).
7. Alfrey, T., and C. C. Price, *J. Polymer Sci.*, **2**, 101 (1944).
8. Walling, C., *J. Am. Chem. Soc.*, **71**, 1930 (1949).
9. Bamford, C. H., *Trans. Faraday Soc.*, **55**, 179 (1959).
10. Bevington, J. C., and D. E. Eaves, *Trans. Faraday Soc.*, **55**, 1777 (1959).
11. Overberger, C. G., and A. B. Finestone, *J. Am. Chem. Soc.*, **78**, 1638 (1956).
12. Van Hook, J. P., and A. V. Tobolsky, *J. Am. Chem. Soc.*, **80**, 779 (1958).
13. Bonsall, E. P., L. Valentine, H. W. Melville, *Trans. Faraday Soc.*, **48**, 763 (1952).
14. Bradbury, J. H., and H. W. Melville, *Proc. Roy. Soc. (London)*, **A222**, 456 (1954).

Résumé

On a étudié la copolymérisation de l'acrylonitrile (AN) avec le *p*-styrène-sulfonate de sodium (SSS) en solution dans le diméthylsulfoxyde. Les rapports de réactivité des monomères à 45°C pour AN et SSS sont $r_1 = 0.15 \pm 0.02$, $r_2 = 0.55 \pm 0.03$. À partir de ces valeurs, on a calculé les valeurs de Price Q et e pour SSS qui sont 0.44 et -0.38 respectivement. On trouve que ces valeurs sont différentes de celles obtenues en solutions aqueuses et peuvent être attribuées aux distributions électroniques différentes dans

les solvants. Avec l'azobisisobutyronitrile comme initiateur, on a déterminé les vitesses initiales de la copolymérisation à 45°C dans le domaine complet de composition depuis AN pur jusqu'à SSS pur et on a trouvé qu'il y avait une légère augmentation des vitesses de copolymérisation pour 90-95 mole% de SSS monomère ce qui est attribué à la co-existence de liquides de différentes densités optiques. On a également étudié l'homopolymérisation de AN et SSS dans le diméthylsulfoxyde et on a trouvé des valeurs de δ ($= k_t^{1/2}/k_p$) égales à 3.55 (mole/sec/l)^{1/2} et 2.46 (mole/sec/l)^{1/2} pour AN et SSS respectivement. À partir de ces valeurs, on calcule une constante de terminaison croisée égale à 6.5.

Zusammenfassung

Die Kopolymerisation von Acrylnitril (AN) mit Natrium-*p*-styrolsulfonat (SSS) in Dimethylsulfoxydlösung wurde untersucht. Die Monomerreaktivitätsverhältnisse wurden für AN und SSS bei 45°C zu $r_1 = 0,15 \pm 0,02$, $r_2 = 0,55 \pm 0,03$ bestimmt, woraus Price-*Q*- und *e*-Werte für SSS von 0,44 bzw. 0,38 berechnet wurden. Diese Werte unterscheiden sich von denjenigen in wässriger Lösung, was der verschiedenen Elektronenverteilung in den Lösungsmitteln zugeschrieben werden kann. Die Anfangsgeschwindigkeit der Kopolymerisation bei 45°C mit Azobisisobutyronitril als Starter wurde im ganzen Zusammensetzungsbereich von reinem AN zu reinem SSS bestimmt und ein kleiner Anstieg der Polymerisationsgeschwindigkeit bei 90-95 Molprozent SSS in der Monomermischung gefunden, was auf die Koexistenz von Flüssigkeiten mit verschiedener optischer Dichte zurückgeführt wird. Weiters wird die Homopolymerisation von AN und SSS in Dimethylsulfoxyd untersucht und δ ($= k_t^{1/2}/k_p$) für AN und SSS zu 6,55 (Mol. sec/l)^{1/2} bzw. 2,46 (Mol. sec/l)^{1/2} bestimmt. Aus diesen Werten wird die gekreuzte Abbruchkonstante φ zu 6,5 berechnet.

Received September 29, 1964

Revised January 14, 1965

Prod. No. 4638A

Synthesis of Condensation Polyesters Containing the Bis(halomethyl) Group

HIDEO MIYAKE, KOICHIRO HAYASHI, and SEIZO OKAMURA,
Department of Polymer Chemistry, Kyoto University, Kyoto, Japan

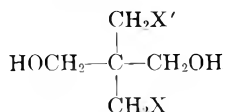
Synopsis

Methods of preparing polyesters from 2,2-bis(halomethyl)-propanediols were investigated. Linear solid polyesters were obtained by the reaction with dicarboxylic acid chlorides, and this was the most suitable method of preparing polyesters from these diols. The polyoxalate, polysuccinate, and polyadipate of 2,2-bis(chloromethyl)-1,3-propanediol were crystalline, but the poly(*o*-, *m*-, *p*-)phthalates were amorphous. Polyadipates of 2,2-bis(bromomethyl)- and 2-chloromethyl-2-bromomethyl-propanediol were also crystalline, and polyadipates of 2,2-bis(iodomethyl)- and 2-chloromethyl-2-iodomethylpropanediols were amorphous.

Introduction

It is known that polyesters and polyethers, such as poly- α,α -bis(chloromethyl)- β -propiolactone^{1,2} and poly-3,3-bis(chloromethyl)oxetane, containing a bis(chloromethyl) group at a carbon on the polymer chain are highly crystalline and resist solubilities in a number of solvents. These polymers were obtained by a process of ring-opening polymerization. The synthesis of polyesters by polycondensation reactions from diols containing a bis(halomethyl) group have been investigated in our laboratory. Condensation polyesters containing halogens are also very interesting polymers, but few polyesters from halogenated diols have been reported.³⁻⁷

This paper describes the synthesis and preliminary characterization of polyesters by polycondensation reactions from five 2,2-bis-(halomethyl)-1,3-propanediols (I-V) synthesized from pentaerythritol. Unlike 2,2-dimethyl-1,3-propanediol which has a structure similar to that of these diols, only low molecular weight polyesters were obtained by direct esterification and transesterification. Linear solid polyesters, however, were obtained by the reaction with dicarboxylic acid chlorides.



- (I) X = X' = Cl
(II) X = X' = Br
(III) X = X' = I
(IV) X = Cl, X' = Br
(V) X = Cl, X' = I

2,2-Bis(halomethyl)-1,3-propanediol

Results and Discussion

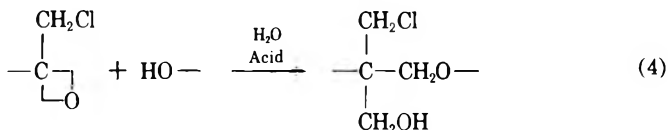
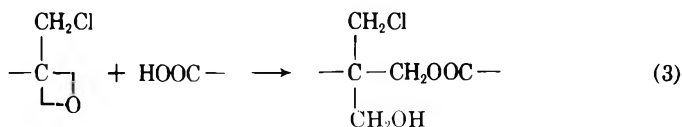
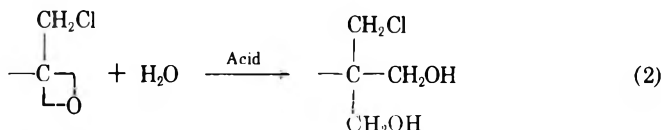
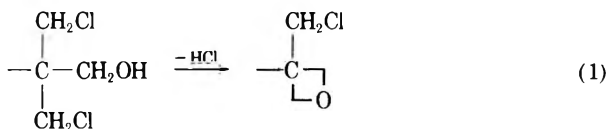
Experiments were carried out mainly on diol I. Four general methods of preparing polyesters from I were investigated under melt conditions with the use of various catalysts (except for method 4): (1) direct esterification with adipic, sebacic, and terephthalic acid; (2) transesterification with dimethyl esters of these three dicarboxylic acids; (3) acidolysis reaction between diacetate of I and adipic and sebacic acid; (4) reaction between I and seven kinds of dicarboxylic acid chlorides. Polyesters from II, III, IV, and V were prepared by the reaction with adipoyl chloride.

It is well known that ethanols halogenated at the β -carbon do not esterify readily with carboxylic acids in the presence of acid catalysts. In the case of I which has two chloromethyl groups at the β -carbon, polyesters were not readily prepared by direct esterification. Direct esterification (and transesterification) in various mole ratios with a variety of catalysts and at various temperatures and times gave only slightly reacted liquids, colored viscous liquids, or gels. The reason why I, unlike most glycols, does not esterify readily is probably not only the steric hindrance of the two bulky chloromethyl groups, but also the electron attraction by the chloromethyl groups. In fact, an aqueous solution of I was observed as an acid as follows; pH = 5.35 for 0.0101 mole/l., pH = 5.15 for 0.0012 mole/l. (cf. pH = 5.2 for 0.010 mole/l. aqueous solution of phenol). The pH's indicate that diol I is an acidic diol. The withdrawal of electron density from the oxygen to the chloromethyl group gives the oxygen positive charge. Then, the reactivity of conjugated acid converted from dicarboxylic acid with I is considerably less than that obtained with normal alcohols. 2,2-Dimethyl-1,3-propanediol, with less bulky and electron-donating methyl groups esterified readily to high molecular weight polyester.⁸ Terephthalic acid immiscible with I and hardly reacted, even when a large excess of I was used.

Some of the slightly colored, viscous liquid polymers prepared by direct esterification and transesterification showed bands in the infrared spectra characteristic of ester, polymethylene, and carbon-chlorine bonds. The chlorine content by elemental analysis was also near the theoretical value. It is suggested that polymers prepared by these two methods were low molecular weight polyesters.

High reaction temperature and long reaction time led to formation of a gel, but the gelation did not always depend on coloring. A characteristic pungent odor of the gas evolved was observed, especially at reaction temperatures over 200°C. An aqueous solution of the exit gas showed acidity, and chlorine ion was detected; this suggested that dehydrochlorination occurred. Dehydrochlorination, which might be the main cause for the gelation, is most likely to occur at the terminal group of the polyester, considering the reactivity between the chloromethyl and hydroxymethyl groups. In view of the fact that the little gelation occurs in transesterification and acidolysis, the gelation seems to result from reactions

occurring after the oxetane ring at the end of the polyester is formed by dehydrochlorination [eq. (1)]. Opening of the oxetane ring occurs by the reaction with water⁹ produced by the condensation, in the presence of acid as a catalyst [eq. (2)], by reaction with the carboxy group [eq. (3)] and by reaction with the hydroxy group¹⁰ [eq. (4)] in the presence of acid or water as catalyst. Then, the hydroxymethyl group formed condenses with the end of the polyester and reacts with another chloromethyl group to form a new oxetane ring, and so on. These complicated reactions cause the reaction mixture to turn into a gel.



Diol I itself is not so stable at elevated temperature. When I was heated at 220°C. for 4 hr. under purified nitrogen or in a tube sealed under vacuum, it turned into brown liquid at room temperature. Bubbling the gas evolved into 2 ml. water yielded a solution showing pH below 1 in 15 min. and containing chloride ion.

The transesterification, method (2), was poorer in reactivity and the viscosity of the product was lower compared with direct esterification. Many authors have reported that base catalysts (especially, alkali catalysts) were much better for the transesterification than acid catalysts. However, base catalysts are not suitable for use with I because it is an acidic diol and, furthermore, reacts quite easily with base to form oxetanes. Aluminum alcoholate¹¹ and zinc powder,¹² which are useful for the transesterification with alcohols sensitive to base, did not give better results. Dimethyl terephthalate was immiscible with I, as was terephthalic acid.

The acidolysis reaction did not take place, even when butyl orthotitanate or titanium dioxide, which are superior catalysts for preparing polyesters from bisphenols¹³ by the acidolysis reaction, was used. The reactants were

recovered from the reaction mixture. However, the acidolysis reaction between diacetates of hydroquinone¹⁴ or bisphenols^{13,15} led to polyesters with high molecular weight.

It seemed that there were differences between reactivities in the three methods of preparing polyesters from I. To compare the reactivities quantitatively, molecular weights were measured after the reactions were carried out under similar conditions. Results are listed in Table IA; conditions are given in Table IB. The viscous liquid polyesters obtained were pale colored and transparent.

TABLE IA
Relative Reactivity of Methods of Preparing Polyesters from 2,2-Bis(chloromethyl)-1,3-propanediol

Method	Dibasic acid or diester ^a	Mole ratio ^b	Catalyst		
			Type	Wt., mg.	Molecular weight ^c
Direct esterification	AA	1.00	<i>p</i> -TSA ^d	2	4,500
	AA	2.00	<i>p</i> -TSA	2	5,000
	AA	3.00	<i>p</i> -TSA	2	4,700
	SA	2.00	<i>p</i> -TSA	3	7,300
Transesterification	DMA	1.00	Ca(OAc) ₂ ·2H ₂ O	10	1,800
	DMA	2.00	Ca(OAc) ₂ ·2H ₂ O	10	2,200
	DMA	3.00	Ca(OAc) ₂ ·2H ₂ O	10	1,700
	DMS	1.50	Ca(OAc) ₂ ·2H ₂ O	15	4,200
Acidolysis	AA	2.00	TiO ₂	15	Almost unreacted
	AA	6.00	TiO ₂	15	"

^a AA = adipic acid; SA = sebacic acid; DMA = dimethyl adipate; DMS = dimethyl sebacate.

^b Mole ratio = I or diacetate of I/AA,SA,DMA or DMS.

^c By the method of determining endgroups.

^d *p*-Toluenesulfonic acid.

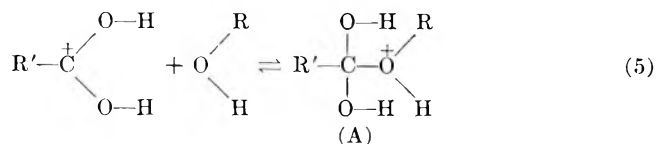
TABLE IB
Reaction Conditions^a

Method	Temp., °C.	Time, hr.	Pressure
Direct esterification	150	10	Atmospheric
Transesterification	170	5	Water pump
	180	10	<2 mm. Hg
	150	15	Atmospheric
Acidolysis	150	15	Atmospheric
	170	5	Water pump

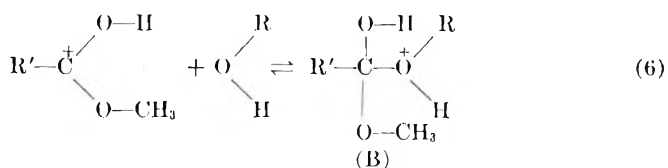
^a 0.050 mole of I was charged.

The results show that the relative rate of polycondensation reactions for direct esterification and transesterification was about 2:1. The rate-determining steps in direct esterification, transesterification, and acidolysis reaction are supposed on the basis of the mechanisms given in many references to be as shown in eqs. (5)–(7).

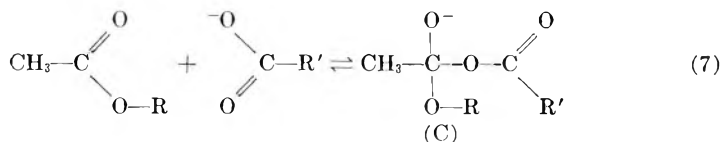
Direct esterification:



Transesterification:



Acidolysis:¹⁶



Here R = residue of I or polyester; R' = residue of dicarboxylic acid or polyester.

The ease with which tetrahedral intermediates are formed from the bulky and electron-attracting chloromethyl groups probably decreases in the order (A) > (B) > (C), and the formation of (C) seems to be almost impossible.

The esterification which does not involve a tetrahedral intermediate, namely, the reaction with acyl cations from dicarboxylic acid chlorides, was quite suitable for preparing polyesters from I, as shown in Table II.

TABLE IIA
Polyesters from 2,2-Bis(chloromethyl)-1,3-propanediol and Dicarboxylic Acid Chlorides

Dicarboxylic acid chloride	Melting point, °C.	Intrinsic viscosity ^a	Chlorine content, %		Melting point of polyester from neopentyl glycol, °C.
			Found	Calcd.	
Oxalyl	119-122	0.14	32.23	31.23	111 ^b
Succinyl	72-74	0.19	28.28	27.80	86 ^b
Adipoyl	104-108	0.35	25.71	25.04	37 ^b
Sebacoyl	35-38	0.63	22.01	20.90	26 ^b
Phthaloyl	76-80	0.18	23.94	23.39	—
Isophthaloyl ^c	180-185	0.22	24.36	23.39	—
Terephthaloyl	115-123	0.25	24.24	23.39	140 ^d

^a Measured in *sym*-tetrachloroethane/phenol (50/50, w/w) at 30°C.

^b Data of Doak and Campbell.¹⁷

^c Reacted at 200°C. instead of 180°C.

^d Data of Hill and Walker.¹⁸

TABLE IIB
 Reaction Conditions^a

Temp., °C.	Time, hr.	Pressure
100-180	ca. 0.5	Atmospheric
180	1	Atmospheric
180	1	<2 mm. Hg

^a 0.050 mole of I was charged.

Results from experiments under the same reaction condition are given in Table IIA. In the last column in Table IIA, melting points of polyesters from 2,2-dimethyl-1,3-propanediol and various dicarboxylic acids reported in the literature, are compared.

The colorless, transparent, glasslike products obtained were dissolved in *sym*-tetrachloroethane (TCE) and reprecipitated in methanol. The yields of white or off-white powder polymer reprecipitated were over 95%, based on the reactants used. The polymer from sebacoyl chloride was reprecipitated at 0°C.

Infrared spectra by a potassium bromide disk technique showed identifiable bands for the ester bond and for the carbon-chlorine bond at 703-698 cm.⁻¹. Chlorine contents found by elemental analyses were close to theoretical values. All polymers were soluble in *sym*-TCE and *m*-cresol (polymers from oxalyl and isophthaloyl chloride were in hot *m*-cresol). These results and intrinsic viscosities indicate that linear polyesters were obtained from I and dicarboxylic acid chlorides.

Polyesters having intrinsic viscosities different from these in Table IIA were also prepared for each of the polyesters under various reaction conditions. Infrared spectra, x-ray diffraction patterns, solubilities, melting points, and chlorine contents of these polyesters were almost the same as those in Table IIA.

Melting points depend on dicarboxylic acid residues. It was quite unexpected that the polymer from isophthalic acid had a higher melting point than that from terephthalic acid. Unlike the polyesters from 2,2-dimethyl-1,3-propanediol, the polyadipate of I had a higher melting point than the polysuccinate of I and, moreover, a much higher melting point than the polyadipate of 2,2-dimethyl-1,3-propanediol. Solubilities varied also with dicarboxylic acid residues in the polyester. The polyphthalate and polyterephthalate were soluble in chloroform, *sym*-TCE, *m*-cresol, dimethylformamide (DMF), and dimethylaniline (DMA). The polysuccinate and polysebacate were insoluble in DMA, and the polyadipate was insoluble in DMA and DMF. The polyoxalate and polyisophthalate dissolved only in *sym*-TCE.

Since the high melting points and relative insolubilities of some of these polyesters suggested possible crystallinity, x-ray analyses also were obtained. Diffraction patterns for the polyesters given in Table II are shown in Figure 1. The polyoxalate, polysuccinate, and polyadipate were crystalline, while the poly(*o*-, *m*-, *p*-)phthalates were amorphous. The same pat-

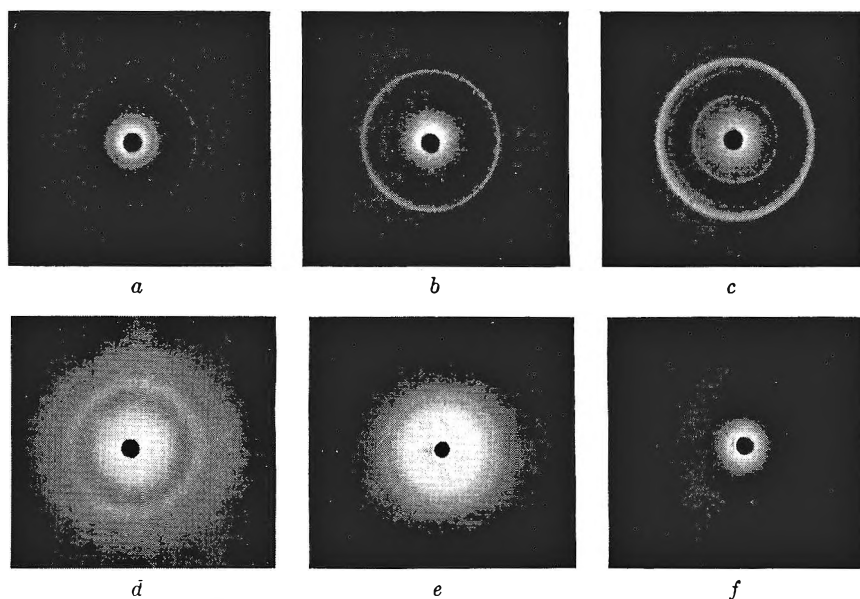


Fig. 1. X-ray diffraction patterns: (a) poly-2,2-bis(chloromethyl)trimethylene oxalate; (b) poly-2,2-bis(chloromethyl)trimethylene succinate; (c) poly-2,2-bis(chloromethyl)trimethylene adipate; (d) poly-2,2-bis(chloromethyl)trimethylene phthalate; (e) poly-2,2-bis(chloromethyl)trimethylene isophthalate; (f) poly-2,2-bis(chloromethyl)trimethylene terephthalate. The polyesters listed in Table IIA were used.

terns were obtained from the polyesters with different intrinsic viscosities.

The results of preparing polyesters from 2,2-bis(halomethyl)-1,3-propanediols (II, III, IV, and V) and adipoyl chloride (AC) under similar reaction conditions are given in Table III. Products in the reaction tubes were all transparent and pale brown to brown in color. The yield of pale brownish-white powder reprecipitated was over 88% based on the reactants used.

It was confirmed from the following results that linear polyesters were obtained. Infrared spectra showed characteristic bands for the carbon-halogen bond: C—Br, 660 cm^{-1} for II and AC, C—I, 790 cm^{-1} for

TABLE IIIA
Polyesters from II, III, IV, or V and Adipoyl Chloride

2,2-Bis(halomethyl)-1,3-propanediol	Melting point, °C.	Intrinsic viscosity ^a	Halogen content, %	
			Found	Calcd.
II (X = X' = Br)	116-120	0.17	42.40	42.96
III (X = X' = I)	80-85	0.31	55.45	54.46
IV (X = Cl, X' = Br)	108-111	0.31	35.78	35.22
V (X = Cl, X' = I)	79-84	0.14	46.10	43.34

^a Measured in *sym*-tetrachloroethane/phenol (50/50 w/w) at 30°C.

TABLE IIIB
 Reaction Conditions^a

2,2-Bis(halomethyl)- 1,3-propanediol	Temp., °C.	Time, min.	Pressure
II, IV	100-160	25-30	Atmospheric
	160	60	Atmospheric
	160	60	<2 mm. Hg
III, V	100-130	10-13	Atmospheric
	130	60	Atmospheric
	130	60	<2 mm. Hg

^a 0.050 mole of diol was charged.

III and AC, C—Cl, 690 cm.^{-1} , C—Br, 661 cm.^{-1} for IV and AC, and C—Cl, 688 cm.^{-1} , C—I, 810 cm.^{-1} for V and AC. (The characteristic bands for these carbon-halogen bonds were determined, compared with distinctive absorptions in the range of 900–650 cm.^{-1} on infrared spectra obtained from diols I, II, III, IV, and V: C—Cl, 690 cm.^{-1} , C—Br, 660–56 cm.^{-1} , and C—I, 801–9 cm.^{-1} .) The characteristic absorptions for the ester bond were also very clear. Halogen contents by elemental analysis were close to theoretical values. All the polymers were soluble in chloroform, *sym*-TCE and *m*-cresol, and had intrinsic viscosities over 0.14.

Polyesters having intrinsic viscosities different from those in Table III were also prepared for each of the polyesters, whose physical properties found were almost the same as those in Table III. Some reactions attempting to prepare polyesters from II or III and adipic acid, succinic anhydride, and dimethyl terephthalate led to dark-colored, cloudy gel in a short time.

Polyadipates of II, IV, and V were obtained as pale brownish-white powders, and, interestingly, the polyadipate of III was pale brownish-white, hard, rubbery polyester. Polyadipates of II and IV had melting points near that of the polyadipate of I and were crystalline as well, as shown in Figure 2, where the x-ray diffraction pictures of three of the

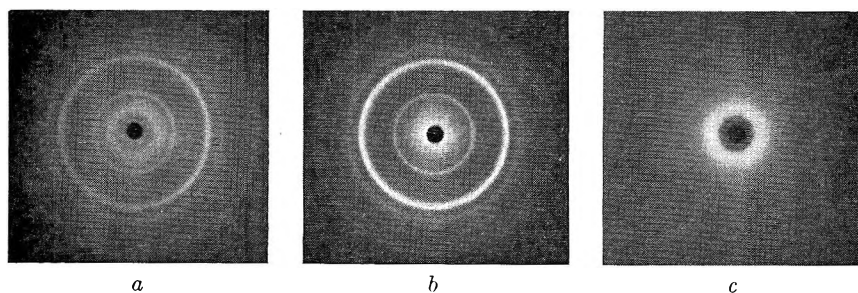


Fig. 2. X-ray diffraction patterns: (a) poly-2,2-bis(bromomethyl)trimethylene adipate; (b) poly-2-chloromethyl-2-bromomethyltrimethylene adipate; (c) poly-2-chloromethyl-2-iodomethyltrimethylene adipate. The polyesters listed in Table IIIA were used.

polyesters in Table III are given. The polyadipate of V was amorphous. It appears that the residues of III and V with the iodomethyl group are so bulky as to affect the crystallinity of the polyadipate to some extent.

EXPERIMENTAL

Starting Materials

2,2-Bis(chloromethyl)-1,3-propanediol (I) was prepared from pentaerythritol tetraacetate and hydrogen chloride by the conventional method and purified by distillation (b.p. 155–156°C./10 mm. Hg); (lit.¹⁹ 158.5–160°C./12 mm. Hg) and finally by recrystallization from benzene (m.p. 80°C.; lit.²⁰ 79–80°C.).

ANAL. Calcd. for $C_5H_{10}O_2Cl_2$: C, 34.74%; H, 5.83%; Cl, 40.98%. Found: C, 34.73%; H, 5.81%; Cl, 40.93%.

2,2-Bis(bromomethyl)-1,3-propanediol (II) 2,6-dioxaspiro-(3,3)-heptane (m.p. 90°C.; lit.²¹ 89–90°C.), prepared from I and potassium hydroxide in absolute ethanol, was treated with hydrobromic acid. II was purified by recrystallizations from benzene (m.p. 112–112.2°C.; lit.²² 109–110°C.).

ANAL. Calcd. for $C_5H_{10}O_2Br_2$: C, 22.92%; H, 3.85%; Br, 60.01%. Found: C, 22.94%; H, 3.83%; Br, 59.95%.

2,2-Bis(iodomethyl)-1,3-propanediol (III) was prepared by a procedure similar to that used in preparation of II by using hydriodic acid and purified by recrystallization from ethylene dichloride (m.p. 133.8–134°C.; lit.²³ 130.5°C.).

ANAL. Calcd. for $C_5H_{10}O_2I_2$: C, 16.87%; H, 2.83%; I, 71.31%. Found: C, 16.94%; H, 2.90%; I, 71.40%.

2-Chloromethyl-2-bromomethyl-1,3-propanediol (IV); 3-chloromethyl-3-hydroxymethyl-oxetane (b.p. 111–113°C./5 mm. Hg), prepared from I and potassium hydroxide (half mole ratio with respect to I), was treated with hydrobromic acid. IV was purified by recrystallization from chloroform (m.p. 96–96.3°C.; lit.²⁴ 95–95.5°C.).

ANAL. Calcd. for $C_5H_{10}O_2BrCl$: C, 27.61%; H, 4.63%; Br-Cl, 53.05%. Found: C, 27.70%; H, 4.69%; Br-Cl, 52.91%.

2-Chloromethyl-2-iodomethyl-1,3-propanediol (V) was prepared by a procedure similar to that used in preparation of IV by using hydriodic acid and purified by recrystallizations from chloroform (m.p. 99.5–100°C.; lit.²⁴ 95–95.5°C.).

ANAL. Calcd. for $C_5H_{10}O_2ClI$: C, 22.70%; H, 3.81%; Cl-I, 61.39%. Found: C, 22.74%; H, 3.81%; Cl-I, 61.25%.

2,2-Bis(chloromethyl)trimethylene diacetate (diacetate of I) was obtained from I and acetic anhydride and purified by distillation (b.p. 123.5–124°C./2 mm. Hg; lit.²⁵ 146–148°C./6 mm. Hg).

ANAL. Calcd. for $C_9H_{14}O_4Cl_2$: C, 42.04%; H, 5.49%; Cl, 27.58%. Found: C, 42.00%; H, 5.52%; Cl 27.68%.

Commercially available adipic acid, sebacic acid, and dimethyl terephthalate were purified by recrystallization. Dimethyl esters of adipic acid and sebacic acid were prepared by conventional procedures. Purified dimethyl terephthalate was saponified to very pure terephthalic acid. Dicarboxylic acid chlorides, except oxalyl chloride, were prepared from the dicarboxylic acid and thionyl chloride and purified by fractional distillations. Catalysts used were of commercial guaranteed grade.

Preparation of Polyesters

The methods of preparing polyesters were carried out by the usual procedure. Nitrogen was purified through Fieser's solution, concentrated sulfuric acid, and phosphorus pentoxide.

Molecular weights of polyesters, listed in Table I, were determined by titrating excess potassium hydroxide with 0.1*N* hydrogen chloride-ethanol solution, after a benzene solution of polyester and 1*N* potassium hydroxide-ethanol solution were mixed and reacted with gently stirring at 50°C. for 1 hr. By this procedure, two kinds of endgroups on polyesters of the three —COOCH₃, —COOH, and C(CH₂Cl)₂·(CH₂OH)₂— could be determined by one analytical procedure.

In preparing polyesters from dicarboxylic acid chlorides, the transparent solid polyesters in the reaction tubes were dissolved in *sym*-TCE to 5% solution, reprecipitated in methanol, filtered, and dried in vacuum at room temperature. Polyesters obtained by this procedure were used for the measurement of melting point, intrinsic viscosity, infrared spectra, elemental analysis, solubility, and x-ray diffraction patterns.

The authors wish to express their appreciation to Mr. H. Watanabe, of Textile Research Institute, Toyo Spinning Co., for his helpful comments and technical assistance during this investigation.

References

1. Reynolds, J. W., and E. J. Vickers, U. S. Pat. 2,853,474 (1958).
2. Okamura, S., K. Hayashi, and H. Watanabe, paper presented at the 12th Annual Meeting of Society of Polymer Science, Japan (1963); paper presented at the 12th Discussion Meeting on Polymers, Japan (1963).
3. Reynolds, J. W., and E. J. Vickers, U. S. Pat. 2,848,441 (1958).
4. Al'shits, I. M., et al., *Zh. Prikl. Khim.*, **34**, 468 (1961).
5. Smith, D. D., U. S. Pat. 2,902,473 (1959).
6. Schweiker, G. C., and P. Robitschek, *J. Polymer Sci.*, **24**, 33 (1957).
7. Gouinlock, E. V., Jr., et al., *J. Appl. Polymer Sci.*, **1**, 361 (1959).
8. Caldwell, J. R., and R. Gilkey, U. S. Pat. 2,891,930 (1959).
9. Pritchard, J. G., and F. A. Long, *J. Am. Chem. Soc.*, **80**, 4162 (1958).
10. Searles, S., and C. F. Butler, *J. Am. Chem. Soc.*, **76**, 56 (1954).
11. Rosemund, K. W., *Arch. Pharm.*, **286**, 324 (1953).
12. Strassburg, R. W., U. S. Pat. 2,446,114 (1948).
13. Conix, A., *Ind. Eng. Chem.*, **51**, 147 (1959).

14. Walsgrove, E. R., and F. Reeder, Brit. Pat. 636,429 (1950); J. G. N. Drewitt and J. Lincoln, Brit. Pat. 621,102 (1947).
15. Levine, M., and S. C. Temin, *J. Polymer Sci.*, **28**, 179 (1958).
16. Temin, S. C., *J. Org. Chem.*, **26**, 2518 (1961).
17. Doak, K. W., and H. N. Campbell, *J. Polymer Sci.*, **18**, 215 (1955).
18. Hill, R., and E. E. Walker, *J. Polymer Sci.*, **3**, 609 (1948).
19. Mooradian, A., and J. B. Cloke, *J. Am. Chem. Soc.*, **67**, 942 (1945).
20. Rapoport, H., *J. Am. Chem. Soc.*, **68**, 341 (1946).
21. Abdun-nur, A., and C. H. Issidorides, *J. Org. Chem.*, **27**, 67 (1962).
22. Bincer, H., and K. Hess, *Ber.*, **61b**, 537 (1928).
23. Backer, H. J., and K. J. Keunung, *Rec. Trav. Chim.*, **53**, 812 (1934).
24. Issidorides, C. H., et al., *J. Org. Chem.*, **21**, 997 (1956).
25. Dobryanskiĭ, A. F., and A. P. Sivertsev, *Zh. Obshch. Khim.*, **17**, 902 (1947).

Résumé

On a étudié les méthodes de préparation de polyester à partir de 2,2-bis-(halométhyl)-propane-diols. Des polyesters solides, linéaires ont été obtenus par la réaction avec des chlorures d'acides dicarboxyliques. Cette méthode est la meilleure pour préparer des polyesters à partir de ces diols. Le polyoxalate, le polysuccinate et le polyadipate du 2,2-bis(chlorométhyl)-1,3-propane-diol sont cristallins, mais les poly(o-,m-,p-) phtalates sont amorphes. Les polyadipates du 2,2-bis(bromométhyl) et du 2-chlorométhyl-2-bromométhyl-propane-diol sont également cristallins, et les polyadipates du 2,2-bis(iodométhyl)-et du 2-chlorométhyl-2-iodo-méthyl-propane-diol sont amorphes.

Zusammenfassung

Methoden zur Darstellung von Polyestern aus 2,2-Bis(halomethyl)-propandiolen wurden untersucht. Lineare feste Polyester wurden durch Reaktion mit Dicarbonsäurechloriden erhalten, was sich als günstigste Methode zur Darstellung von Polyestern aus diesen Diolen erwies. Polyoxalat, Polysuccinat und Polyadipat von 2,2-Bis(chloromethyl)-1,3-propandiol waren kristallin, Poly(o-, m-, p-)phthalat hingegen amorph. Polyadipate von 2,2-Bis(bromomethyl)- und 2-Chlormethyl-2-brommethylpropandiol waren ebenfalls kristallin und Polyadipate von 2,2-Bis(jodmethyl)- und 2-Chlormethyl-2-jodmethylpropandiol waren amorph.

Received September 2, 1964

Revised December 17, 1964

Prod. No. 4641A

Polymer-Solvent Interactions of Bisphenol A Polycarbonate in Different Solvents*

GULLAPALLI SITARAMAIAH, *Borg-Warner Research Center, Des
Plaines, Illinois*

Synopsis

Bisphenol A polycarbonate (Lexan, General Electric) was fractionated from methylene chloride by progressive precipitation with methanol and the fractions were characterized by osmometry, light scattering, and viscometry. Intrinsic viscosities of eight fractions in the molecular weight range 10,000-70,000 were obtained in five solvents at different temperatures to study the molecular expansion of polycarbonate. Light-scattering molecular weights, measured for the three high viscosity fractions, agreed within $\pm 5\%$ with the \bar{M}_v values. The \bar{M}_v/\bar{M}_n ratio of the fractions was between 1.1 and 1.3, as compared to 2.7 for the unfractionated polymer. This indicates a relatively narrow distribution of the fractions. The exponent, a , in the Mark-Houwink equation showed no appreciable change with temperature. Values of $d[\eta]/dT$ were generally negative. The unperturbed dimensions of polycarbonate, evaluated by the relation $[\eta] = KM^{1/2}\alpha^2$,^{4,3} suggest a stiff molecule. Values of K and $d \log \alpha^3/dT$ indicate increased chain flexibility at higher temperatures. Experimental data demonstrate that the Kurata-Stockmayer-Roig expression, based on the equivalent ellipsoidal model of a linear polymer molecule, is well suited to interpret the molecular expansion of polycarbonate. The Flory relation, $\alpha^5 - \alpha^3$ versus $M^{1/2}$, is found to be of limited applicability.

INTRODUCTION

Interactions of dilute solutions of linear polymers have long been interpreted in terms of the Flory-Fox theory,¹⁻³ in which the relationships of interest are

$$[\eta] = \phi (\bar{R}_0^2/M)^{3/2} M^{1/2} \alpha^3 = KM^{1/2} \alpha^3 \quad (1)$$

$$[\eta]/[\eta]_\Theta = \alpha^3 \quad (2)$$

$$\alpha^5 - \alpha^3 = 2C_M (1/2 - \chi) M^{1/2} \quad (3)$$

where \bar{R}_0^2 , α , and χ are respectively the mean square end-to-end length in the unperturbed state, the expansion factor due to polymer-solvent interactions, and the Flory-Huggins interaction parameter.

By taking into account the non-Gaussian character of the chains with excluded volume, Kurata and Yamakawa⁴ modified eq. (2) to give

$$[\eta]/[\eta]_\Theta = \alpha^{2.43} \quad (4)$$

* Paper presented at the 148th Meeting of the American Chemical Society, Chicago, Illinois, August 31-September 4, 1964.

Experimental evidence in the past^{3,5,6} suggested that the Flory ratio $(\alpha^5 - \alpha^3)/M^{1/2}$, evaluated from the intrinsic viscosity data, either displayed a maximum at some molecular weight or increased with M . When the expansion factor was obtained by means of eq. (4) instead of eq. (2), it was observed that the Flory ratio increased monotonically with M . To resolve these anomalies, Kurata, Stockmayer, and Roig recently proposed a new theory of excluded volume effect of linear polymer molecules in solution and derived the relation

$$\frac{\alpha^3 - \alpha}{N^{1/2}} = \frac{1}{(1 + 1/3\alpha^2)^{3/2}} \left(\frac{4}{3}\right)^{5/2} \left(\frac{3}{2\pi}\right) \beta/a^3 \quad (5)$$

where a is the effective bond length, β the binary cluster integral, and N is the number of segments in the polymer chain. These authors found that eq. (5) was more appropriate to interpret the existing viscosity data for several polymers in dilute solution. Other investigators^{8,9} also observed that eq. (5) was more satisfactory to interpret their viscometric data.

Earlier studies by Schulz and Horbach¹⁰ on bisphenol A polycarbonate were concerned with the determination of molecular weights and molecular constants of the fractions in solution. In the present investigation, the viscometric behavior of the bisphenol A polycarbonate has been studied, with special emphasis on the expansion of the molecule under a variety of conditions of solvent and temperature. Intrinsic viscosities of eight fractions, in the molecular weight range 10,000–70,000, have been obtained in five solvents at different temperatures. These data have been interpreted in terms of eq. (5) and the Flory theory. Few studies of this nature are available for polyesters covering this low molecular region.

EXPERIMENTAL AND RESULTS

Fractionation

Bisphenol A polycarbonate (Lexan, General Electric), which had an $[\eta]$ value of 0.68 dl./g. at 25°C. in methylene chloride, was fractionated from 1% solutions (w/v) of methylene chloride at $25 \pm 0.1^\circ\text{C}$. Methanol was used as precipitant and was gradually added to arbitrary turbidity with vigorous stirring. The stirring was continued for 6–8 hr. The gel-like precipitate was allowed to settle overnight, dissolved in a small quantity of methylene chloride, and reprecipitated by dropwise addition of the solution to excess methanol in a Waring Blendor. The fractions were dried at 70°C. for a few hours and then in vacuum for several hours.

Fractionation of the polymer was reproducible, as seen from the integral distribution curve for two fractionations (Fig. 1). Fractions of almost identical viscosity were solution blended to give eight representative fractions, designated A–H; their characteristics are shown in Table I.

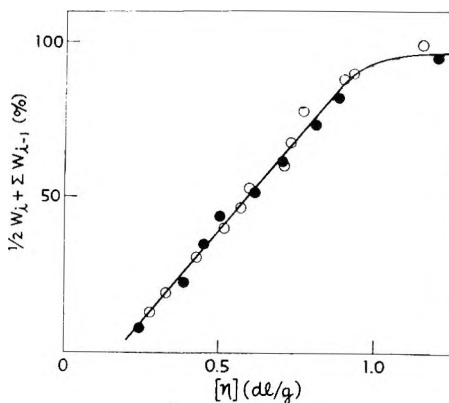


Fig. 1. Integral distribution curve of bisphenol A polycarbonate (Lexan): (O) First fractionation; (●) repeat fractionation.

TABLE I
Characteristics of the Fractions

Fraction	$M_r \times 10^{-4}$	$M_{LS} \times 10^{-4}$	$\bar{M}_n \times 10^{-4}$	\bar{M}_w/\bar{M}_n	M_{LS}/\bar{M}_n	$[\eta]$ in CH_2Cl_2 , dl./g.
A	6.97	7.20	6.00	1.11	1.20	1.00
B	5.61	5.74	5.35	1.05	1.08	0.83
C	4.60	4.80	4.27	1.08	1.12	0.74
D	4.08	—	3.57	1.14	—	0.64
E	3.27	—	2.95	1.11	—	0.56
F	2.58	—	2.33	1.11	—	0.46
G	1.91	—	1.51	1.27	—	0.36
H	1.09	—	0.93	1.17	—	0.26

Intrinsic Viscosities

Dilute solution viscosities of the fractions were measured at $25 \pm 0.01^\circ\text{C}$. by means of a Cannon-Ubbelohde dilution viscometer, for which kinetic energy corrections were negligible. All solvents and solutions were filtered through a medium sintered filter before the measurement of efflux times. Shear dependence, as observed from the viscosity determinations in a Cannon four-bulb shear viscometer, was within the normal limits of experimental error.

Viscosities were measured at 25°C . in methylene chloride, tetrachloroethane, chloroform, tetrahydrofuran, and ethylene dichloride, and in the last four solvents the measurements were extended to high temperatures, up to 70°C . The usual precautions for the evaporation of solvent at higher temperatures were taken and corrections were made for the changes in solution concentration wherever necessary. No degradation of the polymer was observed in these solvents up to the duration of one week. All solvents used were Fisher reagent grade.

Intrinsic viscosities $[\eta]$ were obtained from the reduced viscosity at four concentrations by means of the Huggins relationship

$$\eta_{sp}/c = [\eta] + k' [\eta]^2 c \quad (6)$$

where k' is known as the Huggins constant. Values of $[\eta]$ at different temperatures are given in Table II. Typical graphs of η_{sp}/c versus c of polycarbonate fractions in ethylene chloride are shown in Figure 2.

TABLE II
Values of $[\eta]$

Solvent	Fraction	$[\eta]$, dl./s.					
		25°C.	32°C.	40°C.	48°C.	56°C.	70°C.
Chloroform	A	1.12	1.03	1.01	0.98	—	—
	B	0.94	0.87	0.84	0.85	—	—
	C	0.82	—	—	—	—	—
	D	0.69	0.67	0.64	0.64	—	—
	E	0.63	—	—	—	—	—
	F	0.52	—	—	—	—	—
	G	0.40	0.37	0.36	0.36	—	—
	H	0.27	0.25	0.25	0.24	—	—
Tetrachloroethane	A	1.15	1.07	—	0.96	0.96	0.96
	B	1.09	0.98	0.89	0.76	0.74	0.76
	C	0.80	—	—	—	—	—
	D	0.70	0.69	0.62	0.58	0.56	0.53
	E	0.60	—	—	—	—	—
	F	0.55	—	—	—	—	—
	G	0.35	0.30	0.27	0.29	0.31	0.25
	H	0.28	0.28	0.26	0.23	0.18	0.20
Tetrahydrofuran	A	0.95	0.92	0.87	0.86	0.82	—
	B	0.85	0.84	0.82	0.77	0.77	—
	C	0.71	—	—	—	—	—
	D	0.64	0.60	0.61	0.56	0.55	—
	E	0.57	—	—	—	—	—
	F	0.49	—	—	—	—	—
	G	0.38	0.37	0.36	0.34	0.33	—
	H	0.25	0.26	0.25	0.24	0.23	—
Ethylene chloride	A	0.98	0.94	0.95	—	0.86	0.87
	B	0.83	0.81	0.76	—	0.74	0.68
	C	0.70	—	—	—	—	—
	D	0.62	—	—	—	—	—
	E	0.55	0.55	0.53	—	0.46	0.52
	F	0.49	—	—	—	—	—
	G	0.37	0.35	0.34	—	0.34	0.31
	H	0.25	0.24	0.25	—	0.23	—

Molecular weights, \bar{M}_v , of the fractions were calculated from intrinsic viscosities in methylene chloride at 25°C. by using the $[\eta]$ - M relationship given by Schulz and Horbach.¹⁰ The \bar{M}_v values were in the range of 10,000–70,000 and are shown in Table I.

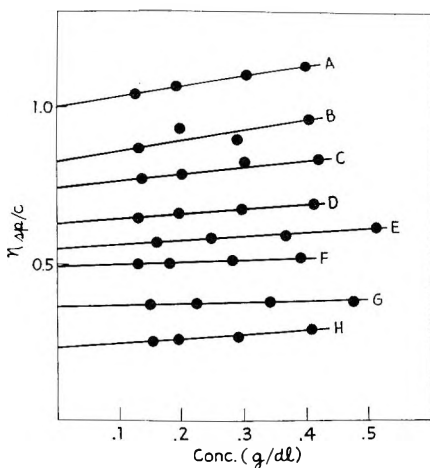


Fig. 2. Viscosity-concentration graphs of polycarbonate fractions in ethylene chloride at 25°C.

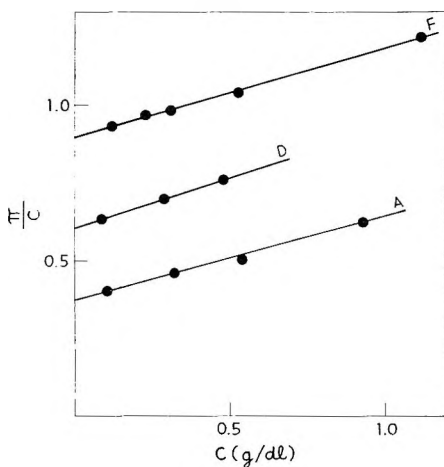


Fig. 3. Osmotic pressure-concentration graphs for fractions A, D, and F (π in cm. of solvent and $RT = 2.14 \times 10^4$).

Osmometry

Number-average molecular weights \bar{M}_n were obtained from ethylene chloride solutions of the fractions by means of the Mechrolab high-speed osmometer, and use of the gel cellophane (No. 600) membranes. The membranes were conditioned by the usual procedure. Except in the case of lowest molecular fraction, H, where some membrane permeation was detected, the osmotic pressures were reproducible at all concentrations. \bar{M}_n values were obtained from the relationship

$$\pi/c = [RT (1/\bar{M}_n) + A_2 c] \quad (7)$$

where π is the osmotic pressure and A_2 is the virial coefficient of interaction of polymer with the solvent. A typical graph of π/c versus c is shown in Figure 3. The osmotic molecular weights are shown in Table I. Values of A_2 have been of the order of $1.3 \pm 0.2 \times 10^{-3}$ cm.³-mole / g.² for polycarbonate fractions in ethylene chloride at 25°C., and no trend of A_2 with molecular weight was noted.

Light Scattering

Measurement of light scattering of chloroform solutions of the fractions was made with a Brice-Phoenix photometer.¹¹ Scattered light intensities were measured for the wavelength of 5461 Å. at angles of 45, 90, and 135° to the primary beam. All solvents and solutions were filtered through a fine sintered filter to eliminate dust and colloidal debris. The instrument was calibrated with Ludox colloidal silica by the standard procedure.^{12,13} The measurement was limited to the three high molecular fractions and was not extended to lower molecular weight fractions because of the large experimental errors arising from the low intensity of scattering of the solutions.

The Debye dissymmetry method was used for computing the molecular weights, by using the relation

$$Kc/R_{90} = (1/M_w) + 2A_2c \quad (8)$$

where

$$K = 2 \pi^2 n_0^2 (dn/dc)^2 / \lambda^4 N$$

in which λ is the wavelength of light and n_0 is the refractive index of chloroform. The value of dn/dc was obtained by means of a Ziess laboratory interferometer, using 8 cm. cells, and was found to be 0.162 at 5461 Å. in chloroform. No dissymmetry correction was applied to the scattering data as the values of intrinsic dissymmetry were close to unity.

DISCUSSION

Intrinsic Viscosities and Molecular Weights of the Fractions

The intrinsic viscosities of the polycarbonate fractions, as seen from Table II, are in the order of tetrachloroethane > chloroform > methylene chloride > ethylene chloride > tetrahydrofuran. In the region of 10,900–70,000 molecular weight, a fourfold increase of viscosity was observed, and the viscosities generally decreased with the increase of temperature. In all cases, no dependence of the Huggins interaction constant k' on molecular weight, solvent, or temperature was observed.

The closeness of the viscosity-average molecular weights calculated from the equation of Schulz and Horbach¹⁰ for the three fractions, A, B, and C, with the light-scattering values in Table I indicates that the \bar{M}_v values are practically the weight averages. As is evident from the values of \bar{M}_v/\bar{M}_n ,

fall between 1.1 and 1.3, fractions with relatively narrow distribution were obtained in the fractionation, as compared to a \bar{M}_v/\bar{M}_n value of 2.7 measured for the original polymer.

Intrinsic Viscosity—Molecular Weight Relationships

The dependence of viscosity on molecular weight is usually expressed by the Mark-Houwink relationship^{14,15}

$$[\eta] = K'M^a \quad (9)$$

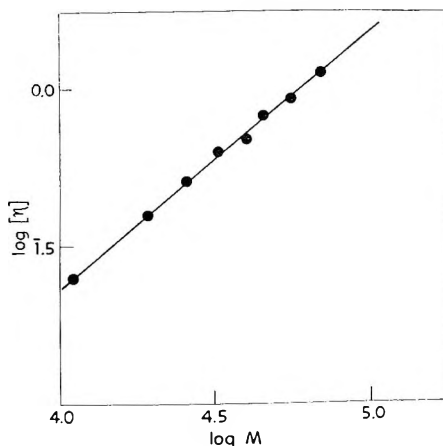


Fig. 4. Intrinsic viscosity-molecular weight relationship for polycarbonate fractions in chloroform at 25°C.

where a is the exponent which generally varies between 0.5 and 0.8 for synthetic polymers.³ Linear log-log graphs of $[\eta]$ versus M were obtained in all solvents, and such a typical graph for chloroform is shown in Figure 4. The relationships obtained at 25°C. are presented in Table III, and it can be seen that the exponent was found to be 0.82 in the good solvents, like tetrachloroethane and chloroform, whereas in ethylene chloride and tetrahydrofuran, which are poorer solvents for polycarbonates, values of 0.76 and 0.70 were obtained. The same value of 0.70 for tetrahydrofuran was found by Schulz and Horbach.¹⁰ From the exponent of the molecular weight, the conclusion may be drawn that the polycarbonate molecule has

TABLE III
Values of K' and a in $[\eta] = K'M^a$, at 25°C.

Solvent	K'	a
Ethylene chloride	2.04×10^{-4}	0.76
Tetrachloroethane	1.34×10^{-4}	0.82
Tetrahydrofuran	3.89×10^{-4}	0.70
Chloroform	1.20×10^{-4}	0.82

a configuration between that of a free-draining and a solvent-immobilizing coil.

No gradual change of the exponent with temperature was observed in the case of polycarbonate and this may be attributed to the low molecular weight of the fractions investigated, for which the changes in chain conformation with temperature may be small. As was pointed out by earlier authors,¹⁶ the exponent, a is not sensitive to small changes in chain conformation.

Determination of Unperturbed Dimensions

The unperturbed dimensions of a polymer molecule are usually obtained by employing eq. (1), when light-scattering methods are not satisfactory. Where Θ -solvent viscosities are not available, as in the present case, K values were usually obtained by the Flory-Fox-Schaeffgen method,^{17,18} for which the equation of interest is

$$[\eta]^{2/3}/M^{1/3} = K^{2/3} + 2C_M'(1/2 - \chi) K^{2/3} M/[\eta] \quad (10)$$

This method, although attractive, leads to an underestimation of K in good solvents. For methyl methacrylate in the good solvent, methyl ethyl ketone, a K value of 0.9×10^{-4} was obtained by Chinai and Samuels,¹⁹ which is much lower than the correct value of 4.7×10^{-4} .

Another method of evaluation of K is based on the equation

$$[\eta]^{2/3}/M^{1/3} = K^{2/3} + 0.363\Phi_0 B[g(\alpha)M^{2/3}/[\eta]^{1/3}] \quad (11)$$

which was derived by Kurata and Stockmayer²⁰ and applied to a number of experimental data already available. It has been shown that this procedure gives the same value of K irrespective of solvent. A more direct method has recently been published by Stockmayer and Fixman.²¹ Their equation reads

$$[\eta] = KM^{1/2} + 0.51\Phi_0 BM \quad (12)$$

in which B is the polymer-solvent interaction parameter. This relationship is almost identical with a semiempirical equation derived by Krigbaum^{22,23} some years ago.

Now it is worthwhile to consider whether the above relationships, eqs. (11) and (12), could be applied to the relatively low molecular polycarbonate fractions used in the present study. Kurata and Stockmayer²⁰ applied eq. (11) to the polyethylene oxide data of Sadron and Remp²⁴ and of Bailey and Callard²⁵ and showed that the data fit very well with eq. (11), in the molecular weight ranges of 3,000–20,000 (Sadron) and 20,000–5,000,000 (Bailey). The value of K found for the two molecular weight regions was almost identical. Similarly, it was also shown that the applicability of eq. (11) may be extended to a molecular weight of 1,000 for polystyrene.

In Figures 5 and 6, the data for polycarbonate fractions in methylene chloride are plotted in terms of eqs. (11) and (12), and a K value of 15 ± 1

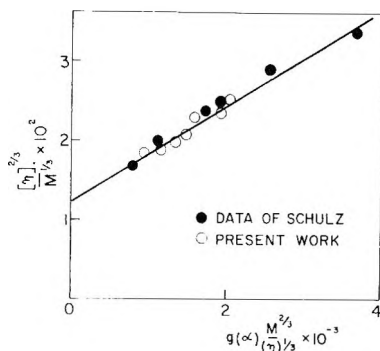


Fig. 5. Evaluation of K for polycarbonate in methylene chloride at 25°C.

TABLE IV
Values of K and α

Solvent	Temp., °C.	α					$K \times 10^3$
		Fraction A	Fraction B	Fraction D	Fraction G	Fraction H	
Chloroform	25	1.55	1.49	1.41	1.31	1.25	1.39
	32	1.53	1.48	1.43	1.30	1.24	1.36
	40	1.55	1.49	1.44	1.32	1.27	1.33
	48	1.58	1.55	1.40	1.36	1.30	1.32
Methylene chloride	25	1.48	1.45	1.37	1.26	1.23	1.42
	25	1.56	1.59	1.43	1.24	1.26	1.35
Tetrachloroethane	25	1.55	1.55	1.45	1.19	1.30	1.03
	40	1.53	1.42	—	1.33	1.29	1.03
	48	1.57	1.48	1.43	1.25	1.27	0.95
	56	1.63	1.52	1.46	1.33	1.19	0.54
Tetrahydrofuran	25	1.44	1.43	1.37	1.28	1.21	1.67
	32	1.45	1.46	1.37	1.30	1.26	1.68
	40	1.45	1.47	1.41	1.32	1.28	1.74
	48	1.50	1.49	1.42	1.33	1.30	1.45
Ethylene dichloride	56	1.53	1.54	1.45	1.36	1.32	1.49
	25	1.46	1.42	1.36	1.27	1.21	1.51
	32	1.47	1.44	1.37	1.27	1.23	1.46
	40	1.51	1.43	1.38	1.28	1.26	1.44
Ethylene dichloride	56	1.55	1.61	1.39	1.37	1.31	1.19
	70	1.64	1.71	1.54	1.39	1.21	0.44

$\times 10^{-4}$ has been obtained by both methods. Because of the simplicity of eq. (12), all K values were obtained directly from the ordinate intercept of $[\eta]/M^{1/2}$ versus $M^{1/2}$ graphs.*

The K and α values, evaluated by eqs. (1), (4) and (12), are shown in Table IV. At 25°C., where the viscosity data are expected to be most accu-

* All graphical extrapolations were performed on a Recomp III digital computer by use of least-square polynomial curve fitting.

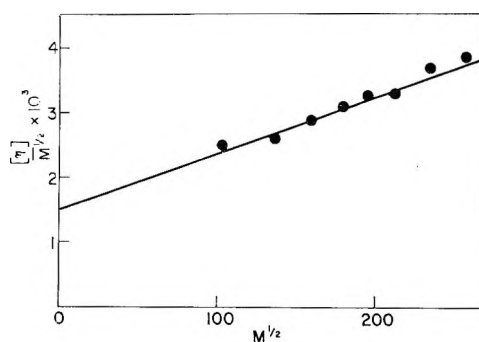


Fig. 6. Stockmayer-Fixman plot for evaluation of K for polycarbonate in methylene chloride at 25°C.

rate, the K value of $1.5 \pm 0.13 \times 10^{-3}$ has been obtained. As seen in Table IV, in general the K values in good solvents are lower than in the poorer solvents, which may be attributed at least partially to short-range interactions of solvent on the dimensions of the molecule. Evidence for such short-range interactions was found by Bianchi, Magnasco, and Rossi from their study of polystyrene fractions in various mixed θ solvents.²⁶

Values of K obtained for polycarbonate are generally higher than those for other synthetic polymers. The value of 1.5×10^{-3} at 25°C. corresponds to a $(\bar{R}_0^2/M)^{1/2}$ value of 840×10^{-11} , which is much higher than 655×10^{-11} , obtained for methyl methacrylate polymer.²⁰ It may be noted from the review article of Kurata and Stockmayer²⁰ that many synthetic polyesters, polycarbonate included, possess a stiff chain conformation approaching that of many cellulose esters. The decrease of K at higher temperatures is due to increased flexibility of the polymer chain.

Molecular Expansion in Terms of Flory Theory

Although a small measure of specific interaction of the polymer with solvent is not ruled out, it is considered satisfactory to assume K independent

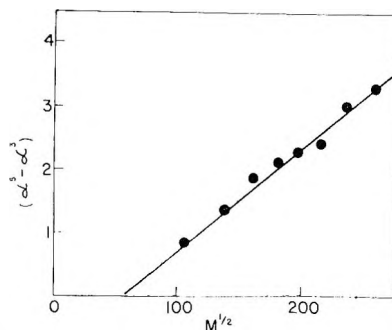


Fig. 7. Graph of $\alpha^5 - \alpha^3$ vs. $M^{1/2}$ for polycarbonate in tetrahydrofuran at 25°C., in terms of the Flory theory.

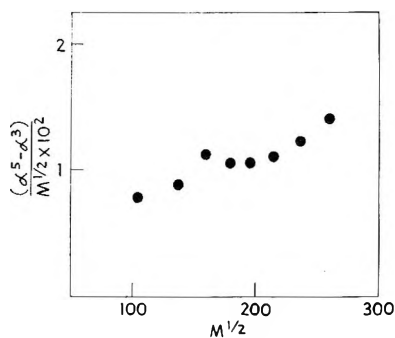


Fig. 8. Flory plot of polycarbonate in ethylene chloride at 25°C.

of solvent and calculate α values. As seen in Table IV, the values of α increase with the increase of molecular weight, solvent power, and temperature, indicating increased expansion of the molecule. Graphs of $\alpha^5 - \alpha^3$ versus $M^{1/2}$ and $(\alpha^5 - \alpha^3)/M^{1/2}$ versus M (Figs. 7 and 8) in all cases show a monotonic increase of $\alpha^5 - \alpha^3$ and $(\alpha^5 - \alpha^3)/M^{1/2}$ with molecular weight. However, graphs of $\alpha^5 - \alpha^3$ versus $M^{1/2}$, although linear, do not pass through the origin but give an abscissa intercept corresponding to about 6000 molecular weight.

Temperature dependence of viscosity may be expressed by the relation:²⁷

$$d \log [\eta]/dT = d \log [\Phi]/dT + 3/2 d \log (\bar{v}v^2/M)/dT + d \log \alpha^3/dT \quad (13)$$

As seen in Table V, negative temperature coefficients have been obtained and are of the same order of magnitude as for other synthetic polymers.²⁸

TABLE V
Temperature Dependence of $[\eta]$ and α^3

Solvent	Temp., °C.	α^3 (for fraction D)	$d \log [\eta]/dT$ $\times 10^2$	$d \log \alpha^3/dT \times 10^2$
Chloroform	25	2.86		
	32	2.94		
	40	3.01	0.15	0.23
	48	3.34		
Tetrachloroethane	25	2.92		
	32	3.05		
	40	2.87	0.18	0.26
	48	2.91		
	56	3.09		
Ethylene dichloride	25	2.51		
	32	—		
	40	—	0.16	0.33
	56	2.70		
Tetrahydrofuran	25	2.58		
	32	2.58		
	40	2.79	0.19	0.26
	48	3.04		

Although the polycarbonate molecule is almost as stiff as cellulose esters, values of $d \log \alpha^3/dT$ are higher for polycarbonate, indicating greater chain flexibility at higher temperatures.²⁷ Analysis of the data to evaluate the theta temperature, as well as heat and entropy parameters, was not possible because the data did not fit into the Flory graphs for that purpose.

Test of Kurata, Stockmayer, and Roig Relation

As seen from Figures 9 and 10, graphs of $(\alpha^3 - \alpha) (1 + 1/3 \alpha^2)^{3/2}$ versus $M^{1/2}$ are linear and pass through the origin in all cases. This suggests that the data fit in excellently with the Kurata-Stockmayer-Roig (K-S-R) equation. The slopes of these graphs are a measure of the polymer-solvent interaction. Similarly, the slopes of $[\eta]/M^{1/2}$ versus $M^{1/2}$ in the Fixman-Stockmayer (F-S) equation also indicate the magnitude of interaction.

These slopes are shown in Table VI, and good agreement of the slopes in the two equations is evident. Increase of the slopes with solvent power is

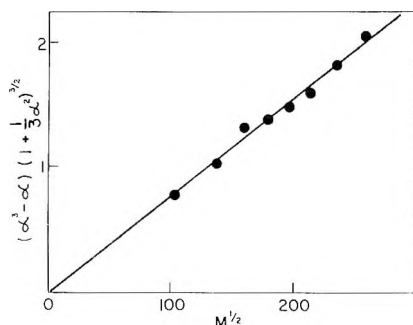


Fig. 9. K-S-R plot of polycarbonate in ethylene chloride at 25°C.

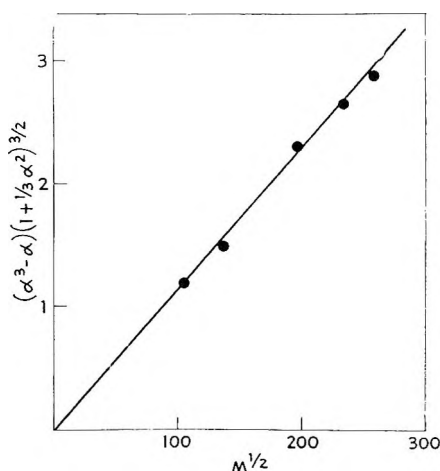


Fig. 10. K-S-R plot of polycarbonate in chloroform at 48°C.

observed; however, no striking trend with temperature can be noticed. This is probably due to the small temperature dependence of interaction for these fractions.

CONCLUSIONS

The molecular expansion of bisphenol A polycarbonate can best be interpreted in terms of the expression of Kurata, Stockmayer, and Roig, and the Flory relations are not satisfactory for this purpose. The equivalent ellipsoidal model, assumed to explain the volume effects of polymers in solution,^{4,6,29} is applicable for the expansion of polycarbonate in solution. This explains the absence of any trend in the molecular weight exponent a , for, in the low molecular region investigated, changes in solvation of the polymer influence the molecular expansion far more than changes in chain conformation. Short-range interactions of the solvent on polycarbonate are not altogether absent. The polycarbonate molecule, although stiff, has considerable flexibility at higher temperatures.

The author's grateful thanks are due to Drs. Eugene P. Goldberg and Frank Chang for continued encouragement, to Jack Gawlik for the technical assistance, and to Borg-Warner Corporation for permission to publish this work.

References

1. Flory, P. J., *J. Chem. Phys.*, **17**, 303 (1949).
2. Fox, T. G., Jr., and P. J. Flory, *J. Am. Chem. Soc.*, **73**, 1909 (1951).
3. Flory, P. J., *Principles of Polymer Chemistry*, Cornell Univ. Press., Ithaca, N. Y., 1953.
4. Kurata, M., and H. Yamakawa, *J. Chem. Phys.*, **29**, 311 (1958).
5. Krigbaum, W. R., and P. J. Flory, *J. Polymer Sci.*, **11**, 37 (1953).
6. Notley, N. T., and P. Debye, *J. Polymer Sci.*, **24**, 275 (1957).
7. Kurata, M., W. H. Stockmayer, and A. Roig, *J. Chem. Phys.*, **33**, 151 (1960).
8. Okada, R., Y. Tcyoshima, and H. Fujita, *Makromol. Chem.*, **59**, 137 (1963).
9. Utraki, L., and R. Simha, *J. Chem. Phys.*, **67**, 1056 (1963).
10. Schulz, G. V., and A. Horbach, *Makromol. Chem.*, **29**, 93 (1959).
11. Brice, B. A., M. Halwer, and H. Speiser, *J. Opt. Soc. Am.*, **40**, 768 (1950).
12. Goring, D. A. I., M. Senez, B. Melansen, and M. M. Huque, *J. Coll.-Sci.*, **12**, 412 (1957).
13. Sitaramaiah, G., Ph.D. Thesis, McGill University, Montreal, 1961.
14. Mark, H., *Der Feste Korper*, Leipzig, Germany, 1938, p. 103.
15. Houwink, R. H., *J. Prakt. Chem.*, **157**, 15 (1940).
16. Sitaramaiah, G., and D. A. I. Goring, *J. Polymer Sci.*, **58**, 1107 (1962).
17. Flory, P. J., and T. G. Fox, Jr., *J. Am. Chem. Soc.*, **73**, 1904 (1951).
18. Schaeffgen, J. R., and P. J. Flory, *J. Am. Chem. Soc.*, **70**, 2709 (1948).
19. Chinai, S. N., and R. J. Samuels, *J. Polymer Sci.*, **19**, 463 (1956).
20. Kurata, M., and W. H. Stockmayer, *Fortschr. Hochpolymer Forsch.*, **3**, 196 (1963).
21. Stockmayer, W. H., and M. Fixman, *J. Polymer Sci.*, **C1**, 137 (1963).
22. Krigbaum, W. R., *J. Polymer Sci.*, **18**, 315 (1955).
23. Krigbaum, W. R., *J. Polymer Sci.*, **28**, 213 (1958).
24. Sadron, C., and P. Remp, *J. Polymer Sci.*, **29**, 127 (1958).
25. Bailey, F. E., and R. W. Callard, *J. Appl. Polymer Sci.*, **1**, 56 (1959).
26. Bianchi, U., and C. Rossi, *Chim. Ind. (Milan)*, **40**, 263 (1958).
27. Moore, W. R., and G. D. Edge, *J. Polymer Sci.*, **47**, 469 (1960).

28. Moore, W. R., and R. J. Fort, *J. Polymer Sci.*, **A1**, 929 (1963).
 29. Ptitsyn, O. B., *Soviet Phys. Uspekhi*, **2**, 796 (1960).

Résumé

Du bisphénol-A polycarbonate (Lexan General Electric) a été fractionné à partir de chlorure de méthylène par précipitation progressive au moyen de méthanol. Les fractions ont été caractérisées par osmométrie, diffusion lumineuse et viscosimétrie. On a obtenu les viscosités intrinsèques de huit fractions de poids moléculaires situés entre 10.000 et 70.000, dans cinq solvants à différentes températures en vue d'étudier l'extension moléculaire du polycarbonate. Les poids moléculaires obtenus par diffusion lumineuse déterminés pour les trois fractions de viscosité élevée, concordent à $\pm 5\%$ près avec les valeurs de \bar{M}_n . Comparée à la valeur 2.7 pour le polymère non-fractionné, le rapport \bar{M}_v/\bar{M}_n pour les fractions se situe entre 1.1 et 1.3. Cela indique une distribution relativement étroite de fractions. L'exposant a de l'équation de Mark-Houwink ne présente pas de changement appréciable avec la température. Les valeurs de $d[\eta]/dt$ sont généralement négatives. Les dimensions non-perturbées du polycarbonate, évaluées par la relation $[\eta] = KM^{1/2}\alpha^{2.43}$, suggèrent une molécule rigide. Les valeurs de K et de $d \log \alpha^3/dt$ indiquent une augmentation de la flexibilité de la chaîne à températures plus élevées. Les résultats expérimentaux démentent que l'expression de Kurata, Stockmayer et Roig, basée sur le modèle ellipsoïdal équivalent d'une molécule polymérique linéaire, convient bien pour interpréter l'extension moléculaire du polycarbonate. La relation de Flory, $\alpha^4 - \alpha^3$ vs. $M^{1/2}$, semblerait être d'une application limitée.

Zusammenfassung

Bisphenol-A-Polycarbonat (Lexan, General Electric) wurde aus Methylenchlorid durch fortschreitende Fällung mit Methanol fraktioniert und die Fraktionen durch Osmometrie, Lichtstreuung und Viskosimetrie charakterisiert. Zur Untersuchung der Molekülexpansion des Polycarbonats wurde die Viskositätszahl von acht Fraktionen im Molekulargewichtsbereich 10.000-70.000 in fünf Lösungsmitteln bei verschiedenen Temperaturen bestimmt. An den drei höchstviskosen Fraktionen gemessene Lichtstreuungsmolekulargewichte stimmten innerhalb $\pm 5\%$ mit den \bar{M}_n -Werten überein. Das \bar{M}_v/\bar{M}_n -Verhältnis der Fraktionen lag zwischen 1,1 und 1,3, verglichen mit Werten von 2,7 für das unfraktionierte Polymere. Das beweist eine verhältnismässig enge Verteilung der Fraktionen. Der Exponent a in der Mark-Houwink-Gleichung zeigte keine merkliche Temperaturabhängigkeit. Der Wert von $d[\eta]/dt$ war im allgemeinen negativ. Die aus der Beziehung $[\eta] = KM^{1/2}\alpha^{2.43}$ erhaltenen ungestörten Dimensionen des Polycarbonats sprechen für eine steife Molekel. Die Werte von K und $d \log \alpha^3/dt$ zeigen, bei höherer Temperatur die Kettenbiegsamkeit zunimmt. Die Versuchsdaten lassen erkennen, dass der auf dem Äquivalentellipsoidmodell einer linearen Polymermolekel beruhende Ausdruck von Kurata, Stockmayer und Roig zur Interpretation der Molekülexpansion von Polycarbonat gut geeignet ist. Die Flory-Beziehung $\alpha^4 - \alpha^3 \rightarrow M^{1/2}$ ist nur beschränkt anwendbar.

Received November 24, 1964

Revised January 25, 1965

(Prod. No. 4634A)

Absorption Spectra of Poly-*p*-iodostyrene

J. P. LUONGO and R. SALOVEY, *Bell Telephone Laboratories, Incorporated, Murray Hill, New Jersey*

Synopsis

From the infrared and ultraviolet spectra of iodinated polystyrene, the location and amount of the iodine substitution in the polystyrene molecule can be determined. In addition, when isotactic polystyrene is iodinated, the tacticity is retained but the helical conformation of the carbon backbone, both in solution and in the solid state, has been modified. Comparison of the atactic, helical isotactic, and nonhelical iodinated isotactic spectra show that bands at 1297, 585, and 558 cm^{-1} and particularly the 1080/1055 cm^{-1} doublet can be attributed to the helical conformation of the carbon backbone of isotactic polystyrene.

Introduction

Certain differences in the infrared and ultraviolet spectra of polystyrene and iodinated polystyrene indicate the location and content of iodine in the iodostyrene molecule. Of particular interest, however, is how iodination affects the helical conformation of the carbon backbone in isotactic polystyrene. Isotactic polystyrene assumes the conformation of a three-fold helix in the solid crystalline state.¹ Evidence indicates that the helical structure persists in solutions of the isotactic material.² However, x-ray³ and solution⁴ studies demonstrate that atactic and isotactic poly-*p*-iodostyrenes are contracted random coils in solution. In this paper we report on the spectral changes associated with the affect of iodination on the helical conformation of isotactic polystyrene.

Experimental Details

Copolymers of styrene and *p*-iodostyrene were prepared by the iodination of atactic and isotactic polystyrene (The Borden Chemical Co.) according to the procedure of Braun.⁵ Infrared spectra were recorded with a Perkin-Elmer Model 21 spectrometer. Samples were examined in chloroform solution, as films cast from chloroform, and as solids dispersed in potassium bromide pellets. Resultant spectra were essentially independent of sample state.

Reagent isomers of iodotoluene (Eastman Organic Chemicals) were used without purification. Ultraviolet spectra of these and of the copolymers were measured in chloroform solution with a Cary 14 spectrophotometer.

Results and Discussion

In Figure 1 are spectra of polystyrene and iodinated polystyrene. In the iodinated polystyrene spectrum there is a decrease in the ring CH stretching bands near 3030 cm.^{-1} while the intensity of the aliphatic CH stretching band at 2900 cm.^{-1} remains the same. This shows that the ring portion of the molecule has been affected by iodine substitution. In the 2000 cm.^{-1} region the four overtone bands associated with monosubstitution of the rings in polystyrene become a single band at 1900 cm.^{-1} ,

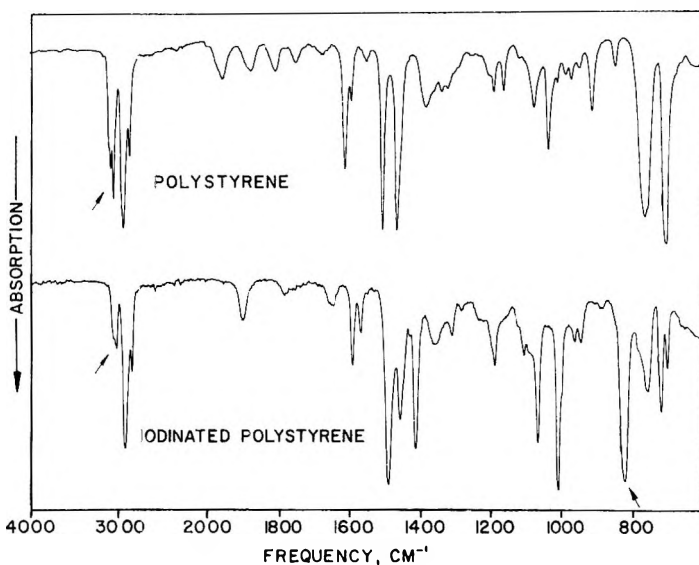


Fig. 1. Spectra of polystyrene and iodinated polystyrene.

showing disubstitution of the ring in iodinated polystyrene. Another significant feature in the infrared spectrum of the iodinated polymer is the strong band at 820 cm.^{-1} which is due to *para* substitution by iodine on the ring.

In the course of this work a series of samples containing various amounts of iodine was prepared. Since the ratio of the 820 cm.^{-1} band and the 760 cm.^{-1} band varied with iodine concentration in these samples, this ratio was plotted versus the known iodine content (determined gravimetrically),* resulting in the curve shown in Figure 2. The theoretical weight of iodine for monosubstitution in the polystyrene molecule is 55.2%. In the curve it can be seen that the ordinate becomes infinite at $\sim 55.1\%$, which agrees with the expected maximum of 55.2% iodine. The spectra of samples containing more iodine showed broad, ill-defined absorptions which prohibited reasonable interpretation.

* Determined by Dr. C. Tiedcke, Teaneck, N. J.

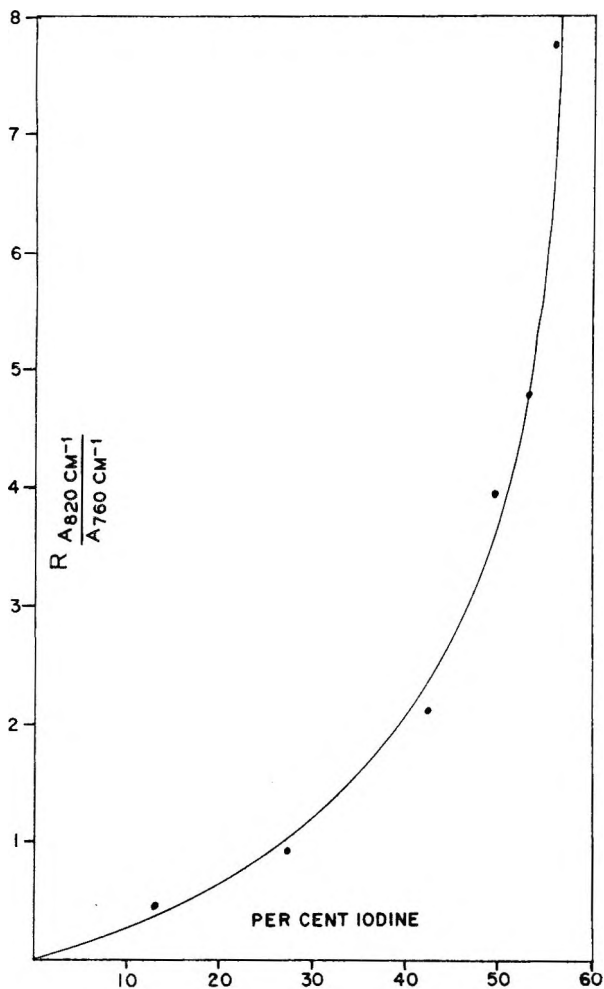


Fig. 2. $A_{820 \text{ cm}^{-1}} / A_{760 \text{ cm}^{-1}}$ vs. iodine content.

According to Natta¹ the structural arrangement in isotactic polystyrene involves alternate *trans* and *gauche* bonds along the carbon chain forming a helix. From steric considerations, this helical arrangement of the isotactic chain allows the bulky aromatic rings to pack closely without significant distortion of chain bonds. In Figure 3 is shown what is believed to be the isotactic polystyrene molecule showing the alternate *trans* (carbon atoms 1 and 4 across bond A) and *gauche* (carbon atoms 2 and 5 across bond B) arrangements along the carbon backbone.

In Figure 4 the top two curves are spectra of isotactic and atactic polystyrene in the 1700–400 cm^{-1} region. (Spectra of all polymers in Fig. 4 were similar in the solid state and in solution.) The profiles of the band near 1365 cm^{-1} differ, the isotactic polymer having a sharper band head at 1365 cm^{-1} . Another difference is the shoulder at 1297 cm^{-1} in the iso-

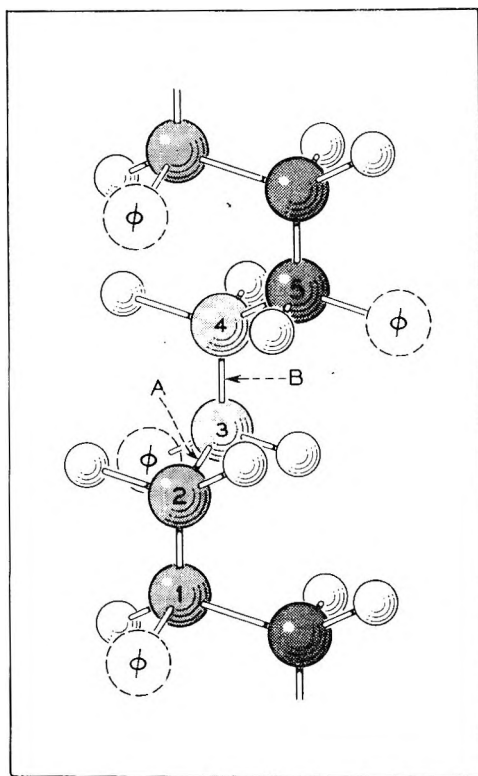


Fig. 3. Carbon backbone of isotactic polystyrene.

tactic and the lack of it in the atactic material. Near 1180 cm.^{-1} , again the profiles are different, the isotactic having a stronger shoulder at 1195 cm.^{-1} . One of the most significant differences occurs in the 1060 cm.^{-1} region. Here the isotactic material has a doublet ($1080/1055\text{ cm.}^{-1}$) and the atactic a singlet at 1056 cm.^{-1} . In the atactic polymer a weak band appears at 940 cm.^{-1} which is not present in the spectrum of the isotactic material. At longer wavelengths, the isotactic polymer has a band at 558 cm.^{-1} with a weak but definite side band at 585 cm.^{-1} . The atactic polymer has a corresponding major band at 537 cm.^{-1} .

When we compare the spectrum of iodinated isotactic polystyrene (bottom curve in Fig. 4) to the spectra of the isotactic and atactic polymers we find that the bands mentioned above are similar to those for atactic polystyrene. The 1365 cm.^{-1} band is considerably weakened. The 1297 cm.^{-1} band is gone, and the 1195 cm.^{-1} shoulder is not as pronounced as in either the atactic or isotactic spectrum. The 940 cm.^{-1} band found in the atactic but not in the original isotactic polymer now appears in the iodinated isotactic polystyrene spectrum. In the long wavelength region, the isotactic band at 558 cm.^{-1} has shifted to 541 cm.^{-1} , which compares to the 537 cm.^{-1} band in the atactic spectrum. The similarities between atactic and

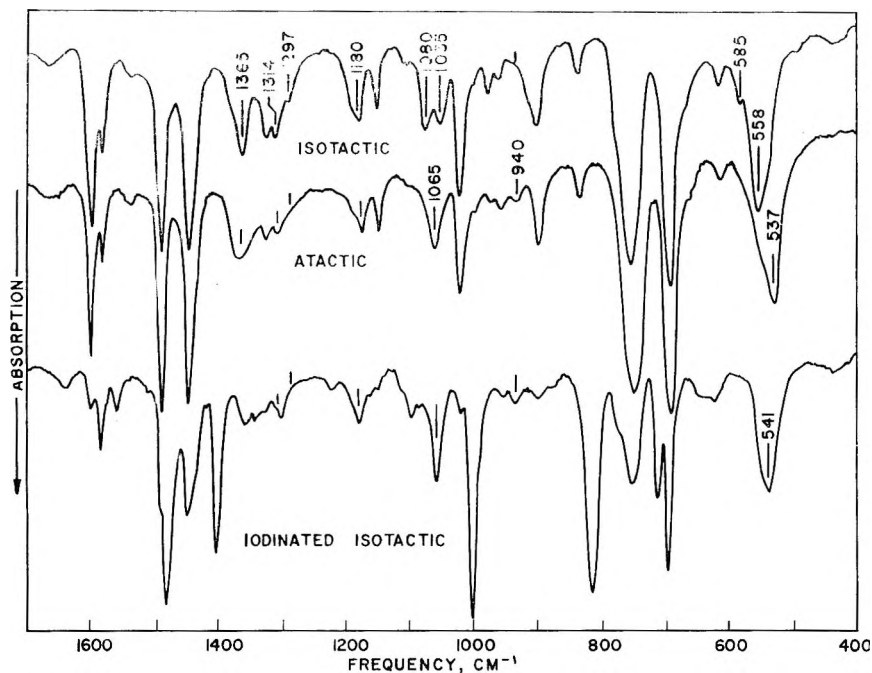


Fig. 4. Spectra of isotactic, atactic, and iodinated isotactic polystyrene in the 1700–400 cm^{-1} region.

iodinated isotactic polystyrene appear to suggest that iodination has affected the tacticity of the isotactic material. However, this would require the unlikely breaking of primary bonds. That this does not happen is supported by light-scattering measurements,⁴ which show that essentially no degradation occurs. X-ray diffraction studies³ of chloroform solutions of *p*-iodotoluene and iodinated isotactic polystyrene indicate randomness of iodine spacings in the iodinated isotactic polymer. The fact that no regular spacings are displayed by the iodinated isotactic material indicates that the helix has been destroyed by iodination. (Regular x-ray spacings can be observed in helical 3,5-dibromotyrosine.⁶)

These results then show that isotactic polystyrene, after iodination, retains an isotactic configuration, but that the helical conformation (i.e., the three-fold screw axis arrangement) has been destroyed. The loss of the helix on iodination may be due to repulsion of iodine atoms at *para* positions on aromatic rings. This in turn, affects certain vibrational modes of the C–H and aromatic groups along the carbon backbone which are reflected as changes in the infrared spectrum.

Most of the absorptions in the polystyrene spectrum are due to either C–H or aromatic ring modes. However, when we compare the spectra of the three polymers in Figure 4, certain absorptions for isotactic polystyrene can be attributed to the helical conformation. Thus absorptions at 1297, the 1080/1055 doublet, 585, and 558 cm^{-1} which appear in the isotactic

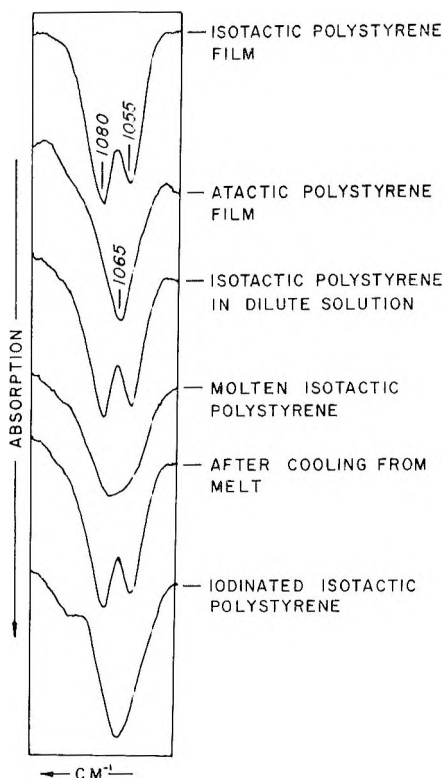


Fig. 5. The 1080–1055 cm^{-1} region in polystyrene.

but neither in the atactic nor the nonhelical (iodinated) isotactic, material can be attributed to the helical conformation in isotactic polystyrene.

The band near 1050 cm^{-1} in which the greatest effect can be observed is shown in Figure 5. The top two curves are from cast films of isotactic and atactic polystyrene. The third curve is from isotactic polystyrene in dilute solution (0.5% in chloroform). The doublet is present in the solution spectrum, indicating the doublet is not due to the crystal state. The next trace shows the isotactic "doublet" at the molten stage in an inert atmosphere ($\sim 260^\circ\text{C}$). At this temperature we would expect the helix to be modified. The next trace is that for the molten sample cooled to room temperature, and again the doublet reappears. It was interesting to note that when the molten run was made in air, the doublet did not reappear when cooled. Since the "molten" spectrum run in air showed C=O groups and the "inert" atmosphere spectrum did not, it is believed that bulky oxygenated groups formed during melting in air prevent reversible formation of the helix.

It has been reported⁷ that bands at 1365, 1314, and 1185 cm^{-1} are also due to the helical conformation of isotactic polystyrene. These assignments were primarily based on an increase of intensity during crystalliza-

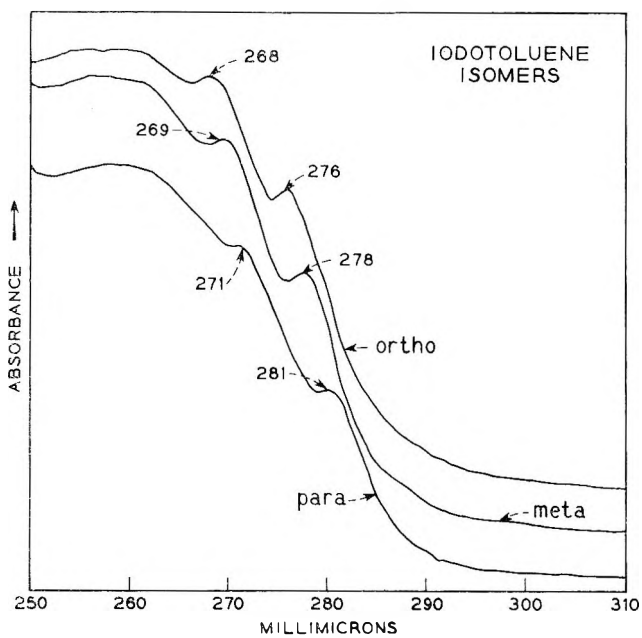


Fig. 6. Ultraviolet spectra of iodotoluene isomers.

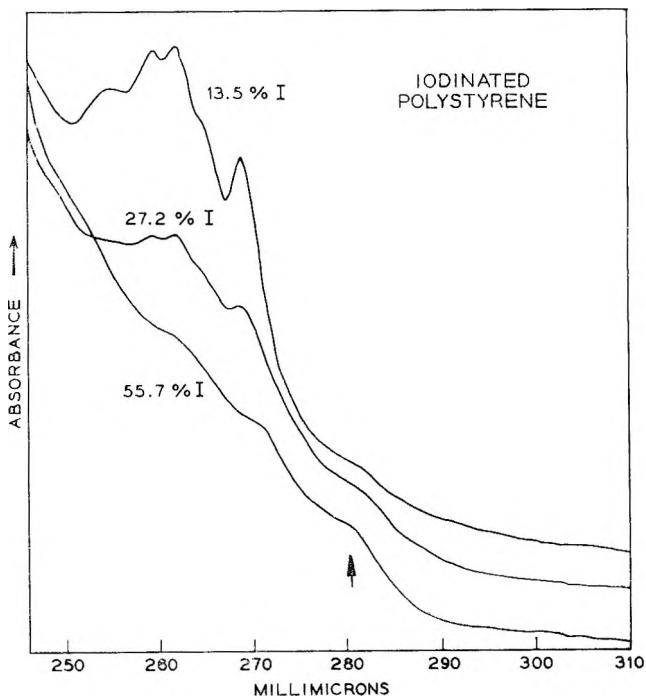


Fig. 7. Ultraviolet spectra of polystyrene containing different amounts of iodine.

tion. However, in our work, we find that, although slightly weakened, the 1314 and 1185 cm^{-1} bands are still present in both the atactic and iodinated isotactic polystyrene (Fig. 4). Also, it is not clear whether the 1365 cm^{-1} band seen in the isotactic spectrum (Fig. 4) is completely gone in either the atactic or iodinated isotactic materials, since both polymers have bands in this region which would overlap the 1365 cm^{-1} band.

Additional evidence regarding the location of iodine in iodinated polystyrene is found in the ultraviolet spectra. In Figure 6 are the ultraviolet spectra of *o*-, *m*-, and *p*-iodotoluene to show how substitution at the *ortho*, *meta*, and *para* positions can be distinguished in the ultraviolet. In Figure 7 are the spectra of polystyrenes iodinated to different extents. The characteristic spectrum of polystyrene is still evident in the sample iodinated to 13.5%. The next curve represents 27.3% iodination, and the bands characteristic of polystyrene are starting to diminish. In both curves, the *para* substitution band at 281 $\text{m}\mu$ can be noted. The bottom curve is completely iodine monosubstituted polystyrene. At this point the spectrum is similar to that of *p*-iodotoluene.

References

1. Natta, G., P. Corradini, and I. W. Bassi, *Nuovo Cimento (Suppl.)*, **15**, 69 (1960).
2. Onishi, T., and S. Krimm, *J. Appl. Phys.*, **32**, 2320 (1961).
3. Brady, G. W., and R. Salovey, *J. Am. Chem. Soc.*, **86**, 3499 (1964).
4. Salovey, R., and M. Y. Hellman, *J. Polymer Sci.*, **B3**, 499 (1965).
5. Braun, D., *Makromol. Chem.*, **30**, 85 (1959).
6. Brady, G. W., private communication.
7. Tadokoro, H., et al., *Bull. Chem. Soc. Japan*, **32**, 313 (1959).

Résumé

A partir des résultats de l'analyse spectrographique dans l'infrarouge et l'ultraviolet du polystyrène iodé, on peut déterminer l'emplacement et l'importance de la substitution par l'iode dans la molécule de polystyrène. De plus, lorsque du polystyrène isotactique est iodé, la tacticité est maintenue mais la structure hélicoïdale du squelette carboné, aussi bien en solution qu'à l'état solide, est modifiée. La comparaison entre les spectres de l'atactique, de l'isotactique hélicoïdal et de l'isotactique iodé non-hélicoïdal, montre que les bandes à 1297, 585 et 558 cm^{-1} et particulièrement le doublet 1080/1055 cm^{-1} peuvent être attribuées à la structure hélicoïdale du squelette carboné du polystyrène isotactique.

Zusammenfassung

Aus den Infrarot- und Ultraviolettpektren von jodiertem Polystyrol kann der Ort und der Betrag der Jodsubstitution in der Molekel bestimmt werden. Ausserdem wird bei der Jodierung von isotaktischem Polystyrol zwar die Reaktivität beibehalten, jedoch die Helixkonformation der Kohlenstoffhauptkette sowohl in Lösung als auch im festem Zustand modifiziert. Ein Vergleich der Spektren der ataktischen, isotaktischen Helix- und odierten isotaktischen Nichthelixform zeigt, dass die Banden bei 1297, 585, und 558 cm^{-1} sowie besonders das 1080/1055 cm^{-1} -Dublett der Helixkonformation der Kohlenstoffhauptkette des isotaktischen Polystyrols zugeordnet werden können.

Received December 17, 1964

Prod. No. 4645A

Polymerization of Acrylonitrile by Electron Transfer Initiation

AKIRA TSUKAMOTO, *Electrochemicals Department, E. I. du Pont de Nemours & Company, Inc., Niagara Falls, New York*

Synopsis

The homogeneous polymerization of acrylonitrile by electron transfer initiators is investigated. In a rigorously purified system at low temperatures it is demonstrated that "living" polyacrylonitrile is formed, and that its molecular weight can be predetermined. The number-average molecular weight of "living" polyacrylonitrile is approximately given by $2M/I$, where M represents grams of monomer and I is the number of moles of the initiator. For polyacrylonitrile prepared by homogeneous anionic polymerization with an electron-transfer initiator, it is found that the viscosity average molecular weight calculated by using the conventional values of K and α in the Mark-Houwink equation is considerably smaller than the osmotic number-average molecular weight. This clearly indicates a structural difference between the free-radical and anionic polyacrylonitrile; the anionic polyacrylonitrile appears to have a highly branched structure formed by a chain transfer process to the polymer.

INTRODUCTION

The polymerization of vinyl monomers by anionic initiators has been extensively studied.¹⁻³ Recently such polymerizations have been carried out in hydrocarbon or ether solvents where chain termination is absent or negligible if the system is rigorously purified and the polymerization is carried out in the absence of moisture or air. Such polymerizations are often called "living" polymerization.⁴ The polymers thus obtained generally exhibit narrow molecular weight distributions and, furthermore, the molecular weight is predetermined.^{5,6} The most clear-cut examples are the polymerizations of conjugated hydrocarbons, such as styrene or butadiene, initiated by rapid electron-transfer reactions. The generally accepted mechanism of the "living" polymerization of styrene consists of electron transfer to styrene monomer to yield a radical anion, followed by coupling to produce a dianion which propagates polymerization from both ends. The "living" polymers so obtained have molecular weights given by $2M/I$, where M is the amount of monomer in grams and I is the number of moles of the initiator. This simple relation has not generally been observed with polar monomers such as methyl methacrylate⁷⁻⁹ or acrylonitrile,¹⁰⁻¹³ although, they are much more reactive in anionic polymerization than styrene. Zilkha and co-workers have studied the anionic polymerization of

acrylonitrile^{10,11} and suggested the presence of a chain transfer reaction to the monomer and chain termination reactions to explain their results. Claes and Smets¹² have shown that termination reactions are present in anionic polymerization of acrylonitrile at 0°C. Graham and co-workers¹⁴ have indicated the "living" characteristics in anionic block copolymerization of acrylonitrile.

We have been investigating homogeneous polymerization of acrylonitrile at low temperatures by electron-transfer initiators and find some results which are not expected from earlier conclusions. Especially, it was found that the structure of the polyacrylonitrile produced differs considerably from that prepared by conventional free-radical polymerization.

EXPERIMENTAL

Materials

Commercial acrylonitrile, washed twice each with dilute hydrochloric acid and dilute sodium hydroxide solutions and then with water, was distilled from P₂O₅. The distilled monomer was degassed and distilled in a high vacuum line before use. Fractionated tetrahydrofuran (THF) was vacuum-distilled from LiAlH₄ and stored over sodium biphenyl under vacuum. Fractionated dimethylformamide (DMF), stored over calcium hydride, was vacuum-distilled into a thoroughly dried reaction flask before use. Other materials were used as supplied.

Preparation of Initiator Solution

The initiator solution was prepared¹⁵ by transferring THF under high vacuum into a tube containing biphenyl and freshly cut sodium metal and stirring the mixture for at least 24 hr. at room temperature. The solution was withdrawn for use through a filter stick. Its concentration was determined by titration for NaOH with 0.1*N* hydrochloric acid after hydrolysis.

Polymerization Procedure

The polymerizations were carried out in a high vacuum line similar to that described by Morton.¹³ The solvents were degassed by two or three freeze-thaw cycles before use. A typical polymerization procedure is described below.

Into a thoroughly dried 500-ml. two-necked flask, equipped with a tube containing a solution of sodium biphenyl in THF and a magnetic stirring bar (encapsulated in Pyrex), was vacuum-distilled 100 ml. of DMF. The flask was then attached to the vacuum line through a flexible glass spiral and the DMF was degassed by two or three freeze-thaw cycles. The flask was maintained at about -50°C. while 100 ml. of THF was distilled in through a vacuum line from a storage flask containing sodium biphenyl. The solvent mixture thus obtained was cooled to -78°C. (Dry Ice-acetone), and a few drops of the initiator solution was added, giving a permanent blue color

to the solution. (If more than 0.02 mmole of initiator is required to remove impurities, the solvent mixture is not suitable for quantitative experiments, since such a solvent was found to be capable of initiating polymerization of acrylonitrile without further addition of the initiator.) With rapid stirring at -78°C ., 0.5 ml. of acrylonitrile was transferred through the vacuum line (the blue color immediately disappeared) and 4.6×10^{-5} mole of the initiator solution was added (the color of the initiator solution disappeared immediately on contact with the reaction mixture). Into the stirred reaction mixture was added 9.5 ml. of acrylonitrile through the vacuum line over a period of 20 min., while a steady increase in viscosity was observed. The reaction was further continued for 1 hr. at -78°C . with stirring. The reaction was stopped by adding 1 ml. of concentrated hydrochloric acid. The polymer was precipitated by dilution with methanol, washed successively with water and acetone in a Waring Blendor, and dried in a vacuum desiccator over silica gel. The yield was 7.95 g. (99% of theoretical), $[\eta] = 0.870$ in DMF at 25°C .

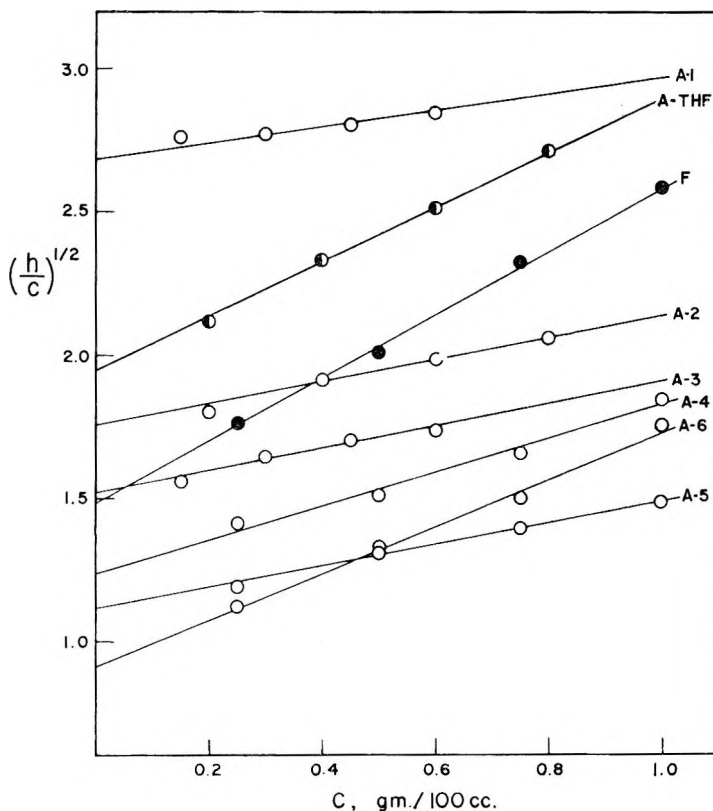


Fig. 1. Osmotic data of polyacrylonitrile in DMF at 30°F .: (F) prepared by free-radical polymerization; (A-1) to (A-6) prepared by homogeneous polymerization with sodium biphenyl initiator; (A-THF) prepared by polymerization in THF with sodium biphenyl initiator.

TABLE I
 Polymerization of Acrylonitrile with Sodium Biphenyl at -78°C .

Run no.	Acrylonitrile, g.	Initiator, mmole	Solvents, ml.		Yield, %	\bar{M}_n^a	$[\eta]$, g./dl.	\bar{M}_v^a	\bar{M}_w^a
			DMF	THF					
1	2.4	0.20	100	100	76	24,000	0.383	17,500	76,800
2	2.6	0.22	100	100	100	24,000	0.572	29,000	36,000
3	3.3	0.26	100	100	70	25,000	0.263	11,000	
4	5.5	0.28	100	100	100	39,000	0.570	27,000	
5	5.5	0.27	100	100	100	41,000	0.490	23,800	78,000
6	4.2	0.21	100	100	90	41,000	0.742	40,000	91,000
7	5.2	0.25	100	100	97	42,000	0.649	34,000	
8	8.8	0.28	100	100	100	62,000	0.693	37,000	
9	8.8	0.26	100	100	100	68,000	0.756	41,000	
10	8.0	0.20	100	100	100	80,000	0.877	49,000	89,000
11	8.8	0.20	100	100	100	88,000	1.006	58,000	87,000
12	8.1	0.18	100	100	100	90,000	0.910	51,500	
13	5.5	0.12	100	100	98	92,000	0.957	55,000	
14	4.8	0.10	100	100	100	96,000	0.779	42,500	

15	12.1	0.24	100	100	100	100	125,000	0.622	32,000	120,000
16	8.0	0.11	100	100	100	100	140,000	0.478	23,000	
17	12.6	0.14	100	100	100	100	180,000	0.683	36,000	228,000
18	7.8	0.09	100	100	100	100	180,000	0.804	44,000	190,000
19	8.8	0.09	100	100	100	100	190,000	0.532	25,000	
20	13.6	0.10	100	100	100	99	285,000	0.995	58,000	
21	7.6	0.07	100	100	100	100	320,000	0.794	43,000	
22	8.2	0.05	100	100	100	97	350,000	0.956	55,000	304,000
23	8.5	0.03	100	100	100	95	450,000	1.52	98,000	
24	8.0	0.20	100 ^b	100	100	100	83,000	0.710	36,000	116,000
25	8.4	0.19	100 ^b	100	100	96	91,000	0.478	23,000	
26 ^c	2.4	0.15	200	0	0	100	32,000	4.96	430,000	
27 ^c	5.6	0.30	150	50	50	90	37,000	1.62	105,000	
28 ^d	5.5	0.30	0	200	200	91	37,000	2.07	145,000	70,000
29 ^d	5.5	0.15	0	200	200	85	73,000	3.01	230,000	

^a \bar{M}_w , \bar{M}_v , and \bar{M}_n are kinetic, viscosity-average, and number-average molecular weight, respectively.

^b Dimethylacetamide.

^c At -55°C , gel formation.

^d The polymer precipitated.

The same results were obtained by single-stage continuous addition of acrylonitrile.

The experimental data are summarized in Table I.

Molecular Weight Determination

Intrinsic viscosities were obtained by graphical extrapolation of relative solution viscosities determined in DMF at 25°C. in a Cannon-Fenske viscometer. Number-average molecular weights were determined in DMF at 30°C. with a Stabin-Shell automatic osmometer. Typical examples of osmotic pressure-concentration plots are given in Figure 1. When the solution was prepared by using DMF as supplied, the osmotic data were very erratic, in accordance to the finding of Krigbaum and Kotliar.¹⁶ Satisfactory results were obtained by using solvent which had been fractionally distilled, followed by either deionization or vacuum distillation immediately before use. DMF purified according to the latter procedure was used for the results reported here.

RESULTS AND DISCUSSION

Homogeneous Polymerization of Acrylonitrile

Zilkha and Avny¹⁰ studied the polymerization of acrylonitrile using several electron-transfer initiators. The polymerizations, carried out in THF, were heterogeneous. Since we wish to avoid possible complexities which might arise in a heterogeneous reaction, attempts were made to carry out the polymerization in homogeneous media.

Aprotic solvents for polyacrylonitriles are limited to tertiary amides and alkyl sulfoxides. Tertiary amides are the only practical solvents for homogeneous polymerization, since sulfoxides react with the alkali metal complexes used as initiators. Although tertiary amides are also sensitive to alkali metal complexes at higher temperature, sodium biphenyl does not react with DMF below -40°C. This was demonstrated by the persistence of sodium biphenyl color for several hours at temperatures below -40°C. However, in DMF extremely fast polymerization of acrylonitrile occurred often with local gel formation. The polymer isolated from such gel was usually highly colored and only difficultly soluble in DMF, and the viscosity-average molecular weight was found to be unusually high. In ether solvents, as described by Zilkha and Avny, the polymer separated from the reaction mixture. However, in a mixture of DMF and THF (40-60, % by vol.) at low temperatures, acrylonitrile polymerized homogeneously by the electron-transfer initiator with a complete conversion of monomer to polymer. Therefore, most of the polymerizations described here were carried out in a 1:1 mixture of DMF and THF at -78°C. Also in a 1:1 mixture of dimethylacetamide (DMAc) and THF, acrylonitrile polymerized homogeneously and completely. The polymerization at higher temperatures is not desirable because of the reac-

tion between the initiator and the solvent. It was also found that the polymerization at higher temperatures resulted in lower yields as well as formation of a colored product. The effect of solvents on the intrinsic viscosity of the products is demonstrated in Table II.

TABLE II
Effect of Solvent on the Intrinsic Viscosity of Polyacrylonitrile

Solvent	Conversion, %	Intrinsic viscosity, dl./g.	Viscosity molecular weight ^a
DMF ^b	100	4.96	430,000
DMF-THF ^b (1:1)	100	0.57	27,700
THF ^b	91	1.97	134,000
DMAc-THF (1:1) ^c	96	0.71	36,000

^a Calculated from the Mark-Houwink equation for $K = 1.55 \times 10^{-4}$ and $\alpha = 0.80$.¹³ The values are given here for comparison with the kinetic molecular weight. The relation between intrinsic viscosity and molecular weight is discussed later.

^b The reaction was carried out by using 5.5 g. of acrylonitrile and 0.30 mmole of sodium biphenyl in total of 200 ml. of the solvent. The kinetic molecular weight is 37,000.

^c Acrylonitrile, 8.8 g., and 0.20 mmole of initiator were used; the kinetic molecular weight is 88,000.

Except for the solvent, the polymerization was carried out in the manner described for the preparation of "living" polystyrene of the narrowest molecular weight distribution.⁸

"Living" Polyacrylonitrile

In spite of the presence of a large number of nucleophile-sensitive nitrile groups, acrylonitrile polymerized without, or with only very slow, termination reaction under suitable reaction conditions. The formation of "living" polyacrylonitrile was demonstrated by resumption of polymerization on adding more acrylonitrile to a system in which polymerization had already stopped by the complete consumption of the monomer. This was shown in a typical reaction in which one-third of the total acrylonitrile was added to the initiator solution in DMF-THF mixture at -78°C ., and the rest was added after allowing the reaction mixture to stand at -78°C . for periods up to 2 hr. (Table III). In all cases polyacrylonitrile was obtained in quantitative yields, indicating that the polymer formed in the first stage was capable of initiating further polymerization.

The formation of "living" polyacrylonitrile suggested that the polymers should have predetermined molecular weights and a narrow molecular weight distribution, since the initiation reaction is believed to be extremely rapid. For rapid initiation by electron transfer and no termination or side reactions, the molecular weight of the polymer formed should equal the kinetic molecular weight, defined by

$$\bar{M}_k = 2M/I$$

TABLE III
 Two-Stage Polymerization of Acrylonitrile^a

Interval between two additions, hr.	Overall yield, %	Kinetic mol. wt.	Intrinsic viscosity, dl./g.	Osmotic mol. wt.
0	100	62,000	0.693	170,000
0.5	98	91,000	0.910	190,000
1	100	68,000	0.756	—
2	99	93,000	0.986	160,000

^a The reactions were carried out by using a total of 8 g. of acrylonitrile and 0.18–0.26 mmole of sodium biphenyl in 200 ml. of a 1:1 DMF-THF mixture at -78°C .

where M is the amount of the monomer in grams and I is the number of moles of initiator. Theoretically, the kinetic molecular weights should give the number-average molecular weights. However, with the expected narrow molecular weight distribution, weight-average and viscosity-average molecular weights should also equal the kinetic molecular weight. Therefore a linear relation between logarithm of kinetic molecular weight and logarithm of intrinsic viscosity is expected for living polymers. Our experimental data are shown in Figure 2. (The straight line represents the theoretical relation, $\bar{M}_k = \bar{M}_v$.)

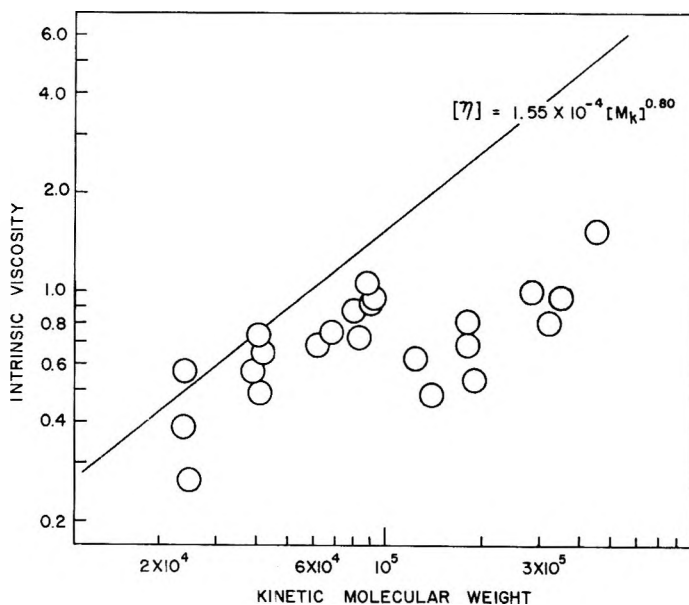


Fig. 2. Relation between the kinetic molecular weight and intrinsic viscosity of polyacrylonitrile polymerized in a 1:1 mixture of THF and DMF with sodium biphenyl initiator.

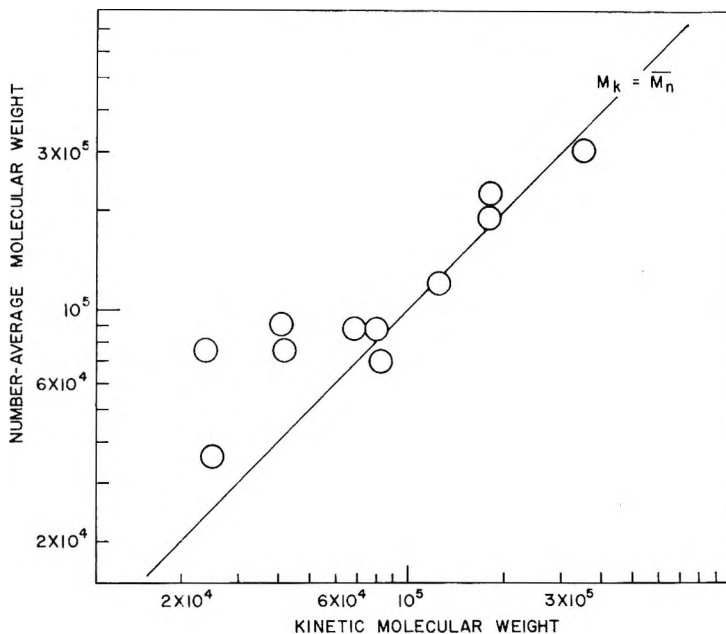


Fig. 3. Relation between the kinetic molecular weight and osmotic number-average molecular weight of polyacrylonitrile prepared by sodium biphenyl initiator.

The deviation from the predicted linear relation is quite marked. Furthermore, the observed intrinsic viscosity is always lower than that predicted from the kinetic molecular weight. Neither polydispersity of the products nor slow termination processes can explain this deviation, since under conditions of complete conversion either should give higher viscosity-average molecular weights than the predicted values. The observed negative deviation could be explained by chain transfer to the monomer, as postulated in the anionic polymerization of acrylonitrile by Zilkha and co-workers.^{16, 18} If chain transfer to monomer is mainly responsible for the low molecular weight products, the product should be polydisperse.¹⁹ In order to investigate this possibility, the number-average molecular weights of our polyacrylonitrile samples were determined osmotically.

Number-Average Molecular Weights

Figure 3 shows the relation between osmotic number-average molecular weights and the kinetic molecular weights for a series of polyacrylonitriles prepared by varying the amount of the initiator and monomer. (The straight line represents the theoretical relation, $\bar{M}_k = \bar{M}_n$.) This linear relation is surprising in view of the nonlinear relationship of intrinsic viscosity and kinetic molecular weight (Fig. 2). Furthermore, viscosity-average molecular weights calculated by the Mark-Houwink equation, using either the constants given by Cleland and Stockmayer²⁰ or Krigbaum and Kotliar,¹⁷ are invariably lower than the osmotic molecular weights of

polyacrylonitrile prepared homogeneously by electron transfer-initiation. This clearly indicates the K and α values in the Mark-Houwink equation determined for free-radical polyacrylonitrile are not applicable to anionically polymerized polyacrylonitrile. For the polymers prepared in this study the osmotic molecular weights and intrinsic viscosities correlate only poorly to give

$$[\eta] = 4.4 \times 10^{-4} \bar{M}_n^{0.62}$$

Poor correlation suggests that the polymers differ somewhat in structure from one run to the next. According to our proposed polymerization mechanism discussed later, it is not surprising that the polymer structure is sensitive to the rate of addition of acrylonitrile, the precise control of which was not maintained in the present study. Thus, there appears to be little significance in attempting the correlation of the intrinsic viscosity and kinetic molecular weight.

The linear relation between number-average molecular weights and kinetic molecular weights (Fig. 3) is further evidence supporting the formation of "living" polyacrylonitrile in homogeneous anionic polymerization at low temperatures.

Structure of Polyacrylonitrile Prepared by Electron-Transfer Initiation

Although the detailed study of structure of anionically polymerized polyacrylonitrile is beyond the scope of the present study, the osmotic molecular weights clearly indicate a structural difference between the polyacrylonitrile samples prepared by free-radical and electron-transfer initiation. Virtually identical infrared spectra were obtained for polyacrylonitrile prepared by either procedure. The only observable difference is in the weak absorption bands at 6.45, 7.04, and 7.40 μ , the first two being absent from free-radical and the latter from anionic polymer. The absence

TABLE IV
Viscosity and Osmotic Data of Polyacrylonitrile

Sample	[η], dl./g.	Molecular weight		$A_2 \times 10^4$, cm. ³ mole/g. ²
		Viscosity ^a	Osmotic	
F ^b	3.37	265,000	120,000	11.8
A-THF ^c	2.07	145,000	70,000	12.2
A-1 ^d	0.253	11,000	36,000	2.7
A-2 ^d	0.877	49,000	87,000	4.7
A-3 ^d	0.622	32,000	120,000	5.0
A-4 ^d	0.804	44,000	190,000	5.6
A-5 ^d	0.683	36,000	230,000	3.2
A-6 ^d	0.956	55,000	300,000	5.6

^a Calculated from [η] for $K = 1.55 \times 10^{-4}$ and $\alpha = 0.80$.

^b Prepared by free-radical polymerization.²⁴

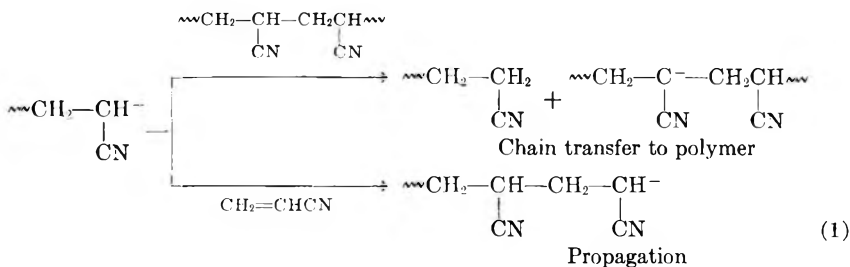
^c Prepared by anionic polymerization in THF.

^d Prepared by homogeneous anionic polymerization.

of color and of infrared absorption at 6.1–6.2 μ (conjugated carbon–nitrogen double bonds) indicates little participation of cyano groups in low-temperature homogeneous anionic polymerization, in contrast to the anionic polymerization at higher temperatures.¹²

On the basis of our finding that anionic polyacrylonitrile exhibited a lower intrinsic viscosity than free-radical polymers of same number-average molecular weight, it is proposed that the anionic polyacrylonitriles have a highly branched structure.^{21,22} Low values of the osmotic second virial coefficient of anionic polymer (Fig. 1) are also in accord with this argument.²³ Viscosity and osmotic data for a few representative polyacrylonitriles are summarized in Table IV.

The branched structure is probably the result of chain transfer process to existing polymer [eqs. (1)].



The tertiary hydrogens in polyacrylonitrile are more acidic than the α -hydrogen of acrylonitrile. Therefore, it is not surprising that in homogeneous polymerization chain transfer reaction to polymer is preferred to the chain transfer of the monomer, especially when the concentration of the monomer is kept low as in the case of our polymerization.

The very low intrinsic viscosity of anionic polyacrylonitrile for a given number-average molecular weight suggests a high degree of branching, perhaps as high as one branch for every 10 monomer units (estimated roughly from $g' = [(1 + m/7)^{1/2} + 4m/9]\pi^{-1/4}$, where g' is the ratio of the intrinsic viscosity of a branched molecule to that of a linear molecule of the same molecular weight, m is average number of branch units per molecule, and π has the usual significance),²² yet we were unable to observe significant changes in the infrared adsorption. This eliminates the possibility that the cyano group is involved in the branching reaction. The proposed mechanism finds further support in the fact that a linear relation between kinetic and viscosity-average molecular weights is observed for anionically polymerized methacrylonitrile in which the tertiary hydrogen atom is replaced by a methyl group.^{14,24}

Earlier an effect of the polymerization solvent on the intrinsic viscosity of the product was demonstrated (Table II). The data in Table IV show that the structure of the polyacrylonitrile prepared by anionic polymerization in THF is similar to that of free-radical polymers, rather than to those prepared homogeneously by electron-transfer initiation. The number-average molecular weight of the anionic polymer prepared in THF

agrees with the kinetic molecular weight (70,000 vs. 37,000), while the viscosity-average molecular weight is much higher than that of corresponding anionic polymer prepared under homogeneous conditions (Table II). Apparently the heterogeneous reaction broadens the molecular weight distribution, and it appears to make chain branching more difficult, as suggested by the higher value of the second virial coefficient, A_2 , for this polymer.

The author wishes to thank Prof. W. R. Krigbaum of Duke University, Prof. W. H. Stockmayer of Dartmouth College, and Dr. W. P. Baker, Jr., of Film Department, E. I. du Pont de Nemours & Company, for their information and helpful discussions.

References

1. Szwarc, M., *Makromol. Chem.*, **35**, 132 (1960).
2. Mulvaney, J. E., C. G. Overberger, and A. M. Schiller, *Fortschr. Hochpolymer-Forsch.*, **3**, 106 (1961).
3. Szwarc, M., in *Advances in Chemistry Series; Polymerization and Copolymerization Processes*, American Chemical Society, Washington, D. C., **1962**, pp. 96-110.
4. Szwarc, M., M. Levy, and R. Milkovitch, *J. Am. Chem. Soc.*, **78**, 2656 (1957).
5. Szwarc, M., R. Waack, A. Rembaum, and J. D. Coombes, *J. Am. Chem. Soc.*, **79**, 2026 (1957).
6. Gold, L., *J. Chem. Phys.*, **28**, 91 (1958).
7. Szwarc, M., and A. Rembaum, *J. Polymer Sci.*, **22**, 189 (1956).
8. Wenger, F., *Chem. Ind. (London)*, **1959**, 1094.
9. Graham, R. K., D. L. Dunkelberger, and E. S. Cohen, *J. Polymer Sci.*, **42**, 501 (1960).
10. Zilkha, A., and Y. Avny, *J. Polymer Sci.*, **A1**, 547 (1963).
11. Ottolenghi, A., S. Barzakay, and A. Zilkha, *J. Polymer Sci.*, **A1**, 3643 (1963).
12. Claes, P., and G. Smets, *Makromol. Chem.*, **44-46**, 212 (1961).
13. Ottolenghi, A., and A. Zilkha, *J. Polymer Sci.*, **A1**, 687 (1963).
14. Graham, R. K., J. R. Panchok, and M. J. Kampf, *J. Polymer Sci.*, **44**, 411 (1960).
15. Morton, M., R. Milkovitch, D. B. McIntyre, and L. J. Bradley, *J. Polymer Sci.*, **A1**, 443 (1963).
16. Wenger, F., *Makromol. Chem.*, **36**, 200 (1960).
17. Krigbaum, W. R., and A. M. Kotliar, *J. Polymer Sci.*, **32**, 323 (1958).
18. Zilkha, A., B.-A. Feit, and M. Frankel, *J. Polymer Sci.*, **49**, 231 (1961).
19. Litt, M., and M. Szwarc, *J. Polymer Sci.*, **42**, 159 (1960).
20. Cleland, R. L., and W. H. Stockmayer, *J. Polymer Sci.*, **17**, 473 (1955).
21. Thurmond, C. D., and B. H. Zimm, *J. Polymer Sci.*, **8**, 477 (1952).
22. Zimm, B. H., and R. W. Kilb, *J. Polymer Sci.*, **37**, 19 (1959).
23. Krigbaum, W. R., and Q. A. Trementozzi, *J. Polymer Sci.*, **28**, 295 (1958).
24. Sorenson, W. R., and T. W. Campbell, *Preparative Methods of Polymer Chemistry*, Interscience, New York, 1961, pp. 168-169.
25. Overberger, C. G., E. M. Pearce, and N. Mayes, *J. Polymer Sci.*, **34**, 109 (1959).

Résumé

On a étudié la polymérisation homogène de l'acrylonitrile initiée par transfert électronique. Dans un système rigoureusement purifié et à basse température, on démontre qu'il se forme du polyacrylonitrile "vivant" et que son poids moléculaire peut être prédéterminé. Le poids moléculaire moyen en nombre du polyacrylonitrile "vivant" est donné approximativement par $2M/I$, où M représente les grammes de monomère et I le nombre de moles d'initiateur. Pour du polyacrylonitrile préparé par polymérisation anionique homogène, initiée par transfert électronique, on a trouvé que le

poids moléculaire viscosimétrique, calculé à partir des valeurs conventionnelles de K et de α dans l'équation de Mark-Houwink, est beaucoup plus petit que le poids moléculaire moyen en nombre obtenu par osmose. Cela indique clairement une différence de structure entre le polyacrylonitrile obtenu par polymérisation radicalaire et anionique; le polyacrylonitrile anionique semble posséder une structure fortement ramifiée provoquée par un processus de transfert de chaîne sur le polymère.

Zusammenfassung

Die homogene Acrylnitrilpolymerisation bei Anregung mit Elektronenübertragerstartern wird untersucht. In einem extrem gereinigten System wird bei niedrigen Temperaturen "living" Polyacrylnitril gebildet und sein Molekulargewicht kann vorausbestimmt werden. Das Zahlenmittelmolekulargewicht von "living" Acrylnitril ist angenähert durch $2M/I$ gegeben, wo M die Gramm von Monomerem angibt und I die Anzahl Initiator-mole. Bei Darstellung von Polyacrylnitril in einer homogenen anionischen Polymerisation mit einem Elektronenübertragungsstarter erweist sich das mit den üblichen K - und α -Werten der Mark-Houwink-Gleichung berechnete Molekulargewicht des Polyacrylnitril als beträchtlich kleiner als das osmometrische Zahlenmittelmolekulargewicht. Dies bildet einen klaren Hinweis auf einen Strukturunterschied zwischen dem radikalischen und dem anionischen Polyacrylnitril; das anionische Polyacrylnitril scheint eine hochgradig verzweigte, durch Kettenübertragung zum Polymeren gebildete Struktur zu besitzen.

Received October 1, 1964

Revised January 28, 1965

Prod. No. 4660A

Copolymerization Studies. VI. Spontaneous Copolymerization of Bicyclo[2.2.1]hept-2-ene and Sulfur Dioxide. Evidence for Propagation by Biradical Coupling*

N. L. ZUTTY, C. W. WILSON, III, G. H. POTTER, D. C. PRIEST, and C. J. WHITWORTH, *Union Carbide Corporation, Plastics Division, Research and Development Department, South Charleston, West Virginia*

Synopsis

The alternating copolymerization of bicyclo[2.2.1]hept-2-ene and sulfur dioxide has been found to be quite unusual for a free-radical polymerization: (1) the initiation of copolymerization is spontaneous, even at -40°C .; (2) solution copolymerization is extremely fast, yielding very high molecular weight polymer within a few seconds; (3) conversions are high (up to 93% within a minute); (4) molecular weight during copolymerization increases at essentially constant conversion; (5) the reaction is incapable of being chemically inhibited indefinitely, short of exhausting one of the constituent monomers; (6) at elevated temperatures, the monomers and copolymer appear to be in equilibrium; (7) large concentrations of free radicals have been detected by electron paramagnetic resonance to be associated with the bulk copolymerization; and (8) the copolymerization appears to result in "living" free-radical polymers. A copolymerization mechanism is proposed to explain these observations. Bicycloheptene and sulfur dioxide initially form a 1:1 molecular charge transfer complex which rearranges to a biradical; subsequent coupling of biradicals with each other (and possibly also with the molecular complexes themselves) leads to rapid propagation to high molecular weight, alternating copolymer. Speculations that similar mechanisms may be important in other copolymerization reactions are also made.

INTRODUCTION

While investigating the polymerization of compounds containing the bicyclo[2.2.1]heptane nucleus,² an experiment carried out by Caldwell and Hill^{3,4} was repeated, in which it was reported that bicycloheptene and sulfur dioxide formed an alternating copolymer initiated by a free-radical catalyst within several hours.

Surprisingly, upon mixing a toluene solution of pure bicycloheptene with liquid sulfur dioxide at -20°C . in the absence of initiator, rapid reaction occurred which almost instantly led to high yields of a white solid. By solution viscosity and elemental analyses, the solid was found to be a high molecular weight copolymer containing equimolar amounts of sulfur dioxide

* For a preliminary report on this work see Zutty and Wilson.¹

and bicycloheptene. Repeating this experiment in the absence of toluene, *in vacuo*, led to the same results.

Preliminary experiments also showed the reaction apparently unaffected by water, hydrogen chloride, and free-radical initiators; however, addition of hydroquinone led to induction periods followed again by vigorous reaction and yielded polymer of somewhat lower molecular weight than that formed in the absence of inhibitor. Copolymers containing equimolar comonomer concentrations were obtained for monomer ratios throughout the range from 1:9 to 9:1. Copolymerization was also found to proceed in precisely the same manner in the dark.

The literature describes several polymolecular, spontaneous, radical-forming processes which occur at relatively low temperature. The thermal polymerization of styrene is thought to involve a termolecular reaction leading to free radicals.⁵ Bartlett and co-workers^{6,7} have shown that the 1,2-addition of chlorotrifluoroethylene to dienes involves the intermediate formation of biradicals, and Poutsma⁸ postulates that the chlorination of cyclohexene at low temperatures is a polymolecular, spontaneous, radical-forming process. The mechanism for the spontaneous copolymerization of perfluoronitrosomethane and tetrafluoroethylene at -30°C . also indicates a similar process.⁹

RESULTS AND DISCUSSION

Proof that the reaction of bicyclo[2.2.1]hept-2-ene and sulfur dioxide was not a kinetically "normal" free-radical copolymerization came from the following simple set of experiments. Identical reactions were set up whereby, under nitrogen, equal weights of bicycloheptene and sulfur dioxide at a total concentration of 15 wt.-% in cyclohexanone were allowed to polymerize at 0°C . for varying lengths of time, after which the reaction was stopped by flooding with hydroquinone dissolved in cyclohexanone. Time zero was taken at the addition of liquid sulfur dioxide to the olefin-cyclohexanone solution, and the reaction time was the time elapsed at the addition of the hydroquinone.

The data obtained from these experiments (open circles) are shown in Figure 1. It can be seen that, after 10 sec. of reaction, polymer having a reduced viscosity of about 0.3 is formed, and conversion to polymer is around 65%. After about 40 sec. the copolymer reduced viscosity is 1.8, but conversion has remained essentially constant. After about 1 min. both reduced viscosity (about 2.0) and conversion remain constant. Several experiments were also carried out at equimolar concentrations of reactants (Fig. 1, closed circles). Essentially the same results were obtained although conversions to polymer were higher.

The copolymer density at 23°C . was 1.263. Ultracentrifuge experiments* showed that a copolymer reduced viscosity of 1.09 corresponds to a weight-average molecular weight of about 2.2×10^6 .

* We are indebted to Dr. J. A. Faucher for these measurements.

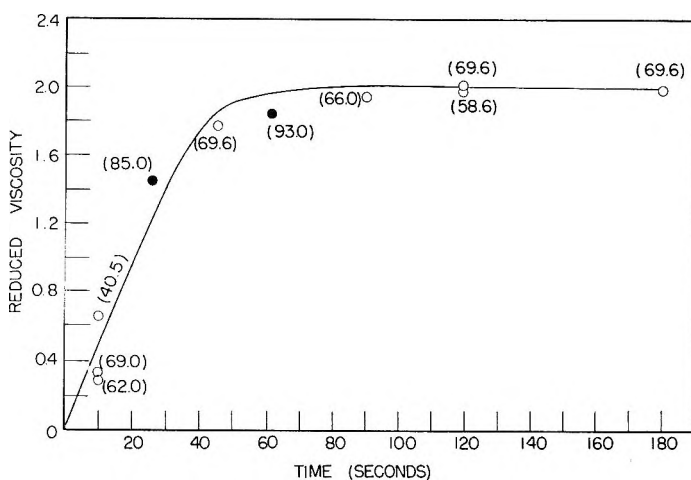
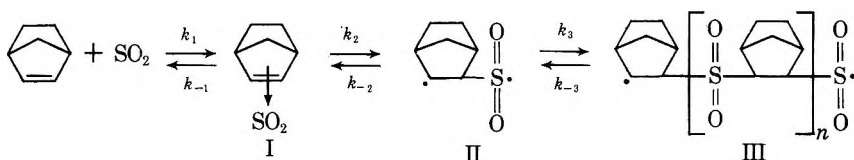


Fig. 1. Solution copolymerization of bicyclo[2.2.1] hept-2-ene and sulfur dioxide at 0°C.; (O) equal weight concentrations of monomers; (●) equimolar concentrations. All solutions were 15% by weight of reactants in cyclohexanone. Figures in parentheses by data points give per cent conversion to copolymer.

The results of these experiments (increasing molecular weights with time at constant, high conversions) are, of course, contrary to those obtained during conventional, free-radical polymerizations (where molecular weights remain essentially constant and conversions increase with time) and are analogous to reactions of bifunctional species, such as in condensation polymerizations.

These data led to the postulation of a mechanism for the reaction which involves initially the formation of a complex between reactants (I), followed by rearrangement of this complex to a biradical (II), and propagation to copolymer (III) by condensation of biradicals.



The copolymerization behavior outlined above is consistent with the proposed mechanism.

Inherent in this mechanism are the facts that few, if any, termination reactions leading to "inactive" polymer chains can occur. Of the usual termination reactions, radical coupling is the same as propagation, while disproportionation could regenerate monomers which would spontaneously repolymerize. The strain energy liberated upon conversion of bicyclo[2.2.1]hept-2-ene to the substituted bicyclo[2.2.1]heptane would also make the reverse reaction difficult at the low polymerization temperature. Therefore, molecular weights are limited only by diffusion.

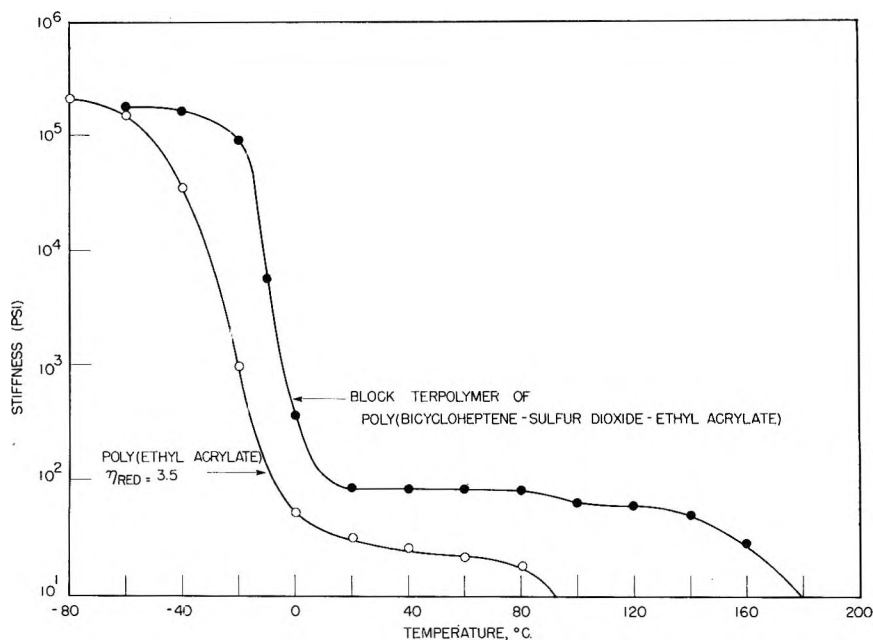


Fig. 2. Stiffness-temperature comparison of (O) ordinary poly(ethyl acrylate), with (●) a presumed block terpolymer (84 mole-% of ethyl acrylate, 8 mole-% each of bicycloheptene and sulfur dioxide). Both resins had 3.5 reduced viscosities.

That "living" free-radical ends are present and termination is unlikely is supported by the electron paramagnetic resonance (EPR) data below. However, it is also supported by experiments whereby polymerizing bicycloheptene-sulfur dioxide solutions are added to ethyl acrylate at room temperature. When this is done, immediate and normal polymerization of the ethyl acrylate takes place and leads to polymers whose properties are indicative of block polymers containing long segments of predominantly alternatingly copolymerized bicycloheptene-sulfur dioxide, followed by long segments of predominantly poly(ethyl acrylate). Thus, if 0.05 mole of bicycloheptene and 0.05 mole of sulfur dioxide, in cyclohexanone at 0°C., are allowed to polymerize for a minute or so and added to 0.9 mole of ethyl acrylate and the reaction allowed to proceed for 30 min. at room temperature, about 50% of the ethyl acrylate is consumed, leading to resin of reduced viscosity 3.48. This resin was transparent when molded, in contradistinction to mixtures of the component resins. The stiffness-temperature curve for this polymer, shown in Figure 2, indicates the multiple transition behavior normally associated with block polymers. The resin analyzed for 8 mole-% each of bicycloheptene and sulfur dioxide and 84 mole-% of ethyl acrylate. For comparison purposes, the stiffness-temperature curve for poly(ethyl acrylate) of 3.5 reduced viscosity is also shown in Figure 2. The glass transition of the bicycloheptene-sulfur dioxide copolymer is 285°C.^{3,4} It should be noted that the results of this type of experiment

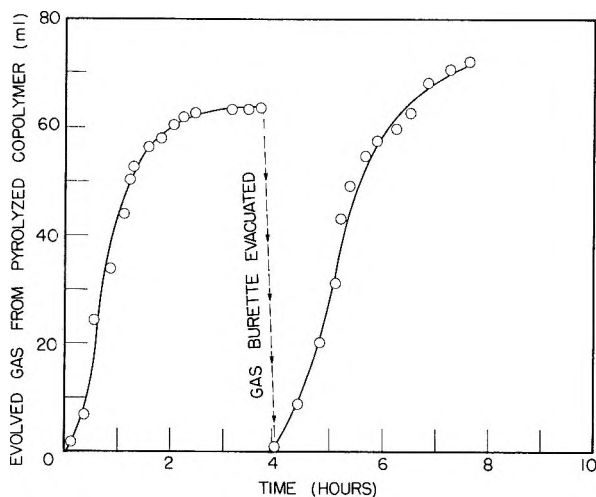


Fig. 3. Evolution of gas with time during pyrolysis of bicycloheptene-sulfur dioxide copolymer at 150°C. Gas buret at room temperature connected to pyrolysis tube was evacuated after about 4 hr.

could only be reproduced about 50% of the time, and the transition temperatures in the resulting block polymers were variable. It is believed that this is because the bicycloheptene-sulfur dioxide copolymerization is too rapid to allow ready control of "block" length and hence transition temperatures. Neither bicycloheptene nor sulfur dioxide alone polymerized ethyl acrylate.

The pyrolysis of bicycloheptene-sulfur dioxide copolymers also supports the proposed polymerization mechanism. Thus, if in a closed system at atmospheric pressure, under nitrogen, a freshly prepared bicycloheptene-sulfur dioxide copolymer of reduced viscosity 1.87, is pyrolyzed at 150°C. for 7 hr., 33% of the resin is lost from the pyrolysis flask, the reduced viscosity of the remaining copolymer being then 1.03. The resin, after pyrolysis, remained white, opposed to propylene-sulfur dioxide copolymers which blackened under the same conditions. These data are indicative of degradation occurring from the ends of the copolymer chain, since the reduced viscosity, after pyrolysis, was not low enough to predict random chain scission. Mass spectra showed the gases evolved during pyrolysis to be entirely bicycloheptene and sulfur dioxide, but quantitative estimates of their amounts were precluded, since considerable repolymerization of the gaseous pyrolysis products occurred in the gas buret, which was kept at room temperature. The behavior of the pressure of the system during pyrolysis indicated the monomers (and/or biradicals) and copolymer were in equilibrium. Figure 3 shows the effects of pyrolyzing the resin at 150°C. The reaction is apparently near completion after 4 hr.; however, if at this time, the gases in the gas buret are removed from the system and the pyrolysis continued, gases are again evolved at roughly the same rate as that at the start of the experiment.

Experiments designed to produce biradicals in the vapor phase which would condense upon polymerizing were unsuccessful. When gaseous bicycloheptene and gaseous sulfur dioxide were brought together in a closed chamber no polymerization (as would have been noticed by a decrease in the pressure of the system) occurred (Table I).

TABLE I
Attempted Vapor-Phase Copolymerization of Bicyclo[2.2.1]hept-2-ene
and Sulfur Dioxide

Concentration of monomers ^a in vapor phase, mole $\times 10^3$		Temperature, °C.
Bicycloheptene	Sulfur dioxide	
1.6	2.3	25
1.8	3.0	70
2.0	4.5	100

^a Monomers assumed to be perfect gases.

Although these experiments did not allow the formation of biradicals or polymers, it was noticed that if the bicycloheptene were present, in the system, in the solid or liquid phase (m.p. 44.5°C., sealed tube) polymerization occurred immediately upon the addition of the gaseous sulfur dioxide.

If the biradical-coupling propagation mechanism is correct, it might be expected that large concentrations of free radicals (structures II and III) would accompany the copolymerization. Accordingly, EPR studies of the reaction were undertaken. Temperature equipment being unavailable all measurements were carried out at room temperature. Initially solutions of bicycloheptene and sulfur dioxide were made in toluene or cyclohexanone at -80°C ., placed in EPR sample tubes, sealed under nitrogen, and warmed to room temperature before placing in the EPR spectrometer, a process which took 2-3 min. In the time required to warm these tubes to room temperature, polymerization occurred and appeared complete prior to the first measurement. Hence, in the case of solution copolymerization no free-radical EPR signal could be observed, indicating that radical concentrations less than about $10^{-7}M$ were present or that radical lifetimes were so short that the EPR signal was so broadened as to be undetectable, or both. In light of the extreme rapidity of copolymerization these results were not surprising.

In the next experiments bicycloheptene was melted into the EPR sample tube, the tube cooled to -80°C ., liquid sulfur dioxide injected on to the surface of the bicycloheptene, and the tube sealed under nitrogen. If such sample tubes were allowed to remain at room temperature a solid, clear layer (copolymer) was observed to grow between the bicycloheptene and sulfur dioxide layers. The surfaces of this copolymer layer were not smooth so that its rate of growth could not be studied accurately. If, however, these sample tubes were inverted at -80°C ., so that only sulfur dioxide

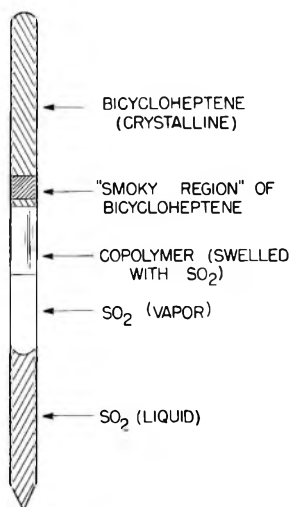


Fig. 4. Drawing of typical glass sample tube, in inverted position, of bulk copolymerizing bicycloheptene-sulfur dioxide, after several days of reaction at room temperature. Tube dimensions: 5 mm. o.d., 180 mm. long. Smoky region of solid bicycloheptene phase contains substantial free-radical concentration.

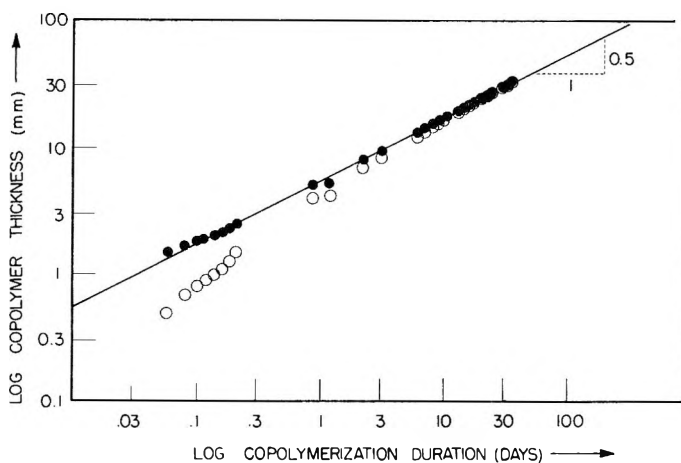


Fig. 5. Room temperature growth of (visible) copolymer layer thickness with time for bulk copolymerizing bicycloheptene-sulfur dioxide: (O) observed thickness; (●) modified data (see text). Copolymer grows approximately with the square root of time.

vapor was in contact with the solid bicycloheptene when warmed to room temperature, the growing copolymer phase was observed to have smooth surfaces at both ends. Figure 4 shows this type of sample orientation. (Further explanation of Fig. 4 is given below.)

One such inverted tube was photographed over a period of 35 days. The length of the clear polymer section formed as a function of time is presented in Figure 5 (open circles). The theoretically predicted behavior that the polymer thickness should increase with the square root of the time

after initiation, if the growth-limiting step is random diffusion of monomer (through previously formed polymer) to the opposite polymer-monomer interface, is shown as a dashed line of slope $1/2$ in this figure. The divergence of observation from theory at short times can be accounted for by the inexact location of the polymer-bicycloheptene boundary; if it is considered that there is a transition region, part polymer and part bicycloheptene, of about 1.0 mm. mean thickness, and this is added to the measured length of the clear polymer section, then the experimental data, thus corrected, fall along the dashed line of slope $1/2$ shown in Figure 5 (closed circles).

Two additional observations were made on a series of samples. First, by breaking the sealed tubes, it was found that the copolymer was swelled by sulfur dioxide. When the sulfur dioxide evaporated, a hard, brittle copolymer of high molecular weight (reduced viscosity around 3.6) remained, indicating that polymer growth consisted predominantly of diffusion of sulfur dioxide through the copolymer phase to the bicycloheptene-polymer interface. The illusion that the copolymer phase is growing almost equally in both directions was due to the fact that the copolymer phase plasticized with sulfur dioxide can be extruded as necessary in the direction of the liquid sulfur dioxide phase as new copolymer is formed at the polymer-bicycloheptene boundary. Second, in support of this observation, small chips of poly(tetrafluoroethylene) (density, 2.2) when placed at the bicycloheptene-sulfur dioxide boundary at -80°C . prior to warming, were found to move along with the polymer surface toward the sulfur dioxide phase during copolymerization. Thus, it seems certain that the polymer-sulfur dioxide boundary is not an active site of polymerization, and that practically all copolymerization occurs in the region of the polymer-bicycloheptene interface.

Upon scanning the entire sample tube it was only near this copolymer-bicycloheptene interface that concentrations of free radicals could be detected by EPR. The operating procedure for making EPR measurements was to place the samples in the spectrometer after warming from Dry Ice to room temperature (1-2 min.). The 5 mm. O.D. Pyrex sample tubes were made in three forms—straight, L-shaped, or U-shaped—so that it was optional whether sulfur dioxide vapor or liquid was in contact with the solid bicycloheptene. Neither bicycloheptene nor sulfur dioxide alone gave rise to detectable EPR signals; during the bulk copolymerization, no EPR signals could be measured in the liquid sulfur dioxide phase.

In the preliminary report of this work,¹ the precise location of the free radicals was in doubt; specifically, it was unknown whether the free radicals existed in the copolymer phase, or at the visible copolymer-bicycloheptene interface, or still further ahead in the bicycloheptene phase. By following the process with EPR for several months, the question of radical location has now been settled: No radicals can be detected either in the sulfur dioxide-swelled copolymer region or at the visible interface between copolymer and bicycloheptene; instead, all measurable radicals exist, quite

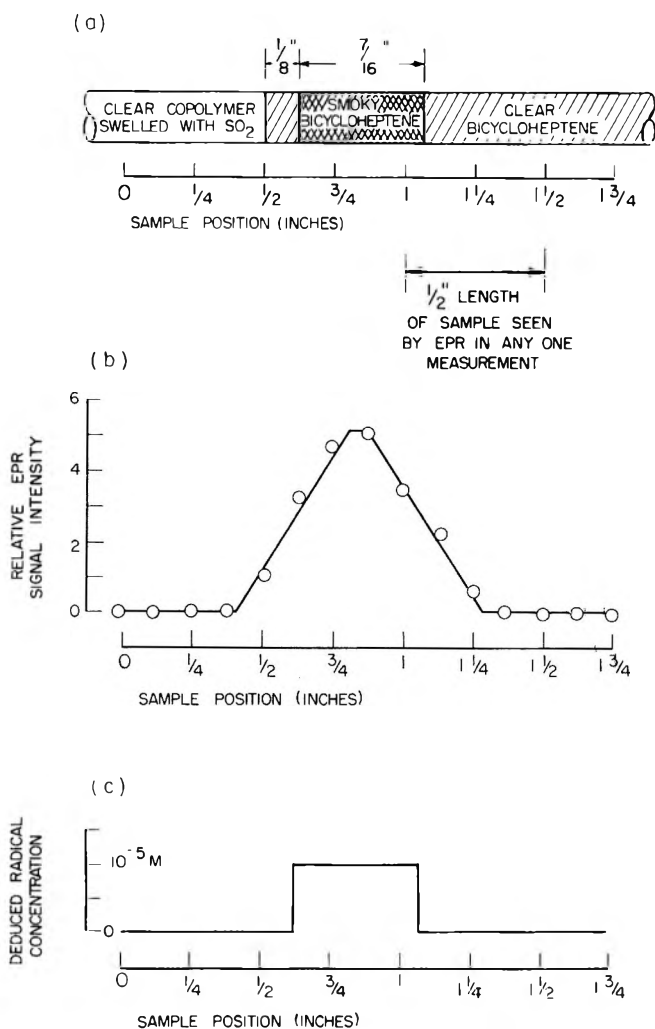


Fig. 6. EPR experiment showing that free radicals observed during the bulk copolymerization of bicycloheptene and sulfur dioxide reside in measurable concentrations only in the smoky-appearing regions of crystalline bicycloheptene: (a) EPR sample tube; (b) observed EPR signal intensity along tube; (c) deduced free-radical concentration along tube.

stably and in uniform concentrations of roughly $10^{-5}M$, throughout a "smoky" region of the bicycloheptene phase that may be 0.7–1.1 cm. in length and that may remain 0.1–0.3 cm. ahead of the advancing copolymer–bicycloheptene visible interface. The detailed situation found in one illustrative sample is shown in Figures 4 and 6. Figure 4 is a schematic representation of the sample tube in an inverted position so that only SO_2 vapor can contact the bicycloheptene or copolymer phases. The so-called smoky region of the bicycloheptene phase where radicals are found is indicated in this sketch. Figure 6 illustrates the variation of EPR signal

intensity across the sample; to understand this figure note that our EPR spectrometer effectively measures all radicals occurring over a length of about 1.3 cm. of sample tube, so that while high geometric resolution is impossible, localization of radicals in a region smaller than this length can be deduced simply from the measurements.

It is evident from these measurements that sulfur dioxide is diffusing into the crystalline bicycloheptene phase to form biradicals with bicycloheptene, which then become immobilized in the crystalline matrix. As further sulfur dioxide molecules diffuse into the smoky region, they become trapped—apparently preferentially near existing biradical sites, since the total radical concentration remains so nearly uniform throughout this region—and added to a copolymerizing radical chain in what amounts to a solid-state copolymerization, under these conditions. Eventually, this originally crystalline bicycloheptene region becomes predominantly copolymer swelled by further sulfur dioxide infusion, and the bulk copolymerization in this region becomes complete as long as biradical chains add links or couple together during the diffusional freedom accorded them in the plasticized copolymer phase.

One sample tube was prepared containing a small amount of sulfur dioxide and a large molar excess of bicycloheptene. It was warmed to room temperature in darkness, and has remained thus for more than 15 months, except for visual and EPR examination. Liquid sulfur dioxide was never permitted to contact the solid bicycloheptene or copolymer phases. Copolymerization began immediately, and in several weeks, no liquid sulfur dioxide remained; copolymer swollen with sulfur dioxide adjoined the bicycloheptene phase in which the usual smoky region appeared. Over the months, the smokiness diffused uniformly throughout the entire bicycloheptene phase, and eventually the copolymer portion of the tube assumed a shrivelled appearance, indicating that its excess sulfur dioxide plasticizer had been depleted. EPR measurements show a nearly uniform, $10^{-5}M$ concentration of free radicals throughout the entire length (over 6 cm.) of the crystalline bicycloheptene region.

The growth in the intensity of free radicals measured by EPR in the $1/2$ -in. layer of solid bicycloheptene adjacent to, and including, the copolymer-bicycloheptene interface is shown in Figure 7, for the first several hours of the bulk copolymerization at room temperature. Only one type of EPR signal line shape has ever been observed, regardless of the time or the sample position of the observation. This line shape is shown in Figure 8. It was previously uncertain¹ whether this line shape was attributable to one type of radical (exhibiting g -anisotropy¹⁰) or to the two species of radicals ($-\text{SO}_2\cdot$ and $-\text{BCH}\cdot$) having slightly different g values. It is now believed that EPR is detecting only a single radical species. Since the radicals are found to exist only in the crystalline bicycloheptene phase, restricted radical mobility is to be expected, and g anisotropy is a consequence. The line shape indicates that the observed radical has axial symmetry, with $g_{\perp} = 2.0030$ and $g_{\parallel} = 2.0124$. Both the line width and

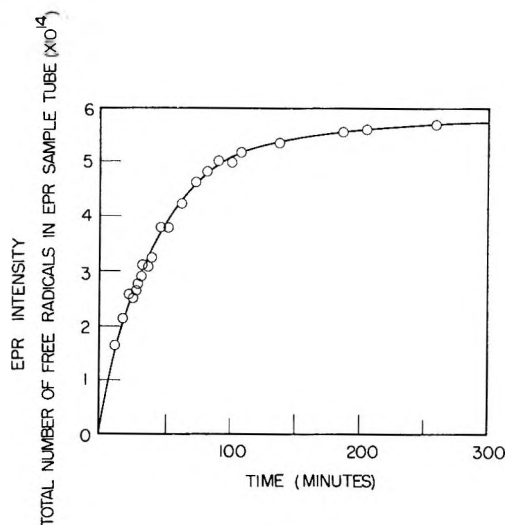


Fig. 7. Growth of EPR signal intensity with time for bulk copolymerizing bicycloheptene-sulfur dioxide, during early stages, for the $\frac{1}{2}$ -in. long section of the bicycloheptene phase including the copolymer-bicycloheptene interface.

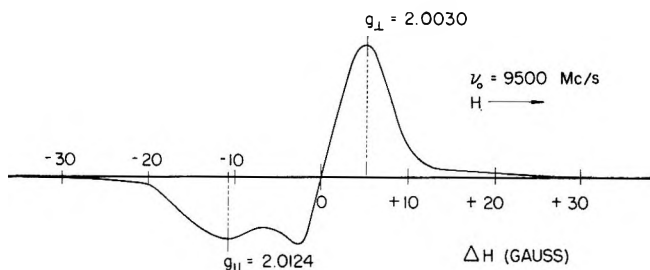


Fig. 8. Line shape derivative of EPR signal from crystalline bicycloheptene phase during bulk copolymerization of bicycloheptene and sulfur dioxide.

the line shape reflect no large hyperfine or dipolar splitting by intramolecular protons. Thus, it appears that the signal detected by EPR arises exclusively from free radicals of the type, $-\text{SO}_2\cdot$. At this point, it is still not clear whether the reason we detect only the $-\text{SO}_2\cdot$, but not the $-\text{BCH}\cdot$ radical also, is because the latter is too broad, diffuse, and complex to be measured by our present EPR spectrometer, or because in fact there is a tendency for the $-\text{BCH}\cdot$ radicals to add a single molecule of SO_2 and thus to assume preferentially the more stable $-\text{SO}_2\cdot$ configuration. Since it is expected that growing polymer chains terminating on both ends with $-\text{SO}_2\cdot$ would have a lower energy of formation than ones with $-\text{BCH}\cdot$ on both ends, this argues in favor at least of a preponderance of the $-\text{SO}_2\cdot$ structure.

From *a priori* considerations, it is not surprising that one radical species predominates in this type of diffusion-controlled experiment if it is recalled

(Fig. 1) that experiments at equimolar monomer ratios led to higher conversion of copolymer than those at equal weight ratios where sulfur dioxide is in stoichiometric excess.

EPR measurements on bicycloheptene and sulfur dioxide polymerizing in solution at lower temperatures, where the reaction might be slower, are needed to resolve these points.

In any event, these EPR experiments lend support to the spontaneously initiated biradical-coupling mechanism by showing that high concentrations of free radicals (perhaps biradicals) do, indeed, exist during the copolymerization of bicycloheptene and sulfur dioxide.

If the proposed mechanism is correct, it should be impossible to inhibit the reaction permanently, short of exhausting one of the monomers. Thus, experiments were carried out whereby the effect of inhibitors on the reaction of bicycloheptene and sulfur dioxide was observed.

The inhibitors used were: 2-*tert*-butyl-4-methoxy-phenol (BMP), monoethylether of hydroquinone (MEEHQ), and 2,2-diphenyl-1-picrylhydrazyl (DPPH). Each was found effective in delaying the onset of polymerization when used in quantities of 2% or more by weight of bicycloheptene; with 1% or less inhibitor concentration (which in most radical chain reactions is quite a massive concentration) no visual inhibition was noted.

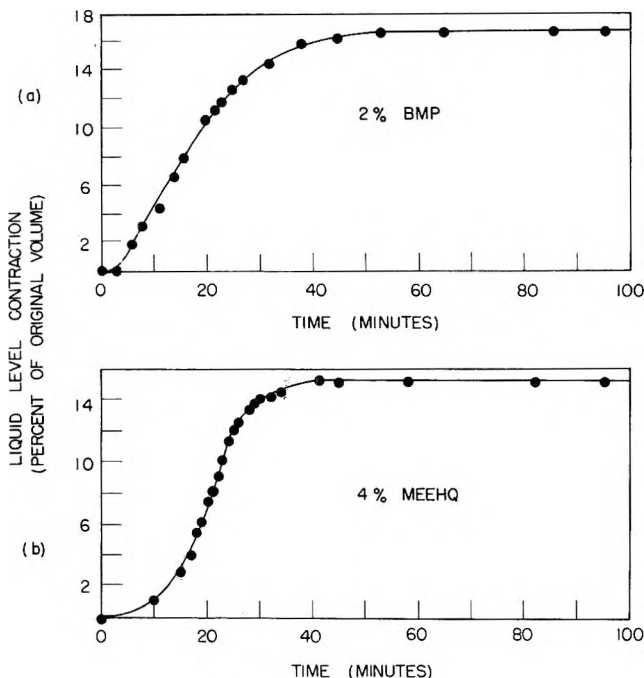


Fig. 9. Volumetric contraction at room temperature vs. copolymerization reaction time for two liquid systems of bicycloheptene-sulfur dioxide-benzene containing inhibitors: (a) inhibitor: 2% by weight of 2-*tert*-butyl-4-methoxy-phenol (BMP); (b) inhibitor: 4% by weight of monoethyl ether of hydroquinone (MEEHQ).

These studies were carried out in EPR sample tubes in the absence of oxygen. It was found that a 3:1 (v/v) bicycloheptene-benzene mixture would remain liquid at room temperature, and this composition was used throughout. The inhibitor was placed in this phase. After loading the bicycloheptene-containing phase in the sample tubes, they were frozen in Dry Ice, and the sulfur dioxide was injected as a top layer. Polymerization was initiated by warming the samples to room temperature. After warming, the samples were shaken vigorously to produce a uniform sample mixture.

The course of the reactions could be followed by the liquid level in the sample tubes, as well as by quickly inverting the tubes to check qualitatively on the sample viscosity. Volumetric contractions during the copolymerization amounted to 15 to 20% over the course of the reaction in the samples studied. Figures 9a and 9b illustrate the results of following the copolymerization by measuring liquid levels in the tubes at various times when 2% BMP and 4% MEEHQ, respectively, are used as inhibitors. DPPH gave qualitatively quite similar results, although comparable quantitative results were not recorded.

The addition of more inhibitor retards both the onset of copolymerization and the time to complete the copolymerization reaction. In an extreme case, when 10% MEEHQ was added per unit amount of bicycloheptene, more than 12 hr. was required before the solution became too viscous to flow by inverting the sample tube; however, even in this case, reasonably high polymer was eventually formed.

Electron paramagnetic resonance scans were made on these same or duplicate samples, with the use of all three inhibitors (BMP, MEEHQ, and DPPH). No EPR signals were ever seen in the solutions inhibited by BMP or MEEHQ. In the case of DPPH-inhibited solutions, EPR signals arising from DPPH could be measured to diminish in intensity with time, qualitatively as expected.

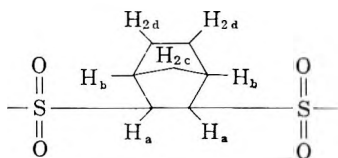
TABLE II
Elemental Analyses and Reduced Viscosities for Several Inhibited Solution
Copolymerizations of Bicyclo[2.2.1]hept-2-ene and Sulfur Dioxide

Copolymer	Elemental analysis			Reduced viscosity
	C, %	H, %	S, %	
Theoretical copolymer structure, $\text{+C}_7\text{H}_{10}\text{-SO}_2\text{+}_n$	53.14	6.37	20.27	(>1)
Copolymer obtained in presence of inhibitors				
2% MEEHQ/unit wt. bicycloheptene	55.39	6.59	19.54	0.42
{ 2% MEEHQ/unit wt. bicycloheptene O ₂ bubbled through bicycloheptene phase prior to freezing	51.23	6.26	19.86	0.42
2% MEEHQ/unit wt. bicycloheptene	52.69	6.55	19.22	0.38
4% MEEHQ/unit wt. bicycloheptene	51.98	6.22	19.53	0.34
2% BMP/unit wt. bicycloheptene	49.20	6.15	18.35	0.26
2% DPPH/unit wt. bicycloheptene	54.59	6.62	18.88	0.31

Reduced viscosities and elemental analyses for several samples prepared with BMP, MEEHQ, and DPPH as inhibitors are shown in Table II. It thus is clear that even when enormous quantities of inhibitor are added to benzene solutions at room temperature containing bicycloheptene and sulfur dioxide, alternating polymer of high molecular weight is formed. Inhibitors delay the onset of such solution copolymerizations, but when consumed by reaction with the bicycloheptene-sulfur dioxide radicals, the copolymerization proceeds spontaneously to high polymer, as dictated by the proposed mechanism.

Preliminary high-resolution proton NMR spectra are in agreement with structure III, and assignments of major peaks of the proton NMR spectrum are presented in Table III.

TABLE III
High-Resolution Proton NMR Chemical Shifts and Integrated Intensities for
Bicycloheptene-Sulfur Dioxide Copolymer



Protons	Chemical shifts τ , ppm ^a	Line widths, cycles/sec. ^b	Integrated relative spectral intensities (approx.)
H _a	5.93	35	2
H _b	7.07	15	2
H _c , H _d	8.37	45	6

^a Measured at room temperature with a 15% solution of copolymer in CDCl₃, using 1% tetramethylsilane as internal reference. Positions of the maxima of the broad, unresolved peaks are listed.

^b Width at half-height of the broad, poorly resolved peaks. In no case could spin-spin coupling be observed.

CONCLUSIONS AND SPECULATIONS

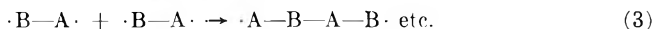
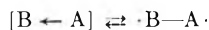
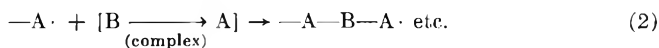
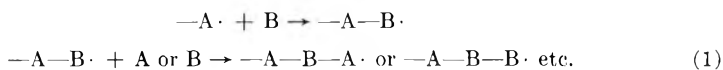
It is clear from the above experiments that the copolymerization of bicycloheptene and sulfur dioxide is unusual in many respects. Unique are the facts that: (1) at relatively low temperatures initiation of copolymerization is spontaneous; (2) the reaction is probably the fastest free-radical polymerization known, high molecular weight copolymer being formed very rapidly; (3) very high conversions invariably accompany these very rapid copolymerizations; (4) during the copolymerization, copolymer molecular weight increases at constant conversion, in sharp contrast to conventional vinyl polymerizations where conversion increases at approximately constant molecular weight; (5) the reaction leads to "living" free-

radical polymers, incapable of termination; (6) large concentrations of free radicals are associated with the copolymerization; (7) the reaction is incapable of being chemically inhibited indefinitely, short of exhausting one of the component comonomers; (8) at elevated temperatures the monomers and copolymer are in equilibrium.

The proposed mechanism, as well as the evidence described above, certainly does not clearly indicate the relative importance of each step toward the formation of final product. It is not impossible that the coupling of biradicals is not solely responsible for propagation, but that propagation, in part, occurs by the addition of biradical to complex. On the other hand, it might be that the biradical II is in an even lower energy state than the complex I and that propagation occurs predominantly through the biradical.

It is quite possible that the above mechanism is a more general phenomenon than heretofore supposed.

For example, consider three possible and different copolymerization propagation mechanisms shown in eqs. (1)–(3).

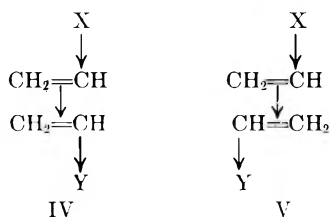


Case (1) is the classical way in which copolymerizations are considered, and it most likely is correct when monomers A and B do not have widely different double bond polarities. Case (3) has, above, been shown to be probable for the uncatalyzed copolymerization of bicyclo[2.2.1]hept-2-ene and sulfur dioxide. In olefin-sulfur dioxide copolymerizations involving less strained olefins, initiator is required,^{11,12} but one current thought advanced by Barb¹³ and Matsuda and Tokura,¹⁴ although disputed by Walling,¹⁵ is that to explain the kinetics of normal olefin-sulfur dioxide copolymerization requires a mechanism similar to case (2), (a propagating radical reacting with the olefin-sulfur dioxide charge-transfer complex). Olefin-sulfur dioxide charge transfer complexes¹⁶ are shown to exist in solution in reasonable concentration at normal polymerization temperatures.

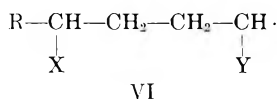
A copolymerization, which involves charge transfer complexes, is that of *trans*-stilbene and maleic anhydride.⁷ Neither of these monomers readily forms homopolymer. Upon mixing the two colorless compounds in solution, a yellow-green color results, which is retained at the polymerization temperature (without catalyst) of around 140°C. High molecular weight alternating copolymer slowly forms. Although case (2) or (3) might operate here, another possibility is that the complex is involved only in initiation leading to a diradical which then propagates classically according to eq. (1).

The relative ease of alternating copolymerization of difficultly free-radical-homopolymerizable monomers might be explained by considering a charge transfer complex as an intimate part of the polymerization mechanism and not simply due to "a large difference in ϵ values." Oppositely polarized monomer pairs known to lead reasonably rapidly to high molecular weight alternating copolymer, with or without initiator, are vinylidene cyanide-styrene¹⁸ and α -cyanoacrylate ester-isobutylene.¹⁹

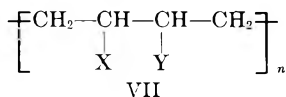
If it is assumed that charge-transfer complex formation might influence copolymerization reactions, several ramifications result, which, unfortunately, due to the symmetrical structure of the bicycloheptene-sulfur dioxide copolymer, could not be tested in this work. For, example, it might be expected that, for electronic reasons, complexes having schematic structure IV rather than V will result.



If this is the case and structure type IV predominates, by analogy with many photodimerizations, it might be expected that under the influence of a propagating radical [eq. (2)], intermediate radicals of structure VI would be present.

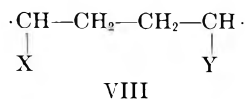


Structure VI, upon subsequent reaction with additional complex, could lead to alternating copolymers of structure VII.



Structure VII would be a head-to-head polymer.

If the mechanism of eq. (3) were operative, structure IV would open up to the most stable diradical, VIII.



which via coupling would also lead to head-to-head copolymer, VII.

EXPERIMENTAL

Purification of Reagents

Bicyclo[2.2.1]hept-2-ene. The purification of this monomer was critical. Upon repeated fractionation of purchased monomer (Roberts Chemical Co.) (under high purity nitrogen) through a spinning band column (Nester-Faust, 36 in. column) the spontaneous and instant copolymerization temperature (no induction period) was reduced so that the very purest samples instantly copolymerized in cyclohexanone at around -40°C . This was eventually used as a test of monomer purity. Extraction of crude monomer prior to fractionation, with concentrated aqueous alkali, although removing a yellow substance, did not decrease the number of fractionations necessary to obtain the most active monomer (about three). Extraction of monomer with aqueous ferrous sulfate prior to final distillation also had no effect on its activity, nor did a final distillation from metallic sodium. It should be mentioned that although the bicycloheptene was chromatographically pure after one fractionation its activity was increased upon further distillation.

Sulfur Dioxide. Matheson C. P. material was used throughout this work. Three bulb-to-bulb distillations followed by drying over Linde 4A molecular sieves had no visible effect on its reactivity. The addition of small amounts of hydrochloric acid or water to the polymerization experiments also had, qualitatively, no effect on the copolymerization.

Solvents. The polymerization solvents were fractionated under high purity nitrogen and stored over Linde 4A molecular sieves. Reduced viscosity determinations were made at 30°C . with 0.2 wt.-% solutions, usually in cyclohexanone or methylene chloride. The copolymers were soluble in higher ketones, aromatic solvents, tetrahydrofuran, and halogenated aliphatics.

EPR Measurements

EPR studies were made with a Varian V-4500 EPR spectrometer operating at 9500 Mcycles/sec. with 200 cycle/sec. magnetic field modulation. Both intensity and magnetic field calibrations were comparatively crude, being based on freshly prepared benzene solutions²⁰ of 2,2-diphenyl-1-picrylhydrazyl (DPPH) purchased from Distillation Products Industries. Measurements of g values also assumed that the bulk DPPH resonance signal was centered at $g = 2.0036$.

NMR and Stiffness-Temperature Measurements

High-resolution proton NMR measurements were made with both Varian A-60 and DP-60 NMR spectrometers by use of standard techniques. Stiffness-temperature measurements were carried out on an Instron tensile tester and calculated as secant moduli.

The valuable assistance of Mr. D. M. Harmon and Mr. R. E. Dodd in the preparation of samples as well as in other phases of the experimentation described above is gratefully acknowledged.

References

1. Zutty, N. L., and C. W. Wilson, III, *Tetrahedron Letters*, **30**, 2181 (1963).
2. Zutty, N. L., *J. Polymer Sci.*, **A1**, 2231 (1963).
3. Caldwell, J. R., and E. H. Hill, U.S. Pat. 2,899,412 (1959).
4. Hill, E. H., and J. R. Caldwell, *J. Polymer Sci.*, **A2**, 1251 (1964).
5. Hiatt, R. R., and P. D. Bartlett, *J. Am. Chem. Soc.*, **81**, 1149 (1959).
6. Bartlett, P. D., L. K. Montgomery, and B. Seidel, *J. Am. Chem. Soc.*, **86**, 616 (1964).
7. Montgomery, L. K., K. Schueller, and P. D. Bartlett, *J. Am. Chem. Soc.*, **86**, 622 (1964).
8. Poutsma, M., *J. Am. Chem. Soc.*, **85**, 3510 (1963).
9. Crawford, G. H., D. E. Rice, and B. F. Landrum, *J. Polymer Sci.*, **A1**, 565 (1963).
10. Kueubuhl, F. K., *J. Chem. Phys.*, **33**, 1074 (1960).
11. Dainton, F. S., J. Diaper, K. J. Ivin, and D. R. Sheard, *Trans. Faraday Soc.*, **53**, 1269 (1957).
12. Hazell, J. E., and K. J. Ivin, *Trans. Faraday Soc.*, **58**, 176,342 (1962).
13. Barb, W. G., *Proc. Roy. Soc. (London)*, **A212**, 66, 177 (1952).
14. Tokura, N., and M. Matsuda, *Sci. Rept. Res. Inst. Tohoku Univ.*, **A12**, 280 (1960).
15. Walling, C., *J. Polymer Sci.*, **16**, 315 (1955).
16. Booth, D., F. S. Dainton, and K. J. Ivin, *Trans. Faraday Soc.*, **55**, 1293 (1959).
17. Wagner, T.-J., *Ber.*, **63**, 3213 (1930).
18. Gilbert, H., F. F. Miller, S. J. Averill, E. J. Carlson, V. L. Folt, H. J. Heller, F. J. Stewart, R. F. Schmidt, and H. L. Trumbull, *J. Am. Chem. Soc.*, **78**, 1669 (1956).
19. Kinsinger, J., Michigan State Univ., private communication.
20. Ueda, H., Z. Kuri, and S. Shida, *J. Chem. Phys.*, **36**, 1676 (1962).
21. Atherton, N. M., H. Melville, and D. H. Whiffen, *J. Polymer Sci.*, **34**, 199 (1959).

Résumé

On a trouvé que la copolymérisation alternée du bicyclo [2.2.1]hept-2-ène et de l'anhydride sulfureux était tout à fait inhabituelle pour une polymérisation radicalaire: (1) L'initiation de la copolymérisation est spontanée, même à -40°C ; (2) la copolymérisation en solution est extrêmement rapide, fournissant du polymère de poids moléculaire très élevé endéans quelques secondes; (3) les conversions sont élevées (jusqu'à 93% après une minute); (4) le poids moléculaire augmente pendant la copolymérisation pour une conversion essentiellement constante; (5) la réaction est incapable d'être inhibée chimiquement d'une façon indéfinie, en éliminant rapidement un des monomères; (6) à température élevées, les monomères et le copolymère semblent être en équilibre; (7) on a détecté par résonance paramagnétique électronique que de grandes concentrations en radicaux libres sont associés à la copolymérisation en bloc; (8) la copolymérisation semble résulter de polymères radicalaires "vivants." On propose un mécanisme de copolymérisation pour expliquer ces observations: le bicycloheptène et l'anhydride sulfureux forment initialement un complexe moléculaire de transfert de charge 1:1 qui se transforme en un biradical; le couplage subséquent des biradicaux avec un autre biradical (ce qui est également possible, avec les complexes moléculaires aux-mêmes) conduit à une propagation rapide jusqu'à un poids moléculaire élevé du copolymère alterné. On a également spéculé sur le fait que des mécanismes semblables pourraient être importants dans d'autres réactions de copolymérisation.

Zusammenfassung

Die alternierende Kopolymerisation von Bicyklo[2.2.1]hept-2-en und Schwefeldioxyd weist für eine radikalische Polymerisation ganz ungewöhnliche Züge auf: (1) der Kopolymerisationsstart ist sogar bei -40°C spontan; (2) die Lösungskopolymerisation ist extrem rasch und liefert innerhalb einiger Sekunden sehr hochmolekulare Polymere; (3) der Umsatz ist hoch (bis zu 93% innerhalb einer Minute); (4) das Molekulargewicht nimmt während der Kopolymerisation bei im wesentlichen konstantem Umsatz zu; (5) die Reaktion kann chemisch nicht unbegrenzt knapp vor dem Verbrauch eines der Monomerbestandteile inhibiert werden; (6) bei erhöhter Temperatur scheinen die Monomeren und das Polymere im Gleichgewicht zu sein; (7) mittels elektronparamagnetischer Resonanz wurde gefunden, dass bei der Kopolymerisation in Substanz hohe Konzentrationen an freien Radikalen auftreten und (8) die Kopolymerisation scheint zu "living" Polymerradikalen zu führen. Ein Kopolymerisationsmechanismus zur Erklärung dieser Befunde wird aufgestellt: Bicyklohepten und Schwefeldioxyd bilden anfangs einen Ladungsübergangskomplex im Molverhältnis 1:1, welcher sich zu einem biradikalischen umlagert; darauffolgende Kopplung der Biradikale untereinander (und möglicherweise auch mit den Molekülkomplexen selbst) führt zu einem raschen Wachstum zu hochmolekularen, alternierenden Kopolymeren. Ähnliche Mechanismen könnten auch bei anderen Kopolymerisationsreaktionen von Bedeutung sein.

Received December 3, 1964

Revised February 19, 1965

Prod. No. 4661A

Thermodynamic Stability of Polymer Crystals.

III. Torsional and Longitudinal Chain Vibrations

A. PETERLIN and CHR. REINHOLD, *Camille Dreyfus Laboratory,
Research Triangle Institute, Durham, North Carolina*

Synopsis

The free energy density of a folded-chain crystal varies with the length of the straight-chain section between consecutive folds. It is always minimum at infinite length. Another minimum at finite length L appears below a critical temperature T_0 which among other things depends on the surface energy of the fold-containing planes. This minimum is a result of the smearing out of the nonharmonic lattice potential energy field by the incoherent vibrations of adjacent chains. In the present paper the simultaneous influence of both longitudinal and torsional vibrations of polyethylene chains in the orthorhombic lattice is considered. Due to the relative smallness of the amplitude of the potential energy for chain translation in comparison to that for chain rotation the calculated equilibrium length L at any temperature does not appreciably differ from the value obtained formerly for the torsional vibrations only. L increases with temperature and is maximum at the critical temperature. With increasing surface energy the equilibrium long period at constant temperature increases, and the critical temperature decreases. The calculated values fit fairly well the experimental data of polyethylene crystals grown from dilute solution if one admits that the surface energy varies slightly from solvent to solvent.

Introduction

The thermodynamic stability theory¹⁻⁵ explains the observed long period L of polymer single crystals by the relative minimum of free energy density occurring at finite crystal thickness. Another minimum always exists at infinite L so that according to the thermodynamic theory one can expect folded and extended-chain crystals. Which minimum is lower depends on temperature. At sufficiently low temperature T the minimum at finite L is rather deep and definitely lower than that at infinite L . With increasing T it moves to larger L , becoming more and more shallow, rising over the minimum at infinite L , and finally completely disappearing above a limited T_0 which depends on the value of surface energy at the fold containing surfaces. The appearance of a minimum of free energy density is due to two contributions. The first contribution $ab\sigma/L$ stems from the surface energy, steadily decreases with L , and yields the minimum at infinite L . The second contribution is the potential energy. The incoherent vibrations of adjacent macromolecules smear out the lattice field and hence decrease the amplitude of potential energy. This reduction increases with the vibration amplitude.

The square of this amplitude is roughly proportional to the number of chain elements in the straight section between two folds, i.e., proportional to the long period L . Consequently the free energy density contains a positive term increasing with L and $ab\sigma/L$ which together create a minimum at finite L .

Previously the role of longitudinal¹⁻³ and torsional⁴⁻⁵ vibrations of polyethylene chains were treated separately. In both cases the potential energy field was assumed to be sinusoidal. The arbitrary assumption³ that the amplitude of the potential energy for chain translation decreases as $\exp(-\alpha T)$ leads to a very rough agreement between the calculated and the observed L . In particular, it yields the increase of long period with increasing crystallization temperature. For torsional vibrations⁵ the temperature dependence of the potential energy amplitude was calculated from unit cell expansion data. The resulting stable long periods agreed well with data observed with polyethylene single crystals grown from dilute solutions.

In the actual crystal the polyethylene chains are subject to longitudinal and torsional vibrations. Therefore, in a realistic treatment of free energy density as function of crystal thickness both types of vibration have to be considered simultaneously. Their influence on the lowering of potential energy will be calculated as function of temperature, by use of simplified models of a polyethylene chain.

Molecular Model

The free energy density [eq. (4)] contains the elastic spring constants and the amplitudes of potential energy for translational and rotational vibration. In order to simplify the calculation three slightly different molecular models were chosen for the determination of spring constants (Fig. 1a), energy amplitudes for rotation (Fig. 1b), and energy amplitudes for translation (Fig. 1c). As the molecules are immobilized at their equilibrium positions in the crystal lattice, the temperature dependence of the potential energy field is calculated from known unit cell dimensions under the assumption of a slightly anisotropic Lennard-Jones type interaction between any two CH_2 groups. The so obtained field is then approximated by a sinusoidal function in the chain direction and for chain rotation with corresponding amplitudes ϕ_0 and ϕ_{10} . The thermal vibration of adjacent chains reduces the potential energy amplitudes to ϕ_t and ϕ_{t_1} , respectively.

For calculation of the spring constants the polyethylene chain is represented by an arrangement of dumbbells as shown in Figure 1a. Each dumbbell contains two CH_2 groups, 0.88 Å. apart, exhibiting a mass $2m_{\text{CH}_2} = 4.68 \times 10^{-23}$ g. and a moment of inertia $\theta = 2.07 \times 10^{-39}$ g.-cm.². The distance between two dumbbells in the direction of the chain axis is $c = 2.53$ Å. The connecting springs permit longitudinal and torsional vibrations. The corresponding spring constants $f_t = 10^5$ erg/cm.² and $f_{t_1} = 0.51 \times 10^{-12}$ erg are derived from evaluation of infrared spectra.^{1,5,6} The

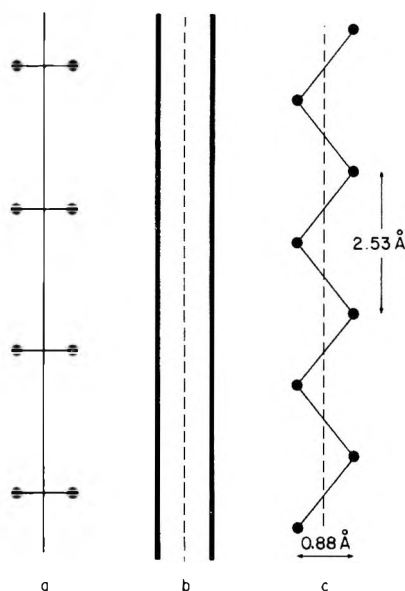


Fig. 1. Diagram of models used for the calculations of (a) the longitudinal and torsional vibrations of a free chain; (b) the potential energy for chain rotation (ϕ_{t0}); (c) the potential energy along the chain (ϕ_{l0}). The masses of the CH_2 groups are localized at the points shown. In the case b the mass is assumed to be evenly distributed along the lines.

highest eigenfrequencies of the model are those where the adjacent dumbbells vibrate with opposite phase:

$$\omega_{0l} = (4 f_l / 2m_{\text{CH}_2})^{1/2} = 0.925 \times 10^{14} \text{ sec.}^{-1}$$

$$\omega_{0t} = (4 f_t / \theta)^{1/2} = 0.315 \times 10^{14} \text{ sec.}^{-1}$$

Because f_l takes into account the combined action of valence bond stretching and valence angle deformation, one must not expect ω_{0l} to agree exactly with any polyethylene infrared eigenfrequency.⁶

The potential energy in the polyethylene crystal lattice results primarily from the attraction and repulsion forces between CH_2 groups. It is very nearly a sinusoidal function with period c in the chain direction and with period π for chain rotation. The energy fields and corresponding amplitudes ϕ_{l0} and ϕ_{t0} were calculated on the basis of the Lennard-Jones potential energy

$$U = -2\epsilon(R_{\text{min}}/R)^6 + \epsilon(R_{\text{min}}/R)^{12} \quad (1)$$

between two CH_2 groups in a distance R . One has $\epsilon = 1.135 \times 10^{-14}$ erg/ CH_2 group. The anisotropy of the force field yields $R_{\text{min}} = 4.28$ A. and 4.74 A. when the vector in the ab plane connecting the interacting chains is in the (110) and (010) directions, respectively. The latter value drops to 4.59 A. when the temperature is raised from 123 to 403°K. The dependence on direction and temperature was obtained from the condition

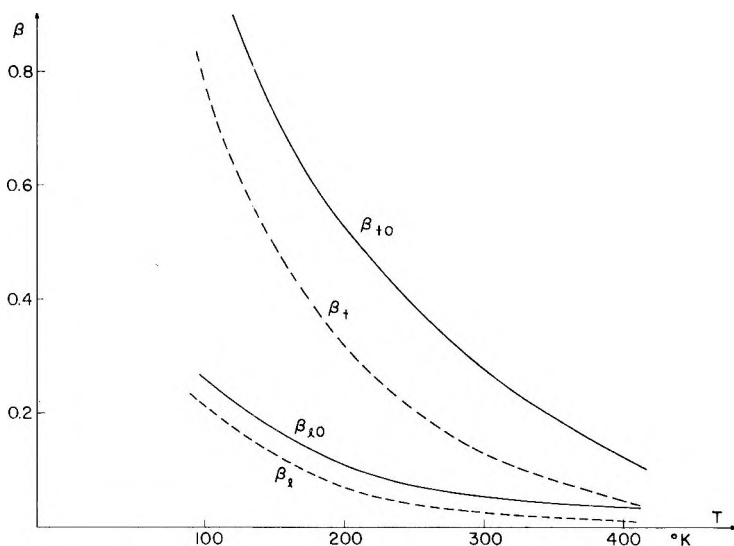


Fig. 2. Potential amplitudes for chain rotation (index l) and along the chain (index t) as function of temperature: (—) molecules being at rest; (---) vibrations taken into account of adjacent chains of the length 126 Å. ($N = 50$).

that every chain in the actual crystal lattice must be located in a minimum of potential energy.⁵

The potential energy field for rotation was calculated with a model (Fig. 1b) having the CH_2 groups evenly distributed along two infinite parallel lines separated by a distance 0.88 Å. The equivalence of the models of Figures 1b and 1c with regard to this potential energy has been shown previously.⁴ The energy field in the c axis was calculated with the original zig-zag chain model (Fig. 1c). The rapid decrease of contribution with increasing distance makes it sufficient to consider six closest neighboring molecules only. The resulting amplitudes $\beta_{t0} = \phi_{t0}/kT$ and $\beta_{l0} = \phi_{l0}/kT$ are plotted in Figure 2 as function of temperature. They can be approximated by

$$\begin{aligned}
 \phi_{t0} &= 2.1 kT \exp \{-0.007T\} \\
 \phi_{l0} &= 0.345 kT \exp \{-0.0058T\} & (223 < T < 373^\circ\text{K}) \\
 \phi_{t0} &= 0.639 kT - 0.129 \cdot 10^{-2} kT^2 \\
 \phi_{l0} &= 0.115 kT - 0.02 \cdot 10^{-2} kT^2 & (353 < T < 403^\circ\text{K}) \quad (2)
 \end{aligned}$$

β_{l0} is much less than β_{t0} in good agreement with estimates derived from the rate of long period growth during annealing.⁷

The torsional and longitudinal chain vibrations smear out the sinusoidal energy yielding a new amplitude ϕ_t and ϕ_l smaller than ϕ_{t0} and ϕ_{l0} . As a first approximation one may assume that the influence of both types of vibration is independent of each other so that one obtains

$$\begin{aligned}
 \beta_t &= \beta_{t0} \exp \left\{ -\frac{\pi^2 N k T}{5 c^2 f_t} \right\} \exp \left\{ -N k T / 5 f_t \right\} \\
 \beta_l &= \beta_{l0} \exp \left\{ -N k T / 5 f_l \right\} \quad (3)
 \end{aligned}$$

The dependence of β_t and β_l for $N = 50$ is also shown in Figure 2. Longitudinal vibrations do not influence β_t because the model has already a uniform charge distribution along the chain axis.

Free Energy of the Folded-Chain Crystal

The free energy density reads

$$F/NkT = -\ln(2kT/\hbar\omega_{0t}) - \ln(2kT/\hbar\omega_{0l}) + 2(\beta_{t0} - \beta_t + \beta_{l0} - \beta_l) + (1/N)[2ba\sigma/kT + \ln(2kT/\hbar\omega_{0t}) + \ln(2kT/\hbar\omega_{0l}) + 0.5 \ln(N + 8N^3kT\beta_t/\pi^2f_t) + 0.5 \ln(N + 8N^3kT\beta_l/c^2f_l)] \quad (4)$$

From the minimum of F/NkT plotted over N one obtains the stable single crystal thickness $L = N_{\min} \times 2.53 \text{ \AA}$. L is plotted in Figure 3 as function of temperature for different surface energies. Solid lines indicate values obtained when both torsional and longitudinal vibrations are considered, broken lines indicate torsional vibrations only. The two sets of curves do not differ very much because, due to the smallness of β_{l0} , the contribution of longitudinal vibrations is much less than that of torsional vibrations.

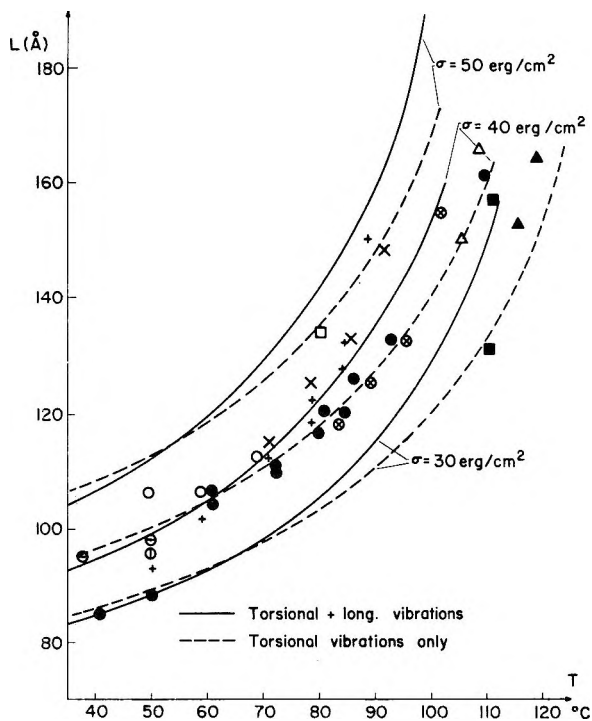


Fig. 3. Long period L of polyethylene crystals grown from solution as function of crystallization temperature: points give experimental data for (O) tetrachloroethylene,⁸ (●) xylene and butyl acetate,⁹ (+) xylene,^{10,11} (□) *p*-xylene,⁸ (Δ) butyl acetate,⁸ (■) butyl stearate,¹² (▲) glycol dipalmitate,¹² (⊕) toluene,¹³ (⊖) xylene,¹³ (×) xylene,¹⁴ and (⊗) octane¹⁴; theoretical curves show stable thickness L for different surface energies with and without longitudinal vibrations taken into account.

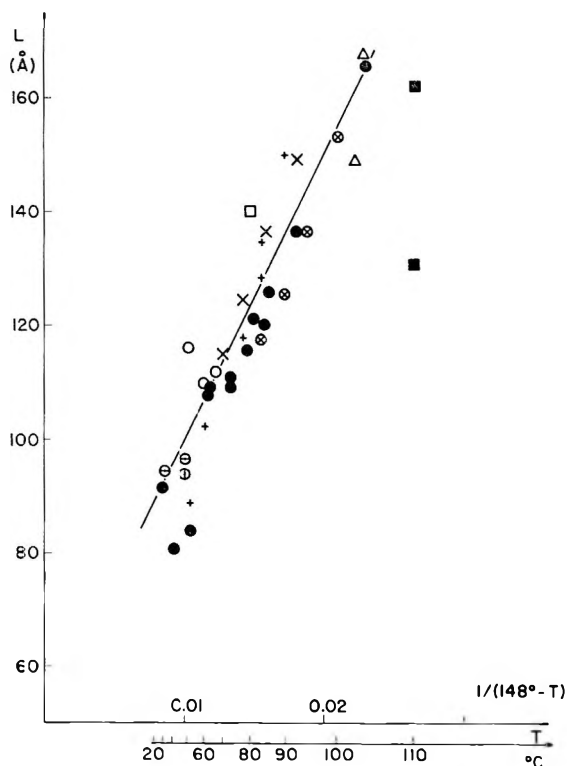


Fig. 4. Stable thickness L for $\sigma = 40$ erg/cm.² as function of $1/(148^\circ\text{C.} - T)$. Torsional and longitudinal vibrations are taken into account. The experimental data correspond to those in Fig. 3.

The larger slope of the new curves fits better the recent data of Kawai and Keller¹⁴ on polyethylene crystals from xylene and octane solutions. By comparison with all experimental data for crystals grown from solution one may conclude that $\sigma = 40$ erg/cm.² yields the best fitting curve. The same value was adopted in the previous paper⁵ where only the torsional vibrations were taken into account. In the temperature range not too close to T_0 a very good approximation for $L(T)$ reads

$$L = A + B / (T^* - T) \quad (5)$$

For $\sigma = 40$ erg/cm.² we obtain $A = 49$ Å., $B = 5000$ Å.-deg., $T^* = 148^\circ\text{C.}$ In this case T_0 is 106°C. In the validity range of this approximation the observed long periods are situated on a straight line if plotted versus $1/(T^* - T)$. Such a plot is shown in Figure 4 with $T^* = 148^\circ\text{C.}$ The experimental points are indeed very nearly on a straight line. The approximative eq. (5) is plotted in Figure 5 as a broken line. Equation (5) has the same structure as equations for long periods derived from the kinetic theory of crystallization¹⁵

$$L = 2\sigma/\Delta h\Delta T + kT/\sigma b_0 \quad (6)$$

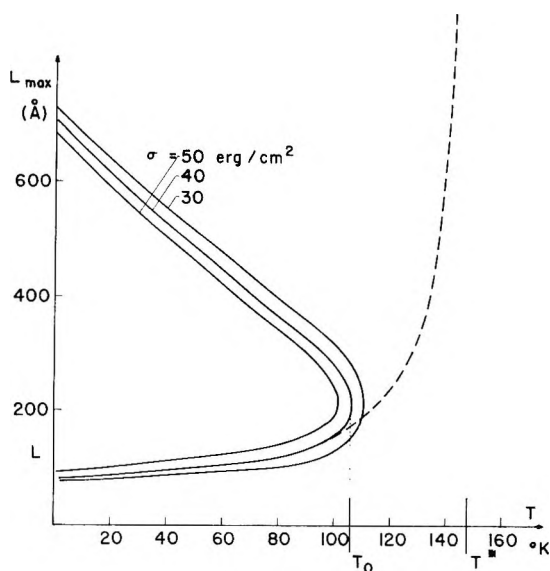


Fig. 5. L_{\max} and L as function of temperature for different surface energies σ . The broken line indicates the approximation of $L(T)$ by eq. (5). The deviation below 100°C . is negligible.

with $\Delta h = 2.8 \times 10^9 \text{ erg/cm}^2$; $b_0 = 5 \times 10^{-8} \text{ cm}$. The surface energy of the (110) plane is $\sigma_e = 10 \text{ erg/cm}^2$.

The minima at finite and infinite L are separated by a maximum at L_{\max} which with increasing temperature moves closer to L and finally at T_0 merges with it, as shown in Figure 5. If at any temperature the crystals have a thickness above L_{\max} they will tend to grow in order to reduce the free energy density. The observability of such a growth strongly depends on chain mobility which is sufficiently large only in a rather narrow temperature range below the melting point. This may be deduced from the fact that long period changes were only observed above 100°C . At 110°C . a discontinuity of long period growth was reported by Fischer and Schmidt¹⁶ agreeing with the prediction of the thermodynamic theory that a stable finite length is only to be expected below 110°C . Above this temperature there exists only the minimum of free energy at infinite length. The question is open whether the discontinuity at 100°C . of the thermal expansion coefficient of polyethylene in the a direction as found by Moore and Matsuoka¹⁷ has the same origin. Figure 5 also shows that for constant temperature the stable finite length increases with increasing surface energy σ , a result which has also been derived by the kinetic theory.¹⁵ Increasing surface energy yields a decrease of the critical temperature T_0 and a slight increase of the corresponding maximum stable length.

Discussion

The present calculations do not take into account the influence of crystal defects and in particular of the free ends of the polyethylene molecules.

The specific influence of the solvent may show up in the surface energy. Also, in bulk samples and drawn material, when the number of chain folds is markedly below one-half per chain, one can expect substantial changes in σ and hence in L . The predictions of the kinetic and the thermodynamic theory are again very similar so that it is not easy to decide which better reproduces the experimental data. There are some deficiencies in both theories. The thermodynamic theory lacks any prediction above T_0 , i.e., for temperatures where crystallization from the melt occurs. The value A in eq. (5) is about four to five times larger than the kinetic theory predicts. A particular difficulty for the kinetic theory is also the fact that according to Zahn and Pieper¹⁸ the chains already fold in oligomers where the chain length is only 50% larger than the crystal thickness. Their experimental data on oligomers of polyurethane, nylon 66, and nylon 6 show that the long period L characteristic for very long molecules is established as soon as the chain length is 50% larger than L . With shorter chains a reduction of L is observed, indicating that the number of crystal defects due to the free ends is reduced by a detracting of the crystal yielding a decrease in thickness.

One may speculate that the kinetic theory of crystallization rules the kinetic effects, i.e., the primary nucleation for crystal formation, the secondary for new layer deposition on a completed (110) face, and tertiary nucleation for completion of the layer. Accordingly, the long period of the deposited chains exhibits a nonnegligible fluctuation, and the fold surface is coarse and uneven. Before the next layer is added the chain mobility is still large enough not only to smooth the folds but also to reach the configuration corresponding to the free energy minimum. This means the value L of the thermodynamic theory is established. The crystal is now stable and has no tendency to change its thickness as long as it remains at the same temperature. Although cooling to a lower temperature shifts the equilibrium length to a smaller value the gentle slope of the strongly unsymmetrical free energy minimum does not produce enough driving force to overcome the drastically reduced chain mobility at lower temperatures. Therefore, the long period remains unchanged. An increase of temperature, certainly above 100°C., increases sufficiently the mobility and also produces a substantially larger driving force so that crystal starts to grow in thickness. Below T_0 the growth has to stop as soon as the equilibrium thickness L is reached. Above T_0 , however, the growth proceeds until the chains are fully extended.

The authors gratefully acknowledge the financial support of this work by the Camille and Henry Dreyfus Foundation.

References

1. Fischer, E. W., *Z. Naturforsch.*, **14a**, 584 (1959).
2. Peterlin, A., and E. W. Fischer, *Z. Physik*, **159**, 272 (1960).
3. Peterlin, A., *J. Appl. Phys.*, **31**, 1934 (1960).
4. Reinhold, Chr., Thesis, University of Mainz, Germany, 1962.

5. Peterlin, A., E. W. Fischer, and Chr. Reinhold, *J. Polymer Sci.*, **62**, S59 (1962); *J. Chem. Phys.*, **37**, 1403 (1962).
6. Kuhn, H., and W. Kuhn, *Helv. Chim. Acta*, **29**, 1095 (1946).
7. Peterlin, A., *J. Polymer Sci.*, **B1**, 279 (1963).
8. Rånby, B. G., and H. Brumberger, *Polymer*, **1**, 399 (1960); B. G. Rånby, F. F. Morehead, and N. M. Walker, *J. Polymer Sci.*, **44**, 349 (1960).
9. Fischer, E. W., and G. F. Schmidt, see reference 5.
10. Holland, V. F., and P. H. Lindenmeyer, *J. Polymer Sci.*, **57**, 589 (1962).
11. Keller, A., *Growth and Perfection of Crystals*, Wiley, New York, 1958, p. 499; A. Keller and A. O'Connor, *Polymer*, **1**, 163 (1960).
12. Ryan, Y., unpublished data, quoted in P. H. Geil, *Polymer Single Crystals*, Interscience, New York, 1963.
13. Hirai, N., T. Tokumori, T. Katayama, S. Fijita, and Y. Yamashita, *Repts. Res. Lab. Surface Science, Okayama Univ.*, **2**, 91 (1963).
14. Kawai, T., and A. Keller, to be published.
15. Hoffman, J. D., *SPE Trans.*, **4**, 315 (1964).
16. Fischer, E. W., and G. F. Schmidt, unpublished data; see reference 5.
17. Moore, R. S., and S. Matsuoka, *J. Polymer Sci.*, **C5**, 163 (1964).
18. Zahn, H., and W. Pieper, *Kolloid-Z.*, **180**, 97 (1962).

Résumé

La densité de l'énergie libre d'une chaîne cristalline repliée varie avec la longueur de la réaction de chaîne rectiligne entre les plis consécutifs. Elle est toujours minimum pour une longueur infinie. Un autre minimum pour une longueur finie L apparaît en-dessous d'une température critique T_0 qui dépend entre autres de l'énergie superficielle des plans contenant des plis. Ce minimum résulte d'une répartition du champ de l'énergie potentielle du réseau non-harmonique par les vibrations incohérentes des chaînes adjacentes. Dans cet article on considère l'influence simultanée des vibrations longitudinales et de torsion des chaînes de polyéthylène dans le réseau orthorhombique. À cause de la petitesse relative de l'amplitude de l'énergie potentielle pour la translation de chaînes en comparaison de celle pour la rotation, la longueur L , calculée à l'équilibre pour chaque température, ne diffère pas d'une façon appréciable de la valeur obtenue précédemment pour les vibrations de torsion seules. L augmente avec la température et est maximum à la température critique. Lorsque l'énergie superficielle augmente, la longue période d'équilibre à température constante augmente et la température critique diminue. Les valeurs calculées correspondent très bien avec les résultats expérimentaux concernant la croissance des cristaux de polyéthylène à partir de solution diluée si on admet que l'énergie superficielle varie légèrement d'un solvant à un autre.

Zusammenfassung

Die Freie-Energiedichte eines gefalteten Kettenkristalls hängt von der Länge des geraden Abschnitts zwischen aufeinanderfolgenden Faltungen ab. Sie hat in allen Fällen bei unendlicher Länge ein Minimum. Ein weiteres Minimum erscheint bei endlicher Länge L unterhalb einer kritischen Temperatur T_0 , welche unter anderem von der Oberflächenenergie der die Faltungen enthaltenden Ebenen abhängt. Dieses Minimum kommt durch die Ausschmierung des nicht-harmonischen Feldes der potentiellen Gitterenergie durch die inkohärenten Schwingungen benachbarter Ketten zustande. In der vorliegenden Mitteilung wird der gleichzeitige Einfluss von Longitudinal- und Torsionsschwingungen von Polyäthylenketten im orthorhombischen Gitter betrachtet. Wegen der im Vergleich zur Kettenrotation relativ kleinen Amplitude der potentiellen Energie bei der Kettentranslation unterscheidet sich die berechnete Gleichgewichtslänge L bei einer bestimmten Temperatur nicht wesentlich von dem früher für die Torsionsschwingungen allein erhaltenen Wert. L nimmt mit der Temperatur zu und erreicht bei der kritischen Temperatur ein Maximum. Mit steigender Oberflächenenergie nimmt die

Gleichgewichtslangperiode bei konstanten Temperaturen zu und die kritische Temperatur ab. Die berechneten Werte stimmen recht gut mit den Ergebnissen an aus verdünnter Lösung gewachsenen Polyäthylenkristallen überein, unter der Annahme, dass die Oberflächenenergie sich von Lösungsmittel zu Lösungsmittel schwach ändert.

Received February 16, 1965

Prod. No. 4664A

Raman Spectra of Polymers in Solution

TSUNEO YOSHINO and MASAYASU SHINOMIYA, *Basic Research Laboratories, Toyo Rayon Company, Kamakura, Kanagawa, Japan*

Synopsis

The intensity and the depolarization ratio of a Raman line measured on a turbid polymer solution were related to the true intensity and the depolarization ratio, and the relations were confirmed by experiments. Apparent depolarization ratios measured on a polymer rod or solution are different from the corrected values obtained by using these relations, especially for polarized lines. The intensity per monomer unit of a polymer Raman line is equal to the intensity of the corresponding line of a model compound. No effect of polymer tacticity on Raman spectra was found.

Measurements of Raman spectra have been made on polymers in the form of rods,¹⁻⁴ powders,⁵⁻⁷ pellets,^{8,9} or melts,¹⁰ but scarcely any studies have been carried out with polymer solutions, probably because of the difficulty of measurement due to low solubility of polymers and the turbidity of the solutions which decreases Raman intensity and reflects incident light. A fairly transparent rod of a polymeric substance if obtainable, yields far better Raman spectra than a pellet, melt, or powder of the polymer. The depolarization ratios of Raman lines are important for assignments of spectral lines and for determination of molecular structures. The ratios obtained from a polymer rod were, however, found to be much different from their correct values as shown below.

Results and Discussion

The present study showed that (a) Raman lines of a polymer in solution nearly equal in number to those from its rod are obtainable; (b) correct depolarization ratios for the polymer Raman lines can be obtained by varying the concentration of the polymer in solution, (c) the relative intensity of a polymer Raman line to a solvent line of nearly equal depolarization ratio is independent of polymer concentration and is equal to the relative intensity of the corresponding Raman line of a compound with molecular structure similar to the monomer unit of the polymer; and (d) frequencies and intensities of Raman lines are nearly the same for isotactic and atactic polymers.

Some examples of Raman spectra of polymers in solution are shown in Figure 1. The optimum polymer concentration was found to be 3-10 vol.-%.

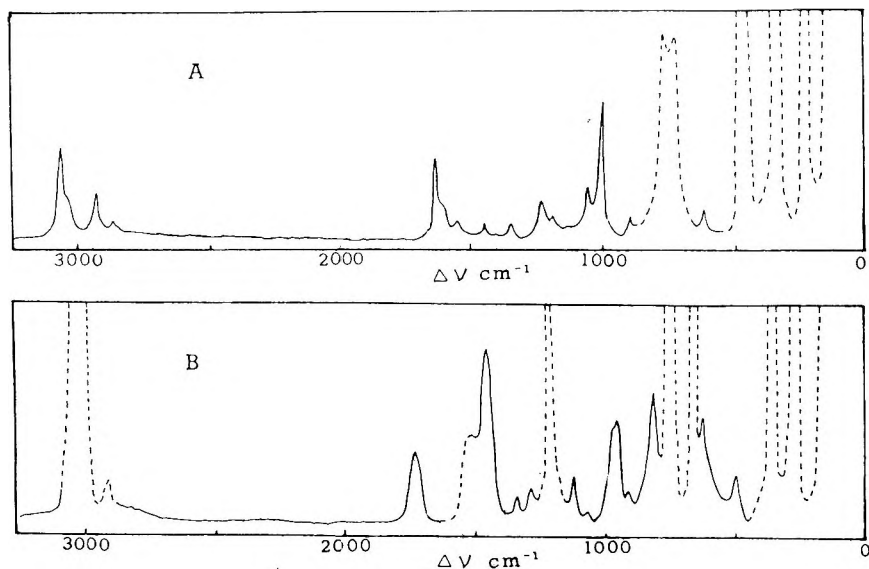


Fig. 1. Raman spectra of polymer solutions: (A) polystyrene in carbon tetrachloride solution; (B) poly(methyl methacrylate) in chloroform solution.

When a molecule which is allowed to assume all orientations with equal probabilities is placed in the electric field of exciting light polarized along the x direction, the x , y , and z components of the intensity of Raman scattering due to the anisotropic part γ of a derived polarizability are in 4:3:3 ratio, while Raman light due to the isotropic part α of a derived polarizability has only the x component, as confirmed for a transparent liquid or gas.¹¹ However, reflection or scattering of a light beam by small particles in a polymer solution changes the direction of propagation and polarization, and the degree of polarization. Raman light polarized along the direction of observation X when it is emitted from a molecule acquires Y and Z components when it goes through a turbid polymer solution and becomes observable, while Raman light originally polarized along the Y (or Z) direction partly loses the intensity of the Y (or Z) component.

In consideration of the effect of turbidity mentioned above, the intensities I_{\parallel} , I_{\perp} , and I of a Raman line measured with polarizer axes parallel and perpendicular to X and without polarizer, respectively, are given by eqs. (1)–(3):

$$I_{\parallel} = 45\alpha^2[I_X f_+(\tau) + (i_Y + i_Z) f_-(\tau)]a + \gamma^2[(6I_X + 7i_Y + 7i_Z) f_-(\tau) + (4I_X + 3i_Y + 3i_Z) f_+(\tau)]a \quad (1)$$

$$I_{\perp} = 45\alpha^2(I_Y + I_Z) f_-(\tau)a + \gamma^2[(7I_Y + 7I_Z) f_-(\tau) + 3(I_Y + I_Z) f_+(\tau)]a \quad (2)$$

$$I = 45\alpha^2[I_X f_+(\tau) + (I_Y + I_Z) f_-(\tau)]a + \gamma^2[(6I_X + 7I_Y + 7I_Z) f_-(\tau) + (4I_X + 3I_Y + 3I_Z) f_+(\tau)]a \quad (3)$$

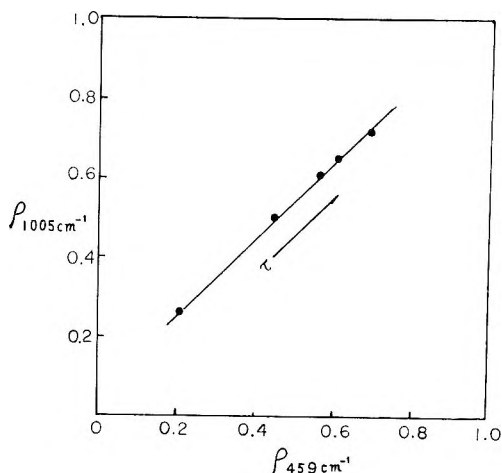


Fig. 2. Relation between changes with turbidity of ρ_{app} of the 1005 cm^{-1} line of polystyrene and the 459 cm^{-1} line of carbon tetrachloride measured for carbon tetrachloride solutions of polystyrene containing methanol.

Here i_Y is the Y component of the exciting light intensity in a Raman cell due to nonvertical incidence, I_Y is the Y component of the intensity in the Raman cell of the exciting light which is incident vertically and nonvertically, $f_+(\tau)$ and $f_-(\tau)$ are functions of turbidity τ , and a is a constant determined by the apparatus used; $i_Y = i_Z$, $I_Y = I_Z \approx I_X/2$,

$$0 \leq f_+(\tau) \leq f_-(\tau), f_-(\infty) = f_+(\infty) = f_+(0) = 0, \text{ and } f_-(0) = 1.$$

Explicit forms of $f_-(\tau)$ and $f_+(\tau)$ depend on the apparatus used. Magnitudes of I_X , I_Y , and I_Z in eq. (3) are different from those in eqs. (1) and (2).

Equations (1)–(3) show that (1) they apply to Raman lines of both polymer and solvent, (2) the apparent depolarization ratio ρ_{app} ($=I_{\parallel}/I_{\perp}$) increases with τ , (3) the increase of ρ_{app} with τ is larger for Raman lines of higher polarization, (4) the change of ρ_{app} with τ is nearly the same for highly polarized (that is, $45\alpha^2 \gg 7\gamma^2$) Raman lines, and (5) the relative intensities of Raman lines with ρ_{app} values not much different from each other are almost independent of τ .

To confirm these points by experiment, the ρ_{app} values of the 459 cm^{-1} line of carbon tetrachloride and the 1005 cm^{-1} line of polystyrene were measured for carbon tetrachloride solutions of polystyrene with equal polymer concentration but with different turbidities caused by addition of various small amounts of methanol. When observed values of ρ_{app} of the 1005 cm^{-1} line are plotted against those of the 459 cm^{-1} line, a straight line with slope equal to one is obtained, as shown in Figure 2, and this confirms points (1), (2), and (4) mentioned above.

The values of ρ_{app} for the depolarized Raman lines at 314 and 217 cm^{-1} of carbon tetrachloride in the polymer solution and the intensity ratios of the 1005 to the 459 cm^{-1} line and the 314 to 217 cm^{-1} line were found to

change little with change of τ , which verifies points (3) and (5) mentioned above.

Since the effect of turbidity on Raman intensity and depolarization ratio was found to be expressed by eqs. (1)–(3), we wished to determine whether or not Raman lines of a polymer in solution are comparable with those of a nonpolymeric liquid. For this purpose, the intensity of the 1005 cm^{-1} line of polystyrene relative to the 459 cm^{-1} line of carbon tetrachloride was measured for carbon tetrachloride solutions of polystyrene of various polymer concentrations, and compared with relative intensity of the 1003 cm^{-1} line of toluene in carbon tetrachloride, which is considered to correspond to the 1005 cm^{-1} line in the vibrational mode. As shown in Figure 3, the relative intensity of the 1005 cm^{-1} line was observed to be proportional to polymer concentration (though its absolute intensity was of course not),

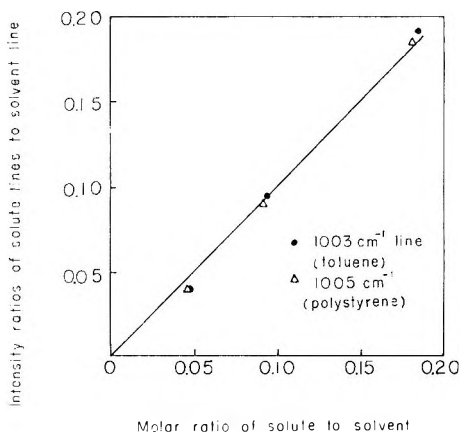


Fig. 3. Intensity ratios of the 1005 cm^{-1} line of polystyrene to the 459 cm^{-1} line of carbon tetrachloride measured on carbon tetrachloride solutions of polystyrene of various concentrations, and intensity ratios of the 1003 cm^{-1} line of toluene to the 459 cm^{-1} line measured on carbon tetrachloride solutions of toluene of various concentrations.

and the relative intensity per monomer unit was found to be equal to the relative intensity of the 1003 cm^{-1} line. For the same purpose, changes with polymer concentration of the ρ_{app} of the 1005 and 459 cm^{-1} lines were also measured, and these were found to be in the same relation as that shown in Figure 2 for changes of ρ_{app} with τ . The change of ρ_{app} with polymer concentration is, therefore, due to change of τ , and the correct depolarization ratio* of the 1005 cm^{-1} line of polystyrene, for example, is given by extrapolation of the straight line in Figure 2, which gives at the same time the depolarization ratio† of the 459 cm^{-1} line of pure carbon tetrachloride measured by the same apparatus. The correct depolarization

* Not corrected for nonvertical incidence of the exciting line and other nonideal conditions of the measuring apparatus.

† The depolarization ratio was found to be 0.18.

ratio of a polymer Raman line thus obtained can be compared with the depolarization ratio of a Raman line of a nonpolymeric liquid.

The correct depolarization ratios of the 1005 cm^{-1} line of polystyrene and the 1729 cm^{-1} line of poly(methyl methacrylate) in carbon tetrachloride were found to be 0.22 and 0.40, respectively, while the depolarization ratios of these lines obtained from polymer rods are 0.88 and 0.67, respectively, which are nearly equal to the depolarization ratios of depolarized Raman lines.

The frequencies and intensities of Raman lines are nearly the same for isotactic and atactic polystyrenes dissolved in bromoform and for isotactic and atactic poly(methyl methacrylates) dissolved in chloroform, and that depolarization ratios of the 1005 cm^{-1} lines of isotactic and atactic polystyrenes are equal to each other.

Experimental

The isotactic polystyrene was prepared at 80°C . in *n*-heptane with the use of triisobutylaluminum-titanium tetrachloride as catalyst, and the atactic portion was removed with methyl ethyl ketone extraction.¹² Isotactic poly(methyl methacrylate) was prepared at 0°C . in toluene by use of phenylmagnesium bromide as catalyst.¹³ The tacticity of these polymers was established from the NMR and infrared spectra.

Undissolved material in polymer solutions was removed by filtration and centrifugation. Polymer rods were prepared by polymerization of the liquid monomers in glass tubes of 7 mm. in diameter, which were removed before Raman measurement. Raman spectra were obtained with a Cary 81 spectrometer at 35°C ., with a 4358 Å. light source.

References

1. Signer, R., and J. Weiler, *Helv. Chim. Acta*, **15**, 649 (1932).
2. Palm, A., *J. Phys. Chem.*, **55**, 1320 (1951).
3. Ferraro, J. R., J. S. Ziomek, and G. Mack, *Spectrochim. Acta*, **17**, 802 (1961).
4. Matsui, Y., T. Kubota, and H. Tadokoro, *Bunko Kenkyu*, **10**, 107 (1962).
5. Tobin, M. C., *J. Opt. Soc. Am.*, **49**, 850 (1959).
6. Tadokoro, H., A. Kobayashi, Y. Kawaguchi, S. Sobajima, S. Murahashi, and Y. Matsui, *J. Chem. Phys.*, **35**, 369 (1961).
7. Nikitin, V. N., and L. I. Maklakov, *Optika i Spektroskopiya*, **13**, 343 (1962).
8. Nielsen, J. R., and A. H. Woollett, *J. Chem. Phys.*, **26**, 1391 (1957).
9. Tobin, M. C., *J. Phys. Chem.*, **64**, 216 (1960).
10. Brown, R. G., *J. Chem. Phys.*, **38**, 221 (1963).
11. Wilson, E. B., J. C. Decius, and P. C. Cross, *Molecular Vibration*, McGraw-Hill, New York, 1955, pp. 46, 47.
12. Overberger, C. G., F. Ang, and H. Mark, *J. Polymer Sci.*, **35**, 381 (1959).
13. Goode, W. E., F. H. Owens, R. P. Fellmann, W. H. Snyder, and J. E. Moore, *J. Polymer Sci.*, **46**, 317 (1960).

Résumé

L'intensité et le rapport de dépolarisation d'une bande Raman mesurée sur une solution trouble de polymère ont été comparés à l'intensité vraie et au rapport de dépolarisa-

tion véritable, et les relations ont été confirmées par les expériences. Les rapports apparents de dépolarisation mesurés sur une barre de polymère ou sur une solution sont différents des valeurs corrigées en utilisant ces relations, spécialement pour les bandes polarisées. L'intensité par unité monomérique pour une bande Raman dans le cas d'un polymère est égale à l'intensité de la bande correspondante d'un composé modèle. On n'a pas trouvé d'influence sur les spectres Raman de la tacticité du polymère.

Zusammenfassung

An einer trüben Polymerlösung gemessene Werte der Intensität und des Depolarisationsverhältnisses einer Ramanlinie wurden zu den entsprechenden wahren Werten in Beziehung gesetzt und die Beziehungen experimentell bestätigt. Scheinbare, an einem Polymerstab oder einer Lösung gemessene Depolarisationsverhältnisse unterscheiden sich besonders bei den polarisierten Linien von den mittels dieser Beziehungen korrigierten Werten. Die Intensität einer Polymer-Ramanlinie pro Monomereinheit ist gleich der Intensität der entsprechender Linie einer Modellverbindung. Es konnte kein Einfluss der Polymertacticität auf Ramanspektren festgestellt werden.

Received June 9, 1964

Revised December 9, 1964

Prod. No. 4670A

Electron Traps in Polyethylene

R. H. PARTRIDGE,* *Physics Branch, Royal Military College of Science, Shrivenham, Swindon, Wilts, England*

Synopsis

Qualitative and quantitative results from previous studies of the thermoluminescence induced in polyethylene by irradiation are used in an attempt to deduce the main polyethylene electron traps. It is concluded that the most probable traps are the molecular chains themselves, the different degrees of molecular motion in different structural regions of polyethylene being responsible for the untrapping of the trapped electrons at different rates and hence the appearance of multiple glow peaks in the glow curve. An explanation is given for the correspondence between the activation energies of thermoluminescence, radiation induced electrical conductivity, and molecular chain motion (as measured by NMR) in polyethylene.

Introduction

Previous studies¹⁻⁴ have shown that the thermoluminescence glow curve of γ -ray or ultraviolet irradiated polyethylene *in vacuo* contains three main glow peaks in the temperature range -196 to 0°C ., designated α , β , and γ for convenience in order of ascending temperature. In the presence of molecular oxygen the β and γ glow peaks are completely removed (at low irradiation doses) and replaced by a new peak, ϵ , at somewhat lower temperature. The general mechanism of thermoluminescence in polyethylene, as in many other materials, seems to be the ionization of "luminescence centers" followed by trapping of the ejected electrons while the sample remains at low temperature. Warming allows the electrons to escape from their traps and recombine with the luminescence centers with emission of light.

The existence of several glow peaks in a glow curve is often ascribed to the presence of different types of electron traps (in which case each glow peak will generally have a different activation energy) or to different types of luminescence centers (in which case each glow peak will have a different emission spectrum). However, for polyethylene Charlesby and Partridge¹ have found that the activation energies of the α , β , and γ glow peaks are identical, within experimental error, at temperatures below the structural transitions of polyethylene and that the thermoluminescence emission spectra of the α , γ , ϵ , and probably β , glow peaks are also identical.^{3,4}

* Present address: Institute of Molecular Biophysics, Florida State University, Tallahassee, Florida, U. S. A.

The luminescence centers producing the actual luminescence emission are carbonyl groups (probably situated on the ends of side chains) produced by oxidation of the polymer both during and after manufacture.^{3,4} Hence it seems likely that the α , β , γ , and ϵ peaks share the same luminescence centers and may also, with the exception of the ϵ peak, share the same electron traps. The ϵ peak electron trap is almost certainly molecular oxygen^{3,4} but the α , β , and γ electron traps have not previously been identified. Measurements with single crystals of polyethylene⁵ have shown the difference between the α , β , and γ peaks to be that the α peak comes from the crystalline regions of polyethylene (impermeable to oxygen) the γ peak from the amorphous region, and the β peak from a region apparently intermediate between these two (possibly the surfaces of the crystallites).

Experimental Evidence on the α , β , and γ Electron Traps

The available evidence on the nature of the α , β , and γ traps in polyethylene is as follows.

(a) The α traps exist in the crystalline regions of polyethylene, the γ traps in the amorphous regions, and the β traps possibly in or around the surfaces of the crystallites.

(b) The traps are not due to chemical impurities introduced during manufacture, such as catalysts, since the α , β , and γ peaks are observed (*in vacuo*) in a wide variety of both low- and high-density commercial polyethylenes, with and without various antioxidant additives, in single crystals of polyethylene, and in highly purified paraffins.^{1,3-5}

(c) The traps either exist in high concentration or have high electron capture probabilities. This can be shown in two ways

Firstly, although thermoluminescence is a bimolecular process the decay of luminescence at constant temperature appears to be exponential for all the glow peaks at all temperatures,¹ i.e., the rate-determining process is the untrapping of electrons and not their subsequent recombination with luminescence centers. This is not merely due to a large excess of trapped electrons over luminescence centers, since for ultraviolet irradiation (which gives the same glow peaks as γ -radiation) the carbonyl luminescence centers are probably themselves the only source of the electrons as only they can absorb the ultraviolet radiation initially.^{3,4} The short recombination time suggests that the ejected electrons are trapped close to their parent luminescence centers and hence that the electron traps must be in high concentration or of high efficiency.

Secondly, and confirming the above, we can very roughly estimate the average diffusion distance of an electron from its parent luminescence center by using the data of Charlesby and Partridge² on the oxygen effect in polyethylene. Oxygen molecules were found to approximately halve the β and γ peak outputs when present in the amorphous region at a concentration of about 2×10^{17} cc.⁻¹ (about half the quantity that is present when samples are in equilibrium with air at atmospheric pressure). At this concentration the average separation of the oxygen molecules is about

170 Å. and, assuming a uniform distribution, no luminescence center should be more than about 120 Å. from an oxygen molecule. In this situation it is unlikely that the electron will be able to diffuse as much as 200 Å. before being captured with approximately equal probability by the highly effective oxygen molecules or by the β or γ traps. (It now seems that oxygen molecules function purely as electron traps in polyethylene, not as luminescence centers as suggested earlier² since the oxygen-induced ϵ glow peak has been found to have the same emission spectrum as the α , β , and γ peaks.) In contrast Nikol'skii, Tochin, and Buben⁶ found that radiation-produced alkyl radical electron traps became competitive with the "shallow" (α , β , γ) traps only at doses of 5–10 Mrad, corresponding to a concentration of around 10^{19} cc.⁻¹ or a furthest luminescence center-alkyl radical separation of around 35 Å. Although the alkyl radicals have unpaired spins they are clearly much less efficient electron traps than oxygen molecules and so to be effective must be present in much greater concentration.

The luminescence center concentration may be as low as 10^{15} cc.^{-1,3,4} corresponding to an average separation of 1000 Å., while from the above the electron diffusion distance in the presence of β and γ traps alone is probably not much above 200 Å. Thus it seems most unlikely that an electron ejected from one center will be able to diffuse as far as any other center, as is confirmed by the unimolecular thermoluminescence kinetics.

(*d*) The α , β , and γ traps give rise to thermoluminescence activation energies and frequency constants which, as will be seen, compare quite closely with those for molecular chain motion in polyethylene.

Discussion

As a result of (*a*) the γ traps can scarcely be due to structural defects since they exist in a completely disordered region, although this is a possibility for the α and β traps. Using (*b*) we can exclude all foreign chemical impurities introduced by any particular manufacturing process, especially as the oxygen effect shows thermoluminescence to be very sensitive to the presence of efficient electron traps in low concentration. Chemical impurities in the molecular chains themselves must also be considered, such as unsaturation, chain branching, crosslinks, peroxide bridges, and radiation-produced free radicals. Branching and unsaturation seem unlikely, as the concentrations of these vary greatly between the various types of low and high density polyethylenes yet all have thermoluminescence outputs of the same order and all are equally sensitive to the presence of molecular oxygen. Crosslinks and peroxide bridges are produced only by irradiation (and the latter only after warming if the irradiation is at low temperature) and hence for low doses (γ -ray doses of as little as 0.8 rad have been used in this work) the probabilities of these being produced near the comparatively few carbonyl luminescence centers attached to the molecular chains, as required by (*c*), must be very small indeed. Furthermore successive irradiations will increase the density of crosslinks and peroxide bridges, yet the thermoluminescence efficiency always decreases.^{1,3,4} The action of

(radiation-produced) free radicals as electron traps is also most unlikely at low doses for similar reasons, but the work of Nikol'skii, Tochin, and Buben⁶ suggests that alkyl radicals do act as electron traps to a significant extent for large single doses.

One of the few remaining possibilities is that the molecular chains themselves may constitute the α , β , and γ traps, i.e., that the electron affinity of a methylene group in a polyethylene chain may be sufficient for the group to trap electrons. This would clearly satisfy (a) and (b), and also (c), since although the methylene groups probably have a very small electron capture probability they are, as the fundamental constituents of polyethylene, present in enormous concentration. But better still, by making some assumptions about the nature of this suggested trapping the quantitative agreement between thermoluminescence and molecular chain motion kinetic constants indicated in (d) can be explained.

As noted in (c), the thermoluminescence emission of polyethylene at constant temperature decays exponentially at a rate different for each glow peak, suggesting a relation

$$n = n_0 e^{-pt}$$

where n_0 is the initial number of trapped electrons per unit volume, n the corresponding number after time t , and p the probability constant for the process. $p = \ln 2 / t_{1/2}$, where $t_{1/2}$ is half life of decay, may be plotted as $\log p$ against $1/T$ in accordance with the Boltzmann relation

$$p = se^{-E/kT} \quad (1)$$

TABLE IA
Activation Energies of Molecular Chain Motion and
Thermoluminescence in Polyethylene

Temperature region	Activation energy, e.v.	
	NMR data ^a	Thermoluminescence data ^b
Below first structural transition	0.035 \pm 0.01 ^c	0.027 \pm 0.005
Above first structural transition	0.22 (average of several values)	0.21 (average of ultraviolet components of β and γ peaks)
Above second structural transition	\sim 0.5 (low-density polyethylene), \sim 0.4 (high-density polyethylene)	0.44 (average of visible components of β and γ peaks)

^a Data of Fuschillo and Sauer¹⁰ and Rempel et al.¹¹

^b See text.

^c Data of Charlesby and Partridge.¹

TABLE IB
Frequency Constants of Molecular Chain Motion and
Thermoluminescence in Polyethylene

Temperature region	Jump frequency of molecular chains, sec. ⁻¹ ^a	Frequency constant $\theta\nu_0$, sec. ⁻¹
Below glass transition temperature T_g	$\sim 10^{-1}$ (for most polymers)	4.6×10^{-3} – 1.23×10^{-1} (for α , β , and γ glow peaks)
Above glass transition temperature T_g	Approaching 10^{13} at extremely high temperatures; much lower at more normal temperatures	5×10^2 (ultraviolet component) – 2.5×10^7 (visible component) (for β and γ glow peaks)

^a Data of Bueche.⁸

The activation energies and frequency constants obtained by Charlesby and Partridge¹ from an Arrhenius plot of this type are repeated here in Tables IA and IB. The activation energy E is often taken to be the electron affinity of the electron trap producing the glow curve, while the frequency constant s has often been visualized as the attempt frequency of the electron trying to escape from its trap, where the trap is tacitly assumed to be immobile (e.g. Randall and Wilkins⁷). However, if the polyethylene molecular chains constitute the α , β , γ traps we must consider these traps as possessing a considerable degree of vibrational motion, especially above the structural transition points. Thus, instead of considering an electron attempting to gain sufficient energy to escape from an immobile trap we may have to picture the electron as somewhat loosely bound (by the electron affinity of a methylene group) to a segment of a vibrating molecular chain which is attempting to "shake it off." This vibrational motion might detach the electron completely from the chain but perhaps more likely is that it will cause the electron to "hop" or "slide" along the chain while never at any point completely ionized with respect to the chain. A comparatively small energy should thus suffice to move the electron along the chain until it combines with an alkyl radical, a double bond, a nearby oxygen atom, or (in view of its proximity) most likely of all in the absence of oxygen its parent luminescence center.

To put this concept on a quantitative basis we now define ν_c as the frequency with which the chain segments vibrate (i.e., the frequency with which the chain segments receive sufficient thermal energy E_c to allow them to move from one position to another), and θ as the probability per vibration that an electron trapped on one of these segments will be released to recombine with its parent luminescence center (for the "hopping" mechanism θ would be an average value over the whole process). Thus we can write the rate of electron-luminescence center recombination as

$$dn/dt = -\theta\nu_cn \quad (2)$$

where n is the number of electrons per unit volume still trapped on the polymer chain at time t .

The luminescence intensity L at any time t will be proportional to dn/dt , i.e.,

$$L = -\eta dn/dt \quad (3)$$

where η is the luminescence constant.

Integrating eq. (2) at constant temperature yields

$$n = n_0 e^{-\theta v_c t} \quad (4)$$

Combining eqs. (2), (3), and (4) we have

$$L = (\eta \theta n_0) v_c e^{-\theta v_c t} \quad (5)$$

Equation (5) gives the decay of thermoluminescence at constant temperature for the α , β , γ peaks assuming electron trapping on the molecular chains. It is exponential in time as required, since η , θ , and v_c will be constant at constant temperature.

It remains to consider how v_c and θ may vary with temperature. v_c is generally known as the "jump frequency" and it has long been established⁸ that this can be approximately represented by a Boltzmann-type formula at temperatures above the glass transition, whether the material concerned is composed of simple molecules or macromolecules. In the former case the jump frequency is the frequency of individual molecules and in the latter case it is the frequency of segments of the molecular chains. Thus we can write

$$v_c = v_0 e^{-E_c/kT} \quad (6)$$

where E_c is the activation energy of the molecular chain motion, as defined earlier, and v_0 , although not quite constant, is far less temperature-sensitive than the exponential. Below the glass temperature the activation energy for many materials tends to become itself a function of temperature.⁹ However, over a moderate temperature range just below the glass point we may take the activation energy to be roughly constant, and eq. (6) will probably hold approximately over this limited temperature range.

θ might be a function of the amplitude and frequency of the molecular vibrations, but we are probably justified in considering it approximately constant over much of the temperature range below the glass point, and also constant (though perhaps of somewhat different value) for temperatures some way above the glass point.

Equations (5) and (6) can be combined as

$$\ln 2/t_{1/2} = \theta v_c = \theta v_0 e^{-E_c/kT} \quad (7)$$

where $t_{1/2}$ is again the half life of the exponential decay. Equation (7) is identical to eq. (1), except that s has been replaced by θv_0 and E by E_c . It thus predicts that the activation energies of the α , β , and γ peaks above and below the structural transition points are in fact the molecular motion

activation energies of the polyethylene chains, while the frequency constants represent the product of the jump frequencies of the molecular chains and the probability constant for electron release from the chains to the luminescence centers. Table I compares the thermoluminescence values of E_c and θv_0 with the values available for E_c from the nuclear magnetic resonance (NMR) measurements of Fuschillo and Sauer¹⁰ and Rempel et al.¹¹ and the range of values of v_0 discussed by Bueche.⁸ It can be seen that agreement is good between the various activation energies and of the right sort of order for the jump frequencies. Special mention must be made of the NMR value of activation energy below the transition points. In their original work the respective authors did not calculate this value, since the NMR derivative line width (broad component), from which it is obtained, appeared to be virtually constant at low temperatures. However a close examination of their data shows that this line width does actually decrease slightly with increasing temperature below the transition points, suggesting a slight increase in molecular motion. The activation energy of this motion was calculated from the data of Fuschillo and Sauer¹⁰ (who provided a more accurate graph of line width versus temperature than Rempel et al.) by using the formula the latter group had employed:

$$v_c/\mu = \Delta v / [\tan(\pi/2)(\Delta v/B)^2]$$

where Δv is the absorption line width, B the line width before motion commences, and μ is a constant.

A plot of $\log v_c/\mu$ against $1/T$, taking B as 15.7 gauss, then gave the apparent activation energy shown in Table I.

A feature of this concept of electron trapping on vibrating molecular chains is that the electron affinity of the chain segments is not measured by the thermoluminescence activation energy. However the electron affinity is actually included in θ , since if the affinity approaches infinity then θ approaches zero. The actual electron affinity of the chain segments would probably be best measured by optical bleaching. Measurements by Nikol'skiĭ, Tochin, and Buben⁶ on the optically activated luminescence emission from electron-irradiated polyethylenes and paraffins showed that untrapping of electrons occurred even at 10,000 Å. (1.24 e.v.). Thus the electron affinity of long-chain saturated hydrocarbon molecules is probably less than 1 e.v. but no actual values for it seem to have been proposed.

The difference between the α , β , and γ glow peaks on this model lies in their θv_0 values, but since either of these quantities could be structure-sensitive it is not clear which has the dominant effect in determining the position of the glow peaks in the glow curve. Also it is not at present obvious why the two activation energies for molecular chain motion above the transition temperatures should be separately associated with the visible and ultraviolet components of the thermoluminescence emission.¹

Although the discussion of this model has hitherto concerned only thermoluminescence and NMR studies of polyethylene it can be seen from Table II that electrical conductivity induced in polyethylene by a prior

irradiation yields activation energies that are in general agreement with those of the other two methods, thus suggesting that the same chain-trapping mechanism (for electrons and possibly even positive charge carriers) may apply to this and other phenomena.

The thermoluminescence mechanism suggested here, in which electrons are released from one type of trap (the molecular chains) to one type of luminescence center (carbonyl ions) differs from the mechanism originally

TABLE II
Activation Energies of Radiation-Induced
Electrical Conductivity in Polyethylene

References	Activation energy, e.v.	
	Below 0°C.	Above 0°C.
12	0.03	
13	0.05	0.26
14		0.35
15		0.35
16		0.36

suggested² in which one type of trap released electrons to a number of different types of luminescence centers of different electron capture probability. This is because the luminescence centers have since been shown to be of only one type,^{3,4} while the difference in glow peak positions in the glow curve is here indicated as being actually due to the different degrees of molecular motion in different structural regions of the polyethylene.

Conclusion

The explanation of the quantitative agreement between the thermoluminescence and molecular chain motion kinetic constants on the basis of the chain trapping model does not by itself exclusively identify the molecular chains with the α , β , and γ traps, since other entities intimately associated with the chains might conceivably be the actual electron traps. Thus, for example, structural defects might be considered as the α , and possibly β , traps and would thus agree with (a), (b), and (d), although not necessarily with (c), as nothing is known of the electron-capture efficiency or concentration of such defects. However the concept of the polyethylene molecular chains themselves being the α , β , and γ traps can, as has been shown, plausibly correlate with all the presently available qualitative and quantitative experimental evidence and it is concluded that this constitutes quite the most likely assignment for these electron traps and possibly for the traps observed in electrical conductivity studies as well. This assignment also fits well with the hitherto rather obscure conclusion of Nikol'skiĭ, Tochin, and Buben⁶ that the electrons trapped in irradiated polyethylene at low temperature are released not by thermal activation but by the "un-freezing of molecular motions" in the material.

The author wishes to thank Prof. A. Charlesby for his continued support and interest in this work.

References

1. Charlesby, A., and R. H. Partridge, *Proc. Roy. Soc. (London)*, **A271**, 170 (1963).
2. Charlesby, A., and R. H. Partridge, *Proc. Roy. Soc. (London)*, **A271**, 188 (1963).
3. Charlesby, A., and R. H. Partridge, *Proc. Roy. Soc. (London)*, **A283**, 312, 329 (1965).
4. Partridge, R. H., Thesis, University of London, 1964.
5. Partridge, R. H. and A. Charlesby, *J. Polymer Sci.*, **B1**, 439 (1963).
6. Nikol'skii, V. G., V. A. Tochin, and N. Ya. Buben, *Fiz. Tverd. Tela*, **5**, 2248 (1963).
7. Randall, J. T., and M. H. F. Wilkins, *Proc. Roy. Soc. (London)*, **A184**, 366 (1945).
8. Bueche, F., *Physical Properties of Polymers*, Interscience, New York, 1962.
9. Bueche, F., *J. Chem. Phys.*, **30**, 748 (1959).
10. Fuschillo, N., and J. A. Sauer, *J. Appl. Phys.*, **28**, 1073 (1957).
11. Rempel, R. C., H. E. Weaver, R. H. Sands, and R. L. Miller, *J. Appl. Phys.*, **28**, 1082 (1957).
12. Mayburg, S., and W. L. Lawrence, *J. Appl. Phys.*, **23**, 1006 (1952).
13. Meyer, R. A., O.N.R. Symposium Report ACR2, Washington, 1954, p. 93.
14. Coleman, J. H., *Conf. Electrical Insulation*, **23**, 51 (NAS-NRC) (1954).
15. Fowler, J. F., *Proc. Roy. Soc. (London)*, **A236**, 464 (1956).
16. Wintle, H. J., Thesis, University of London, 1963.

Résumé

Les résultats qualitatifs et quantitatifs obtenus lors d'études antérieures sur la thermoluminescence induite dans le polyéthylène par irradiation ont été employés en vue de déduire les principaux capteurs d'électrons du polyéthylène. On peut conclure que les capteurs les plus probables sont les chaînes moléculaires elles-mêmes, les différents degrés de mouvement moléculaire dans les différentes régions structurales du polyéthylène étant responsables de la non-capture des électrons piégés à des vitesses différentes et par conséquent de l'apparition de multiples pics de luminescence dans la courbe de luminescence. On donne une explication pour la relation entre les énergies d'activation de la thermoluminescence, la conductivité électrique induite par radiation et la mobilité de la chaîne moléculaire (mesurée par NMR) dans le polyéthylène.

Zusammenfassung

Qualitative und quantitative Ergebnisse früherer Untersuchungen der in Polyäthylen durch Bestrahlung induzierten Thermolumineszenz werden versuchsweise zu Bestimmung der hauptsächlichsten Elektronenfallen in Polyäthylen verwendet. Man kommt zu dem Schluss, dass die wahrscheinlichsten Fallen die Molekülketten selbst sind, wobei die verschiedenen Grade der Molekülbewegung in verschiedenen Strukturbereichen des Polyäthylens für die Freisetzung der eingefangenen Elektronen mit verschiedener Geschwindigkeit und daher für das Auftreten mehrfacher Leuchtmaxima in der Leuchtcurve verantwortlich sind. Eine Erklärung für das Korrespondieren der Aktivierungsenergie bei der Thermolumineszenz, der strahlungsinduzierten elektrischen Leitfähigkeit und der Molekülkettenbewegung (gemessen durch NMR) bei Polyäthylen wird gegeben.

Received September 25, 1964

Revised January 15, 1965

Prod. No. 4671A

Melting of Homopolymers under Pressure

ERIC BAER and JOHN L. KARDOS, *Polymer Science and Engineering, Case Institute of Technology, Cleveland, Ohio*

Synopsis

The effect of pressure on the melting of polyethylene, polypropylene, poly(ethylene oxide), and poly-3,3-bis(chloromethyloxy)cyclobutane (Penton), has been studied up to 3000 atm. The melting temperature-pressure curves for all polymers studied rose indefinitely with pressure, thus behaving in a manner similar to that previously reported for long-chain hydrocarbons. For polyethylene, analysis of the total entropy change on melting, in terms of changes in configurational and volume entropies showed that the percentage of the total entropy change due to change in configurational entropy increased rapidly with pressure, attaining a value of 90% at 3000 atm. The changes in the configurational entropies of melting for polypropylene, poly(ethylene oxide), and Penton were subsequently shown to be lower than that of polyethylene suggesting more melt order. This could arise from helical conformations in the melt for polypropylene and polyethylene oxide and from a stabilized planar zigzag conformation in the Penton melt. A pronounced broadening of the melting range with pressure was attributed to pressure-sensitive transitions which are known to occur near the melting temperature and also to the effect of molecular weight distribution.

INTRODUCTION

Early work on the melting under high pressure of elements, inorganic compounds, and simple organic compounds was conducted primarily by Tammann and Bridgman.¹ More recently Strong² has examined the melting and other solid-phase transitions at very high pressures for several metals. In an effort to bridge the gap between organic materials of low molecular weight and the more complex crystalline polymers, Nelson et al.³ have studied the melting behavior of a series of *n*-paraffins at high pressure.

The melting of a polymer under pressure was first carried out by Wood et al.,⁴ who determined the effect of pressure on the melting temperature of "stark" rubber. The temperature of melting was found to increase on the average 0.029°C./atm. as the pressure was raised to 1000 atm. Since then, measurements of the effect of pressure on the melting of polyethylene have been carried out by several investigators.⁵⁻⁹ In all cases the melting temperature increased about 0.02°C./atm. Also, some melting measurements up to 400 atm. have been reported for polytetrafluoroethylene,¹⁰ polypropylene, and poly(ethylene oxide).¹¹ In a study of the melting of crystalline polyesters up to 2000 atm., Jenckel and Rinkins¹² described the effect of pressure and molecular weight on the shape of the melting curve as well as the melting temperature itself.

Knowledge of the melting transition of crystalline polymers at high pressures is important because both thermodynamic and structural information can be obtained which experiments at atmospheric pressure do not yield directly. Moreover, in order to crystallize a polymer under pressure at a predetermined degree of supercooling, it is necessary to know accurately the effect of pressure on the melting temperature. Accordingly, this paper presents the effect of pressure on the melting points of polyethylene, polypropylene, poly(ethylene oxide), and poly-3,3-bischloromethyloxacyclobutane (Penton), at pressures up to 3000 atm. The data have been analyzed thermodynamically and the results interpreted by suggesting specific structural changes during melting.

EXPERIMENTAL

Apparatus

The high-pressure dilatometer, shown in Figure 1, consisted of three major components: a low-pressure cylinder, an intensifier train, and a high-pressure bomb housing the sample. Proper alignment of the components was maintained by four nickel-steel draw rods connecting two large nickel-steel plates, and a precision ball bushing housed in the top plate which assured linear travel of the intensifier shaft.

The bomb and seal assembly are shown in Figure 2. The bomb was machined from a chromium-vanadium steel rod and polished after heat-treating to yield a smooth, low-friction surface. Closure of the bottom of the sample chamber was accomplished with a compression seal made up of a thin copper disk, a tool-steel plug housing a thermocouple, and a threaded nickel-steel plug. Since motion of the upper seal was necessary, a Bridgman-type unsupported-area closure was employed. The packing consisted of a Teflon ring backed with a copper ring. At low pressures the Teflon ring alone prevented the melted polymer sample from leaking. However, at

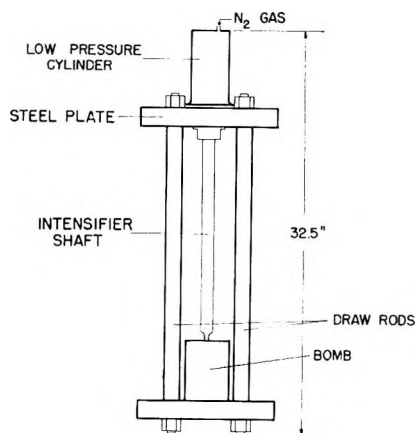


Fig. 1. High pressure bomb and frame assembly.

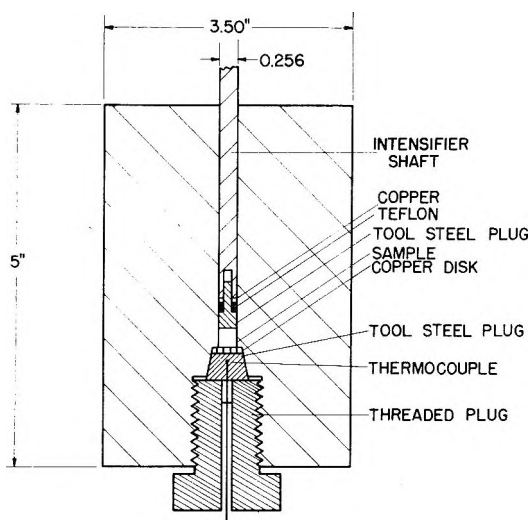


Fig. 2. Sample bomb and seal assembly.

high pressures the Teflon flowed too readily into the clearance around the intensifier shaft, resulting in leaks. The copper ring was added to back up the Teflon to give a leak-free movable seal at all conditions used in this study. Temperature control to within $\pm 1^\circ\text{C}$. up to 250°C . was obtained by submerging the dilatometer into a modified air oven.

Volume changes were measured by detecting the vertical displacement of the intensifier shaft to an accuracy of 0.0001 in. with an Ames dial micrometer. Corrections for the compressibility and thermal expansion of the upper seal and for the thermal expansion of the bomb amounted to less than 2% of the total volume change in a single melting experiment.

Pressure Measurements and Calibration

The source of pressure for this study was provided by a standard 2000 psi cylinder of nitrogen. A Matheson automatic gas regulator having a 1000 psi capacity and a Heise bourdon tube gauge accurate to ± 1 psi for a dial range of 2000 psi served to regulate and measure the pressure in the low-pressure cylinder.

Appropriate reductions in cross-sectional area in the intensifier train provided a theoretical pressure magnification of 138. Due to friction in the packing of the unsupported-area seal, the pressure in the sample chamber differed from that calculated using the intensifier ratio. Therefore, it was necessary to calibrate the apparatus at all temperature and pressure conditions used. This was accomplished by observing the polymorphic transitions of silver iodide and ammonium iodide which were determined accurately by Bridgman.¹³ In this manner, the actual pressure in the sample chamber for a given nitrogen pressure was determined to an accuracy of ± 15 atm.

Materials and Procedure

The crystalline polymers used in this study are listed in Table I. A titration-floatation technique was used to determine densities.

TABLE I
Crystalline Polymers Used in Investigation

Polymer	Trade name	Density at 30°C.	Crystallinity, % (based on density)
Polyethylene		0.932	56
Polypropylene	Profax ^a	0.903	69
Poly-3,3-bis(chloromethyl- oxacyclobutane	Penton ^a	1.399	30
Poly(ethylene oxide)	Carbowax 4000 ^b	1.214	85

^a Registered trademark of Hercules Powder Co.

^b Registered trademark of Union Carbide Chemicals Co.

After loading the bomb with polymer, it was placed in the frame assembly. The sample was compressed for 1 hr. at 100 atm. above the pressure at which the melting was to take place. This allowed a thorough seating of the seal in addition to removing volume changes due to time-dependent compressibility. After decreasing the pressure to the desired value the oven temperature was increased in 20°C. increments resulting in a sample heating rate of about 10°C./hr. In the vicinity of the melting point the heating rate was decreased to a value of 2-7°C./hr., depending on the polymer being melted. Following each melting run, the sample was allowed to crystallize at the melting pressure by slowly cooling to room temperature.

EXPERIMENTAL RESULTS

Three of the isobaric melting curves for polypropylene, whose general shapes are the same for all the polymers studied, are shown in Figure 3. The melting temperature T_m was taken in the usual manner at the point where the specific volume curve suddenly breaks to form a slowly changing plateau region in the melt. This break is quite sharp and leads to an error of less than 1°C. in choosing the melting temperature.

The volume of melting was determined by measuring the difference between the volume at T_m and the volume where the curve begins to deviate from the normal thermal expansion behavior of solid polymer, defined as T' in Figure 3. This change in volume was then corrected for the extrapolated normal thermal expansion of the solid polymer in the temperature interval $\Delta T = T_m - T'$, thus yielding a volume change describing the change from a solid to a melt at the melting temperature. The error in the determination of the volume of melting is $\pm 8\%$ and is due largely to the error in choosing the point of deviation from the normal thermal expansion of the solid polymer. The two outstanding features of Figure 3 are the marked

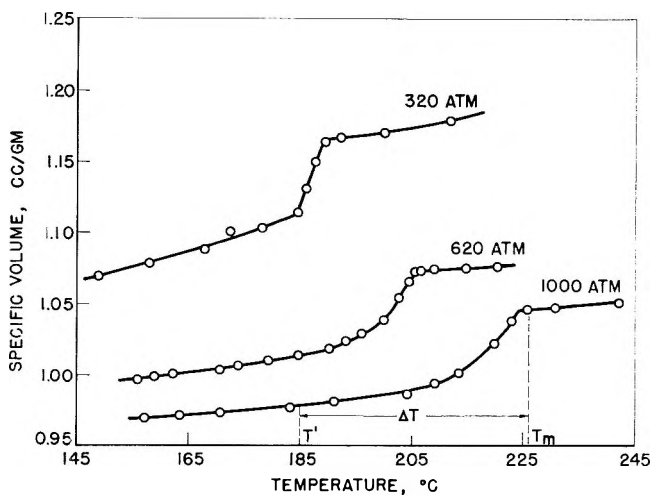


Fig. 3. Specific volume vs. temperature at various pressures for polypropylene.

broadening of the melting range and the pronounced increase of the melting temperature with increase in pressure. Table II illustrates the effect of pressure on the broadening of the melting range, $\Delta T'$. For all the polymers studied, $\Delta T'$ increases significantly with pressure.

TABLE II
Effect of Pressure on the Broadening of the Melting Range

Polymer	Pressure, atm.	T_m , °C.	T' , °C.	$\Delta T'$, °C.
Poly(ethylene oxide)	1	60	54	6
	1500	80	67	13
	3000	94	74	20
Polypropylene	1	174	155	19
	1000	226	185	41
	2000	243	180	63
Polyethylene	1	136	112	24
	1500	177	144	33
	3000	204	145	59
Penton	1	181	161	20
	1500	208	182	26
	3000	222	163	59

The dependence of the melting temperature on pressure is shown in Figures 4 and 5. Both the melting temperature and the volume of melting at 1 atm. were measured with a standard dilatometer by using the technique of Bekkedahl.¹⁴ In all cases, a smooth curve concave toward the pressure axis resulted. From the slope dP/dT_m , shown in Figures 6 and 7, was found to an accuracy of $\pm 5\%$. The results indicate that the melting temperature of polypropylene increases more with pressure than the other polymers studied, and that poly(ethylene oxide) is least affected.

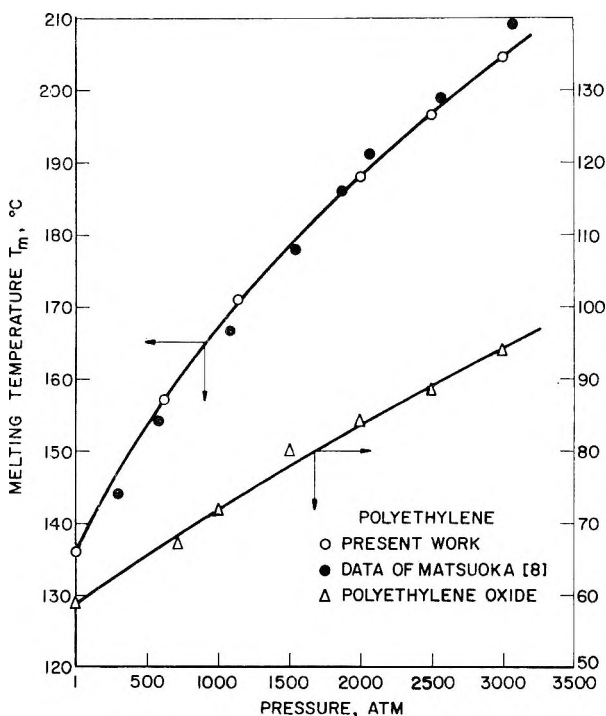


Fig. 4. Effect of pressure on the melting temperature of polyethylene and poly(ethylene oxide).

The volumes of melting as a function of pressure, corrected to 100% crystallinity, are shown in Figure 8. The values at atmospheric pressure were measured in a standard dilatometer with the exception of poly(ethylene oxide) which was obtained by extrapolation. The curves are convex toward the pressure axis, suggesting that they do not approach zero. Once the melting temperature, dP/dT_m , and the volume of melting are known, the

TABLE III
Comparison of the Observed Enthalpy at Atmospheric Pressure with Values Reported in Literature

Polymer	Enthalpy of fusion, cal./g.		Investigator (method)
	Observed	Literature values	
Polyethylene	54.3	66.5	Wunderlich and Dole ²⁶ (calorimetry)
Polypropylene	25.1	35.0	Wilkinson and Dole ¹⁶ (calorimetry)
Poly(ethylene oxide)	50.6	45.0	Mandelkern ³² (melting point depression)
Penton	37.0	35.4	Inoue ³³ (DTA)

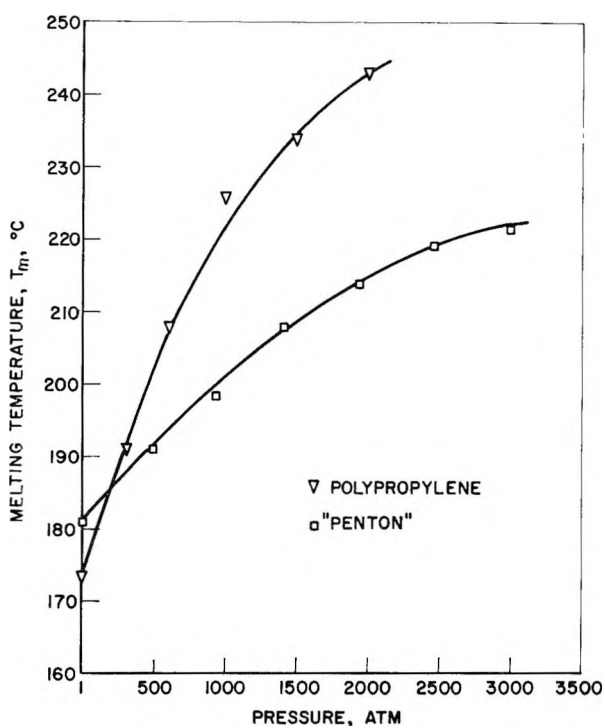


Fig. 5. Effect of pressure on the melting temperature of polypropylene and Penton.

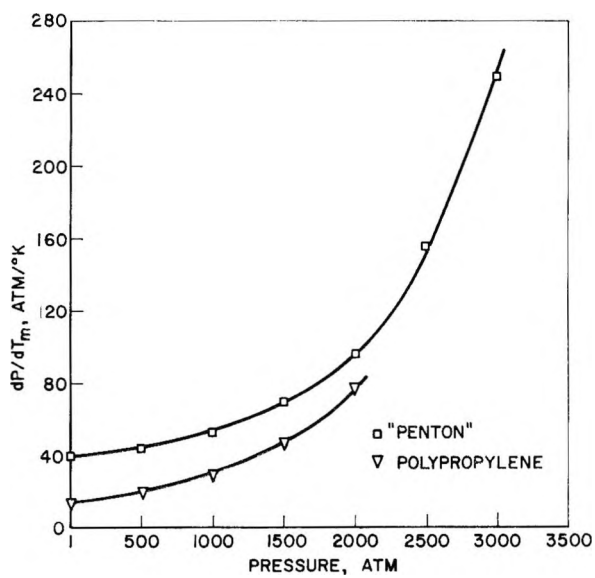


Fig. 6. Effect on pressure on dP/dT_m for Penton and polypropylene.

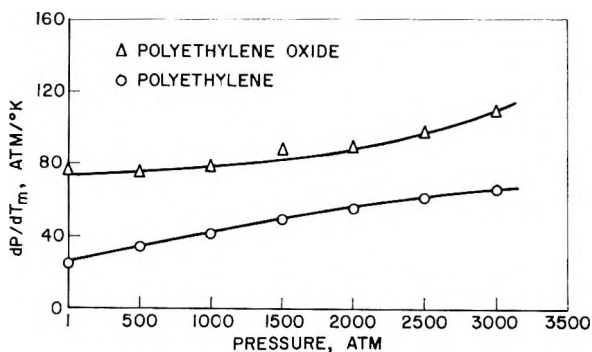


Fig. 7. Effect of pressure on dP/dT_m for poly(ethylene oxide) and polyethylene.

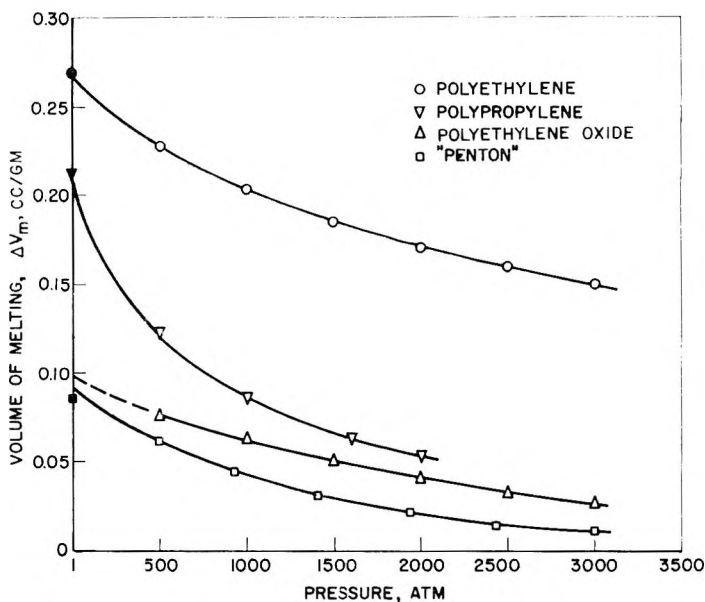


Fig. 8. Effect of pressure on the volume of melting based on 100% crystallinity. Filled symbols indicate dilatometer data.

Clapeyron equation may be employed to determine the enthalpy and entropy of melting.

In Table III, a comparison of the observed enthalpy of melting at atmospheric pressure with values reported in the literature shows fair agreement within experimental error with the exception of polypropylene. By compounding all experimental errors (dP/dT_m , $\pm 5\%$; volume of melting, $\pm 8\%$; and crystallinity values, $\pm 5\%$) the values for ΔH_m and ΔS_m may be in error by as much as $\pm 18\%$. The observed value of ΔH_m for perfectly crystalline polypropylene (25.1 cal./g.) is lower than values reported in the literature, which range from 62 cal./g. as determined by a diluent method¹⁵ to 35 cal./g. by calorimetry.¹⁶ However, some values as

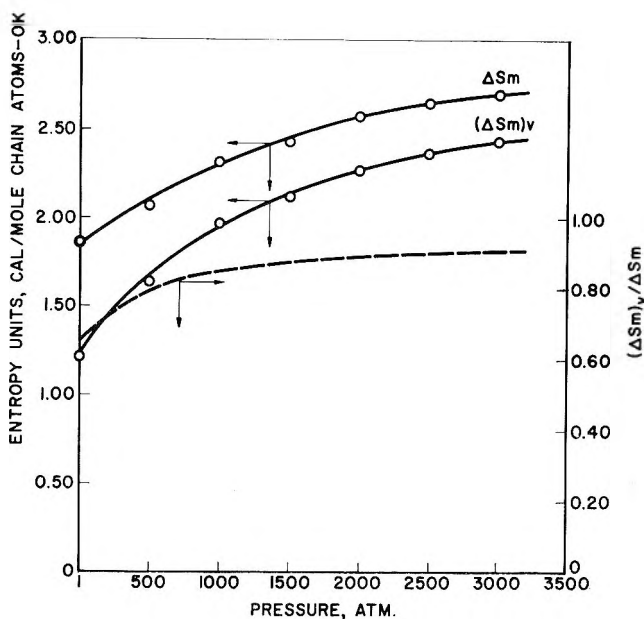


Fig. 9. Effect of pressure on the total, ΔS_m , and the configurational $(\Delta S_m)_v$ entropies of melting for polyethylene. Dashed curve shows the effect of pressure on the ratio, $(\Delta S_m)_v / \Delta S_m$.

low as 15.4 cal./g. have been reported,^{17,18} although it is not clear whether or not these are for perfectly crystalline polypropylene. These wide differences may be due to the method of determining crystallinity as well as to variation in sequence lengths and sequence distribution in the crystallizable polypropylene chain. Consequently, in order to compare enthalpies of fusion for perfectly crystalline polypropylene, knowledge of the specific stereoregularity and the method of crystallinity determination are needed.

Mandelkern¹⁹ has suggested that the total entropy change on melting can be divided into two parts; one due to volume change and the other arising from a change in configurational entropy of melting. In terms of thermodynamic quantities this can be expressed as follows,

$$\Delta S_m = (\Delta S_m)_v + (dP/dT)_v \Delta V_m$$

where ΔS_m is the total entropy of melting, $(\Delta S_m)_v$ is the configurational entropy, $(dP/dT)_v$ is the thermal pressure coefficient at constant volume, and ΔV_m is the volume change on melting per mole of crystalline repeat unit. In order to calculate the configurational entropy of polyethylene, the thermal pressure coefficient was calculated by using the data of Hellwege et al.²⁰ Sufficient data to do likewise for the other polymers studied are not available in the literature.

In Figure 9, the total entropy of melting, the configurational entropy of melting, and the ratio of these quantities for polyethylene are plotted

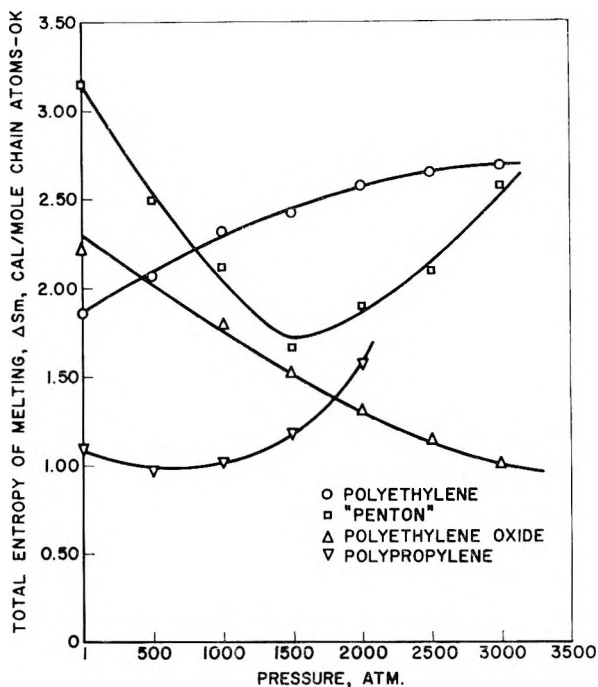


Fig. 10. Effect of pressure on the total entropy of melting.

against pressure. The results indicate that the fraction of the total melting entropy change due to configurational entropy becomes larger as the pressure increases. The configurational and volume entropies at atmospheric pressure (1.22 and 0.64 cal./mole chain atoms—°K.) may be compared with values obtained by Starkweather and Boyd²¹ (1.77 and 0.52 cal./mole chain atoms—°K.). These differences may be attributed to experimental error.

The entropy of melting per mole chain atoms as a function of pressure is shown in Figure 10. It is interesting to note that polyethylene has the highest total entropy of melting at 3000 atm., while at atmospheric pressure it is lower than that of poly(ethylene oxide) and Penton. In addition the curves for Penton and polypropylene show a definite minimum in the pressure range investigated. This rather complex behavior will be analyzed further in the discussion.

DISCUSSION

Bridgman,¹ in his studies of the elements and low molecular weight substances, showed that the melting curve of most materials rises indefinitely with pressure at a continually decreasing rate. Examination of the data in Figures 4 and 5 shows that polymers behave in a similar manner. No maximum in the melting temperature–pressure curve appears possible unless pressure induces chain rupture or a solid–solid transition to a more

TABLE IV
Effect of Pressure on the Melting of Various Substances

Material	Initial dT_m/dP , °C./atm.
Iron ^a	0.0025
Nickel ^a	0.0032
Sodium ^a	0.0089
Poly(ethylene oxide)	0.013
<i>n</i> -C ₉ ^b	0.014
<i>n</i> -C ₂₄ ^b	0.026
Penton	0.026
Polyethylene	0.039
Polypropylene	0.067

^a Data of Strong.²

^b Data of Nelson et al.³

compact structure. Attempts to fit the melting curves to the semiempirical expression proposed by Simon²² were unsuccessful. The equation, which has adequately described some elements and low molecular weight substances,^{2,3,23} is apparently not applicable to polymers. In Table IV, the initial slopes of the melting curves of various materials are compared. The melting points of metals are much less affected by pressure, while long-chain hydrocarbons give values similar to those obtained for polymers.

The complex shape of the total entropy of melting versus pressure curves shown in Figure 10 can be explained as follows. Figure 9 shows that the configurational entropy on melting increases from 60% of the total entropy at 1 atm. to 90% at 3000 atm. Since the volume entropy change decreases with pressure while the configurational entropy change increases, the relative amounts of these opposing pressure effects determine whether the total entropy change will increase or decrease with pressure.

If the volume entropy change decreases with pressure (high melt compressibility) more than the configurational entropy change increases due to increasing temperature, a net decrease in the total entropy change can result. This implies, in agreement with Frenkel,²⁴ that the melt can become more ordered with pressure than the solid. Such behavior is exemplified in Figure 10, where polypropylene, poly(ethylene oxide), and Penton all show initial decreases in the total entropy of melting with pressure. On the other hand, as the pressure is increased further, the configurational entropy change increases, while the volume change portion of the total entropy change becomes small and changes very little with pressure, leading to a net increase in the total entropy change. This explains the minimum observed in the total entropy versus pressure curves for polypropylene and Penton in Figure 10. Although the slope of the poly(ethylene oxide) curve is negative throughout the entire pressure range studied, it becomes less negative with pressure, and a minimum is expected at some higher pressure. Polyethylene, unlike the other three polymers, exhibits an initial increase in the total entropy change with pressure, which suggests

that the decrease in volume entropy change with pressure for polyethylene is quite small (see Fig. 9).

Presumably, any retention of order in the melt or residual melt structure should lead to a low entropy of melting. By comparing the configurational entropy changes on melting for various polymers, the relative degree of melt order may be determined at any pressure. Unfortunately, sufficient data were not available to calculate the configurational entropy for all the polymers studied. However, it was shown that at higher pressures the total entropy change on melting for polyethylene is composed mainly of configurational entropy change (90%). In addition, at 1 atm. the percentage of total entropy change on melting due to configurational entropy change is greater than 60% for poly(ethylene oxide)²⁵ and other polymers not included here.²¹ Also, this percentage increases with pressure for all polymers. Consequently, by comparing the total entropies at a higher pressure, the relative degree of melt order can be determined.

At 1500 atm., the total entropy of melting for polypropylene is the lowest of the four polymers shown in Figure 10. This implies a relatively high degree of melt order which may be due to partial retention of the solid state helical conformation of polypropylene in the melt. Dole and Wunderlich²⁶ have pointed out that polypropylene has a low chain flexibility in the melt due to a high barrier for rotation about the C-C bonds, and recently Beck and Hiltz²⁷ have found a transition in polypropylene about 30°C. above the melting temperature indicating some type of melt order. Poly(ethylene oxide) also exhibits a low total entropy of melting. Again, partial retention of helical order in the melt may be responsible. Penton exhibits a low entropy change on melting, although it is higher than that for either polypropylene or poly(ethylene oxide). Even though Penton has a planar zigzag conformation in the solid like polyethylene, a high barrier to rotation about the C-C bonds can exist in the melt due to the large polar chlorine atoms located on opposite sides of the zigzag plane. The total entropy change on melting for polyethylene is much higher than for any of the other polymers shown in Figure 10. This is reasonable when one considers that the planar zigzag conformation of polyethylene in the solid state is not likely to be stabilized in the melt because of a relatively low rotation barrier which leads to a greater chain flexibility. It is interesting to note that at 1500 atm. the two "helical" polymers, i.e., poly(ethylene oxide) and polypropylene, have more ordered melts than does the chlorine-stabilized Penton. It should be pointed out that although the above comparison was made at 1500 atm., the conclusion that polyethylene exhibits the most melt disorder holds true over the range of 1000-2500 atm. In addition, the fact that at even higher pressures the total melting entropies of polypropylene and Penton approach that of polyethylene is consistent with the above suggestions, since at these pressures the high temperatures may destroy melt order, resulting in a larger total entropy change on melting. The importance of choosing a high pressure at which the configurational entropy change makes up a high percentage of the total entropy change should be empha-

sized. A comparison of the total entropy change for the four polymers at one atm. does not yield explainable melt order information because of the significant contribution of the volume change entropy to the total entropy change on melting.

The "upper part" of the melting transition may be treated as a first-order transition. However, the broadening of the melting range with pressure summarized in Table II indicates that the overall melting process is far more complex. Jerckel and Rinkens¹² have shown that molecular weight affects the broadening of the melting point. However, solid-state transitions near the melting point may also contribute to a broadening of the melting range. In a detailed study of dynamic mechanical behavior of linear polyethylene, Takayanagi²⁸ has isolated two separate loss peaks very near the melting point. From an analysis of the effect of frequency on the loss peaks and an estimate of the energies of activation, he suggests that the transition at about 80°C. is due to rotational vibration around the molecular axis in the crystalline lattice, while that at about 115°C. is due to vibration of chain segments in the direction of the molecular axis in the crystalline lattice. While a portion of the melting interval is undoubtedly due to molecular weight distribution, the pronounced broadening of the melting interval under pressure may also be caused by transitions of the type described above being separated according to their pressure sensitivity.

Recently, a considerable amount of research has been devoted to the crystallization of polyethylene under high pressure from both dilute solutions²⁹ and the melt.³⁰ Geil et al.,³¹ in a study of the morphology of pressure-crystallized polyethylene, have confirmed the presence of extended-chain lamellae and suggested that molecular weight fractionation may take place during the growth of the extended crystals. In order to pin down such phenomena experimentally it is important to know the degree of supercooling of the polymer as it crystallizes isothermally under pressure. The data presented here provide a basis from which crystallization experiments under pressure can be conducted at known degrees of supercooling.

The authors wish to thank the National Science Foundation and the Manufacturing Chemists' Association for their generous financial support of this work.

We are especially indebted to Professors Geil, Koenig, and Maron for their stimulating discussions and suggestions. Special credit is due Mr. A. Christiansen who performed the dilatometric runs at atmospheric pressure.

References

1. Bridgman, P. W., *The Physics of High Pressure*, London, 1949.
2. Strong, H. M., in *Progress in Very High Pressure Research*, F. P. Bundy, W. R. Hibbard, Jr., and H. M. Strong, Eds., Wiley, New York, 1961.
3. Nelson, R. R., W. Webb, and J. A. Dixon, *J. Chem. Phys.*, **33**, 1956 (1960).
4. Wood, L. A., N. Bekkedahl, and R. E. Gibson, *J. Chem. Phys.*, **13**, 475 (1945).
5. Parks, W., and R. B. Richards, *Trans. Faraday Soc.*, **45**, 203 (1949).
6. Matsuoka, S., and B. Maxwell, *J. Polymer Sci.*, **32**, 131 (1958).
7. Matsuoka, S., and C. J. Aloisio, *J. Appl. Polymer Sci.*, **4**, 116 (1960).
8. Matsuoka, S., *J. Polymer Sci.*, **57**, 569 (1962).
9. Hellwege, K. H., W. Knappe, and P. Lehmann, *Kolloid-Z.*, **183**, 110 (1962).

10. McGeer, P. L., and H. C. Duus, *J. Chem. Phys.*, **20**, 1813 (1952).
11. Fortune, L. R., and G. N. Malcolm, *J. Phys. Chem.*, **64**, 934 (1960).
12. Jenckel, E., and H. Rinkens, *Z. Elektrochem.*, **60**, 970 (1956).
13. Bridgman, P. W., *Proc. Am. Acad. Art Sci.*, **51**, 55 (1915); *ibid.*, **52**, 91 (1916).
14. Bekkedahl, N., *J. Res. Natl. Bur. Std.*, **42**, 145 (1949).
15. Danusso, F., G. Moraglio, and E. Flores, *Atti Accad. Nazl. Lincei, Rend. Classe Sci., Fis. Mat. Nat.*, **25**, 520 (1958).
16. Wilkinson, R. W., and M. Dole, *J. Polymer Sci.*, **58**, 1089 (1962).
17. Ke, B., *J. Polymer Sci.*, **42**, 15 (1960).
18. Gee, G., *Proc. Chem. Soc.*, **1957**, 111.
19. Mandelkern, L., *Crystallization of Polymers*, McGraw-Hill, New York, 1964.
20. Hellwege, K. H., W. Knappe, and P. Lehmann, *Kolloid-Z.*, **183**, 110 (1962).
21. Starkweather, H. W., and R. H. Boyd, *J. Phys. Chem.*, **64**, 410 (1960).
22. Simon, F., *Z. Elektrochem.*, **35**, 618 (1929).
23. Bridgman, P. W., *Proc. Am. Acad. Sci.*, **81**, 190 (1952); *ibid.*, **81**, 228 (1952); *ibid.*, **74**, 438 (1942).
24. Frenkel, J., *Kinetic Theory of Liquids*, New York, 1955.
25. Malcolm, G. N., and G. L. D. Ritchie, *J. Phys. Chem.*, **66**, 852 (1962).
26. Dole, M., and B. Wunderlich, *Makromol. Chem.*, **34**, 29 (1959).
27. Beck, D. L., and A. A. Hiltz, *SPE Trans.*, **5**, 15 (1965).
28. Takayanagi, M., *Mem. Fac. Eng. Kyushu Univ.*, **23**, No. 1, 72 (1963).
29. Wunderlich, B., *J. Polymer Sci.*, **A1**, 1245 (1963).
30. Wunderlich, B., and T. Arakawa, *J. Polymer Sci.*, **A2**, 3697 (1964).
31. Geil, P. H., F. R. Anderson, B. Wunderlich, and T. Arakawa, *J. Polymer Sci.*, **A2**, 3707 (1964).
32. Mandelkern, L., *J. Appl. Phys.*, **26**, 443 (1955).
33. Inoue, M., *J. Polymer Sci.*, **A1**, 2697 (1963).

Résumé

On a étudié jusqu'à 3.000 atmosphères l'influence de la pression sur la fusion du polyéthylène, du polypropylène, de l'oxyde de polyéthylène et du poly-(3,3-bischlorométhyl-oxacyclobutane), "Penton." Les courbes de température de fusion-pression pour tous les polymères étudiés s'élevaient indéfiniment avec la pression, se comportant donc d'une façon semblable à celle décrite antérieurement pour les longues chaînes hydrocarbonées. Pour le polyéthylène, l'analyse du changement total d'entropie, par fusion, en fonction des changements dans les entropies de configuration et de volume montre que le pourcentage du changement total d'entropie dû au changement de l'entropie de configuration augmente rapidement avec la pression pour atteindre une valeur de 90% à 3.000 atms. On a montré ultérieurement que les changements dans les entropies de configuration à la fusion pour le polypropylène, l'oxyde de polyéthylène et le "Penton" sont plus faibles que ceux du polyéthylène, ce qui suggère un ordre de fusion de plus. Cela pourrait provenir des configurations hélicoïdales à l'état fondu pour le polypropylène et l'oxyde de polyéthylène et d'une configuration planaire stabilisée en zig-zag dans le "Penton" à l'état fondu. Un élargissement marqué du domaine de fusion avec la pression est attribué aux transitions sensibles à la pression qui sont connues comme ayant lieu aux environs de la température de fusion et également à l'influence de la distribution du poids moléculaire.

Zusammenfassung

Der Einfluss des Druckes auf das Schmelzen von Polyäthylen, Polypropylen, Polyäthylenoxyd und Poly-(3,3-bischlormethyloxacyclobutan), "Penton," wurde bis zu 3000 Atmosphären untersucht. Die Schmelztemperatur-Druckkurve stieg bei allen untersuchten Polymeren mit dem Druck unbegrenzt an und verhält sich daher ähnlich, wie es

früher bei langkettigen Kohlenwasserstoffen gefunden wurde. Bei Polyäthylen zeigte eine Analyse der Gesamtentropieänderung beim Schmelzen durch Zerlegung in Konfigurations- und Volumsentropieänderung, dass der prozentuelle Anteil der Konfigurationsentropieänderung an der gesamten Entropieänderung mit dem Druck rasch zunimmt und bei 3000 at einen Wert von 90% erreicht. Weiters wurde gezeigt, dass die Änderung der Konfigurationsentropie beim Schmelzen für Polypropylen, Polyäthylenoxyd und "Penton" niedriger als die von Polyäthylen war, was für eine höhere Schmelzordnung spricht. Dies konnte durch eine Helixkonformation in der Polypropylen- und Polyäthylenoxydschmelze und durch eine stabilisierte ebene Zick-Zack-Konformation in der "Penton"-Schmelze bedingt sein. Ein ausgeprägte Verbreiterung des Schmelzbereiches mit dem Druck wurde auf druckempfindliche Umwandlungen, welche bekanntlich in der Nähe der Schmelztemperatur auftreten, und auch auf den Einfluss der Molekulargewichtsverteilung zurückgeführt.

Received September 14, 1964

Revised February 24, 1965

Prod. No. 4673A

Integral and Differential Binary Copolymerization Equations*

VICTOR E. MEYER, *Plastics Fundamental Research, The Dow Chemical Company, Midland, Michigan*, and GEORGE G. LOWRY, *Baxter Science Laboratory, Claremont Men's College, Claremont, California*

Synopsis

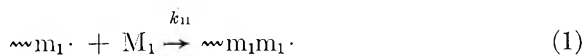
An analytic solution to Skeist's copolymerization equation has been obtained for the case of binary copolymerization. From this solution, a differential copolymer composition equation is also derived. For given values of the reactivity ratios, these equations then permit the convenient calculation of expected binary copolymerization behavior as a function of conversion. Critical conditions leading to incompatible copolymerizations are also discussed.

Introduction

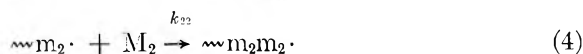
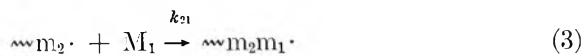
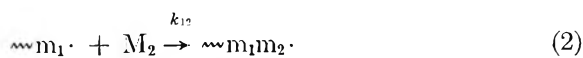
Lewis and Mayo² have developed an equation relating the reactivity ratios to the change in monomer mixture composition during the course of a binary copolymerization. Wall³ derived an equation relating the distribution of chemical composition to degree of conversion, reactivity ratios, and initial monomer mixture composition, but with the restriction that the reactivity ratios be inversely proportional to one another. Walling and Briggs⁴ developed mathematical equations describing the copolymerization of several component systems, but the integration of their equation involved a power series approximation. Skeist⁵ has developed a general formulation of the problem, which requires, however, graphical or numerical methods of evaluation. In this paper, an analytic solution to Skeist's equation is developed for the important case of binary copolymerization. The derivative of this solution then yields the differential copolymer distribution function.

Theory

In the copolymerization of two monomers, M_1 and M_2 , the four different chain growth steps may be indicated by the scheme shown in eqs. (1)-(4) and tabulated in Table I.⁶



* Presented in part to the Division of Polymer Chemistry, 147th meeting of the American Chemical Society, April, 1964.¹



On assuming that the reactivity depends only on the terminal unit and making the steady-state assumption for these free-radical species, an expression may be obtained which relates the instantaneous mole fraction F_1 of monomer M_1 , entering the copolymer from a binary monomer mixture containing f_1 mole fraction of M_1 :^{2,7,8}

TABLE I
Binary Copolymerization Chain Growth Steps

Growing chain	Adding monomer	Rate constant	Reaction product
$\sim\sim m_1 \cdot$	M_1	$\xrightarrow{k_{11}}$	$\sim\sim m_1 m_1 \cdot$
$\sim\sim m_1 \cdot$	M_2	$\xrightarrow{k_{12}}$	$\sim\sim m_1 m_2 \cdot$
$\sim\sim m_2 \cdot$	M_1	$\xrightarrow{k_{21}}$	$\sim\sim m_2 m_1 \cdot$
$\sim\sim m_2 \cdot$	M_2	$\xrightarrow{k_{22}}$	$\sim\sim m_2 m_2 \cdot$

$$F_1 = \frac{r_1 f_1^2 + f_1 f_2}{r_1 f_1^2 + 2f_1 f_2 + r_2 f_2^2} \quad (5)$$

Since, $f_2 = 1 - f_1$, eq. (5) may also be written in a form more convenient for our purposes:

$$F_1 = \frac{(r_1 - 1)f_1^2 + f_1}{(r_1 - r_2 - 2)f_1^2 + 2(1 - r_2)f_1 + r_2} \quad (6)$$

where

$$r_1 = k_{11}/k_{12}$$

$$r_2 = k_{22}/k_{21}$$

$$f_1 = M_1/(M_1 + M_2) = M_1/M = 1 - f_2$$

and

$$F_1 = dM_1/(dM_1 + dM_2) = dM_1/dM = 1 - F_2$$

In general, three different types of copolymerization behavior are normally observed: (1) $r_1 > 1$, $r_2 < 1$ (Fig. 1a); (2) $r_1 < 1$, $r_2 > 1$ (Fig. 1b); and (3) $r_1 < 1$, $r_2 < 1$ (Fig. 1c). The case of both r_1 and r_2 simultaneously being greater than unity does not normally occur.

Since, except at the crossover point,⁸ the instantaneous copolymer composition F_1 is different from the composition of the monomer mixture f_1

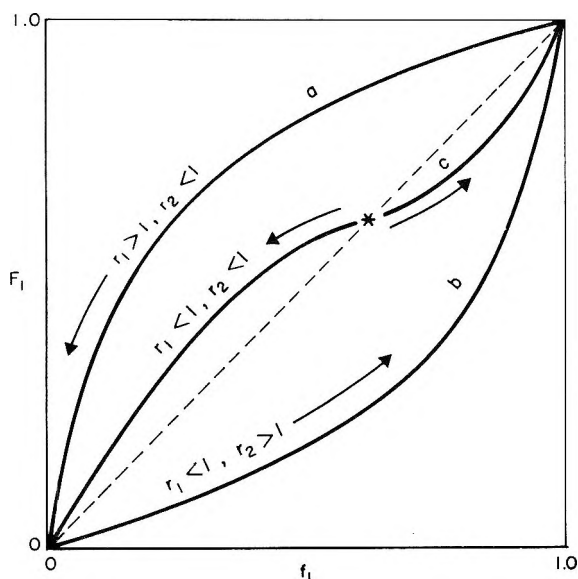


Fig. 1. Instantaneous binary copolymerization behavior. At crossover point (*), $F_1 = f_1 = (1 - r_2)/(2 - r_1 - r_2)$.

from which it is being formed, a drift in both copolymer and monomer mixture composition occurs during the course of a batch-type copolymerization. The direction of drift has been indicated by arrows in Figure 1. It is also to be noted that the direction of drift is in opposite directions about the crossover point.

Skeist⁵ has derived an equation,

$$\ln M/M^0 = \int_{f_1^0}^{f_1} [1/(F_1 - f_1)] df_1 \quad (7)$$

which, for given values of the reactivity ratios, graphical or numerical methods may then be used to calculate the expected change in monomer mixture and copolymer composition corresponding to the mole conversion, $1 - (M/M^0)$.

After substitution of eq. (6) into eq. (7), and rearranging, one obtains:

$$\ln \frac{M}{M^0} = \frac{1}{(2 - r_1 - r_2)} \int_{f_1^0}^{f_1} \frac{(r_1 + r_2 - 2)f_1^2 + 2(1 - r_2)f_1 + r_2}{f_1(f_1 - 1) \left(f_1 - \frac{1 - r_2}{2 - r_1 - r_2} \right)} df_1 \quad (8)$$

Written in this form, eq. (8) may be expanded into easily integrated terms:

$$- \int_{f_1^0}^{f_1} \frac{f_1}{(f_1 - 1)f_1 - \delta} df_1 = \ln \left[\left(\frac{f_1 - 1}{f_1^0 - 1} \right)^{(2 - r_1 - r_2)/(r_1 - 1)} \times \left(\frac{f_1 - \delta}{f_1^0 - \delta} \right)^{(r_2 - 1)/(r_1 - 1)} \right] \quad (9)$$

$$\frac{2(1-r_2)}{2-r_1-r_2} \int_{f_1^0}^{f_1} \frac{df_1}{(f_1-1)(f_1-\delta)} = \ln \times \left[\left(\frac{f_1-1}{f_1^0-1} \right)^{2(r_2-1)/(r_1-1)} \left(\frac{f_1-\delta}{f_1^0-\delta} \right)^{2(1-r_2)/(r_1-1)} \right] \quad (10)$$

and

$$\frac{r_2}{2-r_1-r_2} \int_{f_1^0}^{f_1} \frac{df_1}{f_1(f_1-1)(f_1-\delta)} = \ln \left[\left(\frac{f_1}{f_1^0} \right)^{r_2/(1-r_2)} \times \left(\frac{f_1-1}{f_1^0-1} \right)^{\frac{r_2}{2(r_2-1)} + \frac{r_2(3-2r_2-r_1)}{2(1-r_2)(1-r_1)}} \left(\frac{f_1-\delta}{f_1^0-\delta} \right)^{\frac{r_2}{2(r_2-1)} + \frac{r_2(3-2r_2-r_1)}{2(1-r_2)(r_1-1)}} \right] \quad (11)$$

with the restriction $r_1 \neq 1$, $r_2 \neq 1$.

After collecting terms and rearranging, one obtains:

$$\frac{M}{M^0} = \left(\frac{f_1}{f_1^0} \right)^\alpha \left(\frac{f_2}{f_2^0} \right)^\beta \left(\frac{f_1^0 - \delta}{f_1 - \delta} \right)^\gamma \quad (12)$$

where the constants α , β , γ , and δ have the values: $\alpha = r_2/(1-r_2)$; $\beta = r_1/(1-r_1)$; $\gamma = (1-r_1r_2)/(1-r_1)(1-r_2)$; and $\delta = (1-r_2)/(2-r_1-r_2)$.

The conditions $r_1 = 1$, $r_2 \neq 1$; and $r_2 = 1$, $r_1 \neq 1$ are special cases and are treated separately in Appendices I and II, respectively. The third term on the right of eq. (12) is observed to be a singularity corresponding to azeotropic copolymerizations. It is also observed that if the reactivity ratios are expressed in terms of the number of moles of each component, then eq. (12) may be rearranged to the equation previously derived by Lewis and Mayo.²

The slope of the mole conversion-instantaneous copolymer composition curve, i.e.,

$$\frac{d}{dF_1} \left(1 - \frac{M}{M^0} \right) = - \frac{1}{M^0} \frac{dM}{dF_1} \quad (13)$$

may be obtained from eqs. (12) and (6). Differentiation of eq. (12) yields:

$$\frac{1}{M^0} \frac{dM}{df_1} = \left(\frac{f_1}{f_1^0} \right)^\alpha \left(\frac{f_1-1}{f_1^0-1} \right)^\beta \left(\frac{f_1^0-\delta}{f_1-\delta} \right)^\gamma \left(\frac{\alpha}{f_1} + \frac{\beta}{f_1-1} - \frac{\gamma}{f_1-\delta} \right) \quad (14)$$

which may be simplified to:

$$\frac{1}{M^0} \frac{dM}{df_1} = \frac{M}{M^0} \left(\frac{\alpha}{f_1} - \frac{\beta}{f_2} - \frac{\gamma}{f_1-\delta} \right) \quad (15)$$

Division of eq. (15) by the derivative of eq. (6) then yields the desired differential copolymer composition equation for binary copolymerization as a function of the reactivity ratios and monomer mixture composition:

$$-\frac{1}{M^0} \frac{dM}{dF_1} = -\frac{M}{M^0} \left(\frac{\alpha}{f_1} - \frac{\beta}{f_2} - \frac{\gamma}{f_1 - \delta} \right) \times \frac{[(r_1 + r_2 - 2)f_1^2 + 2(1 - r_2)f_1 + r_2]^2}{[(r_1 + r_2 - 2r_1r_2)f_1^2 + 2r_2(r_1 - 1)f_1 - r_2]} \quad (16)$$

In the case of ideal copolymerization, $r_1 = 1/r_2$, eq. (16) is observed to degenerate to the special case previously considered by Wall.⁸

Incompatibility and phase separation will obviously be favored whenever a wide spread in copolymer composition is made during the course of a batch-type copolymerization. However, this tendency can be expected to be particularly critical whenever homopolymerization occurs during some stage of the polymerization. The critical limiting conditions may be obtained from the preceding analytic equations.

From eq. (5), it is seen that large values of either reactivity ratio will tend to favor the production of a copolymer consisting predominantly of only one of the monomeric species during the initial stages of the polymerization. That is, if $r_1 \gg 0$, then initially the M_1 species will tend to predominate in the copolymer, whereas, if $r_2 \gg 0$, then the M_2 species will tend to predominate in the copolymer formed during the early stages of the copolymerization. This tendency of the predominate polymerization of one of the monomeric species during some stage of the polymerization will be referred to as homopolymerization.

Copolymerization of Styrene and Vinyl Acetate

The system, styrene-vinyl acetate (Fig. 2), is an example in which $r_1 = 55$, i.e. $r_1 \gg 0$; and the homopolymerization of the styrene is favored initially. In Figure 2a, it is seen that over a fairly wide starting composition range, approximately for $0.1 \leq f_1 \leq 1.0$, the copolymer will consist of over 90% styrene units. In Figure 2b, the expected change in monomer mixture composition as a function of conversion for an equimolar mixture of styrene and vinyl acetate has been calculated by means of eq. (12). As part of the same calculation, eq. (5) has been used to calculate the corresponding change in instantaneous copolymer composition (Fig. 2c). Figure 2c shows that during the first half (54%) of the polymerization, a copolymer consisting predominately of styrene units is formed. The last half of the polymerization consists, to an even greater extent, of the homopolymerization of the vinyl acetate. Because styrene tends to serve as a scavenger for the vinyl acetate-polymerizing free-radical species, styrene would only be present in concentrations of the order of parts per million during the last half, i.e., the vinyl acetate portion of the polymerization. The absolute value of the slope of the mole conversion-instantaneous copolymer composition curve (Fig. 2c) may be calculated by means of eq. (16), and is shown in Figure 2d.

Since, both initially and during the final stages of the polymerization, the change in mole conversion, namely $(1/M^0)(dM)$, is not accompanied by a

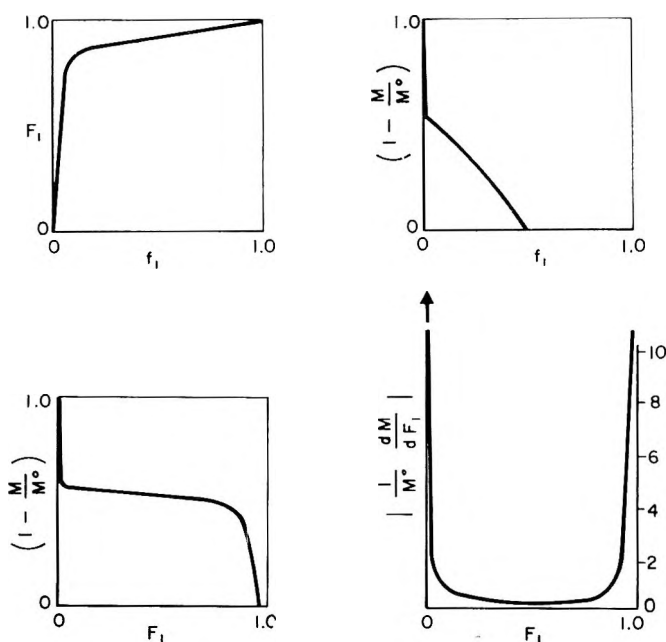


Fig. 2. $M_1 =$ styrene, $M_2 =$ vinyl acetate; $M_1^0 = M_2^0$; $r_1 = 55$, $r_2 = 0.01$.

correspondingly large change in instantaneous copolymer composition, dF_1 , this leads to large values for the slope at these two points, i.e., to the U-shaped differential copolymer composition curve as is observed in Figure 2d and which is considered characteristic of "incompatible" copolymerizations, that is, of copolymerizations in which the homopolymerization of one of the species is favored initially, and the homopolymerization of the other species is favored during the final stages of the polymerization.

Homopolymerization During the Final Stages of Polymerization

First, we consider the case where f_1 and F_1 go to zero as the polymerization goes to completion (Fig. 1a) or, to the left of the crossover point in Figure 1c. From eq. (16), one obtains:

$$\lim_{f_1 \rightarrow 0} \left| \frac{1}{M^0} \frac{dM}{dF_1} \right| = \begin{cases} 0 & 0.5 < r_2 < 1.0 \\ \text{finite} & r_2 = 0.5 \\ \infty & r_2 > 1.0 \text{ or } r_2 < 0.5 \end{cases} \quad (17)$$

In practice, the case of f_1 going to zero, with $r_2 > 1.0$ (see Fig. 1), does not normally occur; therefore, the conditions of eq. (16) may be simplified to:

$$\lim_{f_1 \rightarrow 0} \left| \frac{1}{M^0} \frac{dM}{dF_1} \right| = \begin{cases} 0 & r_2 > 0.5 \\ \text{finite} & r_2 = 0.5 \\ \infty & r_2 < 0.5 \end{cases} \quad (18)$$

For the condition where, $r_2 = 0.5$, since r_2 is then fixed in value, the slope of the mole conversion–instantaneous composition curve, which is finite, will then depend solely on r_1 .

The possibility also exists for f_1 and F_1 to go to unity as the polymerization goes to completion (Fig. 1a) or, to the right of the crossover point in Figure 1c. In this case the simplified limiting conditions become:

$$\lim_{f_1 \rightarrow 0} \left| \frac{1}{M^0} \frac{dM}{dF_1} \right| = \begin{cases} 0 & r_1 > 0.5 \\ \text{finite} & r_1 = 0.5 \\ \infty & r_1 < 0.5 \end{cases} \quad (19)$$

For the condition of finite slope, $r_1 = 0.5$, since r_1 is fixed, the limiting slope will then depend solely on r_2 .

From the preceding discussion, it is clear that the behavior of the limiting slope of the mole conversion–instantaneous copolymer composition curve may be used to define conditions under which homopolymerization of one of the species would be expected to occur during the final stages of a copolymerization.

The various possibilities contained in eqs. (18) and (19) are shown in Figure 3, where again, the direction of drift, which is in opposite directions about the crossover point, has been indicated by arrows.

Thus, if f_1 and F_1 approach zero during the course of a binary copolymerization, to the left of the crossover point in Figure 3, then if, $r_2 < 0.5$ (regardless of the value of r_1), at some point during the final stages of the polymerization, the homopolymerization of the M_2 species will be expected

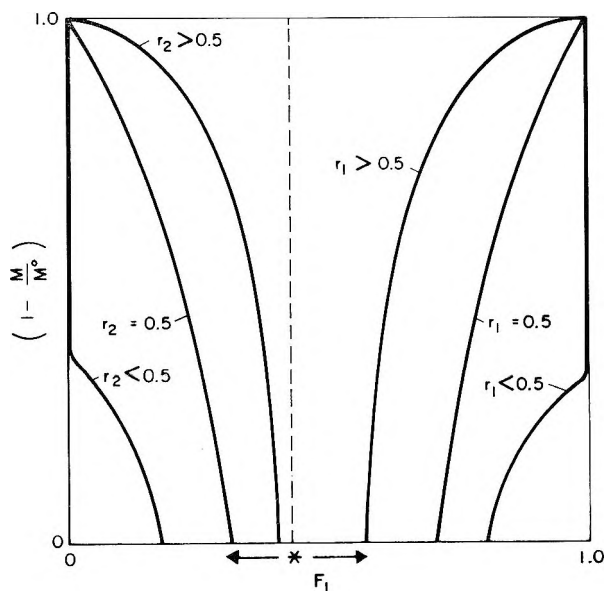


Fig. 3. Binary copolymerization system with a crossover point (*) at $r_1 < 1.0$, $r_2 < 1.0$

to occur. As r_2 approaches 0.5 in value, the behavior of the two curves ($r_2 < 0.5$, and $r_2 > 0.5$) both approach the curve for $r_2 = 0.5$ in behavior. For example, in the copolymerization of a mixture of 1 mole of styrene with 4 moles of acrylonitrile ($f_1 = 0.2$, $r_1 = 0.40$, $r_2 = 0.03$), a conversion-composition curve such as is indicated by the curve for $r_2 < 0.5$ in Figure 3 is obtained, whereas, in the copolymerization of 1 mole of styrene with 4 moles of methyl methacrylate, ($f_1 = 0.2$, $r_1 = 0.53$, $r_2 = 0.49$), the conversion-composition curve will be almost indistinguishable from the curve for $r_2 = 0.5$, i.e., the slope will be infinite, such as is indicated in the curve for $r_2 < 0.5$, only during the very last 2% conversion portion of the curve. Conversely, if the direction of drift is to the right during the polymerization, then, if $r_1 < 0.5$ (again regardless of the value of r_2), the homopolymerization of the M_1 species would be expected to occur at some point during the final stage of the polymerization. Again, depending on the composition and specific values of the reactivity ratios, a continuous range of copolymerization behavior will be observed. However, all binary copolymerizations, insofar as they can be described by two reactivity ratios and the theoretical treatment given here, will be found to fall into one of the six classifications as indicated in Figure 3.

Thus, in agreement with Skeist,⁵ the value of 0.5 for the reactivity ratios is found to be critical. However, this is not a sufficient condition, since whether or not homopolymerization would be expected to occur during the final stages of a binary copolymerization depends both on the direction of drift and the critical value of 0.5 for the appropriate reactivity ratio.

Conclusions

Equations have been derived which allow the convenient calculation of expected copolymerization behavior. Side effects, such as phase separation and depolymerization, are not taken into account.

APPENDIX I

For the special case of $r_1 = 1$, $r_2 \neq 1$, eq. (8) becomes:

$$\ln \frac{M}{M^0} = \int_{f_1^0}^{f_1} \frac{-f_1^2 + 2f_1 + r_2/(1 - r_2)}{f_1^3 - 2f_1^2 + f_1} df_1$$

which may be expanded into easily integrated terms to yield:

$$\ln \frac{M}{M^0} = \ln \left[\left(\frac{f_1}{f_1^0} \right)^{\frac{r_2}{1-r_2}} \left(\frac{f_1^0 - 1}{f_1 - 1} \right)^{\frac{1}{1-r_2}} \right] + \left(\frac{1}{1-r_2} \right) \left[\frac{1}{f_1^0 - 1} - \frac{1}{f_1 - 1} \right]$$

with the restriction, $r_2 \neq 1$.

APPENDIX II

For the special case of $r_2 = 1$, $r_1 \neq 1$, eq. (8) becomes:

$$\ln \frac{M}{M^0} = \int_{f_1^0}^{f_1} \frac{(r_1 - 1)f_1^2 + 1}{(1 - r_1)f_1^3 + (r_1 - 1)f_1^2} df_1$$

which again may be expanded, integrated, and rearranged to yield:

$$\ln \frac{M}{M^0} = \ln \left[\left(\frac{f_1}{f_1^0} \right)^{\frac{1}{r_1 - 1}} \left(\frac{f_1^0 - 1}{f_1 - 1} \right)^{\frac{r_1}{r_1 - 1}} \right] + \left(\frac{1}{r_1 - 1} \right) \left(\frac{1}{f_1^0} - \frac{1}{f_1} \right)$$

with the restriction, $r_1 \neq 1$.

References

1. Meyer, V. E., and G. G. Lowry, *ACS Polymer Preprints*, **5**, 60 (1964).
2. Lewis, F. M., and F. R. Mayo, *J. Am. Chem. Soc.*, **66**, 1594 (1944).
3. Wall, F. T., *J. Am. Chem. Soc.*, **63**, 1862 (1941).
4. Walling, C., and E. R. Briggs, *J. Am. Chem. Soc.*, **67**, 1774 (1945).
5. Skeist, I., *J. Am. Chem. Soc.*, **68**, 1781 (1946).
6. Alfrey, T., Jr., J. J. Bohrer, and H. Mark, *Copolymerization*, Vol. 8 of High Polymers Series, Interscience, New York, 1952, p. 9.
7. Alfrey, T., Jr., and G. Goldfinger, *J. Chem. Phys.*, **12**, 205 (1944).
8. Wall, F. T., *J. Am. Chem. Soc.*, **66**, 2050 (1944).

Résumé

On a obtenu une solution analytique à l'équation de copolymérisation de Skeist dans le cas de la copolymérisation binaire. A partir de cette solution, on a également déduit une équation différentielle de la composition du copolymère. Pour des valeurs données des rapports de réactivité, ces équations permettent le calcul facile du comportement de la copolymérisation binaire prévue en fonction de la conversion. On discute également des conditions critiques conduisant à des copolymérisations incompatibles.

Zusammenfassung

Für den Fall einer binären Copolymerisation wurde eine analytische Lösung der Copolymerisationsgleichung von Skeist erhalten. Aus dieser Lösung wird auch eine Gleichung für die differentielle Copolymerzusammensetzung abgeleitet. Für gegebene Werte des Reaktivitätsverhältnisses erlauben dann diese Gleichungen eine bequeme Berechnung des binären Copolymerisationsverhaltens als Funktion des Umsatzes. Schliesslich werden die kritischen Bedingungen, die zur Unverträglichkeit bei der Copolymerisation führen, diskutiert.

Received November 12, 1964

Revised February 20, 1965

Prod. No. 4668A

Ziegler Polymerization of Olefins without Added Metal Alkyls

A. S. MATLACK and D. S. BRESLOW,
Research Center, Hercules Powder Company, Wilmington, Delaware

Synopsis

Ethylene has been polymerized under mild conditions by (1) transition metals plus alkyl halides, (2) transition metal hydrides, (3) certain transition metals alone, and (4) certain divalent transition metal halides and oxides. Propylene has been polymerized to mixtures of amorphous and crystalline polymer in low conversions by (1) transition metals plus alkyl halides and (2) certain divalent transition metal halides. A vibratory ball mill was used as the polymerization vessel to provide a continuous supply of fresh catalyst surface during the polymerizations. The transient existence of transition metal alkyls is postulated to account for the observed catalysis. This work provides one of the most direct proofs that polymerization occurs on the transition metal, rather than on aluminum, zinc, or other metals usually associated with it in typical Ziegler catalysts.

INTRODUCTION

The conversion of ethylene to high molecular weight linear polyethylene by titanium tetrachloride alone, which had been irradiated by γ -rays, has been described by Oita and Nevitt.¹ Recently several other papers dealing with the Ziegler polymerization of olefins without metal alkyls²⁻⁴ have appeared. These papers have prompted us to report some work done in this area several years ago. While most of this work has appeared in the patent literature,⁵ it appears to have gone largely unnoticed.

Although a bewildering number of catalysts have been reported for the low pressure polymerization of ethylene,⁶ by and large they can be considered to contain a transition metal compound capable of being alkylated, an alkylating agent, and a Lewis acid. Often, of course, a catalyst ingredient serves more than one function. Ziegler polymerization is generally agreed to involve, somehow or other, a transition metal alkyl;^{1,6,7} the present study arose from our interest in the preparation of transition metal alkyls by processes other than those involving alkylation by an organometallic compound.

The preparation of most metal alkyls depends ultimately on the reaction of a metal with an alkyl halide.^{8,9} Such derivatives of transition metals have limited stability and are often short-lived.^{10,11} To provide intimate contact between reagents and to use the transition metal alkyl as it was formed, the polymerizations were carried out in vibratory ball mills.

TABLE I
 Polymerization of Ethylene

Catalyst	Yield, %	RSV	Sulfate ash, %	Structure by infrared spectrum					Melting point, °C.
				Methyl, wt.-%	<i>trans</i> , wt.-%	Vinyl, wt.-%	Vinylidene, wt.-%		
Ti + C ₂ H ₅ Br	94	5.2	15.8 ^a	N.D. ^b	0.035	N.D.	N.D.	130	
Ti + C ₂ H ₅ Br ^c	14	2.3		2.22	0.050 ^d	0.031 ^d	0.034 ^d	132	
Ti + ClCH ₂ CH ₂ Cl	49	3.4	0.71	0.42	0.031	0.070	0.005	131	
V + C ₂ H ₅ Br	52	1.0	0.70	0.74	0.081	0.006	0.009	117	
6 g. Cr + C ₂ H ₅ Br	78	3.1	1.87	0.70	0.046	0.075	—	132	
Mn + C ₂ H ₅ Br	45	2.3	0.94	0.91	0.039	0.013	0.019	134	
V	53	1.1	10.1	1.6	0.15	N.D.	N.D.	130	
Nb	48	4.2	0.56	0.63	0.065	0.058	0.003	139	
Ta	46	1.7 ^e	0.42	2.00	0.200	0.033	0.025	140	
2.3 g. La ^f	48 ^g	1.0	14.5	0.95	0.053	0.005	0.006	134	
2.5 g. Ce ^h	47 ^g	1.8	31.6	0.78	N.D.	0.009	0.009	131	
Tl	65 ⁱ	1.8		0.76	0.039	0.016	0.009	136	
1.4 g. U ^j	76 ⁱ	4.9		0.63	0.020	0.009	0.006	136	
TiCl ₄ + C ₂ H ₅ Br ^k		17.5	1.58	0.31	N.D.	Trace	N.D.	137	
TiCl ₂ ^l	61	3.5	1.68	0.94	0.040	0.021	0.005	125	
0.5 g. Ti + TiCl ₃ ^m	63	1.0		0.88	0.098	0.027	0.010	130	
VCl ₄ ⁿ	27	2.8	0.27	0.78	0.031	0.008	0.007	128	

0.5 g. V + VCl ₃ ^a	78	1.5		0.71	0.043	N.D.	0.009	131
5 g. TiO	91	2.8	0.38	0.74	0.081	0.011	0.006	
1.0 g. V ₂ O ₅ + 0.45 g. Al	81	1.2		0.86	0.109	0.029	0.018	130
TiH ₂ ^b	40	0.4	0.38	1.77	0.064	N.D.	0.043	128
Ti + H ₂	31	39.0	1.72	0.18	N.D.	Trace	Trace	135
ZrH ₂ ^c	63	4.2	0.57	0.40	0.043	0.003	0.004	136
V + H ₂	86	4.0	1.39	1.38	0.057	0.025	0.023	131
1.0 g. NbH ^d	73	3.2	0.48	1.16	0.049	0.185	0.019	131
TaH ^e	67	3.2	0.44	0.87	0.053	0.197	0.021	130
Mn + H ₂	25	Insoluble	0.33	1.84	0.110	0.027	0.014	132

^a Polymer deashed by adding 50/50 1-butanol-concentrated hydrochloric acid and heating for 8 hr. under reflux instead of by the usual workup.

^b N.D. = not detected.

^c Run in carbon tetrachloride instead of heptane.

^d These are maximum values due to an interfering band.

^e Incomplete solution.

^f The bulk material was reduced to filings before use.

^g After the regular workup, the polymer was dissolved in boiling kerosene and filtered to remove ash.

^h Filings from the bulk material were used. It may spark in moist air during filing.

ⁱ After the regular workup, the polymer was dissolved in boiling xylene and filtered to remove the ash.

^j Filled from a disk onto an asbestos sheet frequently emptied. Much sparking occurred.

^k Run in a pop bottle. See experimental section for amounts.

^l 1.0 ml. of 1.2*M* slurry in heptane; average particle size, 2 μ .

^m 3.0 ml. of 0.54*M* slurry in heptane was used; average particle size, 2 μ .

ⁿ 11.5 ml. of 0.087*M* slurry in heptane.

^o 5 ml. of 0.59*M* slurry in heptane, average particle size, 2 μ .

^p The formula shown is a limiting structure; the amount of hydride usually does not reach this limit.

RESULTS

Ethylene

When milled with ethylene overnight at room temperature, combinations of the transition metals, titanium, vanadium, chromium, and manganese, with ethyl bromide catalyzed polymerization to high melting, relatively linear polyethylene. The results are shown in Table I. The runs were normally made in heptane. In one, with titanium, in carbon tetrachloride, the solvent was involved in chain termination or chain transfer, as shown by the lower yield and lower viscosity of the polymer formed. Ethylene dichloride also proved a suitable alkyl halide for use with titanium.

In carrying out control runs, vanadium was found to catalyze the polymerization even in the absence of an alkyl halide. The other Group VB elements, niobium and tantalum, as well as lanthanum and cerium from the rare earth series, and thorium and uranium from the actinide series, also polymerized ethylene in the absence of an alkyl halide. The polymers from these runs were comparatively linear (relative to low-density polyethylene) with reduced specific viscosities in the range from 1.0 to 4.9.

Metal alkyls, although most often formed from the reaction of a metal with an alkyl halide (aside from preparation by transalkylation reactions), can sometimes be made by the action of an alkyl halide on a divalent metal halide, the metal becoming tetravalent in the process.



This process is known for the Group VA metals, tin, germanium, and lead.⁸ Thus, the combination of titanium dichloride with ethyl bromide was tried and found to catalyze the formation of polymer. Here again, a control run showed the ethyl bromide to be unnecessary. Furthermore, the advantage of the use of the vibratory ball mill as a reaction vessel was demonstrated by the catalyst level of 12 mmole/l., whereas a level of 100 mmole/l. was required to get a reasonable polymerization rate with preground catalyst in a stirred reactor under similar conditions of temperature and pressure.

A combination of titanium and titanium trichloride was also an effective catalyst, presumably through the *in situ* formation of titanium dichloride, because neither component was active alone. Vanadium dichloride and a combination of vanadium and vanadium trichloride were also active. For the latter, it is impossible to tell whether the actual catalyst is vanadium metal or vanadium dichloride formed *in situ*, because both are active alone. That chloride ion was not essential in the metal compound was shown through the use of titanium monoxide. Although vanadium monoxide was not available to test, a combination of aluminum with vanadium pentoxide proved to be a catalyst, suggesting its formation *in situ*.

Another route to metal alkyls is the addition of metal hydrides to olefins. Titanium, zirconium, niobium, and tantalum hydrides proved to be catalysts. The hydrides were probably intermediates in the catalysis by the combinations of titanium and manganese with hydrogen, because neither metal is active alone. Much higher molecular weights were obtained when the hydrides were prepared *in situ* than when the preformed compounds

were used. Although the use of hydrogen to control the molecular weights of polyolefins is well established,^{6,12} the conditions of use here were evidently not such as to reduce the molecular weights to the levels found when preformed hydrides were used as catalysts. The preformed hydrides presumably are more efficient initiators, or possibly more effective chain transfer agents. In the combination of vanadium plus hydrogen, it is impossible to say whether vanadium or vanadium hydride was the actual catalyst.

Propylene

A number of the catalyst systems for ethylene (and analogs of them) above proved active also in the polymerization of propylene, mixtures of amorphous and crystalline polymers being obtained in a maximum total conversion of 40%. The results are given in Table II.

In the class of metals plus alkyl halides, combinations of vanadium and thorium with ethyl bromide gave only amorphous polymer, whereas some crystalline polymer was also formed when titanium was used with ethyl bromide.

TABLE II
Polymerization of Propylene

Catalyst	Polymer isolated, g. ^h		Yield, %	RSV ^h		Melting point of insoluble polymer, °C.
	Soluble	Insoluble		Soluble	Insoluble	
Ti + C ₂ H ₅ Br	0.81	0.23	7	0.7	4.2	162
V + C ₂ H ₅ Br	0.88	0	6	2.2		
Th + C ₂ H ₅ Br	2.16	0	14	0.03		
1.0 g. Ti + TiF ₄ ^a	6.07	0	40	0.04		
0.5 g. Ti + TiCl ₄ ^b	0.17	0	1	—		
1.0 g. Ti + TiCl ₃ ^c	3.84	1.40	35	0.3	1.9	160
1.0 g. Ti + TiBr ₄ ^d	1.38	1.18	17	0.8	5.2	162
1.0 g. Ti + 0.16-g. HCl ^e	1.2	0.67	12	0.9	3.7	161
1.0 g. Ti + 1.0 g. I ₂	2.53	3.44	40	1.2	5.4	163
ZrH ₂ + 0.16 g.-HCl ^e	2.77	1.62	29	0.7	4.9	160
0.5 g. V + VCl ₃ ^f	4.2	1.5	38 ^g	0.3	1.9	153

^a 5 ml. of 0.95*M* slurry in heptane.

^b 2.0 ml. of 1*M* solution in pentane.

^c 5 ml. of 0.6*M* slurry in heptane.

^d 5 ml. of 0.5*M* solution in heptane.

^e Injected as a gas. The mill was shaken 5 min. before addition of propylene, which was added last.

^f 5 ml. of 0.59*M* slurry in heptane.

^g After 16 hr., the mill, now at 12 psig, was repressured to 50 psig with propylene, then run an additional 16 hr.

^h Soluble and insoluble are used relative to the polymerization medium, i.e., heptane. The soluble polymer is amorphous; the insoluble crystalline.

Most of the catalysts found for propylene polymerization are those which might involve the intermediate formation of the divalent metal halides. Thus, combinations of titanium with titanium tetrafluoride, titanium tetrachloride, titanium trichloride, or titanium tetrabromide catalyzed the formation of polymer, as did a combination of vanadium and vanadium trichloride. With the first two catalyst combinations, only amorphous polymer was obtained. In the others, mixtures of amorphous and crystalline polymers were obtained. Other catalyst combinations which also gave mixtures of the two types of polymer were titanium with hydrogen chloride, titanium with iodine, and zirconium hydride with hydrogen chloride. Of all the catalysts tested, the maximum yield of crystalline polymer was obtained with titanium plus iodine. In general, the molecular weights of the crystalline polymers were substantially higher than those of the amorphous ones.

DISCUSSION

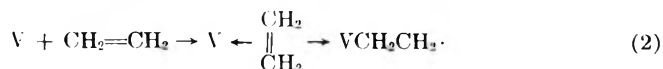
These experiments provide some additional evidence bearing on some of the controversial questions concerning the mechanism of Ziegler catalysis.⁷ Does chain growth occur on the transition metal, or on the metal from the metal alkyl used to alkylate the transition metal? Are two metals needed? If so, what are their roles in determining the specificity of the polymerization?

Here, as in the already known polymerizations by methyl titanium trichloride, mixed with its decomposition products,¹³ and by γ -irradiated titanium tetrachloride,¹ olefins are polymerized by monometallic catalysts. Chain growth can only occur on the one metal present. Whatever stereospecificity is involved must come from the one metal and its immediate environment. In fact, polymerization of ethylene by metals alone would seem to represent the ultimate in simplicity for Ziegler catalysts.

Are transition metal alkyls necessary intermediates in the transition states in Ziegler polymerizations? The answer is probably yes. Although no metal alkyls have been added, they are probably formed *in situ*. While the intermediacy of such species in the present polymerizations is inferred, rather than proved, from the catalyst combinations shown to be active, the data are well rationalized on this basis. With the metals, such as vanadium, and the divalent metal compounds, such as titanium dichloride, which act as catalysts without other additives, the product of the first step of the polymerization may be regarded as the transition metal alkyl involved. Presumably, the metal or metal halide first forms a π -complex with the olefin followed by its rearrangement to a σ -complex. At this point, the next monomer unit which coordinates with the metal inserts. This explanation fits in with the generalized mechanism of Ziegler catalysis as advanced by Cossee and Arlman.⁴⁻¹⁶

There is some precedent for the formation of a metal-carbon σ -bond in the addition of the alkali metals to reactive double bonds to form products formerly written as dimetal salts but now formulated as anion radicals.¹⁷ By analogy with the work of Szwarc^{18,19} on the polymerization of styrene by

anion radicals, in which case the counterion is from an alkali metal, the sequence with vanadium might be:



In contrast to the ionic metal-carbon bond in, for example, sodium anion radicals, the vanadium-carbon bond is probably covalent, by analogy with the volatile methyltitanium trichloride.¹³ Friedlander and co-workers have also written this type of sequence in discussing the mechanism of Ziegler polymerization.²⁰ These authors feel that the need for some decomposition of tetravalent titanium alkyls to get catalytic activity is evidence for the kind of reaction shown (where vanadium would be replaced by titanium with a valence less than four). Following the scheme of Szwarc, the radical might dimerize, add to another molecule of olefin, or acquire an electron from another source, such as more vanadium metal:

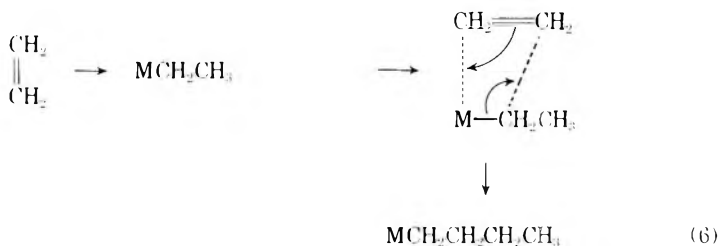
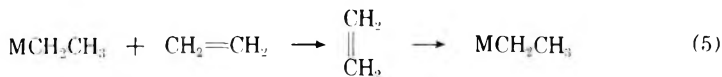


The dimeric radical would disappear sooner or later by further combination, disproportionation, abstraction of a hydrogen atom from the solvent, or by electron transfer to form an anion. The intermediates above would then grow by a coordinated anionic insertion into the vanadium-carbon bond. Although the present work contains no definite proof of such a mechanism, the polymers produced differ from those made with free-radical catalysts under the usual conditions. The latter generally have much lower melting points than, and several times as many methyl groups as, the polymers in Tables I and II. The present polymers are more like those made with ordinary Ziegler catalysts. That sizable molecular weights are obtained in spite of the massive amounts of catalyst used may be due to little or no chain termination or such a need for fresh surface that the number of chains initiated is limited, or both.

Similar mechanisms may be involved in the rhodium chloride-catalyzed polymerization of cyclobutene²¹ and butadiene.^{22,23}

The formation of metal alkyls by the addition of metal hydrides to olefins is well known for nontransition metals such as aluminum,²⁴ boron,²⁵ germanium,²⁶ magnesium,²⁷ tin^{28,29} and others.^{9,10} Although the addition of transition metal hydrides to olefins is less well known, it has been reported for cobalt,³⁰ manganese,^{31,32} and platinum.³³ The addition of transition metal hydrides to olefins has also been postulated as an intermediate step in various hydrogenation reactions. For example, the homogeneous hydrogenation of olefins with mixtures of metal alkyls and transition metal salts as catalysts may involve such an addition.³⁴ Activated olefins, such as styrene, and substituted methacrylic acid have been reduced homogeneously by using potassium hydridopentacyanocobaltate as a catalyst, addition of the hydride to the double bond probably being involved.³⁵

The polymerization of ethylene by the metal hydride can take place as shown in eqs. (4)-(6).



Thus the metal alkyl formed by addition of the hydride to the ethylene probably first forms a π -bond with a second molecule of ethylene. This coordinated ethylene then inserts into the metal carbon bond, the process of coordination and insertion continuing until the chain is terminated or the supply of ethylene exhausted.

The function of the vibratory ball mill is probably to provide a continuous supply of fresh catalyst surface during polymerization. Alternatively, it is possible that sufficient energy may be released in a small area at the moment of impact of a ball to supply the activation energy of the reaction. The energy of grinding may "loosen" metal-metal bonds, creating a disordered structure of higher reactivity. The generation of local "hot spots" by impact is known to initiate the detonation of explosives.⁵⁶

Since the work reported here was completed, a number of patents have appeared which have extended it.³⁷⁻⁴³ The chief modification described in most of these is that of removing the catalyst from the mill before using it in the polymerization. In our hands, this modification has been less desirable (at the same temperature and pressure) because higher levels of titanium dichloride were required to polymerize ethylene, and titanium monoxide failed to polymerize ethylene outside the mill. The use of titanium dichloride as a catalyst has been reported.^{3,4}

EXPERIMENTAL

Materials

Metals and metal salts and their sources are listed in Table III.

Polymerization in Ball Mills

The mills were welded stainless steel (analysis: carbon, 0.008% max.; chromium, 18-20%; nickel, 8.8-10.0%; manganese, 2.0% max.) cylinders with an outlet fitted with an adapter for a conventional bottle cap and self-sealing rubber liner. The internal diameter of the adapter was such that a ball would not pass. A hexagonal nut was used to attach the adapter to the mill over a Teflon gasket. The capacities of the mills when filled to 80% of their depth with 0.5 in. stainless steel balls (SKF Industries, Inc.)

TABLE III
 Sources of Metals and Metal Salts

Material	Source	Grade or purity
Aluminum	Aluminum Co. of America	Albron grade
Cerium	Fairmount Chemical Co.	93%
Chromium	Fisher Scientific Co.	
Lanthanum	Fairmount Chemical Co.	99.5%
Manganese	Fisher Scientific Co.	Pure grade
Niobium	Fairmount Chemical Co.	
Niobium hydride	Delta Chemical Works	
Tantalum	Fairmount Chemical Co.	
Tantalum hydride	Metal Hydrides, Inc.	
Thorium	Fairmount Chemical Co.	
Titanium	Titanium Metals Corp. of America	
Titanium dichloride	New Jersey Zinc Co.	37.81% Ti, 58.33% Cl, Cl/Ti = 2.08
Titanium hydride	Metal Hydrides, Inc.	
Titanium monoxide	Horizons, Inc.	70.1% Ti, 0.25% C
Titanium tetrabromide	Made according to Bond and Crone ⁴⁴	
Titanium tetrafluoride	General Chemical Division of Allied Chemical Corp.	
Titanium trichloride	New Jersey Zinc Co. (for Table I) Stauffer Chemical Co. (for Table II)	30.61% Ti, 69.13% Cl, Cl/Ti = 3.05 99%
Uranium	Mallinckrodt Chemical Works	Analytical reagent
Vanadium	Fairmount Chemical Co.	99.7%
Vanadium dichloride	Delta Chemical Works	
Vanadium pentoxide	Fisher Scientific Co.	
Vanadium trichloride	Delta Chemical Works	
Zirconium hydride	Metal Hydrides, Inc.	

were determined by filling with water to be 660 ml. for the larger model and 410 ml. for the smaller model. A third model, which proved much easier to clean, consisted of a conventional stainless steel high-pressure autoclave (analysis: chromium, 16–18%; nickel, 10–14%; molybdenum, 2–3%) with an adapter attached to a conventional head to take a bottle cap closure. Two steel rings were welded to the outside to balance its weight with that of each of the other mills. Teflon and copper gaskets were used; the latter being annealed at intervals. Its capacity in use was 295 ml.

Four mills at a time were shaken on a Vibraton Schwingmühle [Siebtechnik, G.m.b.H., Mülheim (Ruhr)-Speldorf, Germany], a device that simultaneously imparts a slow rotation (7 rpm) and a high frequency (1500/min.), low-amplitude (4 mm.) circular oscillation to the containers.

A mill, after drying 4 hr. at 120°C., was cooled and charged with 2.0 g. of metal or metal derivative (except as noted in the tables) and 100 ml. of heptane (dried over sodium), then evacuated and filled with nitrogen twice, then evacuated and filled with 50 psig ethylene or propylene (or 40 psig

ethylene plus 10 psig hydrogen). In runs with ethyl bromide, 3 ml. was used with a trace of iodine. In the run with ethylene dichloride, 1 ml. was used without iodine.

After 16 hr. of operation at room temperature (about 30°C.), the mill was vented, uncapped, and the slurry filtered to collect the polyethylene. In propylene runs, the insoluble polymer was separated by centrifugation; the soluble polymer being recovered by evaporation of the filtrate. The product was allowed to stand overnight in a polyethylene beaker with an excess of a 50/50 1-butanol-48% aqueous hydrofluoric acid mixture (except as noted in Table II). After dilution with water, the mixture was filtered to recover the polymer, which was washed free of acid with water and ethanol, then dried overnight at 80°C. at 20 mm. In runs which gave little or no polymer, the catalyst residues had to be handled with caution, since they sometimes ignited if allowed to dry in air. A suitable procedure for handling them was to add the 1-butanol first, then the hydrofluoric acid. If the strong acid was added first, a fire sometimes resulted.

The slurries of metal salts mentioned in Tables I and II were made by milling them in heptane in the same way, then transferring the slurry to pop bottles through needles under nitrogen; the concentration being determined by evaporation of aliquots of the slurry. (Where required by the sensitivity of the materials, a dry box filled with dry argon or helium was used in filling the mills.)

Polymerizations in Glass Pressure Bottles

A 150-ml. capped pop bottle containing 40 ml. of heptane was evacuated and filled with nitrogen twice, then evacuated and filled with ethylene to 30 psig. Ethyl bromide (5 ml. of 1*M* solution in heptane) and titanium dichloride (5 ml. of 1*M* slurry in heptane) were injected. After the bottle had been on a rotation rack in a 30°C. water bath for 1.25 hr., the gage pressure was zero. After the bottle was repressured to 48 psig, agitation was resumed. After 3 hr., when the pressure had dropped to 19 psig, the run was terminated by injection of 1 ml. of 1-butanol. The bottle was vented; the polymer was recovered by filtration, treated first with 10% HCl in methanol under reflux for 30 min., and then recovered by filtration and treated with 4% aqueous sodium hydroxide, containing a small amount of detergent, for 6 hr. at 100°C. After standing over the weekend, the mixture was filtered to remove the polymer which was then held at 100°C. for 3 hr. in 40/40/20 toluene-1-butanol-concentrated hydrochloric acid. The polymer was washed with alcohol until neutral and dried overnight in vacuum at 60°C.

In a second run, a capped 8-oz. pop bottle containing 45 ml. of heptane was evacuated and then connected to a constant ethylene pressure of 50 psig. After injection of 5 ml. of a slurry of titanium dichloride (5 mmole) in heptane, the mixture was stirred (magnetically) overnight at room temperature. The ethylene source was disconnected and the bottle was vented and uncapped. The polymer was removed by filtration, then digested with a 5/5/1 1-butanol-toluene-hydrochloric acid mixture heated under reflux, and finally filtered and washed until neutral with alcohol. After drying, 7.7 g. of polymer remained.

Characterization of the Polymers

The molecular weights of the polymers in Tables I and II are indicated by the reduced specific viscosity (RSV) given for each. By this term is meant the η_{sp}/c determined on a solution of the polymer in decalin containing 0.1 g. of the polymer per 100 ml. of solution at 135°C. The melting point of the polymer given is the temperature at which the birefringence due to crystallinity disappears on remelting after the sample is first melted then cooled and allowed to solidify.

The authors thank Mrs. Seta Olsen and Mr. Norman Newburg for carrying out the experiments with titanium dichloride in bottles. The melting points, viscosity measurements, and infrared spectra were determined by the Analytical and Physical Chemistry Divisions at the Hercules Research Center.

References

1. Oita, K., and T. D. Nevitt, *J. Polymer Sci.*, **43**, 585 (1960).
2. Boor, J., Jr., and E. A. Youngman, *J. Polymer Sci.*, **B2**, 265 (1964).
3. Werber, F. X., C. J. Benning, W. R. Wszolek, and G. E. Ashby, paper presented to Polymer Division, 141st American Chemical Society, Washington, D. C., March 26-29, 1962; *Polymer Preprints*, **3**, No. 1, 122 (1962).
4. Benning, C. J., W. R. Wszolek, and F. X. Werber, paper presented to Polymer Division, 141st Meeting, American Chemical Society, Washington, D. C., March 26-29, 1962; *Polymer Preprints*, **3**, No. 1, 138 (1962).
5. Matlack, A. S., U. S. Pat. 2,891,041-4, 2,913,442 (1959); 2,938,020 (1960); 3,004,962 (1961); Brit. Pat. 848,285 (1961); D. S. Breslow and A. S. Matlack, U. S. Pat. 2,961,435 (1960).
6. Gaylord, N. G., and H. Mark, *Linear and Stereoregular Addition Polymers*, Interscience, New York, 1959.
7. Bawn, C. E. H., and A. Ledwith, *Quart. Revs.*, **16**, 361 (1962).
8. Jones, R. G., and H. Gilman, *Chem. Revs.*, **54**, 835 (1956).
9. Coates, G. E., *Organo-metallic Compounds*, 2nd Ed., Wiley, New York, 1960.
10. Coates, G. E., and F. Gloecking in *Organometallic Chemistry*, H. Zeiss, Ed., Reinhold, New York, 1960, p. 426.
11. Cotton, F. A., *Chem. Revs.*, **55**, 551 (1955).
12. Vandenberg, E. J., U. S. Pat. 3,051,690 (1962).
13. Beerman, C., and H. Bestian, *Angew. Chem.*, **71**, 618 (1959).
14. Cossee, P., *J. Catal.*, **3**, 80 (1964).
15. Arlman, E. J., *J. Catal.*, **3**, 89 (1964).
16. Arlman, E. J., and P. Cossee, *J. Catal.*, **3**, 99 (1964).
17. Schlosser, M., *Angew. Chem.*, **76**, 258 (1964).
18. Szwarc, M., *J. Polymer Sci.*, **C1**, 339 (1963).
19. Szwarc, M., *Proc. Roy. Soc. (London)*, **A279**, 260 (1964).
20. Friedlander, H. N., and K. Oita, *Ind. Eng. Chem.*, **49**, 1885 (1957); H. N. Friedlander and W. Resnick, in *Advances in Petroleum Chemistry and Refining*, Vol. 1, K. A. Kobe and J. J. McKetta, Jr., Eds., Interscience, New York, 1958, pp. 550-553.
21. Natta, G., G. Dall'Asta, and G. Motroni, *J. Polymer Sci.*, **B2**, 349 (1964).
22. Rinehart, R. E., H. P. Smith, H. S. Witt, and H. Romeyn, Jr., *J. Am. Chem. Soc.*, **83**, 4864 (1961); *ibid.*, **84**, 4145 (1962).
23. Canale, A. J., W. A. Hewett, T. M. Shryne, and E. A. Youngman, *Chem. Ind. (London)*, **1962**, 1054.
24. Ziegler, K., in *Organometallic Chemistry*, H. Zeiss, Ed., Reinhold, New York, 1960, p. 215.
25. Brown, H. C., *Hydroboration*, Benjamin, New York, 1962.
26. Quane, D., and R. S. Bottei, *Chem. Revs.*, **63**, 403 (1963).
27. Podall, H. E., and W. E. Foster, *J. Org. Chem.*, **23**, 1848 (1958).
28. Noltes, J. G., *Functionally Substituted Organotin Compounds*, Drukkerij Schotanus and Jens, Utrecht, 1958, p. 15.

29. van der Kerk, G. J. M., J. G. A. Luyten, and J. G. Noltes, *Chem. Ind. (London)*, **1956**, 352.
30. Heck, R. F., and D. S. Breslow, *J. Am. Chem. Soc.*, **83**, 4023 (1961).
31. Treichel, P. M., E. Pitcher, and F. G. A. Stone, *Inorg. Chem.*, **1**, 511 (1962).
32. McClellan, W. R., H. H. Hoehn, H. N. Cripps, E. L. Muetterties, and B. W. Howk, *J. Am. Chem. Soc.*, **83**, 1601 (1961).
33. Chatt, J., and B. L. Shaw, *J. Chem. Soc.*, **1962**, 5075.
34. Sloan, M. F., A. S. Matlack, and D. S. Breslow, *J. Am. Chem. Soc.*, **85**, 4014 (1963).
35. Kwiatek, J., I. L. Mador, and J. K. Seyler, *J. Am. Chem. Soc.*, **84**, 304 (1962).
36. Bowden, F. P., and A. D. Yoffe, *Endeavour*, **21**, 125 (1962).
37. Societe des Usines Chimiques Rhone-Polenc, Belgian Pats. 562,860; 567,208 (1958).
38. Imperial Chemical Industries, Ltd., British Pat. 838,723 (1960).
39. D'Alenio, G. F., U. S. Pats. 3,038,864 (1962); 3,092,589; 3,095,383 (1963).
40. Benning, C. J., U. S. Pat. 2,956,050 (1960).
41. W. R. Grace & Co., Belg. Pat. 588,973 (1960); Brit. Pats. 872,861; 872,970 (1961); 891,575 (1962); French Pats. 1,254,783; 1,261,536 (1961).
42. Farbenfabriken Bayer Akt.-Ges., Brit. Pat., 825,958 (1959).
43. Pechiney-Compagnie de Produits Chimiques et Electrometallurgiques, French Patent 1,155,962 (1958).
44. Bond, P. A., and E. B. Crone, *J. Am. Chem. Soc.*, **56**, 2028 (1934).

Résumé

L'éthylène a été polymérisé dans des conditions douces au moyen (1) de métaux de transition plus des halogénures d'alcoyle, (2) d'hydrures de métal de transition, (3) de certains métaux de transition seuls et (4) de certains halogénures et oxydes de métaux de transition bivalents. Le polypropène a été polymérisé pour fournir des mélanges de polymères amorphes et cristallins à de faibles conversions par (1) des métaux de transition plus des halogénures d'alcoyle et (2) certains halogénures et oxydes de métaux de transition bivalents. Un broyeur à boulets vibrants a été employé comme récipient de polymérisation afin de fournir un approvisionnement continu de la surface catalytique à l'état frais pendant la polymérisation. L'existence temporaire d'alcoyle métal de transition est postulée pour interpréter la catalyse observée. Ce travail fournit une des preuves les plus directes que la polymérisation a lieu sur le métal de transition plutôt que sur l'aluminium, le zinc ou d'autres métaux habituellement associé avec lui dans les catalyseurs du type Ziegler.

Zusammenfassung

Äthylen wurde unter milden Reaktionsbedingungen mit (1) Übergangsmetallen plus Alkylhalogeniden, (2) Übergangsmetallhydriden, (3) gewissen Übergangsmetallen allein und (4) gewissen Halogeniden und Oxyden zweiwertiger Übergangsmetalle polymerisiert. Propylen wurde bei geringem Umsatz zu Gemischen amorpher und kristalliner Polymerer durch (1) Übergangsmetalle plus Alkylhalogeniden und (2) gewisse Halogenide zweiwertiger Übergangsmetalle polymerisiert. Eine Schwingkugelmühle wurde als Polymerisationsgefäß verwendet, um eine kontinuierliche Nachlieferung frischer Katalysatoroberfläche während der Polymerisation zu gewährleisten. Zur Erklärung der beobachteten Katalyse wird das vorübergehende Auftreten von Übergangsmetallalkylen angenommen. Die vorliegende Arbeit liefert einen der direktesten Beweise dafür, dass die Polymerisation am Übergangsmetall und nicht an Aluminium, Zink oder anderen Metallen, die üblicherweise in typischen Zieglerkatalysatoren verwendet werden, auftritt.

Received December 15, 1964

Revised February 9, 1964

Prod. No. 4676A

Homogeneous Ionic Copolymerization. A Study of Solvent Effects in the Styrene Systems*

C. G. OVERBERGER, T. M. CHAPMAN, and T. WOJNAROWSKI,†
Department of Chemistry, Institute of Polymer Research, Polytechnic Institute of Brooklyn, Brooklyn, New York

Synopsis

The effect of solvent in the homogeneous anionic copolymerization of styrene with *p*-methylstyrene, *p*-*tert*-butylstyrene, and *m*-methylstyrene has been determined. In nonpolar media where the gegenion is lithium, a nonhomogeneous distribution exists with the more basic monomer in higher concentration at the growing chain end which shows as an enhanced relative reactivity. This is depressed by the addition of a small amount of more polar solvent. The influence of temperature as a function of solvent has been determined for selected anionic systems. In nonpolar media, an increase of temperature favors incorporation of the less basic monomer whereas a more polar solvent has only a small effect and favors a more ideal copolymerization. In cationic copolymerization the effect of hyperconjugation has been demonstrated. This effect of hyperconjugation appears to be enhanced in polar media. The cationic copolymerizations of styrene with *p*-*tert*-butylstyrene in nitrobenzene shows a steric hindrance of the bulkier monomer on its incorporation into the copolymer. Determination of reactivity ratios as defined for radical systems does not fully characterize ionic copolymerizations.

INTRODUCTION

The purpose of this work was to determine parameters which control copolymer composition in homogeneous ionic copolymerization. Such parameters are defined as polar, resonance, inductive, and steric properties of the monomers, the effect of the solvent, and the effect of temperature.

Previous work in this laboratory concerning heterogeneous ionic copolymerization of styrene with some of its ring-substituted derivatives by use of the Ziegler-Natta catalyst, titanium tetrachloride-triisobutylaluminum demonstrated that in any single polymerization several copolymers of different composition were formed.^{2,3} This was explained in part by postulating the existence of different active sites on the surface of the catalyst varying in their specific chemical environment. The work also demonstrated the existence of a penultimate steric effect with *p*-*tert*-butylstyrene in the heterogeneous system which inhibited the addition of the bulky

* This is the 22nd in a series of papers concerned with ionic polymerizations; for the previous paper in this series, see Overberger and Kamath.¹

† Chief of laboratory, Institute of Plastics, Warsaw, Poland, Visiting Scholar, Committee on International Exchange of Persons-Associated Research Councils.

monomer into the growing copolymer. This effect is particularly important in a heterogeneous polymerization where growth occurs on a solid surface, thus preventing random approach of the monomer to the active site. It was important, however, to study similar parameters for ionic copolymerization in homogeneous systems, not only in relation to the above work, but also because very little data is available for such systems.

The copolymerization of equimolar amounts of styrene and its ring-substituted derivatives, *p*-methylstyrene, *p*-*tert*-butylstyrene, and *m*-methylstyrene, was studied. The use of such similar monomers permitted differences in their relative reactivities to be ascribed to specific parameters with some understanding. The effect of solvent in ionic copolymerization was ascertained; cationic copolymerizations were carried out in toluene and nitrobenzene, whereas, anionic copolymerizations were carried out in toluene, in toluene mixtures with diethyl ester, diethyl sulfide, triethylamine, and tetrahydrofuran, and in pure tetrahydrofuran. The effect of temperature was studied for selected anionic systems.

EXPERIMENTAL

Monomer Synthesis

The *p*-*tert*-butylstyrene was prepared according to the procedure of Mowry⁴ from commercial *tert*-butylbenzene. However, the reduction of the ketone was carried out with lithium aluminum hydride rather than catalytically. The *p*-*tert*-butylstyrene was obtained by dropping a benzene solution of the alcohol through a column of activated alumina heated to 310°C. The final product was purified by distillation, b.p. 87–88°C./10 mm. (b.p. 99–100°C./14 mm., $n_D^{25} = 1.5245$).

m-Methylstyrene was prepared by the method of Overberger et al.⁵

p-Methylstyrene was purchased from the Monomer-Polymer Laboratories of the Borden Chemical Company. It was purified by distillation.

Styrene- α -C¹⁴ was prepared by the method described in previous papers.^{3,4}

All monomers were stored in the cold over *p*-*tert*-butylcatechol.

n-Butyllithium was supplied by the Foote Mineral Company as a 15% by weight solution in hexane. This was diluted under nitrogen in five parts of toluene and stored in the cold.

Aluminum bromide was distilled under vacuum and stored in glass ampules. A saturated solution of aluminum bromide in toluene was prepared by dissolving the material in toluene. After several days there was phase separation, leaving a small amount of a very dark, denser phase. Only the upper phase was used.

Benzoyl peroxide (Fisher reagent grade) was used without further purification.

Solvent Purification

Toluene and xylene were shaken with concentrated sulfuric acid until the washings were colorless. This was followed by washings with base and water, drying over molecular sieves, and distillation.

Diethyl ether and tetrahydrofuran were distilled from blue benzophenone ketyl immediately before use.

Diethyl sulfide and triethylamine were distilled and stored over calcium hydride.

Nitrobenzene was steam distilled from dilute sulfuric acid, dried over calcium chloride, and then distilled under reduced pressure.

Copolymerizations

The reaction vessel for the ionic copolymerizations was a four-necked flask fitted with an externally driven magnetic stirrer, a stopcock fitted with a serum cap, and a side-arm to which was attached a 100-ml. round-bottomed flask. The vessel was attached to a high-vacuum manifold.

A solution of 10 ml. of monomer mixture in 35 ml. of solvent was stored over calcium hydride in the round-bottomed flask overnight. The material was then degassed three times at 5×10^{-6} mm. Hg and distilled into the reaction vessel. Nitrogen was then added to the system. It was necessary to purify the nitrogen by passing it through a drying tower and subsequently a solution of benzophenone ketyl and then a cold trap. The ketyl solution was prepared by adding sodium-potassium alloy to a solution of benzophenone in xylene. After shaking, the very deep blue color of the ketyl would appear. The liquid alloy was prepared by crushing sodium and potassium together under xylene with a glass rod. The reaction vessel, now containing monomer and solvent(s), was then brought to temperature. Copolymerizations were carried out at 0°C. except for a number of experiments at 20°C.

Catalyst solution was now added volumetrically by means of a syringe through the serum cap. For the anionic copolymerizations, except those with THF, the *n*-butyllithium solution was added dropwise until the orange-brown color of the styryl anion was stable. Then an additional 0.3 ml. of catalyst solution was added. Copolymerizations were generally carried to under 6% conversion, the required time being from several minutes to 1 hr., depending upon the solvent system. The reaction in tetrahydrofuran was too rapid for this procedure, and it was necessary to determine arbitrarily the number of drops of catalyst solution to give a reasonable conversion. In each of the cationic copolymerizations, 0.15 ml. of catalyst solution was added and the polymerization carried out for 5-10 min.

Radical copolymerizations were carried out in sealed tubes. A 0.35% solution of benzoyl peroxide in monomer mixture was reacted for 4 hr. at 64°C. Conversions were about 10%.

The copolymers were reprecipitated at least twice from toluene-methanol and dried in a pistol over phosphorus pentoxide at 65°C. under oil pump vacuum.

Copolymer Analysis

Copolymer composition was determined by radioactive carbon counting by use of a procedure similar to one described in a previous paper.³ The

styrene used contained styrene- α -C¹⁴. For the anionic polymerization in toluene the isotope effect was determined by comparison of the activity of a high conversion and low conversion homopolymer. The isotope effect did not exceed experimental error which was about 2%. Specifically, 40–60 mg. samples were accurately weighed in tared 2 ml. volumetric flasks. After being brought to volume with purified xylene, 500 and 1000 μ l. aliquots were placed into suitable counting vessels. To these were then added 5 ml. portions of 0.36% 2,5-diphenyl-oxazole in xylene. Radioactivity was measured by an EKCO 612 scintillation counter at -17°C . and an EKCO N53 Scaler at PM voltage 1150 and discrimination bias 12.5 V. The counting vessels were supplied by American Tradair Corporation. Background radiation was subtracted and the specific activity (activity/unit weight) of the samples determined. The specific activity of a homopolymer prepared from the styrene used was determined, and the ratio of the activities gave the weight per cent styrene in the copolymer, from which the mole per cent could be calculated. Copolymerizations were carried out in duplicate.

RESULTS

The effect of solvent on anionic copolymerization in the styrene system is shown in Table I and in Figures 1–3. In each case it is shown that the addition of a small amount of polar solvent to toluene causes a considerable increase in the incorporation of styrene. Of particular interest is the case of *m*-methylstyrene, where an apparent reversal of reactivity with styrene occurs. Further addition of polar cosolvent causes the styrene incorporation to reach a maximum and essentially remain there, within experimental error.

The effect of solvent in cationic copolymerization is shown in Table II. Polar solvent increases the apparent reactivity of *p*-methylstyrene in its

TABLE I
Influence of Diethyl Ether (E) and Tetrahydrofuran (THF) on Anionic Copolymerization with 50 Mole-% Styrene with Various Comonomers

Solvent	Styrene in copolymer, mole-%		
	<i>p</i> -Methylstyrene	<i>p</i> - <i>tert</i> -Butylstyrene	<i>m</i> -Methylstyrene
Toluene (T)	61.8 \pm 2.1	64.4 \pm 0.7	44.0 \pm 1.3
34:1 T-E	71.4 \pm 2.5	73.8 \pm 2.3	53.9 \pm 1.1
32:3 T-E	74.6 \pm 1.0	72.0 \pm 2.9	
30:5 T-E	73.5 \pm 0.0	72.0 \pm 0.9	54.8 \pm 1.6
25:10 T-E	73.1 \pm 0.8	73.5 \pm 1.2	
20:15 T-E	76.5 \pm 1.2	72.5 \pm 0.8	53.4 \pm 1.1
1:2 T-E	68.5 \pm 1.8	68.2 \pm 1.4	
5:30 T-E	71.2 \pm 1.5	69.4 \pm 1.2	52.4 \pm 1.7
34:1 T-THF	75.6 \pm 0.4		
4:3 T-THF	75.1 \pm 0.3		
THF	76.7 \pm 0.7	72.7 \pm 1.2	58.2 \pm 1.3

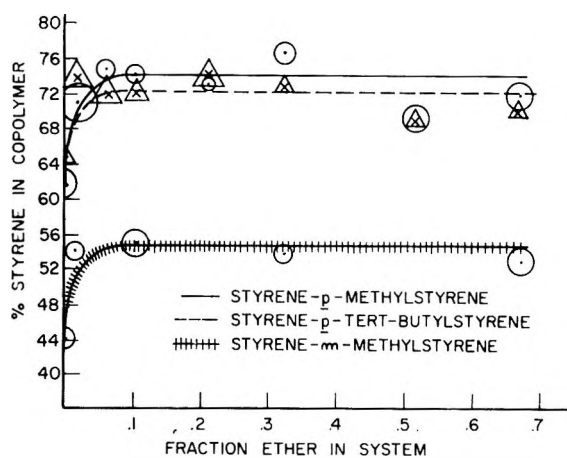


Fig. 1. Effect of diethyl ether in anionic copolymerization.

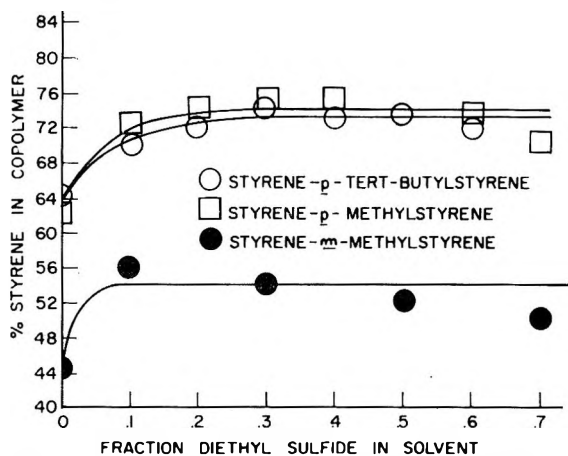


Fig. 2. Effect of diethyl sulfide in anionic copolymerization.

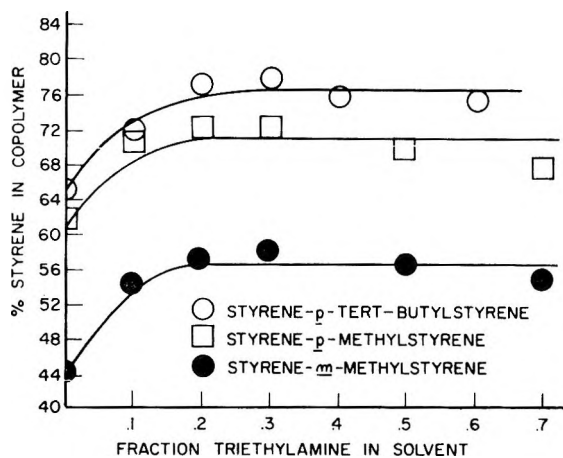


Fig. 3. Effect of triethylamine in anionic copolymerization.

copolymerization with styrene and decreases that of *p-tert*-butylstyrene. For the latter case there is another apparent reversal of reactivity with styrene. There is no effect on the relative incorporation of *m*-methylstyrene.

The effect of substituent on monomer reactivity is readily shown. In anionic copolymerization *p*-methylstyrene \approx *p-tert*-butylstyrene $>$ *m*-methylstyrene. For the cationic systems, *p*-methylstyrene is considerably more reactive than the other substituted styrenes in their copolymerization with styrene.

TABLE II
Cationic and Radical Copolymerization with 50 Mole-% Styrene

Comonomer	Styrene in copolymer, mole-%		
	Cationic		Radical (bulk)
	Toluene	Nitrobenzene	
<i>p</i> -Methylstyrene	38.8 \pm 0.5	34.7 \pm 1.6	48.3 ^a
<i>p-tert</i> -Butylstyrene	49.0 \pm 0.7	54.9 \pm 1.2	52.7 \pm 0.3
<i>m</i> -Methylstyrene	47.5 \pm 0.6	46.9 \pm 1.6	49.8

^a Agrees exactly with a value calculated from reactivity ratios of Wiley and Davis.⁶

TABLE III
Effect of Temperature in Anionic Copolymerization of Equimolar
Styrene-*p*-Methylstyrene

Solvent	Styrene in copolymer, mole %	
	0°C.	20°C.
Toluene	61.8 \pm 2.1	70.1 \pm 0.5
34:1 T-E	71.4 \pm 2.5	73.8 \pm 1.0
4:3 T-E	76.5 \pm 1.2	72.4 \pm 0.9
1:6 T-E	71.2 \pm 1.5	71.4 \pm 1.0

The effect of temperature on the anionic copolymerization of styrene with *p*-methylstyrene in different solvent mixtures is shown in Table III. With temperature increase the effect is small or in the direction of equalizing monomer incorporation when polar solvent is present; however, in toluene solvent the difference in apparent monomer reactivity is accentuated.

DISCUSSION

The effect of solvent in homogeneous anionic copolymerization is open to some discussion. Tobolsky and Boudreau⁷ reported that a study of the copolymerization of substituted styrenes demonstrated that as the solvating power of the solvent increased, the reactivity ratios approached unity. Recently Tobolsky and co-workers⁸ have extended these studies and revised a few of the experimental results given in the earlier paper.⁷ Dawans and

Smets⁹ studied anionic copolymerizations initiated by phenylmagnesium bromide and came to the same conclusions. These results were explained by assuming that reactivity was greater in polar solvents since the overall rates of polymerization were greater. It was further reasoned that since the reactivity is greater in polar solvents, the selectivity of copolymerization would be less—thus the reactivity ratios would approach unity. Recent work of Worsfold and Bywater¹⁰ and Morton et al.,¹¹ however, showed that reactivity actually decreases in polar media. The results reported here show an opposite effect of solvent for the styrene-*p*-methylstyrene and styrene-*p-tert*-butylstyrene systems; an increase in solvent polarity increases the incorporation of the more reactive monomer, styrene. Styrene incorporation is increased also in the *m*-methylstyrene system. The effects of solvent reported by Tobolsky and co-workers^{7,8} are somewhat inconclusive. A comparison is made between sodium in THF (heterogeneous), lithium in THF, and *n*-butyllithium in toluene. To permit any conclusion about solvent, the latter two cases would have to be compared, but in the copolymerizations with lithium metal, it is assumed that radical growth also competes with anionic propagation. The work of Dawans and Smets⁹ is generally with monomers of considerably different electronegativities and of higher polarity than the solvents used; however, for a monomer pair of similar electronegativities, methacrylonitrile and methyl methacrylate, there was no variation in the relative reactivities when the solvent changed from toluene to 11:89 ether in toluene to pure ether.

We explain our results by suggesting a nonhomogeneous distribution of the monomers in the nonpolar toluene medium. The lithium gegenion has a very high charge density and would readily complex with aromatic π -electron systems. Since electron-donating substituents increase the basicity of aromatic rings,¹² it is expected that the substituted styrenes will associate more with the lithium ions than will styrene itself. Since the gegenion is kept in the vicinity of the growing chain end, this would mean a higher local concentration of the substituted styrene there. A slight variation of this explanation is to consider that chain growth is always preceded by coordination of the monomer to the gegenion. This latter hypothesis is being investigated by Szwarc,¹³ who is studying the kinetics of styrene polymerization in THF. He has shown that the bimolecular rate constant of propagation increases as initial styrene concentration decreases and explains this in terms of such a two-step propagation mechanism. In either case, the result would be shown as an enhanced incorporation of the substituted styrene derivative in its copolymerization with styrene. The suggestion of a nonhomogeneous distribution of the monomer is supported by the effect of the addition of polar solvent, the greater reactivity of *m*-methylstyrene over styrene in toluene solvent, and the reversal of this reactivity when polar solvent is added, and the effect of temperature.

The addition of a solvent of higher solvating power than the monomers would displace the monomers from the gegenion and would also make the

gegenion a weaker electrophile. This would minimize the local concentration effect and would show as an increase in styrene incorporation.

Tobolsky and Boudreau⁷ showed that in anionic copolymerization the relative reactivities of styrene with some of its derivatives obeyed the order styrene > *p*-methylstyrene > *p*-methoxystyrene. Szwarc et al.¹⁴ had demonstrated that in THF the rate constant for the addition of substituted styrenes to a polystyrene carbanion followed a Hammett σ - ρ relationship with a ρ value of +5.0. Thus, electron-donating groups in the benzene ring decrease the reactivity of styrene derivatives relative to styrene. The greater reactivity of *m*-methylstyrene over styrene in toluene solvent demonstrated here can best be explained by a concentration or coordination effect. Indeed, the addition of a small amount of polar solvent causes a reversal of the relative reactivities.

Lewis et al.¹⁵ postulated that as temperature increased, reactivity ratios should tend toward unity and showed this to be true for some radical copolymerizations. Investigating anionic systems, Dawans and Smets⁹ showed that in all but one case reactivity ratios remained constant or approached unity as temperature increased. The result we report, the copolymerization in toluene where styrene, the more reactive monomer, becomes even more reactive with a temperature increase, can be rationalized again by assuming a nonhomogeneous distribution of the monomers. A temperature increase would desolvate the gegenion and again the resulting copolymer would have a higher fraction of styrene. Assuming that there would be no tendency toward alternation with such similar monomers the above explanation becomes the only simple explanation of the result.

The concept of selective monomer solvation or coordination with the growing ion pair is not new. Overberger^{1,16} showed the effect to exist in cationic systems if unlike monomers such as isobutylene and *p*-chlorostyrene were used, but not for similar monomers such as styrene and *p*-chlorostyrene. A possible reason why monomer solvation can effect the copolymerization of styrene and its derivatives in the homogeneous anionic systems studied is that the lithium ion has a much higher charge density than a carbonium ion and, therefore, will interact much more strongly with an automatic-electron system. Preferential monomer activation in the anionic copolymerization of styrene and butadiene has been postulated before. Korotov¹⁷⁻¹⁹ showed that although styrene is the more reactive monomer in a homopolymerization, copolymerization gives mostly butadiene. The addition of a small amount of ether greatly increased the styrene incorporation. The results were explained in terms of selective monomer solvation of the butadiene on the growing chain ends. O'Driscoll and Kuntz²⁰ explained these results purely on the basis of copolymerization cross-propagation reactions, but Korotov's mechanism is very plausible.²¹

The anionic copolymerization of styrene with *p*-*tert*-butylstyrene shows no steric control of copolymer composition. This contrasts with the heterogeneous copolymerization of these monomers.²

The results of the cationic copolymerizations demonstrate the strong influence of hyperconjugation. The *p*-methyl substituent is able to stabilize a benzylic carbonium ion much better than a *p*-*tert*-butyl or a *m*-methyl group. Overberger et al.⁵ showed that in the styrene system reactivity ratios follow a Hammett σ relationship, except where strong electron-donating groups such as methoxy or dimethylamino could stabilize the carbon ion. Tobolsky⁷ has demonstrated that the reactivity ratios followed the Brown σ^+ substituent values, thus supporting this view. Yonezawa et al.²² related monomer reactivity to the resonance stabilization energy of the resulting carbonium ion. Thus, the large difference in reactivity between *p*-methylstyrene and *p*-*tert*-butyl styrene is expected, though their respective Hammett substituent constants are similar.

We find that the effect of solvent polarity in the styrene-*p*-methylstyrene cationic copolymerization is such that the styrene content in the copolymer decreases as the polarity of the solvent increases from toluene to nitrobenzene. This agrees with the more recent work of Tobolsky and co-workers,⁸ who revised the earlier results⁷ from their laboratory on this particular system. Since relative reactivity is based on the ability to stabilize the resulting carbonium ion by resonance, an increase in solvent polarity which frees the carbonium ion from the gegenion, thus permitting it to interact more with the aromatic structure, would show as a decrease in styrene content. Solvent has no effect on the copolymerization with *m*-methylstyrene. The copolymerization with *p*-*tert*-butylstyrene is of interest, since there is a reversal of reactivity of the monomers. That *p*-*tert*-butylstyrene should be less reactive than styrene in a cationic system can be explained by imposing some steric control of the copolymer composition. Perhaps there is a built-in steric effect because nitrobenzene is a highly ordered solvent which would cluster around the growing chain end; however, this is difficult to say, since the reactivity does not differ very much from that in a free-radical copolymerization.

This paper comprises a portion of a dissertation submitted by T. M. Chapman in partial fulfillment of the requirements for the degree of Doctor of Philosophy in the Graduate School of the Polytechnic Institute of Brooklyn.

We wish to thank Monsanto, M and T Chemicals, Inc., and the Department of State for their generous support of this work.

References

1. Overberger, C. G., and V. G. Kamath, *J. Am. Chem. Soc.*, **85**, 446 (1963).
2. Overberger, C. G., and F. Ang, *J. Am. Chem. Soc.*, **82**, 929 (1960).
3. Overberger, C. G., and S. Nozakura, *J. Polymer Sci.*, **A1**, 1439 (1963).
4. Mowry, R., M. Renoll, and W. Huber, *J. Am. Chem. Soc.*, **68**, 1105 (1946).
5. Overberger, C. G., L. H. Arond, D. Tanner, J. J. Taylor, and T. Alfrey, Jr., *J. Am. Chem. Soc.*, **74**, 4848 (1953).
6. Wiley, R., and B. Davis, *J. Polymer Sci.*, **26**, 423 (1960).
7. Tobolsky, A. V., and R. J. Boudreau, *J. Polymer Sci.*, **51**, S53 (1961).

8. Phillips, B. D., T. L. Hanlon, and A. V. Tobolsky, *J. Polymer Sci.*, **A2**, 4231 (1964).
9. Dawans, F., and G. Smets, *Makromol. Chem.*, **59**, 163 (1963).
10. Worsfold, D. J., and S. Bywater, *Can. J. Chem.*, **40**, 1564 (1962).
11. Morton, M., L. J. Fetters, and E. E. Bostick, *J. Polymer Sci.*, **C1**, 311 (1963).
12. Hine, J., *Physical Organic Chemistry*, McGraw-Hill, New York, 1962, p. 349.
13. Szwarc, M., and J. Smid, *Progr. Reaction Kinetics*, **2**, 243 (1964).
14. Shine, M., D. N. Bhattacharyya, J. Smid, and M. Szwarc, *J. Am. Chem. Soc.*, **85**, 1306 (1963).
15. Lewis, F. M., C. Walling, W. Cummings, E. R. Briggs, and F. M. Mayo, *J. Am. Chem. Soc.*, **70**, 1519 (1948).
16. Overberger, C. G., and V. G. Kamath, *J. Am. Chem. Soc.*, **81**, 2910 (1959).
17. Rakova, G. V., and A. A. Korotov, *Dokl. Akad. Nauk SSSR*, **119**, 982 (1958).
18. Korotov, A. A., and N. N. Chesnokova, *Vysokomol. Soedin.*, **2**, 365 (1960).
19. Korotov, A. A., S. P. Mitsengendler, and K. M. Aleyev, *Vysokomol. Soedin.*, **2**, 811 (1960).
20. O'Driscoll, K. F., and I. Kuntz, *J. Polymer Sci.*, **61**, 19 (1962).
21. Szwarc, M., and J. Smid, *Progr. Reaction Kinetics*, **2**, 267 (1964).
22. Yonezawa, T., T. Higashimura, K. Karagiri, K. Hayashi, S. Okamura, and K. Fukui, *J. Polymer Sci.*, **26**, 311 (1951).

Résumé

On a déterminé l'influence du solvant lors de la copolymérisation anionique en milieu homogène du styrène avec le *p*-méthylstyrène, le *p*-*tert*-butylstyrène, et le *m*-méthylstyrène. Dans les milieux non polaires où l'ion complémentaire est le lithium, une distribution non homogène existe avec le monomère plus basique en concentration plus élevée sur la chaîne en croissance et qui se révèle comme une réactivité relative exaltée. Ce phénomène est réduit par l'addition d'une petite quantité d'un solvant plus polaire. On a déterminé l'influence de la température en fonction du solvant pour des systèmes anioniques sélectionnés. Dans les milieux non polaires, une augmentation de la température favorise l'incorporation de monomère moins basique tandis qu'un solvant plus polaire a seulement une faible influence et favorise une copolymérisation plus idéale. Dans la copolymérisation cationique on a démontré l'influence de l'hyperconjugaison. Cette influence de l'hyperconjugaison semble être renforcée dans les milieux polaires. Les copolymérisations cationiques du styrène avec le *p*-*tert*-butylstyrène dans le nitrobenzène montrent un empêchement stérique du monomère plus volumineux par son incorporation dans le copolymère. La détermination des rapports de réactivité définis pour les systèmes radicalaires ne caractérise pas complètement les copolymérisations ioniques.

Zusammenfassung

Der Einfluss des Lösungsmittels auf die homogene, anionische Kopolymerisation von Styrol mit *p*-Methylstyrol, *p*-*tert*-Butylstyrol, und *m*-Methylstyrol wurde bestimmt. In unpolaren Medien besteht mit Lithium als Gegenion eine nicht homogene Verteilung, wobei das stärker basische Monomere sich in höherer Konzentration in der wachsenden Kette befindet und eine erhöhte relative Reaktivität zeigt. Dies wird durch Zusatz einer kleinen Menge eines stärker polaren Lösungsmittels unterdrückt. Der Temperatureinfluss wurde als Funktion des Lösungsmittels für ausgewählte anionische Systeme bestimmt. In unpolaren Medien begünstigt eine Temperaturerhöhung den Einbau des weniger basischen Monomeren, während ein mehr polares Lösungsmittel nur einen geringen Einfluss besitzt und eine ideale Kopolymerisation begünstigt. Bei der kationischen Kopolymerisation konnte der Einfluss der Hyperkonjugation nachgewiesen werden. Der Hyperkonjugationseffekt scheint in polaren Medien verstärkt zu sein.

Die kationische Kopolymerisation von Styrol mit *p-tert*-Butylstyrol in Nitrobenzol zeigt eine sterische Hinderung des grösseren Monomeren bei seinem Einbau in das Kopolymere. Die Bestimmung von Reaktivitätsverhältnissen, wie sie für radikalische Systeme definiert wurden, reicht zur vollständigen Charakterisierung der ionischen Kopolymerisation nicht aus.

Received February 1, 1965

Prod. No. 4679A

Preparation and Polymerization of Vinyl Esters of Nonhydroxy Carnuba Wax Acids and Acrylic Esters of Carnuba Wax Alcohols*

C. S. MARVEL, J. H. GRIFFITH, and J. L. COMP,†
Department of Chemistry, University of Arizona, Tucson, Arizona
and J. C. COWAN and J. L. O'DONNELL,
*Northern Utilization Research and Development Division,
Agricultural Research Service, U. S. Department of Agriculture,
Peoria, Illinois*

Synopsis

The acrylic esters of carnuba wax alcohols and the vinyl esters of nonhydroxy carnuba wax acids have been synthesized. The acrylic and vinyl esters have been homopolymerized and copolymerized with vinyl chloride. Acrylonitrile-acrylic ester copolymers also have been prepared. The copolymers were quite brittle when molding was attempted.

INTRODUCTION

Copolymers of vinyl chloride and vinyl esters of long-chain fatty acids have been prepared to determine the degree of internal plasticization by the incorporated vinyl ester. Port and co-workers¹ found that copolymers of vinyl chloride and vinyl acetate were rigid plastics, whereas copolymers of vinyl chloride and vinyl stearate (a C₁₈ acid) were flexible. A copolymer of vinyl behenate (a C₂₂ acid) and vinyl chloride was less plasticized than a copolymer of 13,14-dichlorobehenate and vinyl chloride.² Copolymers of a straight-chain acid vinyl ester of an acid mixture of C₂₂, 78%, C₂₀, 10%, and C₁₈, 7% and of vinyl 9,10-dichlorostearate; vinyl 9,10,12,13-tetrachlorostearate; and vinyl 9(10)-phenylstearate with vinyl chloride have also been prepared and evaluated for internal plasticization² and showed some promise.

To examine the plasticizing effect of an even longer straight-chain hydrocarbon group in a vinyl chloride copolymer, vinyl esters of nonhydroxy carnuba wax acids (VCW) and acrylic esters of carnuba wax

* This is a partial report of work done under contract with four Utilization Research and Development Divisions, Agricultural Research and Development Divisions, Agricultural Research Service, U. S. Department of Agriculture, and authorized by the Research and Marketing Act. The contract was supervised by Dr. J. C. Cowan of the Northern Division.

† Present address: Department of Chemistry, Southwest Texas State College, San Marcos, Texas.

alcohols (ACW) have been copolymerized with vinyl chloride in an emulsion system. The ACW esters also have been copolymerized with acrylonitrile in a solution system. Bulk and solution homopolymers of the VCW and the ACW esters have been prepared and characterized.

The carnuba wax alcohols and nonhydroxy acids were obtained by saponification of Brazil No. 1 carnuba wax with potassium hydroxide. The alcohols were extracted with hot heptane and the acids were extracted as soaps with hot aqueous alcohol. The VCW esters were pre-

TABLE I
Bulk and Solution Homopolymerization of Vinyl Esters of Nonhydroxy Carnuba Wax Acids (VCW) and Acrylic Esters of Carnuba Wax Alcohols (ACW)

Sample	Wt. ester, g.	Con- ver- sion, %	Melting range, °C.	Elemental analysis			η_{inh}^c
				C, %	H, %		
Bulk ^a							
ACW 77-2	1.0	85	175-202	79.50	12.40		Insoluble
VCW 77-1	1.0	82	135-172	77.22	12.93		Insoluble
Solution ^b							
ACW 78-1	1.5	80	79-85	80.00	12.91		0.35
VCW 78-2	1.5	60	Gummy	78.27	12.85		0.28

^a The polymerization tube was heated to 65°C. for 24 hr. and contained 0.020 g. of 2,2'-azobisisobutyronitrile (AIBN).

^b The polymerization tube was heated to 65°C. for 24 hr. and contained 10 ml. of benzene and 0.020 g. of AIBN.

^c Inherent viscosity at 30°C. of 0.4% solution in tetrahydrofuran.

TABLE II
Emulsion Copolymerization of Vinyl Chloride and the Vinyl Esters of Nonhydroxy Acids of Carnuba Wax

Sample	Wt. co- Vinyl polymer ester, isolated, wt.-% ^a		Melting point, °C.	Elemental analysis			m_1/m_2^b	η_{inh}^c
	g.			C, %	H, %	Cl, %		
73-1	30	7.0	95-130	46.29	6.46	40.09	16.2/1	0.746
100-1	20	22.0 ^d	120-150	45.15	5.95	44.82	25.2/1	1.54 ^e
73-2	20	7.5	95-155	44.70	5.86	45.32	26.8/1	0.586
73-3	10	10.3 ^d	110-135	41.68	5.45	51.08	60.2/1	0.393
73-4	5	24.3 ^d	135-165	41.01	5.29	53.86	123.5/1	0.393
73-5	3	23.5 ^d	145-180	40.77	5.34	54.01	130.2/1	0.492
73-6	1	13.2 ^d	150-190	41.04	5.17	52.57	83.2/1	0.750

^a A 10-g. portion of monomer mixture, 40 ml. of water, 3.0 g. of Triton X-301, and 4.0 ml. of 2.5% potassium persulfate solution tumbled for 48 hr. at 60°C.

^b Molar ratio of monomer units in copolymer calculated from elemental analysis; $m_1 = \text{VCl}$, $m_2 = \text{VCW}$.

^c Inherent viscosity at 30°C. of 0.4% solution in tetrahydrofuran.

^d Samples combined from two or three batches.

^e Inherent viscosity at 30°C. of 0.2% solution in tetrahydrofuran.

pared by the vinyl ester exchange procedure of Adelman;³ the ACW esters by trans-esterification with methyl acrylate.

Both ACW and VCW esters were easily homopolymerized in bulk with 2,2'-azobisisobutyronitrile (AIBN). These homopolymers were insoluble in dimethylformamide, dimethyl sulfoxide, tetrahydrofuran, acetone, benzene, and methanol. In all but the last solvent, the mono-

TABLE III
Solution Copolymerization of Vinyl Chloride and Acrylic Esters of Carnuba Wax Alcohols^a

Sample	Acrylic ester, wt.-%	Wt. co-polymer isolated, g.	Melting point, °C.	Elemental analysis			m_1/m_2^b	η_{inh}^c
				C, %	H, %	Cl, %		
72-1	30	4.3	75-85	52.08	7.24	38.62	17.4/1	0.417
72-2	20	17.6 ^d	84-100	50.62	7.23	41.23	21.7/1	0.197
72-3	15	21.4 ^d	125-150	45.58	6.20	46.77	38.1/1	0.234
72-4	10	27.4 ^d	145-160	44.13	5.58	48.89	50.5/1	0.199
72-5	5	19.3 ^d	135-160	42.19	5.45	52.34	96.0/1	0.224
72-6	3	22.6 ^d	130-165	41.08	5.37	52.30	95.0/1	0.243
72-7	4	9.0	135-165	40.57	5.34	53.29	121.1/1	0.219

^a A 10-g. portion monomers in 40 ml. of benzene and 0.2 g. of 2,2'-azobisisobutyronitrile at 60°C. for 48 hr.

^b Molar ratio of monomer units in copolymer calculated from elemental analysis $m_1 = \text{VCl}$, $m_2 = \text{ACW}$.

^c Inherent viscosity at 30°C. of 0.4% solution in tetrahydrofuran.

^d Samples combined from two or three batches.

TABLE IV
Solution Copolymerization of Acrylonitrile and Acrylic Esters of Carnuba Wax Alcohols^a

Sample	Acrylic ester, wt.-%	Wt. co-polymer isolated, g.	Melting point, °C. ^b	Elemental analysis			m_1/m_2^c
				C, %	H, %	N, %	
74-1	0	14.0 ^d	>340	67.40	5.77	25.72 ^e	Homopolymer
74-3	30	19.4 ^d	>340	71.30	7.62	18.49	22.5/1
74-4	25	19.0 ^d	>340	70.67	7.38	19.85	29.7/1
74-5	20	8.7	>340	71.57	7.35	20.74	36.0/1
74-6	15	9.0	>340	69.28	6.81	22.73	61.6/1
74-7	10	8.7	>340	68.58	6.16	23.76	9.9/1

^a A 10-g. portion of monomers, 0.2 g. of 2,2'-azobisisobutyronitrile, and 40 ml. of benzene per batch at 60°C. for 48 hr.

^b No sample melted below 340°C.; 73-1 turned brown at about 300°C., and all the others turned brown at about 230°C.

^c Molar ratio of monomers in copolymer calculated from elemental analysis: $m_1 = \text{ACN}$, $m_2 = \text{ACW}$.

^d Three batches were combined.

^e The theoretical N content of the homopolymer is 26.3%. Since polyacrylonitrile retains dimethyl sulfoxide tenaciously even after drying in vacuum for several days, all these samples may contain some dimethylsulfoxide.

mers were very soluble. These two esters were also homopolymerized in benzene solution with AIBN as the initiator. Soluble polymers were obtained by this procedure. Table I contains the data for the homopolymers.

Copolymers of the VCW esters with vinyl chloride (Table II) were prepared in an emulsion system by using potassium persulfate initiation. The ACW esters were copolymerized with vinyl chloride (Table III) and acrylonitrile (Table IV) in solution systems with AIBN initiation.

Inherent viscosities ranged from 0.39 to 0.75 for the VCW ester-vinyl chloride copolymers (0.4% solutions in tetrahydrofuran) and from 0.19 to 0.41 for the ACW ester-vinyl chloride copolymers. The ACW ester-acrylonitrile copolymers would gel but not dissolve in dimethylformamide or dimethylacetamide. The melting or softening point of the acrylonitrile-ACW ester copolymers was not decreased by an increase in the ester content. Increasing amounts of the VCW and ACW esters in vinyl chloride copolymers decreased the melting points as expected. The vinyl chloride copolymers were all very soluble in the usual organic solvents.

EXPERIMENTAL

Preparation of Compounds

Isolation of Acids and Alcohols of Carnuba Wax. Brazil No. 1 carnuba wax (100 g.) was saponified with potassium hydroxide. The acids were extracted as soaps with hot aqueous alcohol and the alcohols with hot heptane.

Evaporation of the heptane solution gave 53.6 g. of carnuba wax alcohols: m.p. 84–86°C., acid value = 0.23, iodine value = 13.7, 3.72% hydroxyl (hydroxyl equivalent = 457).

The alcoholic extracts were diluted with a large volume of water and acidified with 1*N* hydrochloric acid. The precipitated acids were dissolved in ether, washed free of mineral acid, dried, and filtered, and the solvent was evaporated to yield 41.4 g. of carnuba wax acids: m.p. 73–77°C., neutralization equivalent = 399, 0.67% hydroxyl.

Vinyl Esters of Nonhydroxylated Carnuba Wax Acids. Carnuba wax acids (100 g.) were esterified by refluxing 1 hr. in 320 g. of methanol containing 54 g. of boron trifluoride etherate. After cooling, the reaction mixture was poured into 2 liters of water. The separated esters were dissolved in ether, and the aqueous solution was extracted with ether. The ether solution was washed with water, dried over anhydrous sodium sulfate, and filtered. Evaporation of the ether yielded 95.5 g. of ester: acid value = 5.35, iodine value = 3.1.

The methyl esters (95 g.) and 21 g. of phthalic anhydride in 3 liter of 1:1 heptane-ether solution were heated for 1 hr. on a steam bath. The ether was removed and the residual heptane solution eluted through

basic washed alumina. The phthalic anhydride treatment was repeated with a 3-hr. heating period to remove traces of hydroxy acid. Evaporation of the heptane yielded 45.5 g. of the nonhydroxyl esters, m.p. 55°C.

The nonhydroxyl esters were vacuum-distilled to remove the lower esters. The distillate boiling at 140–175°C./5 μ comprised 17% of the esters. A gas-liquid chromatogram of the residual methyl esters indicated the following composition: 7% C₁₈ and lower, 4% C₂₀, 9% C₂₂, 38% C₂₄, 17% C₂₆, 22% C₂₈, and 3% C₃₀; iodine value = 0. The residual esters were converted to their acids by saponification and acidified: neutralization equivalent = 395. The acids (34 g.) were dissolved at reflux temperature in 250 ml. of vinyl acetate and a catalyst solution of 1.7 g. of mercuric acetate, 0.02 g. of copper resinate, and 0.235 g. of 100% sulfuric acid in 50 ml. of vinyl acetate was added. The solution was refluxed for another 1½ hr. and then shaken and filtered through Celite. The volatiles were removed under reduced pressure. The residue was dissolved in heptane and eluted through a column charged with 9:1 of activated alumina-carbon mixture. The yield of vinyl esters was 30 g.: acid value < 1, iodine value = 61.2.

Acrylate Esters of Carnuba Wax Alcohols. To a 1-liter flask, provided with an efficient distillation column and nitrogen sparge, was added 50 g. of carnuba wax alcohols,⁴ 445 g. of methyl acrylate, 8.1 g. of hydroquinone, and 1.1 g. of concentrated sulfuric acid. The methanol-methyl acrylate azeotrope was continuously removed over a 10-hr. reaction period. The flask's contents were then poured into 1 liter of heptane, and the precipitated hydroquinone was filtered from the solution. The heptane solution was washed repeatedly with water, dried over anhydrous sodium sulfate, and filtered. The solvent was removed under reduced pressure to yield 48 g. of the crude acrylate ester with 0.32% residual hydroxyl.

Acrylic anhydride solution of 1.3 g. in 250 ml. of ether containing 6% hydroquinone was added to the crude ester in 200 ml. of heptane, and the solution was refluxed for 3 hr. The ether was removed under reduced pressure and the heptane solution diluted to 400 ml. with heptane. This solution was eluted through a column charged with 80–20 parts of activated alumina-charcoal. The solvent was stripped off under reduced pressure and 42 g. of white solid was obtained: acid value < 1, saponification equivalent = 511, iodine value = 62, % acrylate ester (corrected for iodine value⁵) = 98. Infrared absorption at 1.41 μ indicated the absence of hydroxyl groups.

Homopolymerization of the ACW and VCW Esters. In polymerization in bulk, 1 g. of ester and 20 mg. of AIBN were placed in a tube connected by standard taper joints to a stopcock. The tube was flushed with nitrogen, evacuated, flushed with nitrogen, and evacuated again before placing in a 65°C. bath. After 24 hr. the tube was opened and the polymer removed. The homopolymers were insoluble in acetone, tetrahydrofuran, dimethylformamide, and dimethyl sulfoxide. After pulverizing the polymers and

washing with these solvents, the polymers, described in Table I, were washed with methanol and dried.

In solution polymerization, 1½ g. of ester, 20 mg. of AIBN, and 10 ml. of benzene (A. R. grade) were placed in the tube described above. Nitrogen was bubbled through the solution and the tube capped, cooled, and evacuated. After 24 hr. in a bath at 65°C., the polymer was coagulated by pouring the solution into methanol. The polymers, described in Table I, were reprecipitated four times from a minimum of benzene into methanol.

Emulsion Copolymerization of Vinyl Chloride (VCl) and the Vinyl Esters of Nonhydroxy Carnuba Wax Acids (VCW). Ace glass polymerization bottles (T 1506, 110 ml.) were charged with an appropriate amount of the VCW ester, 40 ml. of deoxygenated water, 4.0 ml. of a 2.5% potassium persulfate solution, and 3.0 g. of Triton X-301. The bottle was purged with nitrogen and cooled in a solid carbon dioxide-acetone bath. Condensed VCl was added to the bottles and a slight excess allowed to evaporate before capping with crown-type bottle caps. A total of 10 g. of monomer was in each bottle. The bottles were tumbled in a water bath at 60°C. for 48 hr. before coagulating the polymer by pouring the emulsion into 400 ml. of a saturated salt solution. The copolymers were purified by six reprecipitations from tetrahydrofuran into water and three reprecipitations into methanol. The copolymer was filtered, washed two times with methanol, and air-dried for 48 hr. Inherent viscosities were measured on 0.4% solutions in tetrahydrofuran. The copolymers are described in Table II.

Solution Copolymerization of VCl and ACW Esters. A polymerization bottle was charged with an appropriate amount of VCW ester, 0.2 g. of AIBN, and 40 ml. of benzene (A. R. grade). After the bottles were purged with nitrogen and cooled in a solid carbon dioxide-acetone bath, a slight excess of VCl was added. Excess VCl was allowed to evaporate before the bottles were capped. A 10-g. portion of monomer mixture was used in each bottle. After the bottles were tumbled for 48 hr. at 60°C., the copolymer solutions were poured into 400 ml. of methanol. The copolymers were purified by four reprecipitations from tetrahydrofuran into methanol. The copolymer was filtered, washed two times with methanol, and air-dried for 48 hr. Inherent viscosities were measured on 0.4% solutions in tetrahydrofuran. The polymers are described in Table III.

Solution Copolymerization of Acrylonitrile (ACN) and ACW Esters. A polymerization bottle was charged with an appropriate ratio of monomers (a total of 10 g.), 0.2 g. of AIBN, and 40 ml. of benzene (A. R. grade). The solution and bottle were purged with nitrogen and capped with crown-type caps. The bottle was tumbled at 60°C. for 48 hr. and the gelled copolymer was poured into methanol. The copolymers would not completely dissolve in dimethylformamide (DMF). A 15-g. portion of polyacrylonitrile homopolymer (74-1) dissolved completely in 600 ml. of DMF, but 10- and 20-g. samples of the ACW-ACN copolymer would only partially dissolve in 2 liters of boiling DMF. Only a loose gel could be obtained.

The copolymers were reprecipitated three times from DMF into water and then washed with methanol. The finely precipitated copolymers filtered with difficulty. Inherent viscosities measured on the nongel portions of a weighed sample indicated an inherent viscosity of less than 0.2, but attempts to evaporate a known weight-volume sample gave nonreproducible results for the dissolved polymer weight. The tenaciousness with which polyacrylonitrile retains DMF was probably the cause of this difficulty. The polymers are described in Table IV.

Polymer Evaluation

G. R. Riser, of the Eastern Utilization Research and Development Division, USDA, attempted to mold samples of the copolymers prepared from VCl and the VCW esters (Table II). In general, the copolymers were brittle and shattered and chipped when removed from a mold. They showed poor heat stability. Likewise, the copolymers of ACN and the ACW esters (Table III) showed such poor heat stability in the molds that satisfactory testing was not achieved. The VCl-VCW copolymer 100-1 (Table II) had a higher heat stability during molding. However, the brown opaqueness of the molded specimen and the formation of a white area on bending indicate that this copolymer sample was also heterogeneous.

Commercial materials indicated in this manuscript are not recommended over any other such materials of equal quality.

References

1. Port, W. S., E. F. Jordan, Jr., W. E. Palm, L. P. Witnauer, J. E. Hansen, and D. Swern, *Ind. Eng. Chem.*, **47**, 472 (1955).
2. Marvel, C. S., J. C. Hill, J. C. Cowan, J. P. Friedrich, and J. L. O'Donnell, *J. Polymer Sci.*, **A2**, 2523 (1964).
3. Adelman, R. L., *J. Am. Chem. Soc.*, **75**, 2689 (1953).
4. Murray, K. E., and R. Schoenfeld, *J. Am. Oil Chemists' Soc.*, **28**, 461 (1956).
5. Riddle, E. H., *Monomeric Acrylic Esters*, Reinhold, New York, 1954, p. 203.

Résumé

On a synthétisé les esters acryliques des alcools de la cire de Carnauba et les esters vinyliques des acides non hydroxylés de la cire de Carnauba. Les esters acryliques et vinyliques ont été homopolymérisés et copolymérisés avec du chlorure de vinyle. On a également préparé les copolymères acrylonitrile-ester acrylique. Les copolymères sont tout à fait cassants lorsqu'on essaie de les mouler.

Zusammenfassung

Die Acrylester der Carnaubawachsalkohole und die Vinylester der hydroxylgruppenfreien Carnaubawachssäuren wurden synthetisiert. Die Acryl- und Vinylester wurden homopolymerisiert und mit Vinylchlorid copolymerisiert. Weiters wurden Acrylnitril-Acrylestercopolymerere dargestellt. Die Copolymeren erweisen sich bei der Verarbeitung als ziemlich spröde.

Received February 5, 1965
Prod No. 4680 A

NMR Study of Polymers of Ethyl, Isopropyl, and *tert*-Butyl Vinyl Ethers

KERMIT C. RAMEY, NATHAN D. FIELD,*
and ALFRED E. BORCHERT, *The Atlantic Refining Company, Research
and Development Department, Glenolden, Pennsylvania*

Synopsis

The high resolution NMR spectra of poly(vinyl ethyl, isopropyl, isobutyl, and *tert*-butyl ethers), yields, upon examination at 60 and 100 Mcycles/sec., and under the conditions of decoupling, information concerning the various tactic forms present. The spectra are complicated by the number of overlapping resonances to the extent that an unambiguous assignment of the three triad forms could not be made. For poly(vinyl isobutyl ether) the resonances of the α proton decoupled from the β protons exhibits three components which are tentatively assigned to the central monomer units in heterotactic, isotactic, and syndiotactic configurations, with increasing field strength, respectively.

INTRODUCTION

The use of high resolution nuclear magnetic resonance (NMR) in determining the microstructure of polymers has been well documented.¹ In certain cases, particularly that of poly(methyl methacrylate) the normal spectrum is readily interpretable in terms of the three triad forms.¹ In most cases, however, this is not the case, and special techniques such as solvent effects^{2,3} and spin decoupling⁴⁻⁶ must be used to obtain significant results.

Although the chain configuration and crystalline structure of polyvinyl alkyl ethers have been investigated by means of x-ray diffraction, the results are not of a quantitative nature.⁷⁻⁹ A number of NMR studies have also been reported.^{2,3,14,11} However, they have been restricted to poly(α -methylvinyl methyl ether),¹⁰ and poly(vinyl methyl ether).^{2,3,11} In the latter case the spectra showed that the α , β , and methoxyl protons of a central monomer unit are sensitive to the configuration of the adjacent units. Furthermore, the spectra yielded an unambiguous assignment of the three triad forms.³ The object of the present work concerns the use of high resolution NMR to determine and to differentiate between the three tactic forms present in a number of polyvinyl alkyl ethers.

* Present address: General Aniline and Film Corp., Central Research Lab., Easton, Pa.

EXPERIMENTAL

The spectra were obtained with Varian spectrometers operating at 60 and 100 Mcycles/sec., and decoupling was carried out with a Varian integrator utilizing the field sweep technique.¹² The spectra were calibrated by sidebands produced by audiofrequency modulation of the magnetic field. A Hewlett-Packard 200J audiofrequency oscillator in conjunction with a Hewlett-Packard 5512A counter was used. The solutions contained 3–10% (w/v) polymer in a variety of solvents with tetramethylsilane (TMS) as an internal reference and were run at 30°C. unless otherwise specified. The conditions for the various polymerizations are described in the following section.

RESULTS AND DISCUSSION

Poly(vinyl Ethyl Ether)

The 60 Mcycle/sec. spectra of sample I of poly(vinyl ethyl ether) (commercially available from B.A.S.F. Colors and Chemicals Inc.) in solution in C_6H_6 , CH_2Cl_2 , and CS_2 are shown in Figure 1. The spectra consists of three multiplets with chemical shifts ranging from $\tau = 6.47$ to 6.60, 8.17 to 8.40, and 8.82 to 8.90. The downfield multiplet corresponds to the overlap of the resonances for the α proton and the CH_2 protons of the ethyl group. The 100 Mcycle/sec., spectrum of poly(vinyl ethyl ether) in solution in C_6H_6 as obtained at 30°C., is shown in Figure 2A. and depicts quite clearly the advantage of using the higher frequency. At the higher frequency the resonance of the α proton appears as a distinct shoulder on the CH_2 resonance. The relative positions of the two downfield resonances are primarily dependent upon the solvent with C_6H_6 producing the largest separation of those solvents studied. This effect, that of shifting the resonances of the backbone protons downfield relative to that of the side chain group is quite

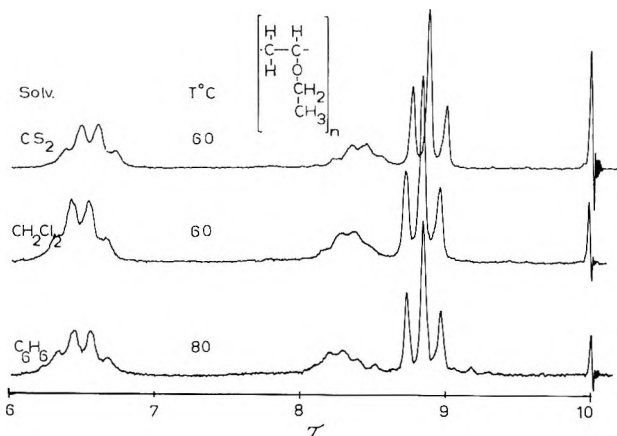


Fig. 1. NMR spectra (60 Mcycles/sec.) of poly(vinyl ethyl ether) in solution in C_6H_6 , CH_2Cl_2 , and CS_2 .

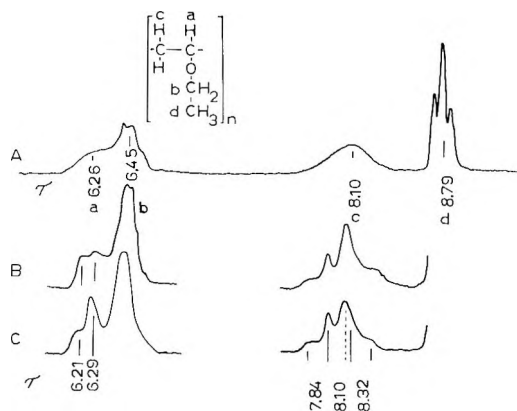


Fig. 2. NMR spectra of poly(vinyl ethyl ether) (100 Mcycles/sec.) in solution in C_6H_6 at $30^\circ C$.: (A) undecoupled spectrum of sample I; (B) decoupled spectra of sample I; (C) decoupled spectra of sample II.

similar to that observed for poly(vinyl methyl ether)³ and is attributed to the spatial relationship of the aromatic ring with respect to the backbone chain of the polymer within the solvated species.

The undecoupled spectrum of sample II of poly(vinyl ethyl ether), which was prepared by using a BF_3 etherate initiator in toluene at $-78^\circ C$., is essentially the same as that of sample I. The decoupled spectra of sample I and II are, however considerably different and are shown in Figures 2B and 2C, respectively. The resonance of the α proton decoupled from the β protons ($\Delta\nu = 1.74$ ppm) exhibits two components at $\tau = 6.21$ and 6.29 which show a considerable variation in intensity with respect to sample. The proximity of the CH_2 resonance of the ethyl group which could overlap the third component of the proton resonance precludes a definite assignment of the two components. The enhancement of the resonance at $\tau = 6.29$ for sample II plus the nature of the catalyst-solvent system used for the polymerization indicates that this resonance corresponds to an isotactic configuration. The resonance of the β protons decoupled from the α proton exhibits an AB quartet ($\nu_A = 7.84$, $\nu_B = 8.32$, $J_{AB} = 15$ cycle/sec. corresponding to isotactic diads and a singlet at $\tau = 8.10$ corresponding to syndiotactic diads. These resonances overlap to the extent that an accurate measurement of their relative areas can not be made. However, the spectra clearly show that sample II is considerably more isotactic than sample I, in agreement with the assignment of the α proton resonances.

Poly(vinyl Isopropyl Ether)

The 100 Mcycle/sec., spectrum of sample I of poly(vinyl isopropyl ether) in solution in CS_2 as obtained at $30^\circ C$. is shown in Figure 3A. Sample I was prepared by using a BF_3 etherate initiator in toluene at $-78^\circ C$. The spectrum consists of four resonances, of which two overlap. The resonances at $\tau = 6.48$ and 8.98 correspond to the isopropyl group while the

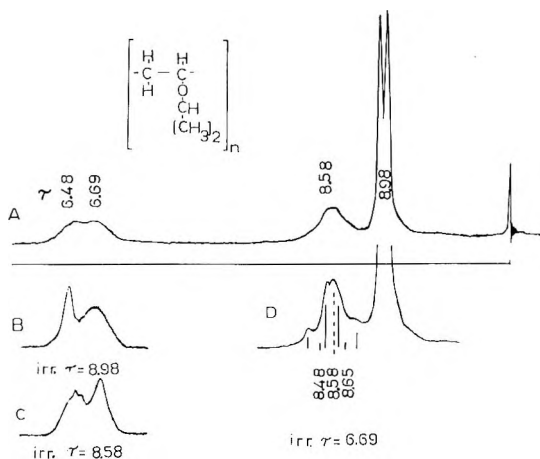


Fig. 3. NMR spectra of poly(vinyl isopropyl ether) (100 Mcycles/sec.) in solution in C_6H_6 at $30^\circ C$.: (A) undecoupled spectrum; (B) resonance of CH proton of isobutyl group decoupled from the CH_3 protons; (C) resonance of the α proton decoupled from the β protons; (D) resonance of the β protons decoupled from the α proton.

resonances of the α and β protons fall at $\tau = 6.69$ and 8.58 , respectively. These assignments were made on the basis of decoupling, and the resulting spectra are shown in Figures 3B, 3C, and 3D. The resonance of the α proton decoupled from the β protons ($\Delta\nu = 1.88$ ppm) exhibits a broad singlet centered at $\tau = 6.69$ as shown in Figure 3C. This could indicate that the α proton is not sensitive to the configuration of the adjacent units. However, the peak is considerably broader than the corresponding decoupled CH resonance of the isopropyl group. This probably indicates that the α proton is sensitive to the configuration of the adjacent units, but that the components are not separated far enough such that they may be resolved under the present experimental conditions. The resonance of the β protons decoupled from the α proton is only partially resolved into an AB quartet and a singlet. The approximate parameters for the AB quartet are $\nu_A = 8.48$, $\nu_B = 8.65$, and $J_{AB} = 15$ cycles/sec., which corresponds to isotactic diads. The singlet corresponding to syndiotactic diads appears at about $\tau = 8.58$. The relative intensities indicate that the sample is predominantly isotactic, perhaps 70%.

Poly(vinyl Isobutyl Ether)

The spectrum of sample I of poly(vinyl isobutyl ether) (commercially available from B.A.S.F. Colors and Chemicals Inc.) in solution in C_6H_6 as obtained at 100 Mcycles/sec., and at $30^\circ C$., is shown in Figure 4. The spectrum consists of five resonances, of which two overlap. The resonances with τ values of 9.10, 8.25, and 6.79 correspond to the isobutyl group, while the α and β protons fall at $\tau = 6.50$ and 8.44. The resonance of the α proton decoupled from the β protons exhibits three components at $\tau = 6.44$, 6.55, and 6.68. The decoupled spectra of samples II, I, and VI are shown in

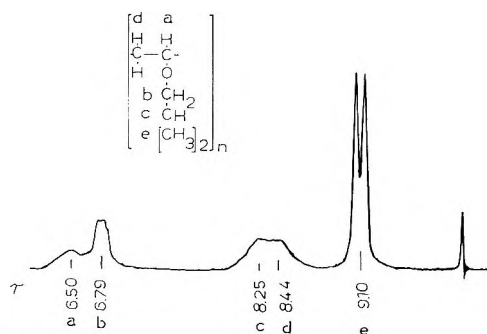


Fig. 4. NMR spectrum of sample I of poly(vinyl isobutyl ether) (100 Mcycles/sec.) in solution in C_6H_6 at $30^\circ C$.

Figures 4A, 4B, and 4C, respectively. The resonance of the β protons decoupled from the α proton did not produce a pattern interpretable in terms of an AB quartet and a singlet. This was due primarily to the overlap of the CH resonance of the isobutyl group.

An unambiguous assignment of the three components of the proton resonance is not possible on the basis of spectral data alone. However, it seems reasonable to assign the peak at $\tau = 6.55$ to isotactic sequences in view of the known chemistry of these polymerizations. Since it is highly improbable that syndiotactic triads would outnumber heterotactic triads in these polymers, the resonances at $\tau = 6.44$ and 6.68 are assigned to heterotactic and syndiotactic sequences, respectively. In Table I are listed the relative areas of the three components of the α proton resonance for the various samples of poly(vinyl isobutyl ether) considered in this study.

TABLE I
Polymerization Conditions and Properties of Some Poly(vinyl Isobutyl Ethers)

Sample no.	Sample type and preparation conditions			Tacticity ^a		
	Catalyst	Solvent	Temp., $^\circ C$.	<i>i</i>	<i>h</i>	<i>s</i>
I	B.A.S.F. commercial	—	—	41	37	22
II	Prepared with BF_3Al $[CH_2CH(CH_3)_2]_3$	$n-C_7H_{16}$	-78	54	27	19
III	MEK-Insoluble fraction of sample II	—	—	75	15	10
IV	Prepared with BF_3	CH_2Cl_2	-78	46	29	25
V	G.A.F. experimental isotactic	—	—	59	21	20
VI	MEK-insoluble fraction of sample V	—	—	64	20	16

^a *i* = isotactic; *h* = heterotactic; *s* = syndiotactic.

Poly(vinyl *tert*-Butyl Ether)

The 100 Mcycle/sec., spectrum of sample I of poly(vinyl *tert*-butyl ether) in solution in CH_2Cl_2 at $30^\circ C$. is shown in Figure 5A and consists of three

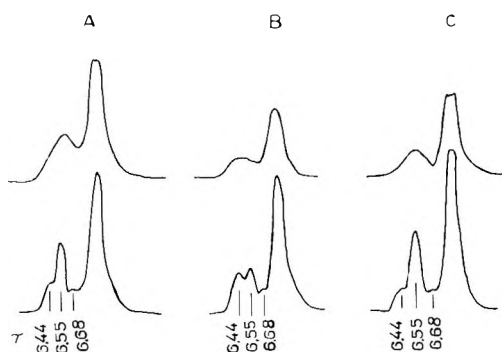


Fig. 5. NMR spectra (100 Mcycles/sec.) of the downfield resonance of poly(vinyl isobutyl ether) in solution in C_6H_6 at $30^\circ C.$, and the resonance of the α proton decoupled from the β protons: (A) sample II; (B) sample I; (C) sample VI.

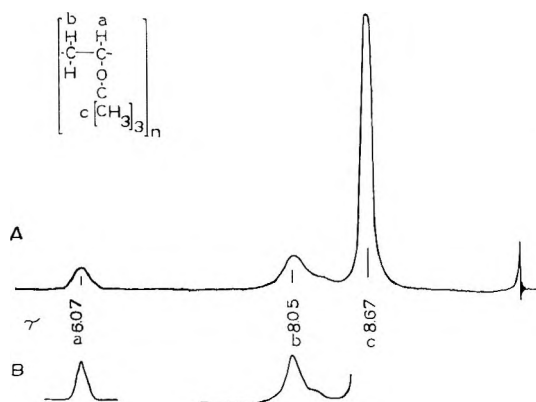


Fig. 6. NMR spectra (100 Mcycles/sec.) of sample I of poly(vinyl *tert*-butyl ether) in solution in CH_2Cl_2 at $30^\circ C.$: (A) undecoupled; and (B) resonance of the α proton decoupled from the β protons and the resonance of the β protons decoupled from the α proton.

resonances with τ values of 6.07, 8.05, and 8.67, corresponding to the α , β , and *tert*-butyl protons, respectively. Sample I was prepared with a 2.5/1.0 molar ratio of $BF_3/Al[CH_2CH(CH_3)_2]_3$ initiator in $n-C_7H_{16}$ at $-78^\circ C.$ The resonance of the α proton decoupled from the β protons and the resonance of the β protons decoupled from the α proton yielded broad singlets in both cases, as shown in Figure 5B. Furthermore, the undecoupled and decoupled spectra of sample II, which was prepared with a BF_3 initiator in CH_2Cl_2 at $-78^\circ C.$, were essentially the same as that of sample I. The spectra may be interpreted in a number of ways: (1) the attached groups are not sensitive to the stereochemical configuration; (2) the random motion of the polymer may not be rapid enough to average out the magnetic effects of a given orientation; (3) only one tactic form is present; or (4) the separation of the three components of the α proton resonance which correspond to the three tactic forms is too small to be resolved under the present

experimental conditions. The possibility that only one tactic form is present was eliminated by converting sample II of poly(vinyl *tert*-buty ether) to poly(vinyl alcohol) by cleavage with HI.¹³ The decoupled spectra of the resulting PVA showed that the former polymer consisted of 40% isotactic, 35% heterotactic, and 25% syndiotactic triads.

An attempt to resolve the assignments for the various tactic forms for the polymers, poly(vinyl ethyl, isopropyl, and *tert*-butyl ethers), by cleavage to the alcohol was however, unsuccessful. The resulting polymers were either crosslinked or only partially cleaved.

References

1. Bovey, F. A., and G. V. D. Tiers, *Fortschr. Hochpolymer. Forsch.*, **3**, 139 (1963).
2. Brownstein, S., and D. M. Wiles, *J. Polymer Sci.*, **2A**, 1901 (1964).
3. Ramey, K. C., N. D. Field, and I. Hasegawa, *J. Polymer Sci.*, **B2**, 865 (1964).
4. Bovey, F. A., E. W. Anderson, D. C. Douglass, and J. A. Manson, *J. Chem. Phys.*, **39**, 1199 (1963).
5. Ramey, K. C., and N. D. Field, *J. Polymer Sci.*, **B2**, 461 (1964).
6. Baldeschwieler, J. D., and E. W. Randall, *Chem. Revs.*, **63**, 81 (1963).
7. Natta, G., *Makromol. Chem.*, **16**, 213 (1955).
8. Natta, G., G. Dall'asta, G. Mazzanti, U. Giannini, and S. Cesca, *Angew. Chem.*, **71**, 205 (1959).
9. Natta, G., I. Bassi, and P. Corradini, *Makromol. Chem.*, **18-19**, 455 (1955).
10. Goodman, M., and Y. Fan, *J. Am. Chem. Soc.*, **86**, 4922 (1964).
11. Kern, R. J., J. J. Hawkins, and J. D. Calfee, *Makromol. Chem.*, **66**, 126 (1963).
12. Johnson, L. F., *Varian Associates Tech. Information Bull.*, **3**, No. 3, 5 (1962).
13. Ramey, K. C., and N. D. Field, *J. Polymer Sci.*, **B3**, 63 (1965).

Résumé

Les spectres NMR à résolution élevée des polyéthers (vinyl-éthylque, isopropylique, isobutylique et-*t*-butylique) fournissent par examen à 60 et 100 Mc./sec. et dans les conditions de découplage, des informations concernant les différentes formes tactiques présentes. Les spectres sont compliqués par le nombre de résonances de recouvrement à telle mesure qu'on ne peut pas faire une attribution inambigue des trois formes de triade. Pour l'éther polyvinyl-isobutylique, les résonances du proton α découplé des protons β montrent trois composantes que l'on attribue expérimentalement aux unités centrales du monomère dans les configurations hétérotactique, isotactique et syndiotactique respectivement accompagnées d'une augmentation de la force du champ.

Zusammenfassung

Die Hochauflösungs-NMR-Spektren von Poly(vinyläthyl-, isopropyl-, isobutyl-, und *t*-butyläthern) liefern bei 60 und 100 HMz und unter Entkopplungsbedingungen Informationen über die verschiedenen vorhandenen taktischen Formen. Die Spektren werden durch die Überlappungsresonanz in einem solchen Ausmass kompliziert, dass eine unzweideutige Zuordnung der drei Triadenformen nicht durchgeführt werden konnte. Bei Poly(vinylisobutyläther) zeigt die Resonanz des α -Protons, entkoppelt von den β -Protonen, drei Komponenten, welche versuchsweise den zentralen Monomereinheiten in heterotaktischen, isotaktischen und syndiotaktischen Konformationen mit zunehmender Feldstärke zugeordnet werden.

Received February 1, 1965
Prod No. 4682A

Studies of Variations in the Properties of Ion-Exchange Resin Particles

DAVID H. FREEMAN, VITHAL C. PATEL, and MARY E. SMITH,
Department of Chemistry, Washington State University, Pullman, Washington

Synopsis

Measurements of the swelling ratio and exchange capacity of individual ion-exchange resin beads are used to compare resin samples, to study interparticle differences, and to help characterize resin degradation. Heterogeneous resin samples were found, along with those of apparent homogeneity. In one extreme case of the former, inert particle cores were found.

The homogeneity of ion-exchange resins is of paramount importance to the establishment of an exact basis for interrelating physical chemical measurements among varied samples of ion-substituted styrene-divinylbenzene co-polymers. Swollen particle density,¹ capacity,² and NMR investigations³ have established the absence of marked interparticle differences. In other studies, interparticle differences in density,⁴ capacity, and specificity⁵ and optical observations⁶ have suggested marked heterogeneity. The apparent disagreement is a possible consequence of variations in the degree of heterogeneity of the different samples or of variations in the experimental sensitivity.

The intercomparison of different particles of the same resin, or of the average particle properties of different resins, depends upon access to appropriate correlating variables. The ratio $q = V(\text{swollen})/V(\text{unswollen})$ for water uptake by cation-exchange resins has been related to the nominal crosslinking X , expressed in divinylbenzene content (% DVB) in the work of Boyd and Soldano⁷ with the expression $(q - 1)X = A$, where A depends upon the counterion. This expression presumes 1:1 substitution, or one exchange site per aromatic group. With different resins, the effect of varied capacity upon water imbibition has been found to be linear⁸ and non-linear,⁹ so that an exact expression which relates the swelling ratio to dry exchange capacity and crosslinking is not yet certain. However, differences in the degree of substitution contribute corresponding changes in swelling ratio; differences in crosslinking also do this, and the two can be distinguished, separately or in combination. If the ion substitution of copolymers does not cause network modifications, the swelling properties of the unsubstituted copolymers must provide a reference behavior for the resin derivatives.

EXPERIMENTAL

The resin samples used in this study were obtained through the courtesy of the Dow Chemical Company and Bio-Rad Laboratories and are of the Dowex 50 W and Dowex 1 types, the sulfonate and methylenetri-methylammonium derivatives, respectively, of styrene-divinylbenzene copolymers. All samples were initially treated by the usual conditioning washes.

The methods of measuring single particle diameters¹⁰ and exchange capacities² have been described. Modifications of these procedures are as follows. Dry resin particle diameters were measured after drying in the sodium or chloride form at 110°C. with vacuum desiccation over P₂O₅ for 5 days. The anhydrous particles were immersed in sodium distilled *n*-octane immediately upon removal from the oven. Prolonged tests revealed no uptake of this solvent by resin, in confirmation of Gregor's finding.¹¹ Weighed amounts of neutron-irradiated sodium carbonate or ammonium bromide were diluted directly to 0.02*N* to prepare tracer solutions of Na²⁴ or Br²⁸. The tracer solutions were used, respectively, for the conversion of hydrogen form cation-exchange resin or hydroxide form anion-exchange resin to the tagged sodium or bromide forms. Integral counting with a well-type scintillation counter and analyzer was carried out below the level of significant coincidence loss. High stability electronic equipment was used, all measurements were made in duplicate at separate times, and a minimum of 40,000 total counts above background were obtained on each particle.

Some of the diameter measurements were obtained with a single microscope objective. Others involved the use of two objectives. The latter method depended upon magnification measurements of high relative accuracy. Corrections for optical distortion and the computations and statistical correlations of capacity, swelling ratio, and particle size were performed by use of a program written for the IBM 709. Less than 5% of the data were rejected on the basis of disagreement beyond 1.5% in the duplicate tracer measurements. Several resin samples and one copolymer sample were found to be contaminated; these were rejected from the study. The specific activities of the tracer solutions were accurate to 1% as judged by the use of different tracer preparations on the same resin sample. The anhydrous resin exchange capacity *C* (in milliequivalents/milliliter) is calculated to have a relative standard deviation of 0.6%, and that for the swelling ratio is 0.4–0.5%.

The swelling ratio for toluene uptake by styrene-divinylbenzene copolymer samples, obtained through the courtesy of the Dow Chemical Company, involved measuring the unswollen particle diameters in water medium. After drying, the particle diameters were measured after swelling with the toluene medium. There is no known matching between the copolymer and resin samples.

RESULTS

Intersample Comparisons

Table I includes the average swelling ratio and exchange capacity measurements which we shall discuss first. The values of \bar{q}_s refer to the average water swelling ratios for anion-exchange resins in the methyl sulfonate form, or for cation-exchange resins in the tetramethyl-ammonium form. The measurements in the columns to the right of this are obtained on sets of N beads whose statistical analysis will be discussed later. The average dry exchange capacity \bar{C} and the average swelling ratio \bar{q} refer to the chloride form anion-exchange resin or to the sodium form cation-exchange resin; the corresponding standard deviations are given as s_c and s_q . The measured capacities may be referred to Pepper's values,⁸ values of 1.48 g./cc. for the density of dry sodium form cation-exchange resin and 1.12 g./cc. for that of dry chloride form anion-exchange resin being used. The comparison suggests that most of the resins used in this study are less than fully substituted, and that there are examples of considerable undersubstitution among the more highly cross-linked resins.

Unsuccessful attempts were made to correct the swelling ratios to a theoretical capacity based upon Pepper's values. A rough evaluation of resin swelling is made by considering its variation with crosslinking alone. For comparison, toluene swelling ratios of 16 copolymer samples were measured after pretreatment involving overnight Soxhlet extraction with toluene. Approximately half of the copolymer samples were found to be fairly homogeneous with standard deviations of 2% or less in the average swelling ratio, and no significant variation of swelling ratio with particle size. Two of the samples showed larger deviations and significant variations of swelling ratio with particle size. In general, the samples were reasonably homogeneous with the following measured swelling ratios: 1% DVB, $\bar{q} = 4.85, 4.48, 4.43, \text{ and } 4.32$; 2% DVB, $\bar{q} = 3.57 \text{ and } 3.43$; 4% DVB, $\bar{q} = 2.50, 2.53, \text{ and } 2.60$; 8% DVB, $q = 1.87, 1.81, \text{ and } 1.80$; 12% DVB, $\bar{q} = 1.61, 1.54, \text{ and } 1.52$; 16% DVB, $\bar{q} = 1.41$. It should be noted from these measurements that the volume fraction of toluene in the swollen copolymer $(q - 1)/q$ varies smoothly with the apparent nominal crosslinking. This precision of swelling behavior is considerably better than that of the resin samples to be described. The ion-exchange resins show substantial scatter among the swelling ratios, and there is no present indication for improvement upon the function given earlier, $(q - 1)X = A$, where $A = 5.6$ for anion-exchange resin chloride and 8.2 for sodium form cation-exchange resin.

The \bar{q}_s measurements refer to the different types of resins having exchange site-counterion combinations that are similar in structure and which should be approximately equally hydrophilic. The measurements bear this out with the previous expression holding fairly well with $A = 5.2$ for the combined measurements. It is evident, in spite of the crudity of the comparison, that the network crosslinking has not been markedly

TABLE I
Averages and Results of Linear Correlation Analysis of Single Resin Particle Measurements

Resin	X, % DVB	\bar{q}_s	\bar{q}	s_q	\bar{C}_c , meq./ ml.	s_c	N	\bar{d} , μ	d_{\max} d_{\min}	R_{C_d}	dC/dd , meq./ml.- mm.	$R_{\theta C}$	dq/dC , ml./meq.	Het.	Unc.	Hom.
Dowex 1	1	6.00	7.00	0.57	4.52	0.17	14	274	1.6	-0.88**	-3.7	0.46*	1.0	X		
"	2	3.58	3.85	0.11	4.98	0.40	3	256	1.3							X
"	2	4.13	4.11	0.31	4.33	0.30	14	298	3.1	-0.78**	-2.8	0.09		X		
"	4	2.36	2.29	0.09	4.57	0.25	7	273	1.4	-0.53		0.62				X
"	4	2.36	2.43	0.03	3.94	0.18	9	374	1.6	-0.94**	-3.3	-0.15		X		
"	7.5		1.705	0.022	4.10	0.21	15	343	2.0	-0.88**	-2.5	-0.15		X		
"	8	1.700	1.785	0.031	4.39	0.11	8	276	1.5	-0.77*	-2.0	0.60			X	
"	8	1.625	1.620	0.030	3.23	0.09	5	273	1.3						X	
"	10	1.538	1.538	0.022	3.18	0.08	7	245	1.5	-0.94*	-2.0	0.95**	0.23	X		
"	10	1.517	1.495	0.056	2.92	0.18	18	234	1.7	-0.87**	-4.6	0.91**	0.29	X		
"	16	1.226	1.261	0.020	2.33	0.17	7	286	1.4	-0.98**	-4.7	0.94*	0.1	X		
Dowex 50W	1		6.90	0.15	7.03	0.29	14	306	1.8	-0.29		0.59*	1.0	X		
"	1	4.67	6.85	0.37	6.04	0.16	9	249	1.3	0.49		0.50			X	
"	2	3.24	4.50	0.33	6.79	0.24	11	178	1.7	-0.18		0.26			X	
"	2	3.69	5.47	0.09	6.73	0.06	10	303	1.2	0.80*	2.0	0.10		X		
"	4	2.10	2.89	0.04	7.24	0.16	18	257	1.4	-0.29		0.56*	0.1	X		
"	4	2.06	2.83	0.05	6.76*	0.11	16	294	1.3	-0.29		-0.02			X	
"	4		2.75	0.09	6.18*	0.21	11	275	1.2	-0.51*	-9.0	0.94**	0.39	X		
"	8	1.587	2.10	0.04	6.59	0.15	14	305	1.2	-0.28		0.62*	0.2	X		
"	8	1.621	2.05	0.04	6.31	0.06	6	304	1.1						X	
"	8		2.28	0.02	6.58 ^b	0.15	19	419	1.5	-0.94**	-3.2	0.68*	0.00	X		
"	8		2.38	0.07	6.52 ^b	0.14	27	413	1.5	-0.73**	-2.6	0.26		X		
"	12		2.12	0.05	7.45	0.04	9	389	1.6	-0.17		0.33				X
"	12	1.385	2.11	0.05	7.38	0.20	11	463	3.2	-0.91**	-0.92	0.33		X		
"	12	1.388	1.761	0.028	6.47	0.14	9	243	1.5	0.16		0.63			X	
"	16	1.257	1.391	0.018	5.32	0.22	19	330	1.2	-0.90**	-12.0	0.56*	0.05	X		

^a See Fig. 1; ^b See Fig. 2. Note that these measurements refer to the hydrogen form, while the other cation-exchange resins have been measured in the sodium form.

altered (or, it has been altered to the same extent, which is unlikely) by the different reactions used to substitute the copolymer during its conversion to ion-exchange resin.

Although the foregoing results are affected by varying degrees of under substitution and heterogeneity, they provide further support to the expectation¹² that homogeneous resins and copolymers should be precisely inter-related on the basis of swelling and capacity measurements.

Intersample Comparisons

The single-particle measurements were treated by statistical analysis with the attempt to develop criteria for heterogeneity. This was based upon tests for linear correlation of dry exchange capacity with particle size, and for that of swelling ratio with the dry capacity. Especially effective in testing for possible linear trend is the correlation coefficient R_{xy} which is defined¹³ as the correlation moment (or covariance) of the quantities x and y divided by the product of the standard deviation of x and that of y . The computed values of R_{cd} and R_{qc} are given in Table I and are referred to a tabulated significance level which implies the probability that the apparent correlation is causal. Those levels in excess of 90% are indicated by a single asterisk, and those in excess of 99.9% by a double asterisk. The observation of marked linear correlations is adequate to justify the suitability of the linear correlation analysis. Statistical evidence for trend is augmented by reference to the least-squares slopes (assuming errors only in the independent variables) dC/dd^* and dq/dC , to the dispersions s_q and s_c , and to the range of sampled particle size d_{\max}/d_{\min} with an average set value of \bar{d} . These considerations led to the assignments of resin heterogeneity, homogeneity, or uncertainty (Het., Hom., and Unc., respectively, in Table I).

The results in Table I show a few of the resins to be apparently homogeneous. However, the majority are heterogeneous with a marked opposite variation of capacity with particle size. This is illustrated in Figure 1 with two nominally identical resin samples: one is apparently homogeneous while the other is clearly heterogeneous. The observed heterogeneity (variations in exchange capacity) is characteristic of diffusion limitations during copolymer substitution, which implies internal heterogeneity in the sense that the capacity within each particle increases radially outwards.

Other tests for heterogeneity show less sensitivity. Where significant, the tabulated correlation of swelling ratio with capacity becomes less marked with increasing cross-linking simply because dq/dX varies approxi-

* The computation of the slope from a narrow range of particle size is more subject to error than the determination of the level of significant of the trend. As a check, the 16% DVB cation-exchange resin was fractionated by back-washing, as described by Hamilton.¹⁴ The end fractions analyzed as follows: 0.10–0.20 mm particles, 4.6 meq./g. of dry hydrogen form resin, and for 0.34–0.48 mm. particles, 4.1 meq./g. This corresponds to a dry sodium form slope dC/dd of -3.4 meq./ml.-mm., as compared to the tabulated value of -12 .

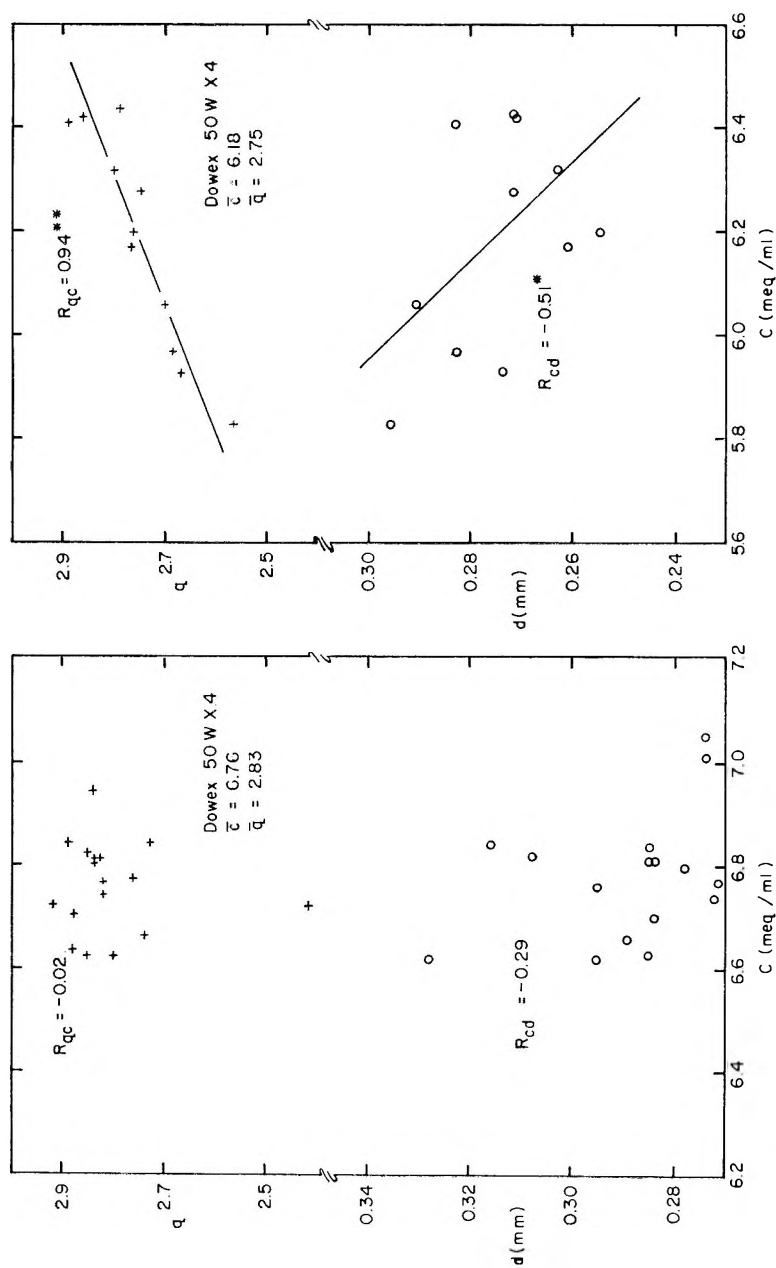


Fig. 1. Results of single-particle measurements of two different resin samples. That on the left shows essentially independent variations of swelling ratio, capacity, and particle diameter, and is classed as apparently homogeneous. The marked trends of the resin shown on the right are evidence for resin heterogeneity.

mately with the inverse square of X . A study of wet capacity was not made: this would involve the ratio C/q and the typical variations of q and C with particle size have a tendency to cancel.

Test of Resin Degradation

We had access to one sample of 8% DVB cation-exchange resin that had been stored at room temperature in the hydrogen form for a period of 5 years. One portion of the sample was stored with excess water, while the other was stored in the air dry form. The effect of the wet storage is determined from the variations of swelling ratio with capacity as shown in

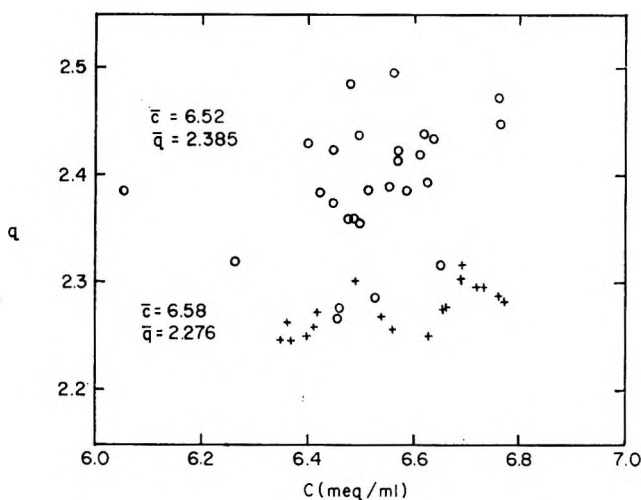


Fig. 2. Intercomparison of measurements on a split sample of hydrogen form Dowex 50W-X8 stored at room temperature for a period of 5 years (+) in the air-dry state and (O) under water. Measurements are confined to dry hydrogen form, particle size region of 340–570 μ . Decrosslinking is indicated for the resin particles stored under water.

Figure 2. The measurements on the dry-stored sample ($C = 6.58$ meq./ml.) and on the wet-stored sample ($C = 6.52$ meq./ml.) are listed under the third and fourth Dowex 50W-X8 entries in Table I. The measurements on these two samples are exceptions in that they refer to the hydrogen form resin. The measurements are confined to the dry, hydrogen form, particle size region of 340–570 μ for both sets of measurements. The dry exchange capacities agree to within experimental error so that substitutional differences appear to be negligible. The swelling ratio correlates with exchange capacity at a level of 99% significance with the dry-stored exchanger and, as given in Table I, this agrees with the capacity variation with particle size. The swelling ratio is nearly independent of the exchange capacity for the wet-stored resin. Thus, apparently pure decrosslinking is indicated by the increased magnitude and dispersion of the swelling ratios. From the $\bar{q} - 1$ ratio for the two samples, it is estimated

that 10% of the crosslinks have been broken in the average wet-stored resin particle.

Resin Morphology

Resin and copolymer samples are expected to show optical isotropy as a result of their statistically isotropic network structure. This was true of the copolymer samples except that very weak birefringence was noted in observation of the swollen or unswollen copolymer samples by using crossed polarizers with a first-order red compensator in 45° position. The same absence of appreciable birefringence was also found with resin samples of less than 8% DVB. More highly crosslinked resins, however, were found to show appreciable positive or negative birefringence with radial symmetry. This effect is also known to occur as a result of stresses which arise during transient swelling processes with ion-exchange resin¹⁰ and with copolymer.¹⁵ The origin of the birefringence with heterogeneous resin is similar, being the result of permanent stress in the region of a radial gradient in the concentration of exchange sites.

Microscopic examinations of the more highly crosslinked resin samples were made in media of matched refractive index. In two cases, there was evidence for an internal boundary which might serve to separate a highly substituted exterior shell from a less substituted particle core: this was found with both of the 16% DVB resins reported in Table I. A single

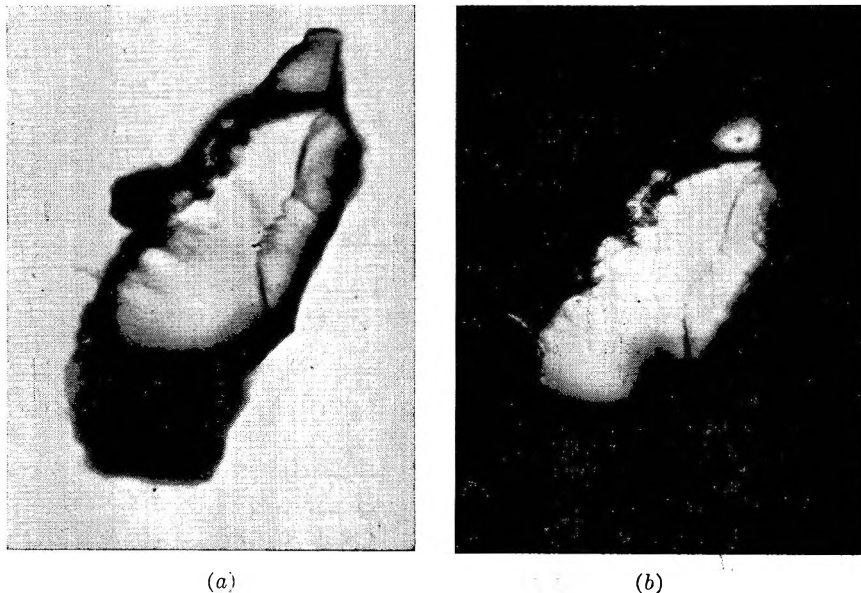


Fig. 3. Photomicrographs of Dowex 1-X16 which has been fragmented and then stained with permanganate solution: (a) fragment shows connecting stained (dark) and unstained (transparent) regions; (b) crossed polarizers have been used to show that transparent region of the same fragment is also birefringent. This illustrates the exceptional finding of a resin particle with a copolymer core. Magnification $450\times$.

boundary was observed for the 16% DVB anion-exchange resin by using phase contrast optics; with the 16% DVB cation-exchange resin, a series of concentric boundaries was observed. Upon first fracturing and then staining the fragments of these two samples, it was evident that the cation-exchange resin was at least partially substituted throughout. With permanganate-treated anion-exchange resin, however, there were several fragments which had connecting stained and unstained regions, the latter being highly birefringent. This is shown in Figure 3, and indicates a completely unsubstituted copolymer core.

CONCLUSIONS

The present work has shown that homogeneous styrene-divinylbenzene copolymers are available, and that homogeneous ion-exchange resins may be prepared from them. From the swelling properties of the former, and from the measured swelling and capacity of the latter, there should be a precise basis for interrelating other measurements which depend upon these properties. At the same time, the study revealed a preponderance of ion-exchange resins with marked variations in their degree of substitution. Such materials are heterogeneous in the sense that their physical properties vary from particle to particle, and within each individual particle. These findings emphasize the importance of incorporating homogeneity tests in all fundamental measurements of ion-exchange phenomena, and they should provide some stimulation for further attention to the improved control of conditions used to prepare ion-exchange resins for fundamental study.

This work was supported by the United States Atomic Energy Commission.

References

1. Suryaraman, M. G., and H. F. Walton, *Science*, **131**, 829 (1960).
2. Moseley, W. D., Jr., and D. H. Freeman, *J. Phys. Chem.*, **67**, 2225 (1963).
3. Gordon, J. E., *J. Phys. Chem.*, **66**, 1150 (1962).
4. Nelson, F., and K. A. Kraus, *J. Am. Chem. Soc.*, **80**, 4154 (1958).
5. Högfeldt, E., *Science*, **128**, 1435 (1958).
6. Abrams, I. M., *Ind. Eng. Chem.*, **48**, 1469 (1956).
7. Boyd, G. E., and B. A. Soldano, *J. Am. Chem. Soc.*, **75**, 6091 (1953).
8. Pepper, K. W., *J. Appl. Chem.*, **1**, 124 (1951).
9. Pepper, K. W., H. M. Paisley, and M. A. Young, *J. Chem. Soc.*, **1953**, 4097.
10. Freeman, D. H., and G. Scatchard, *J. Phys. Chem.*, **69**, 70 (1965).
11. Gregor, H. P., K. M. Held, and J. Bellin, *Anal. Chem.*, **23**, 620 (1951).
12. Kressman, T. R. E., and J. R. Millar, *Chem. Ind. (London)*, **1961**, No. 45, 1833.
13. Nalimov, V. V., (transl. by M. Williams), *The Application of Mathematical Statistics to Chemical Analysis*, Addison-Wesley, Reading, Mass., 1963, p. 192 ff.
14. Hamilton, P. B., *Anal. Chem.*, **30**, 914 (1958).
15. Gurney, E., *J. Polymer Sci.*, **41**, 119 (1959).

Résumé

On a employé des mesures du rapport de gonflement et de la capacité d'échange de résines échangeuses d'ions en perles afin de comparer entre eux les échantillons de résines, d'étudier les différences entre particules et d'aider à caractériser la dégradation

des résines. On a trouvé des échantillons de résines hétérogènes parmi ceux qui possédaient une homogénéité apparente. Dans un cas extrême, on a trouvé des particules inertes.

Zusammenfassung

Messung des Quellungsgrades und der Austauscherkapazität von individuellen Körnern von Ionenaustauscherharzen wird zum Vergleich von Harzproben, zur Untersuchung von Teilchenunterschieden und zur Hilfe bei der Charakterisierung des Harzabbaus herangezogen. Es wurde das Auftreten von heterogenen Harzproben neben solchen von scheinbarer Homogenität festgestellt. Bei ersteren wurden in einem extremen Fall unwirksame Teilchenkerne gefunden.

Received November 16, 1964

Revised February 12, 1964

Prod. No. 4655A

Polymerization of Vinyl Monomers by Organoaluminum Initiators*

HERMAN WEXLER† and JOHN A. MANSON, *Central Research Laboratories, Air Reduction Company, Inc., Murray Hill, New Jersey*

Synopsis

Triethyl aluminum, triisobutylaluminum, and diisobutylaluminum hydride have been utilized to polymerize vinyl acetate, methyl methacrylate, and styrene at temperatures from -80 to 25°C . Linear high polymers were obtained in reasonable yields. Based on kinetic experiments studied in dilatometers, it was possible to observe: (a) the rate decreased steadily with time from an initially high value; (b) the initial rate depended upon catalyst concentration and upon the square of the monomer concentration; (c) the overall energy of activation was 13 kcal./mole, and the energy of activation for the degree of polymerization was about 2 kcal./mole. The copolymerization of methyl methacrylate and styrene produced a polymer that was rich in methyl methacrylate. The polymerization is not clearly free-radical nor ionic, and some form of coordination may take place.

INTRODUCTION

Many applications of complex organometallic catalysts have been demonstrated in the polymerization of α -olefins by Ziegler, Natta, and others. However, the use of these complex catalysts in the polymerization of polar and, especially, oxygen-containing monomers, has been severely limited by the fact that such monomers often tend to poison the catalysts most useful with α -olefins. Accordingly, interest has developed in modifying Ziegler catalysts for use with monomers such as vinyl esters or acrylates; in the past few years, several references and patents have appeared dealing with catalyst systems other than the conventional organoaluminum-titanium halide type.

At the time this work was begun, very little information was available about polymerizations initiated by even simple organometallic catalysts and less about the mechanism and kinetics of such polymerizations. For these reasons, it was decided to investigate the polymerization of some polar and reactive vinyl monomers, such as vinyl acetate, by means of simple organometallic compounds of Group III metals, e.g., aluminum. When initial success was obtained,¹ it was decided to study further the nature of a typical polymerization system in more detail.

* Paper presented in part at the Tenth Canadian High Polymer Forum, Ste. Marguerite, Quebec, September 1960.

† Present address: Research and Development Laboratory, Liquid Carbonic Co., Division of General Dynamics, Chicago, Illinois.

A number of papers have since been published concerning the nature of polymerization induced by simple organometallic compounds.²⁻⁸ With a few exceptions, attention has been focused on boron alkyls, and relatively little has been published regarding the kinetics of polymerization by aluminum alkyls, especially for compounds containing polar groups. Recent work on this topic has prompted us to present the results of our experiments with organoaluminum compounds as polymerization catalysts.

EXPERIMENTAL

Monomers used were carefully purified and stored until use in a refrigerator. No difference was noted in experiments whether or not the monomer was prepolymerized. The nitrogen was Seaford grade. Aluminum alkyls, obtained from the Hercules Powder Company, were used without further purification as solutions in heptane (concentrations of 60-70 vol.-%). One batch was used for all the kinetic work.

Bottle polymerizations and copolymerizations were conducted in 1-oz. brown bottles. After monomer was added under nitrogen, the catalyst solution was introduced by means of a hypodermic syringe and the bottles allowed to stand at the temperature desired. When the desired reaction time had elapsed, the contents were poured into an excess of hexane to precipitate the polymer. Copolymers were extracted with carbon tetrachloride and insoluble residues removed. After washing, the polymers were dried under vacuum to constant weight.

Saponifications were effected by use of methanolic sodium hydroxide and reacylations by means of an acetic anhydride-pyridine mixture.⁹

Initial rates of polymerization were determined by a simple dilatometric technique. Before equilibration, the monomer and catalyst were degassed several times in the conventional manner, thawed, and mixed thoroughly. Although the reaction rate tended to decrease with time, the initial rate was reasonably constant for the first 3-10 min.; no induction periods were observed. Reproducibility was usually within $\pm 20\%$.

The styrene content of copolymers was determined by an ultraviolet technique used successfully by Tobolsky.¹⁰

RESULTS AND DISCUSSION

Polymerization

In spite of the possibility that carbonyl groups would be attacked by the organoaluminum compounds immediately, the polymerization of vinyl acetate and methyl methacrylate by a triisobutylaluminum catalyst proceeded readily under a variety of conditions; styrene was also polymerized, though to lesser extents. Table I lists typical data. Similar results were obtained with triethyl aluminum and diisobutylaluminum hydride, in bulk as well as in various solvents. As a matter of fact, the use of a tetrahydrofuran solvent caused the increase in rate, but decrease in degree of polymerization that has often been associated with anionic polymerization in solvents of high dielectric constant¹¹ due to termination by transfer from

plex nature of catalysis, which makes it difficult to assign a simple mechanism, a series of kinetic studies was made to investigate the effect of reaction variables on the rate and degree of polymerization in order to help elucidate the mechanism of polymerization.

Effect of Time on Polymerization Rate

In all our dilatometric experiments, the rate of polymerization decreased continuously from an initial reasonably steady value. Although this fact complicates the interpretation of dilatometric results, the initial slopes were usually reproducible ($\pm 20\%$). Such effects have been observed for the boron alkyl-oxygen polymerization of methyl methacrylate by Welch¹⁸ and Bawn.⁴

A changing rate was also indicated by bottle experiments, in which most of the polymerization occurred soon after the addition of catalyst. The cause of this behavior may be the rapid depletion of catalyst accompanying very fast initiation. The maximum conversion reached under conditions used here was about 25%—suggesting the possibility that conditions for an equilibrium-type polymerization have been satisfied.¹⁹

As was the case with the first bottle experiments, the rate of polymerization was not noticeably affected by the use of undegassed monomer.

Effect of Catalyst Concentration on Rate and Degree of Polymerization

The best combination of data from both bottle and dilatometric experiments, shown in Figure 1, suggests a dependence of the rate of polymerization upon the first power of the aluminum alkyl concentration. Because of our technique, no attempt was made to measure the effect of any oxygen concentration. The relationship is comparable to that found for the polymerization of vinyl acetate by tributylboron,^{20,21} cationic,²² and anionic polymerizations at low catalyst concentrations.³ However, it differs from normal radical polymerization, where there is a square-root dependence, as well as from cases in which rate is independent of metal alkyl concentration, such as the polymerization of methyl methacrylate by boron alkyls.¹⁸ These are tabulated in Table II.

The poor fit of several points in Figure 1 at low catalyst concentration presents the possibility that the rate might be independent of catalyst concentration, such as for lithium alkyls.³ However, since the active

TABLE II
Effect of Catalyst Concentration on Polymerization
Rate by Organometallic Initiators

Catalyst	Monomer ^a	Concentration effect	Reference
BBu ₃	VAc	[BBu ₃]	21
BBu ₃ -O ₂	VAc	[BBu ₃]	20
BBu ₃ -O ₂	MMA	[Bu ₂ BOOBu], ^{1/2} [BBu ₃] ^{1/2}	12
BEt ₃ -O ₂	MMA	[O ₂], ^{1/2} indep. BEt ₃	18

^a VAc = vinyl acetate; MMA = methyl methacrylate.

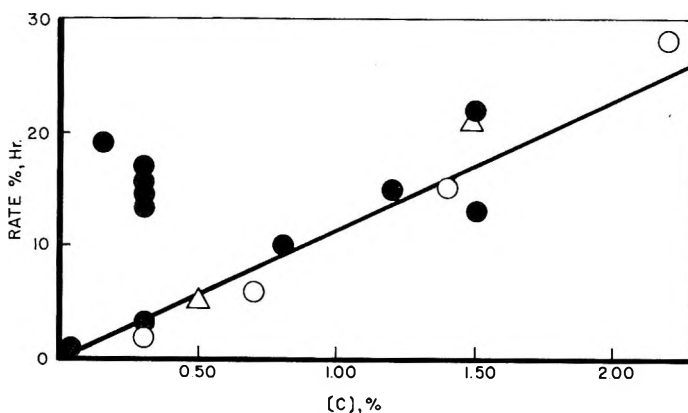


Fig. 1. Effect of triisobutylaluminum concentration upon rate of polymerization at 35°C.; (O) Series 1 in bottles; (Δ) series 2 in bottles; (●) in dilatometers.

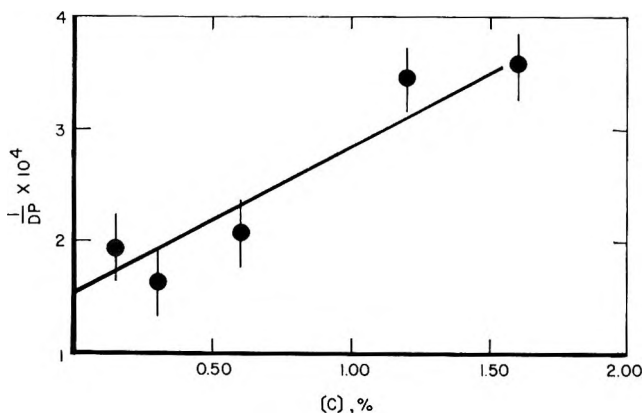


Fig. 2. Effect of triisobutylaluminum concentration upon degree of polymerization at 35°C.

centers in the polymerization are due to the monomolecular aluminum alkyls, this effect might be due to the dissociation of dimeric catalyst at low concentrations. Although triisobutylaluminum is only 1% dimerized,²³ the 10% of diisobutylaluminum hydride present in the catalyst is dimeric, or dimerized with the trialkyl aluminum. It is possible that the dissociation of this material, in dilute solution, might raise the effective catalyst concentration to produce the confusing effect. It was found that the reciprocal degree of polymerization was proportional to the catalyst concentration as shown in Figure 2, which corresponds to the boron alkyl-oxygen polymerization of vinyl acetate.¹⁴

The relationship between rate and catalyst concentration $[c]$ can be expressed as

$$\text{Rate} = [c]$$

If the reaction is a free-radical one, such a dependence would require termination other than by combination or disproportionation, such as termination by destructive chain transfer.

Effect of Temperature on Reaction Rate and Degree of Polymerization

The effect of temperature on the rate and degree of polymerization is shown in the Arrhenius plots of Figure 3. The overall energy of activation for degree of polymerization, E_{DP} is approximately 2 kcal./mole. If data at -78°C . are included, E_p could be as low as 10. It can be seen that the

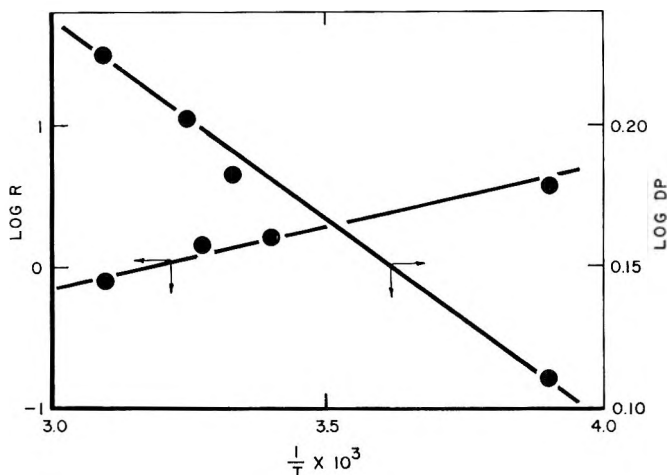


Fig. 3. Effect of temperature upon rate and degree of polymerization. Catalyst concentration, 0.3%. $E_p = 13$ kcal./mole, $E_{DP} = 2$ kcal./mole.

values we report are comparable to those for boron alkyl-initiated polymerization of vinyl acetate²⁰ and methyl methacrylate,^{4,16} both in the presence and absence of air. These values are generally in the range of 13–16 kcal./mole. These data are shown in Table III.

This value falls approximately midway between those reported for cationic polymerization of isobutylene^{27,28} and radical polymerization of styrene,²² which leads us to believe that this reaction is different from standard ionic or radical polymerizations, although the possibility exists of a redox polymerization.

TABLE III
Activation Energy of Polymerizations by Organometallic Initiators

Catalyst	Monomer ^a	Activation energy, kcal./mole	Reference
BBu ₃ -O ₂	VAc	15–16	20
BBu ₃ -O ₂	MMA	13	4
BBu ₃	MMA	15.5	24
BBu ₃ -O ₂	VCl	9.5	25
BBu ₃ -O ₂	MMA	4	18
BBu ₃	VAc	5.8	21
AlEt ₃	Ethylene	21.3	17
AlEt ₃	Propylene	10	26

^a VAc = vinyl acetate; MMA = methyl methacrylate; VCl = vinyl chloride.

Effect of Monomer Concentration

Dilatometric experiments were conducted in two solvents: benzene and ethyl acetate. The results shown in Figure 4 are consistent with the following expression:

$$R_p \propto [M]^2$$

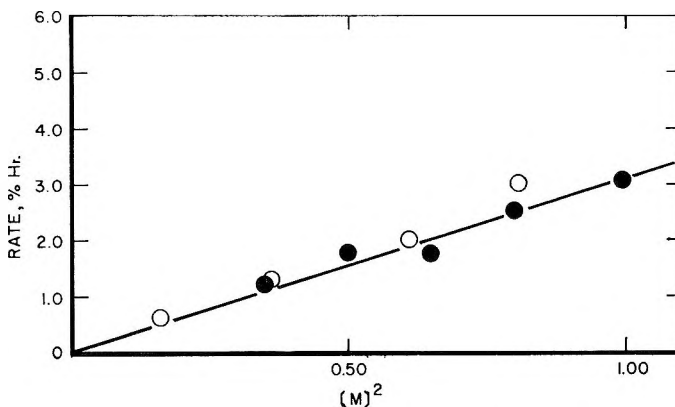


Fig. 4. Effect of monomer concentration upon rate of polymerization at 35°C.: (●) ethyl acetate solution; (O) benzene solution. Catalyst concentration, 0.3%.

but, in no case, can the data be represented by the normal free-radical expression:

$$R_p \propto [M] \quad \text{or} \quad [M]^{3/2}$$

A square dependence has also been reported for the use of boron alkyls for vinyl acetate,^{20,21} although a similar system reports a linear dependence of the rate upon monomer concentration,⁴ as does the polymerization of ethylene by triethylaluminum.¹⁷ Table IV lists representative data.

If the reaction is free-radical, such a dependence could imply participation of solvent²⁹ or monomer³⁰ in the initiation steps. If the reaction is not free-radical, such a dependence would be expected in a medium of moderate dielectric constant.

Copolymerization Experiments

Because the studies of rate and degree of polymerization did not clearly distinguish between a free-radical and non-free-radical mechanism, the copolymerization of styrene and methyl methacrylate was attempted with the use of triisobutyl aluminum as catalyst under both nitrogen and air.

Although control experiments with azobisisobutyronitrile (AIBN) as catalyst yielded copolymers containing approximately 50% styrene units,³¹ the concentration of styrene in the soluble copolymers, obtained in a dozen-odd experiments with the aluminum alkyl, was found to lie in the range of 30–40%.

If the course was the simultaneous occurrence of free-radical and ionic reactions, it should have been affected by changes in temperature and changes in solvent,³² which was not the case.

TABLE IV
Effect of Monomer Concentration on Polymerization Rate
by Organometallic Initiators

Catalyst	Monomer ^a	Concentration effect	Reference
BBu ₃	VAc	[M] ²	21
BBu ₃ -O ₂	VAc	[M] ²	20
BBu ₃ -O ₂	MMA	[M]	4
AlEt ₃	Ethylene	[M]	17

^a VAc = vinyl acetate; MMA = methyl methacrylate.

Further experiments were therefore conducted, the copolymers extracted with acetonitrile, and analyses performed on the extracted and residual material. The following systems were examined: (1) triisobutyl aluminum (2) triisobutylaluminum-oxygen, and (3) triethylaluminum. Results are shown in Table V.

TABLE V
Copolymerization of Styrene and Methyl Methacrylate^a

Catalyst system	Styrene, % (whole polymer)	Styrene, % ^b		Solubility	
		Extract ^c	Residue	Whole polymer ^d	Extract ^e
Al(<i>i</i> -Bu) ₃ -N ₂	30-40(12)	40(2)	40 ± 9(3)	55-46	12-58
Al(<i>i</i> -Bu) ₃ -N ₂		35(1)	39 ± 2(3)	58-30	1-18
Al(<i>i</i> -Bu) ₃ -air		30 ± 2(3)	44(2)	66-25	35-97
AlEt ₃ -N ₂					
ATBN	53 ± 3(3)		Soluble		

^a Number of runs in parentheses.

^b Portion of copolymer soluble in benzene.

^c Acetonitrile-soluble.

^d Benzene- or chloroform-soluble.

^e Acetonitrile-soluble portion of previous column.

Appreciable portions of the copolymers were soluble in acetonitrile, which is a solvent for poly(methyl methacrylate) and nonsolvent for a random 50/50 copolymer, and the per cent styrene in the extracts tended to be low, about 35-40%. The residues also had styrene contents of about 40%. Triethylaluminum tended to give polymers more soluble in both benzene and acetonitrile. The presence of air tended to reduce the amount of the acetonitrile extract, which would suggest the presence of more random copolymer, therefore, greater radical nature of the polymerization.

The results are somewhat similar to those of O'Driscoll and Tobolsky, who postulated the formation of a block polymer.¹⁰ The data are therefore in conflict with those reported for boron alkyls⁸ as well as aluminum alkyls.⁵ In comparing our work with previously published data for aluminum alkyls, we suggest that our use of a monomer containing a carbonyl group led to complexing effects with the metal alkyl, therefore causing a preferred entry of methyl methacrylate into the polymer. Perhaps, too-close analogies should not be drawn between aluminum and boron

alkyls, since the first is capable of initiating polymerization by insertion, whereas the second is reported to be incapable of this.³³

Isolation of Intermediates in the Polymerization of Vinyl Acetate

Finally, stoichiometric amounts of vinyl acetate and aluminum alkyl (1:1, 1:2, and 1:3) were combined, in both the presence and absence of air. In the absence of air it has been possible to isolate carbonyl containing intermediates that, even after storage for prolonged periods of time, can initiate further polymerization. On exposure to air, a higher ester of acetic acid was identified by its infrared spectrum. At the same time, no evidence for the formation of alcohols has been obtained. However, complexing with the carbonyl oxygen, in a nonpermanent manner, was shown by a shift in the carbonyl absorption in the infrared spectrum. This was also verified recently when complexes of aluminum alkyls with the carbonyl group of vinyl acetate and butyl acrylate were shown.¹³

Mechanism

The experimental difficulties for this system have made the mechanism difficult to elucidate. The published data derived from copolymerization experiments, which usually do not involve carbonyl-containing monomers, indicate that boron alkyls^{5,8} and aluminum alkyls⁵ cause polymerization by free-radical mechanisms. However, since the activation energy of the spontaneous thermal decomposition of triethylaluminum is 29 kcal./mole, considerably higher than our value of 13 kcal./mole, it is unlikely that this form of simple decomposition is the source of the polymerization initiator. The inclusion of moderate amounts of oxygen into the system, presumably forming peroxide, produces an enhanced effect upon the alkyls of boron, aluminum, and cadmium,^{7,15,34,35} also emphasizing the possible radical nature of the reactions. Since the completely peroxidized forms of aluminum alkyls¹³ and boron alkyls^{5,36} initiate polymerization too poorly to be effective polymerization catalysts, mechanisms have been postulated whereby the peroxide is decomposed by excess metal alkyl, and these free-radical decomposition products are believed to be the true catalysts.⁴ However, since only traces of boron could be found in a polymer formed by boron alkyl initiation, evidently the boron-containing radical contributes little to the initiation.³⁷

In our own work with aluminum alkyls, although oxygen was usually not included deliberately, the possibility exists that trace quantities may have been present to produce the postulated peroxides or hydroperoxides. However, in spite of the view that initiation by these organometallics cannot occur in the absence of oxygen,^{5,18,38} it could take place with boron alkyl after a very long period of time.³⁹ One mechanism may not be sufficient for all uses of an initiator. For example, the aluminum alkyl-water system seems to act as a cationic initiator for vinyl ethers.⁴⁰ Since our kinetic and copolymerization data do not fit published radical constants except for redox polymerization, and our polymerizations proceed well in the presence of trace amounts of oxygen, at most, we suggest that in the case of the polymerization of vinyl acetate, some of coordination poly-

merization takes place, even though aluminum alkyl peroxides may be present. This may take place by metal complexing with the carbonyl oxygen, while at the same time forming a pseudo six-membered ring during the attack upon the vinyl double bond. A similar mechanism has also been suggested for the polymerization of methyl methacrylate by lithium.⁴¹

CONCLUSION

The suggestion that boron and aluminum alkyls act as free-radical catalysts for vinyl polymerization by virtue of their tendency to react with a cocatalyst such as oxygen is not only possible but also supported by a growing body of evidence.^{4-6,8} Indeed, the anomalous behavior of our system was rather unexpected.

Results of Bawn's experiments⁴ with boron alkyls and oxygen as cocatalyst certainly appeared to follow conventional free-radical kinetics:

$$R_p \propto [C]^{1/2}[O_2]^{1/2}[M]$$

$$1/DP \propto [C]^2$$

Our results, however, can be best explained by a relationship of the form

$$R_p \propto [C]^n[M]^2$$

$$1/DP \propto [C]$$

Under our conditions n probably equals 1. The resulting expression agrees with results of other work with vinyl acetate,^{20,21} and a value of $3/2$ or $1/2$ for n appears most unlikely for our results.

These relationships could easily be consistent with a coordinate, non-free-radical reaction of the type suggested above but could be consistent with a free-radical reaction only if pronounced deviations from the normal behavior are assumed, for example, termination predominantly by destructive chain transfer and participation of the monomer in initiation. If we consider further the unusual results of the copolymerization experiments and the isolation of a polymerization intermediate, the simplest adequate hypothesis would be that of a non-free-radical reaction. Though free-radical reactions can undoubtedly occur, and may predominate under other conditions, we conclude that the possibility of a coordinated, nonionic polymerization should not be excluded for our system.

The authors wish to acknowledge the help through valuable discussions and technical contributions of Drs. E. S. Barabas, H. Sorokin, and G. J. Arquette.

References

1. Air Reduction Co., Inc., Brit. Pat. 880,544 (Oct. 25, 1961); H. Wexler (to Air Reduction Co., Inc.) U. S. Pat. 3,099,645 (July 30, 1963).
2. Kern, W., D. Braun, and M. Herner, *Makromol. Chem.*, **28**, 66 (1958).
3. Welch, F. J., *J. Am. Chem. Soc.*, **81**, 1345 (1959).
4. Bawn, C. E. H., D. Margerison, and N. M. Richardson, *Proc. Chem. Soc.*, **1959**, 397.

5. Zutty, N. L., and F. J. Welch, *J. Polymer Sci.*, **43**, 445 (1960).
6. Furukawa, J., T. Tsuruta, and S. Inoue, *J. Polymer Sci.*, **26**, 234 (1957).
7. Furukawa, J., and T. Tsuruta, *J. Polymer Sci.*, **28**, 227 (1958).
8. Fordham, J. W. L., and C. L. Sturm, *J. Polymer Sci.*, **33**, 503 (1958).
9. McDowell, W. H., and W. O. Kenyon, *J. Am. Chem. Soc.*, **62**, 415 (1940).
10. O'Driscoll, K. F., R. J. Boudreau, and A. V. Tobolsky, *J. Polymer Sci.*, **31**, 115 (1958).
11. Zilkha, A., and Y. Katz, *J. Polymer Sci.*, **62**, 153 (1962).
12. Ide, F., and Y. Takeyama, *Kogyo Kagaku Zasshi*, **63**, 1624 (1960).
13. Ferington, T. E., C. J. Benning, R. N. Chadha, R. S. Gregorian, D. F. Hoeg, F. A. Mirabile, and F. X. Werber, paper presented at 145th Meeting, American Chemical Society, New York, September 1963; *Abstracts of Papers*, p. 28M.
14. Ide, F., and Y. Takayama, *Kogyo Kagaku Zasshi*, **63**, 529 (1960).
15. Furukawa, J., T. Tsuruta, T. Fueno, R. Sakata, and K. Ito, *Makromol. Chem.*, **30**, 109 (1959).
16. Inoue, S., T. Tsuruta, and J. Furukawa, *Kogyo Kagaku Zasshi*, **64**, 492 (1961).
17. Natta, G., P. Pino, and M. Farina, *Ricerca Sci.*, **25A**, 120 (1955).
18. Welch, F. J., *J. Polymer Sci.*, **61**, 243 (1962).
19. Tobolsky, A. V., *J. Am. Chem. Soc.*, **80**, 5927 (1958).
20. Ide, F., and Y. Takeyama, *Kogyo Kagaku Zasshi*, **63**, 533 (1960).
21. Kawakami, H., N. Mori, K. Kawashima, and M. Sumi, *Kogyo Kagaku Zasshi*, **66**, 88 (1963).
22. Pepper, D. C., *Trans. Faraday Soc.*, **45**, 404 (1949).
23. Hoffmann, E. G., *Ann. Chem.*, **629**, 104 (1960).
24. Kolesnikov, H. S., and N. V. Klimentov, *Vysokomolekul. Soedin.*, **1**, 362 (1959).
25. Talamini, G., and G. Vidotto, *Makromol. Chem.*, **49**, 13 (1961).
26. Natta, G., *J. Polymer Sci.*, **34**, 21 (1959).
27. Thomas, R. M., W. J. Sparks, P. K. Fröhlich, M. Otto, and M. Mueller-Cunradi, *J. Am. Chem. Soc.*, **62**, 276 (1940).
28. Flory, P. J., *Principles of Polymer Chemistry*, Cornell Univ. Press, Ithaca, N. Y., 1953, p. 24.
29. Burnett, G. H., and L. D. Loan, *Trans. Faraday Soc.*, **57**, 219 (1955).
30. Jenkins, A. D., *J. Polymer Sci.*, **29**, 245 (1958).
31. Walling, C., E. R. Briggs, W. Cummings, and F. R. Mayo, *J. Am. Chem. Soc.*, **72**, 48 (1950).
32. Overberger, C. G., and V. G. Kamath, *J. Am. Chem. Soc.*, **85**, 446 (1963).
33. Sinn, H., and F. Patat, *Angew. Chem. (Int. Ed. Eng.)*, **3**, 73 (1964).
34. Ashikari, N., and A. Nishimura, *J. Polymer Sci.*, **31**, 247 (1958).
35. Kolesnikov, G. S., and L. S. Fedorova, *Vysokomolekul. Soedin.*, **1**, 1266 (1959).
36. Davies, A. G., and R. B. Moodie, *Chem. Ind. (London)*, **1957**, 1622; *J. Chem. Soc.*, **1958**, 2372.
37. Takeuchi, T., M. Suzuki, and F. Ide, *Kogyo Kagaku Zasshi*, **63**, 2181 (1960).
38. Kolesnikov, G., and L. S. Fedorova, *Izv. Akad. Nauk SSSR, Otd. Khim. Nauk*, **1958**, 906.
39. Schultz, D. R., *J. Polymer Sci.*, **B1**, 613 (1963).
40. Saegusa, T., H. Imai, and J. Furukawa, *Makromol. Chem.*, **63**, 224 (1963).
41. Glusker, D. L., I. Lysloff, and E. Stiles, *J. Polymer Sci.*, **49**, 315 (1961).

Résumé

Le triéthyl-aluminium, le triisobutyl-aluminium et l'hydrure de diisobutyl-aluminium ont été employés pour polymériser l'acétate de vinyle, le méthacrylate de méthyle et le styrène à des températures situées entre -80 et 25°C . On a obtenu des polymères linéaires avec des rendements acceptables. En se basant sur les résultats cinétiques obtenus par dilatométrie, on remarque que: (a) la vitesse diminue d'une façon constante avec le temps à partir d'une valeur initialement élevée; (b) la vitesse initiale dépend de

la concentration en catalyseur et du carré de la concentration en monomère; (c) l'énergie globale d'activation est de 13 kcal./mole, et l'énergie d'activation pour le degré de polymérisation est d'environ 2 kcal./mole. La copolymérisation du méthacrylate de méthyle et du styrène fournit un polymère qui est riche en méthacrylate de méthyle. La polymérisation n'est ni clairement radicalaire ni ionique et une certaine forme de coordination peut avoir lieu.

Zusammenfassung

Aluminiumtriäthyl, Aluminiumtriisobutyl und Diisobutylaluminiumhydrid wurden zur Polymerisation von Vinylacetat, Methylmethacrylat und Styrol bei Temperaturen von -80 bis 25° verwendet. Lineare Hochpolymere wurden in guter Ausbeute erhalten. Dilatometrische kinetische Versuche führten zu folgenden Ergebnissen: (a) Die Geschwindigkeit nimmt mit der Versuchsdauer von einem hohen Anfangswert stetig ab; (b) die Anfangsgeschwindigkeit hängt von der Katalysatorkonzentration und vom Quadrat der Monomerkonzentration ab; (c) die Bruttoaktivierungsenergie beträgt 13 kcal/Mol und die Aktivierungsenergie für den Polymerisationsgrad etwa 2 kcal/Mol. Die Copolymerisation von Methylmethacrylat und Styrol führte zu einem Polymeren mit einem hohen Gehalt an Methylmethacrylat. Die Polymerisation ist weder eindeutig radikalisch noch ionisch; es kann in irgendeiner Weise eine Koordination stattfinden.

Received October 22, 1964

Revised January 26, 1965

Prod. No. 4658A

Variation of Crystallinity with Temperature for Homopolymers and Random Copolymers

WILLIAM R. KRIGBAUM and ICHITARA UEMATSU,
Department of Chemistry, Duke University, Durham, North Carolina

Synopsis

An earlier treatment assumed that crystallization places portions of the polymer molecule between tie-points under strain, which limits the equilibrium crystallinity at any temperature. If these strained chains can be treated in the Gaussian approximation, $(1 - \omega)^{-2}$ should be a linear function of T^{-1} , where ω is the degree of crystallinity. This prediction is unchanged by inclusion of the crystal surface energy. The degree of crystallinity is primarily governed by the deformation entropy at high supercoolings, while near the apparent melting point the crystal surface energy dominates, hence the Hoffman and Weeks procedure for evaluating thermodynamic melting point remains valid. Random introduction of comonomer lowers the apparent melting point and increases the tie-point density. The latter limits both the degree of crystallinity and the initial Young's modulus of a random copolymer at high supercoolings. Values obtained for N (the number of statistical links between tie-points) by fitting crystallinity data near the melting points for isothermally crystallized isotactic polypropylene and linear and branched polyethylene by using the Gaussian approximation, are identical to those previously obtained at high supercoolings by using inverse Langevin statistics. In fact, if the effects of crystal surface energy and the presence of a comonomer are included and the amorphous chains are treated by inverse Langevin statistics, one obtains a satisfactory representation of the variation of crystallinity with temperature over the entire range studied. Finally, the predicted linear variation of ω at high supercoolings with $N^{-1/2}$ is verified for polyethylene.

I. INTRODUCTION

An earlier paper¹ from this laboratory was concerned with the factors which determine the equilibrium degree of crystallinity attained when an initially isotropic, amorphous polymer is cooled below its melting temperature. For the development of this treatment a model of the crystallization process was necessary. Whether one prefers to view a semi-crystalline polymer as a defect crystal or as a two-phase system, the observed bulk mechanical properties would appear to demand that the tiny mosaic blocks having perfect crystalline order be interconnected by polymer chains in the defect (or amorphous) regions. The origin of such tie molecules presents no conceptual difficulty. If one considers a single polymer chain approaching a growing crystal face, the situation must resemble that of a polymer molecule in solution approaching an adsorbing substrate surface. In the latter case it can be shown that the number of

contact points will either be zero or a number greater than unity. The important question is whether the tie chains left at the completion of the crystallization process will be in their unperturbed conformations or will be strained in some manner. The treatment referred to above considered, as a simplified but mathematically tractable model, a chain section composed of N statistical links, both ends of which had deposited on the growing crystal surface. Subsequent crystallization then resulted in the transfer of n links to the crystalline domain. By the use of this model it was possible to demonstrate that the act of crystallization places such tie chains under high tension, and that the crystallization process must stop when the free energy increase produced by this tension balances the decrease associated with the transfer of an additional link of the chain to the crystalline domain. Furthermore, it was shown that the rate of build-up of tension during crystallization depends upon the crystal morphology, and that from an isotropic melt crystallization by chain folding results in less strain in the intervening chains, and hence in higher equilibrium degrees of crystallinity, than is the case for bundlelike crystallites.

The development described thus far has involved the assumption that the set of tie-points formed upon cooling from the melt remains intact and unchanged as the temperature is raised, and thus imposes constraints which dictate the series of pseudo-equilibrium states which the system must traverse in order to reach the melting temperature. There are undoubtedly some situations in which the assumption of a fixed set of tie-points cannot be justified. For example, the very slow "second-stage" crystallization may well involve some readjustment of the tie-point population. Nevertheless, this assumption should furnish a useful approximation if the samples are crystallized as completely as possible at a low temperature, and measurements are then performed at higher temperatures. Furthermore, essentially the same predicted behavior of crystallinity with temperature was obtained from examination of a second model in which the number of tie-points per chain was assumed to vary during the crystallization process, while the crystalline run length n remained constant.

Comparison¹ with experimental data for linear polyethylene showed that the observed variation of crystallinity with temperature could be represented quite well by the folded-chain model, but that the fitted values for the parameter N were unreasonably small. This deficiency is not surprising in view of the oversimplified model employed. Some improvement might result from consideration of pairs of tie-points interconnected by bundles of chains having different lengths. In spite of this shortcoming, the treatment is of value in demonstrating that deformation of the remaining amorphous chains is a primary factor in determining the equilibrium degree of crystallinity.

The same model was subsequently used by the same authors² to predict how the initial Young's modulus should vary with crystallinity or temperature. It was shown that the high moduli observed for semicrystalline polymers are due in part to the fact that the remaining amorphous chains

are near their fully extended lengths, even in the absence of an external force, as a result of the crystallization process. Previous treatments which neglected this circumstance have seriously underestimated the modulus expected for a given degree of crystallinity. Comparison with data for polyethylene revealed that the magnitude of the modulus, and its variation with temperature, could be represented quite adequately by using the same value of the parameter N required to fit the crystallinity-temperature curve.

The foregoing treatments were mainly concerned with the behavior of semicrystalline polymers at temperatures well below the melting point. Here the situation is particularly simple, since the free energy increase due to deformation of the amorphous chains is of paramount importance. These problems become more complicated as the melting temperature is approached, and other factors must then be taken into consideration. Among these are the crystal surface free energy, and the effect of chain ends or copolymer units which cannot enter the crystalline region, both of which depress the melting point. The effect of copolymer units upon the degree of crystallinity and the melting point has been considered by Flory,^{3,4} while Mandelkern⁵ and Hoffman and Weeks⁶ have examined the effect of crystal surface energy upon the melting temperature. Unfortunately, the melting point may also be depressed due to the deformation of the intervening amorphous chains, so that all of these factors must be taken into account if the degree of crystallinity is to be adequately represented near the melting point.

The objectives of this paper are to assess the relative importance of these factors at various levels of supercooling and to obtain, if possible, relationships which are capable of representing the variation of crystallinity with temperature over the entire temperature range. Toward this end, degrees of crystallinity were estimated from dilatometric measurements performed for isotactic polypropylene and for linear and branched polyethylene samples.

II. THEORY

Variation of Crystallinity with Temperature

We will first demonstrate that a simple relationship exists between the degree of crystallinity of a polymer and its temperature for values of the crystallinity which permit the remaining amorphous chains to be represented in the Gaussian approximation. This relationship was first suggested by the theoretical results of Roe, Smith, and Krigbaum.¹ Although we will utilize their model for the derivation of the desired relation, it will later be shown that the result is independent of the model employed. They consider that the act of crystallization pins portions of some of the chains between pairs of tie-points. We focus our attention upon one such chain portion consisting of N equivalent links, and let $\langle r_N^2 \rangle$ be the mean-square displacement vector when the two end segments are first deposited. The

introduction of n links into the growing crystallites deforms the remaining chain of $(N - n)$ links, thereby giving rise to an entropy change. For Gaussian chains this may be written as

$$\Delta S_D = -(3k/2)(\langle r_c^2 \rangle - \langle r_i^2 \rangle)/(N - n)b^2 \quad (1)$$

where k is Boltzmann's constant, $\langle r_i^2 \rangle$ is the mean-square displacement length of the chain of $(N - n)$ links after initial deposition, given in the Gaussian approximation by

$$\langle r_i^2 \rangle = [n(N - n)/N]b^2 + [(N - n)/N]^2 \langle r_N^2 \rangle \quad (2)$$

and $\langle r_c^2 \rangle$ is the corresponding quantity after crystallization of n links.

The latter quantity will depend upon the details of the model employed. For a chain-folded crystallite model, treated in the Gaussian approximation, they obtained a particularly simple result:¹

$$\Delta S_D = -(3k/2)[n/(N - n)] \quad (3)$$

Under these conditions the total free energy change (written on a molar basis) for the transfer of n units to the crystalline region is

$$\Delta F = -n\Delta H_f(1 - T/T_M^\circ) + (3RT/2)[n/(N - n)] \quad (4)$$

where T_M° is the thermodynamic melting point and ΔH_f is the heat of fusion per mole of statistical links. The equilibrium degree of crystallinity, $\omega = n/N$, at temperature T is obtained by setting $(\partial\Delta F/\partial n)_{T,p} = 0$. Their result may be written in the following form:

$$[1/(1 - \omega)]^2 = (2N\Delta H_f/3R)[(1/T) - (1/T_M^\circ)] \quad (5)$$

which suggests that $(1 - \omega)^{-2}$ should be a linear function of T^{-1} so long as the remaining amorphous chains are not sufficiently strained to preclude the application of Gaussian statistics. For the same model the apparent melting temperature, T_M , is obtained upon setting $\omega = 0$

$$1/T_M = (1/T_M^\circ) + (3R/2N\Delta H_f) \quad (6)$$

As pointed out previously,⁷ the treatment of a quite different model by Flory⁸ likewise leads to the prediction of a linear dependence of $(1 - \omega)^{-2}$ upon T^{-1} . We are indebted to R.-J. Roe for the more general derivation of this result which follows. Using ΔS_D as given by eq. (1), rather than eq. (3), we perform the same steps to obtain as the analog of eq. (5)

$$[(\langle r_N^2 \rangle - Nb^2)/Nb^2] + [J/(1 - \omega)^2] = (2N\Delta H_f/3R) \times [(1/T) - (1/T_M^\circ)] \quad (7)$$

where

$$J = (Nb^2)^{-1}[\langle r_c^2 \rangle + (1 - \omega)(\partial\langle r_c^2 \rangle/\partial\omega)] \quad (8)$$

In general $\langle r_c^2 \rangle$ will be a function of ω . We may expand it in a power series

$$\langle r_c^2 \rangle = \langle r_N^2 \rangle + a_1\omega + a_2\omega^2 + \dots \quad (9)$$

where

$$a_1 = (\partial \langle r_c^2 \rangle / \partial \omega)_{\omega=0}$$

$$a_2 = (1/2)(\partial^2 \langle r_c^2 \rangle / \partial \omega^2)_{\omega=0}$$

If our attention is restricted to low values of ω we need retain at most the term $O(\omega^2)$. Then eq. (8) becomes

$$\frac{\langle r_N^2 \rangle - Nb^2 - a_2}{Nb^2} + \frac{\langle r_N^2 \rangle + a_1 + a_2}{Nb^2} \left(\frac{1}{1 - \omega} \right)^2 = \frac{2N\Delta H_f}{3R} \left(\frac{1}{T} - \frac{1}{T_M^\circ} \right) \quad (10)$$

Although the magnitudes of a_1 and a_2 will depend upon the model treated, this will not affect the predicted dependence of $(1 - \omega)^{-2}$ upon T^{-1} . The only approximations involved in the derivation of eq. (10) are the assumption of Gaussian statistics in writing eq. (1), and the neglect of higher terms if the series in eq. (9). In this more general treatment the apparent melting point, T_M , is given by;

$$1/T_M = (1/T_M^\circ) + (3R/2N\Delta H_f)[(2\langle r_N^2 \rangle - Nb^2 + a_1)/Nb^2] \quad (11)$$

Effect of Crystal Surface Energy

Roe, Smith, and Krigbaum¹ pointed out that the energy required to form chain folds was neglected in their treatment. This omission is permissible so long as one is interested only in the crystallinity at temperatures far below the melting point. However, the crystal surface energy assumes increasing importance as the apparent melting point is approached. In order to improve their treatment in the region of low crystallinity, the surface energy must be taken into account. For this purpose we again adopt their chain-folded model. Let us assume that each fold in the crystallite consists of P statistical links, and represent the energy necessary to form the chain fold by ϵ . Equation (4) must then be modified as follows:

$$\Delta F = -n\Delta H_f(1 - T/T_M^\circ) + (3RT/2)[n/(N - n)] + n\epsilon/P \quad (11)$$

and the relation for the equilibrium degree of crystallinity at temperature T becomes

$$[1/(1 - \omega)]^2 = (2N\Delta H_f/3R)\{[1 - (\epsilon/\Delta H_f P)](1/T) - (1/T_M^\circ)\} \quad (12)$$

In the notation of Hoffman and Weeks⁶ the quantity $[1 - (\epsilon/\Delta H_f P)]$ may be written $(1 - 2\sigma_e S/\Delta h_f l)$, where σ_e is the end surface energy per square centimeter, S is the cross-sectional area of the chain in square centimeters, Δh_f is the heat of fusion per cubic centimeter, and l is the crystallite fold length in centimeters.

One important conclusion to be drawn from eq. (12) is that inclusion of the crystal surface energy does not alter the predicted linear dependence of $(1 - \omega)^{-2}$ upon T^{-1} . The apparent melting point deduced from this relation is

$$T_M = T_M^\circ [1 - (\epsilon/\Delta H_f P^*)]/(1 + 3RT_M/2N\Delta H_f) \quad (13)$$

where P^* is the number of statistical links per fold of the largest crystallites present (i.e., the last to melt).

We will now follow the procedure of Hoffman and Weeks,⁶ except that the entropy term associated with the deformation of the remaining amorphous chains will be retained. If eq. (11) is applied to the onset of the crystallization process, the number P of links in the smallest fold which will be stable at a crystallization temperature T_x is found to be

$$\epsilon/P = \Delta H_f(1 - T_x/T_M^\circ) - 3RT_x/2N \quad (14)$$

Following Hoffman and Weeks, we characterize the folds of the last crystallites to melt by the number of links $P^* = 2\beta P$. Hence

$$\epsilon/P^* = (1/2\beta)[\Delta H_f(1 - T_x/T_M^\circ) - 3RT_x/2N] \quad (15)$$

and introduction of this relation into eq. (13) yields

$$T_M = T_M^\circ(1 - 1/2\beta)/(1 + 3RT_M^\circ/2N\Delta H_f) + (T_x/2\beta) \quad (16)$$

The procedure advocated by Hoffman and Weeks for the determination of T_M° involves measurement of the apparent melting temperatures T_M of a number of isothermally crystallized samples covering a range of crystallization temperatures T_x . The observed T_M values are then plotted as a function of T_x and, according to their procedure, T_M° is obtained by extrapolating these points to meet the line $T_M = T_x$. In the present case we designate the intercept of this plot as $T_{M\ddagger}$. According to eq. (16)

$$T_{M\ddagger} = T_M^\circ/(1 + 3RT_M^\circ/2N\Delta H_f) \quad (17)$$

Whether $T_{M\ddagger}$ will, in fact, represent a close approximation to T_M° depends upon the magnitude of N . In this connection it is well to recall that the previous section was concerned with the variation of crystallinity with temperature for a particular sample, and in that case N could be considered constant throughout. The present situation involves comparison of a number of samples crystallized under different conditions, and these will in general have different N values. It may be anticipated that N will be a function of the same variable, $(1 - T_x/T_M^\circ)$, which governs the number P of links in a crystallite fold. However, such a detailed examination is not necessary to demonstrate that the difference between $T_{M\ddagger}$ and T_M° is likely to be completely negligible for any case of interest. To do so we will perform a numerical calculation for polyethylene, taking $T_M^\circ = 418^\circ\text{K}$. and $\Delta H_f = 9.40$ kcal./mole. If $N = 100$, then $T_{M\ddagger} = 0.999 T_M^\circ$. Hence, for these values the procedure of Hoffman and Weeks would underestimate the thermodynamic melting temperature by no more than 0.5°C . While this would be entirely within the experimental error, it is likely that the value of N appropriate for crystallization near the thermodynamic melting point will be much larger than 100, so that the difference between $T_{M\ddagger}$ and T_M° will be much smaller than 0.5°C .

Degree of Crystallinity of Copolymers

The melting point depression caused by the introduction of a second type of repeating unit by random copolymerization was considered many years ago by Flory.³ His treatment implicitly assumed a crystalline phase of negligible surface area, and amorphous regions which could be treated as a separate and distinct phase. In his more recent treatment of non-random copolymers⁴ an expression was obtained for the equilibrium degree of crystallinity. Here the surface free energy was taken into account, but the interconnection of the crystalline regions by amorphous chains was ignored. Our interest will be restricted to random copolymers, but we will take into account both the surface free energy and deformation entropy terms.

Let us consider a random copolymer composed of A units which can crystallize and B units which cannot. If X_A is the mole fraction of A links in the polymer, then when the degree of crystallinity is ω the fraction of crystallizable units remaining in the amorphous regions is $(X_A - \omega)/(1 - \omega)$. Using the folded-chain Gaussian model, and treating the surface free energy as in the preceding section, we obtain for the free energy change on crystallizing n statistical segments from each of a mole of chains

$$\Delta F = -n[\Delta H_f(1 - T/T_M^\circ) + RT \ln \{(X_A - \omega)/(1 - \omega)\}] + (3RT/2)[n/(N - n)] + n\epsilon/P \quad (18)$$

Upon setting $(\partial\Delta F/\partial n)_{T,p} = 0$, the equilibrium degree of crystallinity is found to be

$$\frac{1}{T} \left(1 - \frac{\epsilon}{\Delta H_f P} \right) - \frac{1}{T_M^\circ} = \frac{R}{\Delta H_f} \left[-\ln \left(1 - \frac{X_B}{1 - \omega} \right) + \frac{3}{2N} \left(\frac{1}{1 - \omega} \right)^2 \right] \quad (19)$$

If $X_B/(1 - \omega)$ is small we may expand the logarithmic term and neglect powers beyond the second to obtain

$$\begin{aligned} \frac{1}{T} \left(1 - \frac{\epsilon}{\Delta H_f P} \right) - \frac{1}{T_M^\circ} - \frac{R}{\Delta H_f} \left[\frac{X_B}{1 - \omega} + \frac{X_B^2}{2(1 - \omega)^2} \right] \\ = \frac{3R}{2N\Delta H_f} \left(\frac{1}{1 - \omega} \right)^2 \quad (20) \end{aligned}$$

Equation (20) shows that $(1 - \omega)^{-2}$ is no longer a linear function of T^{-1} for a copolymer. A numerical calculation must again be resorted to in order to illustrate the relative importance of the amorphous deformation and copolymer terms at various levels of crystallinity. As an example we consider $X_B = 0.05$ and $N = 50$. The ratio of the second to the first term in the square brackets in eq. (19) then decreases from 2.6 at $\omega = 0.80$ to 0.6 when ω is zero. Clearly the copolymer term becomes more important as the melting point is approached. However, it also imposes an upper limit on the degree of crystallinity at high supercoolings, since $(1 - \omega)$ must always exceed X_B .

III. EXPERIMENTAL RESULTS

In our preceding paper,⁹ specific volume data were reported for isotactic polypropylene samples which had been crystallized isothermally. Hercules Profax polypropylene was dissolved in tetralin, filtered, and reprecipitated. The precipitate was extracted for 24 hr. with boiling heptane, and the residue was used for sample preparation. Values for the degree of crystallinity, ω , were estimated through use of the specific volume relationships of Danusso et al.¹⁰ for crystalline and amorphous polypropylene:

$$\bar{v}_c = 1.059 + 4.25 \times 10^{-4}t$$

$$\bar{v}_a = 1.1340 + 9.28 \times 10^{-4}t$$

where t is in degrees Centigrade.

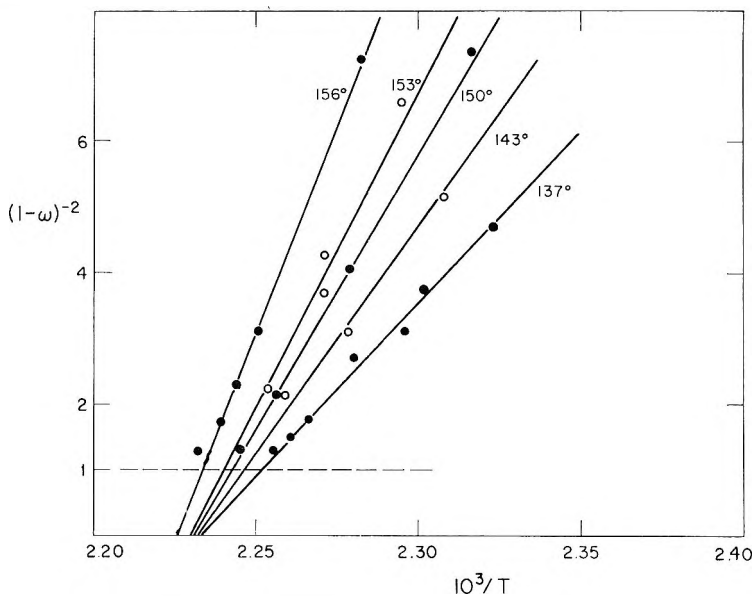


Fig. 1. Data for the degree of crystallinity ω of isotactic polypropylene plotted as $(1 - \omega)^{-2}$ vs. T^{-1} . The isothermal crystallization temperature for each sample is indicated.

According to the theory given above $(1 - \omega)^{-2}$ should be a linear function of T^{-1} . Data obtained for polypropylene crystallized isothermally at five temperatures appear plotted in this manner in Figure 1. These points conform reasonably well with the expected linear relationship. Each line extrapolates to the observed melting point when $(1 - \omega)^{-2} = 1$ and, according to eq. (12), the slope should be given by $(2N\Delta H_f/3R)(1 - \epsilon/\Delta H_fP)$. If the lines are further extrapolated to $(1 - \omega)^{-2} = 0$, the intercept on the abscissa scale is $1/T_M^*$, where $T_M^* = [1 - (\epsilon/\Delta H_fP)]T_M^0$ is the hypothetical melting temperature which would be observed if surface free energy were the sole cause of melting point depression. If the thermo-

dynamic melting point T_M° is known, the intercepts give $[1 - (\epsilon/\Delta H_f P)]$. With this information, and a knowledge of ΔH_f , N may be evaluated from the slope.

Let s be the number of repeating units per statistical segment. We take from our preceding paper⁹ the values $T_M^\circ = 459^\circ\text{K}$. and $\Delta H_f' = \Delta H_f/s = 2.1$ kcal./mole repeating units). Upon setting $\epsilon = 5.7$ kcal./mole (which corresponds to $\sigma_c = 57$ erg./cm.² and $S = 34.8 \times 10^{-16}$ cm.²), we obtain from Figure 1 the values for the average number of repeating units between nuclei, sN , and per fold in the crystallite, sP , which appear in Table I. One sees that both N and P increase with crystallization temperature. While there is considerable uncertainty in these values, it is evident that the magnitude of N obtained in this manner is entirely too small. This behavior was observed previously¹ and, as indicated above, it undoubtedly arises from the use of an oversimplified model.

TABLE I
Parameters for Isotactic Polypropylene

t_c , °C.	t_M , °C.	sN	sP
156	176.8	193	123
153	176.0	150	118
150	175.2	130	112
143	173.5	103	112
137	173.5	79	108

We next turn our attention to a study of linear and branched polyethylene. The four polymers examined were Marlex 50 (No. 6000 and No. 5000), Lupolen, and Yukalon. The latter two polymers have 1.6 and 2.0 branches/100°C, respectively. The samples were melted, crystallized at a fixed temperature for one hour, slowly cooled, and finally annealed for 2 hr. Crystallization and annealing of the Marlex samples were performed at 125°C., while the other two samples were crystallized at 100°C. and annealed at 105°C.

A relatively rapid heating rate of 1°C./5 min. was used for the dilatometric measurements in order to minimize recrystallization. The specific volume data appear plotted as a function of temperature in Figure 2. Crystallinities were estimated through use of the relation of Richardson, Flory, and Jackson:¹¹

$$\bar{v}_c = 0.993 + 3.00 \times 10^{-4}t$$

for the specific volume of the crystalline portion, while for the amorphous portion the specific volume was obtained by linear extrapolation of the values measured in the liquid state. We may remark parenthetically that this procedure apparently fails for polypropylene, so that we were unable to obtain degrees of crystallinity at high supercoolings for that polymer. Values so obtained for the degree of crystallinity of the polyethylene samples appear plotted against temperature in Figure 3. It is

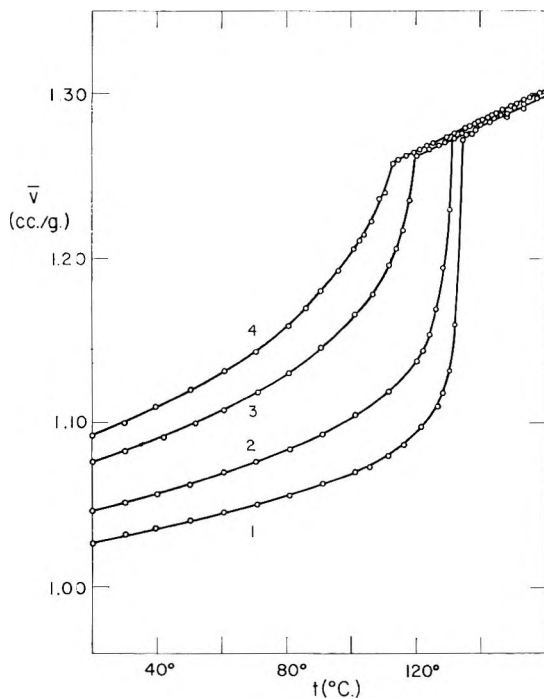


Fig. 2. Specific volume plotted against temperature for four types of polyethylene: (1) Marlex 50 No. 6000; (2) Marlex 50 No. 5000; (3) Lupolen; (4) Yukalon.

evident that the samples having branched chains have lower apparent melting points, and also lower degrees of crystallinity at high supercoolings.

The interpretation of these data is more difficult since, as indicated above, a plot of $(1 - \omega)^{-2}$ versus T^{-1} is not expected to be linear. If the extent of branching is not too large, eq. (19) may be approximated as follows:

$$\left(\frac{1}{1 - \omega}\right)^2 \cong \frac{2N\Delta H_f}{3R} \left(1 - \frac{\epsilon}{\Delta H_f P}\right) \times \left[\frac{1}{T} + \frac{R}{\Delta H_f} \ln \left(1 - \frac{X_B}{1 - \omega}\right) - \frac{1}{T_M^\circ(1 - \epsilon/\Delta H_f P)}\right] \quad (21)$$

This suggests plotting $(1 - \omega)^{-2}$ versus $\left\{\frac{1}{T} + \frac{R}{\Delta H_f} \ln [1 - X_B/(1 - \omega)]\right\}$. The intercept on the abscissa and the slope will have the same significance as in Figure 1. Furthermore, the two plots become identical as X_B approaches zero. The data for the four polyethylene samples are shown plotted in this manner in Figure 4. The values appearing in Table II were calculated with the following assignments: $T_M^\circ = 415^\circ\text{K}$., $s = 10$, $\Delta H_f' = \Delta H_f/s = 0.94$ kcal./mole CH_2 , $\epsilon = 2.55$ kcal./mole (which corresponds to $\sigma_e = 49$ erg/cm.² and $S = 18 \times 10^{-16}$ cm.²), $X_B = 0.10$ for Lupolen and 0.16 for Yukalon.

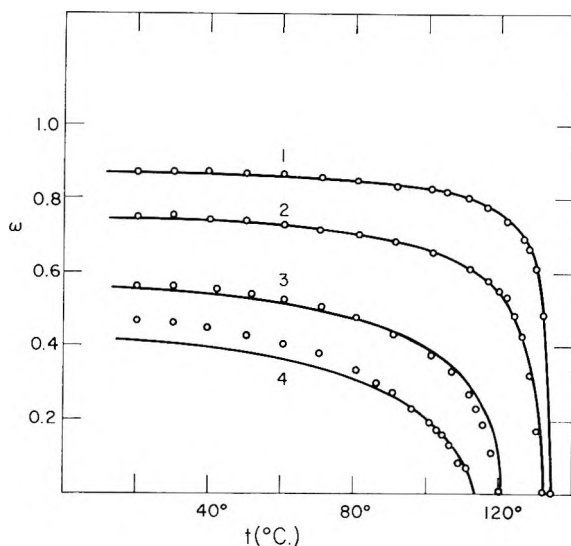


Fig. 3. Variation with temperature of the degree of crystallinity for the four polyethylene samples shown in Fig. 2. The full curves were calculated as described in the text.

We may examine the data in Tables I and II to see how the parameter N varies with crystallization temperature. For this purpose eq. (14) is slightly rearranged;

$$\Delta T/T_M^\circ = (\epsilon/\Delta H_f P) + (3RT_c/2N\Delta H_f) \quad (14)$$

where $\Delta T = T_M^\circ - T_c$. The latter term in eq. (14) was not included in the treatment of Hoffman and Weeks, which permitted them to state that $1/P$ should vary linearly with $\Delta T/T_M^\circ$. In the present case we have no way to predict how the individual terms on the right-hand side of eq. (14) should vary with $\Delta T/T_M^\circ$. In Figure 5 these two quantities are plotted against $\Delta T/T_M^\circ$ for the combined data for polypropylene and polyethylene. Although the points exhibit considerable scatter, a linear variation of each parameter appears to be indicated.

Returning to Table II, the N values are once again found to be too small. However, it is of interest that the N values, 800 and 70, fitted for Marlex and Lupolen by using dilatometric data obtained near the melting point, are identical to those previously found to fit the crystallinities at high supercoolings by use of a different equation derived for inverse

TABLE II
Parameters for Polyethylene

Polymer	t_M , °C.	sN	sP
Marlex 50 (No. 6000)	135.7	800	200
Marlex 50 (No. 5000)	131.2	210	170
Lupolen	120.5	70	123
Yukalon	113.8	40	119

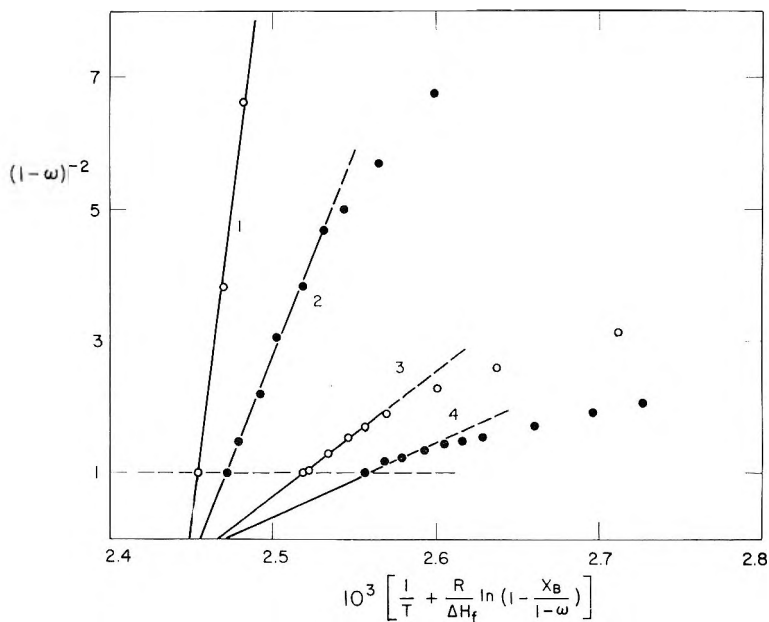


Fig. 4. The polyethylene data plotted as $(1 - \omega)^{-2}$ vs. $1/T + (R/\Delta H_f) \ln [1 - X_B/(1 - \omega)]$, where X_B is the mole fraction of statistical links of noncrystallizable comonomer. Curves are numbered as in Fig. 2.

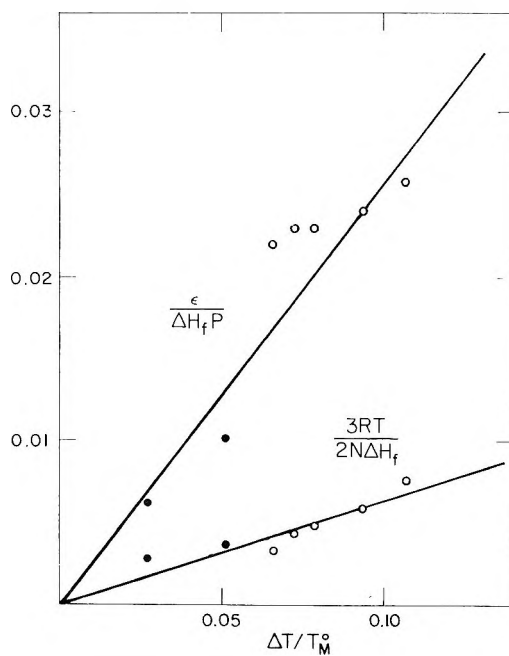


Fig. 5. $\epsilon/\Delta H_f P$ and $3RT_z/2N\Delta H_f$ plotted against $(T_M^0 - T_z)/T_M^0$: (●) polypropylene; (○) polyethylene.

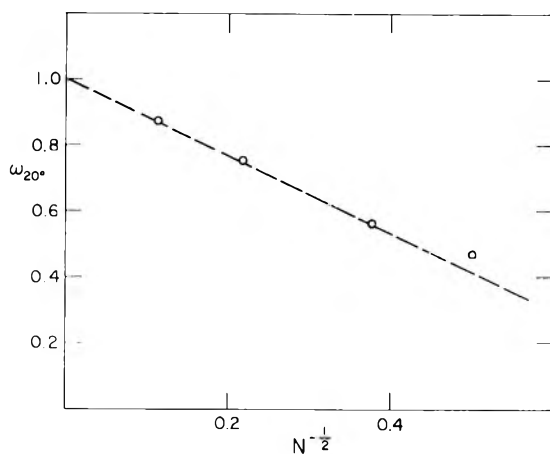


Fig. 6. Degree of crystallinity of polyethylene at 20°C. plotted against $N^{-1/2}$. The dashed line represents the theoretical prediction (see text).

Langevin chains.² This suggests that the departures from linearity in Figure 4 arise from the failure of the Gaussian approximation at higher crystallinity levels. The full curves in Figure 3 represent values calculated by using the analog of eq. (19) for inverse Langevin, rather than Gaussian, chains. The N values fitted near the melting point were employed. It is seen that this procedure furnishes a reasonable representation of the variation of crystallinity with temperature over the entire range investigated. Comparison with the results of the previous calculation² shows that the present one affords better agreement near the melting point, as expected, due to inclusion of the surface energy and copolymer effects.

The fact that a single N value suffices for the entire temperature range may be demonstrated in another manner by utilizing the N values fitted near the melting point to predict the maximum crystallinity which can be achieved at very high supercoolings. According to the previous treatment for inverse Langevin chains and chain-folded crystallites¹

$$\omega = 1 - [1/\mathcal{L}(\beta)]N^{-1/2} \quad (22)$$

Thus, at high supercoolings ω should become a linear function of $N^{-1/2}$. We will calculate the theoretical slope for polyethylene at 20°C., since this is the lowest temperature at which data were obtained. Substitution of the appropriate values given above leads to $A = (\Delta H_f/R)(1/T - 1/T_M^\circ) = 4.35$. Since $(\sinh \beta)/\beta = e^A$, this corresponds to $\beta = 7$, or $\mathcal{L}(\beta) = \coth \beta - 1/\beta = 0.86$. Hence, we conclude that the slope of ω versus $N^{-1/2}$ should be -1.17 . The ω values measured for the polyethylene samples at 20°C. appear in Figure 6 plotted against $N^{-1/2}$, where N is assigned the value fitted near the melting temperature. The dashed line has the predicted slope, and it is seen to furnish a satisfactory representation of the data. The theoretical slope is dependent to some extent

upon the value of s , and better agreement could have been obtained by selecting a value slightly less than 10 CH₂ units per statistical link.

Krigbaum, Roe, and Smith² have shown that the limiting value of Young's modulus, E_0 , at high supercoolings is a linear function of $(1 - \omega)^{-1}$. Equation (22) indicates that $(1 - \omega)^{-1}$ varies linearly with $N^{1/2}$. We conclude that the limiting value of E_0 at high supercoolings will be directly proportional to $N^{1/2}$. Thus, the density of tie-points formed in the sample determines both the level of crystallinity and the Young's modulus which will be exhibited at low temperatures.

CONCLUSIONS

The present paper represents an amplification and extension of the treatment of Roe, Smith, and Krigbaum.¹ For low degrees of crystallinity, their folded chain Gaussian model predicts that $(1 - \omega)^{-2}$ should be a linear function of T^{-1} . A similar conclusion can be drawn from the earlier treatment due to Flory⁸ and, in fact, in the present paper it is shown that any treatment of the crystallinity of homopolymers which involves the Gaussian approximation must inevitably lead to this predicted dependence. This prediction is confirmed by our data obtained for polypropylene and polyethylene near their respective melting points. At lower temperatures (or higher crystallinities) deviations occur due to departures of the remaining amorphous chains from Gaussian behavior.

The predicted dependence mentioned above is not altered by inclusion of the crystal surface energy. The effect of the latter upon the degree of crystallinity at high supercoolings is shown to be negligible when compared to that of amorphous deformation; however, near the melting point these roles are reversed and surface energy far outweighs the contribution of the amorphous chains. As a result of this latter circumstance, the procedure proposed by Hoffman and Weeks⁶ for evaluation of the thermodynamic melting temperature of a polymer remains valid. Our data suggest that both the crystallite fold length and the number of chain links between tie-points vary inversely with $T_M^\circ - T_c$, where T_M° is the thermodynamic melting point and T_c the crystallization temperature.

Two separate effects are encountered when random copolymers are considered. Firstly, as is well known, the chemical potential of the crystallizable units in the amorphous phase is depressed due to the second comonomer by an amount which varies with the degree of crystallinity. This lowers the apparent melting point, and results in a nonlinear variation of $(1 - \omega)^{-2}$ with T^{-1} . If the comonomer cannot enter the crystal lattice, its presence will impose an upper limit upon the level of crystallinity which the copolymer will exhibit at high supercoolings. The melting point depression also affects the crystallinity in a second, and more subtle, manner. For a given crystallization time, it implies that ΔT must be larger, which will result in a higher density of tie-points and smaller N values. This effectively limits both the equilibrium degree of crystal-

linity, and the initial Young's modulus, which a copolymer will exhibit at temperatures far below the melting point.

We are pleased to acknowledge financial support for this investigation through National Science Foundation grant NSF-G20533.

References

1. Roe, R.-J., K. J. Smith, Jr., and W. R. Krigbaum, *J. Chem. Phys.*, **35**, 1306 (1961).
2. Krigbaum, W. R., R.-J. Roe, and K. J. Smith, Jr., *Polymer*, **5**, 533 (1964).
3. Flory, P. J., *J. Chem. Phys.*, **17**, 223 (1949).
4. Flory, P. J., *Trans. Faraday Soc.*, **51**, 848 (1955).
5. Mandelkern, L., *J. Polymer Sci.*, **47**, 494 (1960).
6. Hoffman, J. D., and J. J. Weeks, *J. Res. Natl. Bur. Std.*, **66A**, 13 (1962).
7. Krigbaum, W. R., and R.-J. Roe, *J. Polymer Sci.*, **A2**, 4391 (1964).
8. Flory, P. J., *J. Chem. Phys.*, **15**, 397 (1947).
9. Krigbaum, W. R., and I. Uematsu, *J. Polymer Sci.*, **A3**, 767 (1965).
10. Danusso, F., G. Moraglio, W. Ghiglia, L. Motta, and G. Talamini, *Chim. Ind. (Milan)*, **41**, 748 (1959).
11. Richardson, J. J., P. J. Flory, and J. B. Jackson, *Polymer*, **4**, 221 (1963).

Résumé

Une étude antérieure supposait que la cristallisation place des portions de molécules de polymère entre des points de liaison soumis à une déformation, ce qui limite la cristallinité à l'équilibre pour chaque température. Si ces chaînes déformées peuvent être traitées au moyen d'une approximation gaussienne, $(1 - \omega)^{-2}$ devrait être une fonction linéaire de T^{-1} , où ω est le degré de cristallinité. Cette prévision est inchangée par l'introduction de l'énergie superficielle du cristal. Le degré de cristallinité est essentiellement régi par l'entropie de déformation lors des surfusions élevées, tandis qu'aux environs du point de fusion apparent, l'énergie superficielle du cristal domine. Par conséquent la méthode de Hoffman et Weeks en vue d'évaluer le point de fusion thermodynamique reste valable. L'introduction statistique du comonomère abaisse le point de fusion apparent et augmente la densité des points de liaison. Cette dernière limite le degré de cristallinité ainsi que le module initial de Young pour un copolymère statistique lors des surfusions élevées. Les valeurs obtenues pour N , (le nombre de liens statistiques entre les points de liaison) en interprétant les résultats de la cristallinité aux environs des points de fusion pour du polypropylène isotactique cristallisé isothermiquement et pour du polyéthylène linéaire et ramifié au moyen de l'approximation gaussienne, sont identiques à celles obtenues antérieurement lors de surfusions élevées en employant les statistiques inverses de Langevin. En fait, si l'influence de l'énergie superficielle du cristal et la présence de comonomère sont comprises et si les chaînes amorphes sont analysées en utilisant les statistiques inverses de Langevin, on obtient une représentation satisfaisante de la variation de cristallinité avec la température dans tout le domaine étudié. Finalement, la variation linéaire prévue pour ω aux surfusions élevées en fonction de $N^{-1/2}$ est vérifiée pour le polyéthylène.

Zusammenfassung

In einer früheren Abhandlung wurde angenommen, dass durch die Kristallisation Teile des Polymermoleküls zwischen verformungsbeanspruchte Verbindungspunkte gebracht werden, was die Gleichgewichtskristallinität bei einer gegebenen Temperatur begrenzt. Wenn eine Behandlung dieser verformten Ketten in der Gaußschen Näherung möglich ist, sollte $(1 - \omega)^{-2}$ eine lineare Funktion von T^{-1} sein, wo ω den Kristallinitätsgrad bedeutet. Diese Forderung wird durch Berücksichtigung der Kristalloberflächenenergie

nicht geändert. Der Kristallinitätsgrad wird bei starker Unterkühlung hauptsächlich durch die Deformationsentropie bestimmt, während in der Nähe des scheinbaren Schmelzpunkts die Kristalloberflächenenergie ausschlaggebend ist. Es bleibt daher das Verfahren von Hoffman und Weeks zur Ermittlung des thermodynamischen Schmelzpunkts gültig. Ungeordnete Einföhrung eines Comonomeren erniedrigt den scheinbaren Schmelzpunkt und erhöht die Verknüpfungspunktdichte. Letztere begrenzt sowohl den Kristallinitätsgrad als auch den Anfangs-Young-Modul eines statistischen Copolymeren bei starker Unterkühlung. Für N (Anzahl statistischer Glieder zwischen Verknüpfungspunkten), durch Anpassung der Kristallinitätsdaten in der Nähe des Schmelzpunkts für isotherm kristallisiertes isotaktisches Polypropylen sowie lineares und verzweigtes Polyäthylene an die Gauss'sche Näherung, erhaltene Werte sind mit den früher bei starker Unterkühlung mittels inverser Langevin-Statistik erhaltenen Werten identisch. Tatsächlich erhält man bei Berücksichtigung des Einflusses der Kristalloberflächenenergie und der Gegenwart eines Comonomeren und bei Behandlung der amorphen Ketten durch eine Langevin-Statistik eine befriedigende Darstellung der Kristallinität von der Temperatur im ganzen untersuchten Bereich. Schliesslich wird die erwartete lineare Abhängigkeit von ω von $N^{-1/2}$ bei starker Unterkühlung an Polyäthylene verifiziert.

Received August 5, 1964

Revised December 5, 1964

Prod. No. 4649A

Existence of Long-Lived Radicals in the γ -Radiation Induced Polymerization of Ethylene

SUEO MACHI, MIYUKI HAGIWARA, MASAO GOTODA, and
TSUTOMU KAGIYA, *Japan Atomic Energy Research Institute, Takasaki
Radiation Chemistry Research Establishment, Gunnan-mura Gomma, Japan*

Synopsis

In the γ -radiation-induced bulk polymerization of ethylene under high pressure, the growing polymer radical is shown to have a long lifetime at low temperatures (30°C.). Separation of the propagation reaction from other elementary reactions is possible. During the propagation reaction the molecular weight of the polymer increases with polymer yield when irradiated with an extremely low dose rate. At elevated temperatures (100°C.), the lifetime of the growing polymer radical is not prolonged.

Introduction

In a previous paper¹ it was reported that the rate of polymerization and the molecular weight of polymer increase continuously with reaction time in the bulk polymerization of ethylene induced by γ -radiation. From this fact, we have presumed that both chain termination and transfer reactions are almost absent, and the life of polymer radical is long under irradiation.

The purpose of this note is to report new information on the existence of the long-lived polymer radical and to offer an interesting mechanism for chain propagation in radiation polymerization.

Experimental

The reaction vessel, ethylene monomer, and experimental procedure are the same as described in the previous paper.¹ In the present experiment, however, the polymerization was carried out in two different stages. The first irradiation was carried out at a dose rate of 2.5×10^4 rad/hr. at 30°C. for 0.5 hr.; this was followed by a second irradiation at an extremely low dose rate, 300 rad/hr., at various pressures. The temperature was maintained constant within $\pm 0.5^\circ\text{C}$. in the course of a reaction. In order to change the radiation intensity, the distance between the reactor and the Co^{60} source was varied. Interruption of irradiation between the two stages was about 20 min.

Results and Discussion

Figure 1 show a plot of polymer yield against reaction time at various conditions. The irradiation was carried out in two stages that are shown

as period I and period II. In period I, ethylene was irradiated at a dose rate of 2.5×10^4 rad/hr. under a pressure of 400 kg./cm.² at 30°C.; in period II irradiation was continued at a very low dose rate, 300 rad/hr. It can be seen that the polymer yield increases rapidly in period I, while it is proportional to reaction time in period II. The polymer increase in period II is quite considerable, as shown in Figure 1. When the entire polymerization was carried out at the same low dose rate as was used in period II (Fig. 1D), the amount of polymer formed was much less than that formed in period II after the initial high dose rate irradiation (Figs. 1A, 1B). The amount of polymer increase may be caused by the irradiation

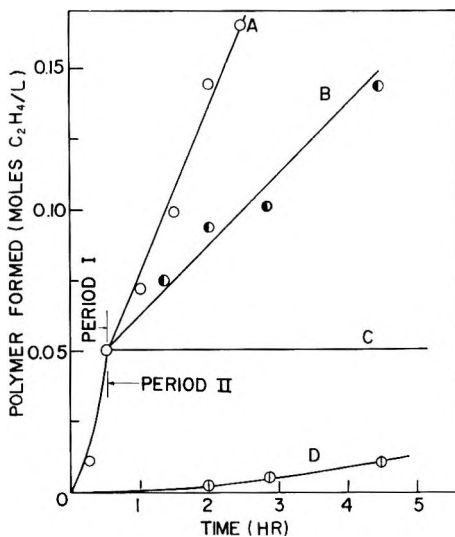


Fig. 1. Polymer yield vs. reaction time: (○) dose rate 2.5×10^4 rad/hr., ethylene pressure 400 kg./cm.², temperature 30°C.; (●) dose rate 300 rad/hr., pressure 400 kg./cm.², temperature 30°C.; (⊕) dose rate 300 rad/hr., pressure 200 kg./cm.², temperature 30°C.; (—) dose rate 0, pressure 400 kg./cm.², temperature 30°C.; (⊕) dose rate 300 rad/hr., pressure 200 kg./cm.², temperature 30°C.

tion in period I. This fact may indicate that the polymer radical introduced in period I survives and the polymer chain growth can occur at a low dose rate in period II. However, since no polymer increase in period II is observed without irradiation in this period, post-polymerization does not occur.

Table I shows the characteristic effect of temperature on the polymer increase in period II. As is seen in run 5, when the polymerization in period I is carried out at 100°C., the amount of polymer increase in period II is nearly equal to the yield of polymer in run 2. While in the case of run 3, the polymer increase in period II greatly exceeds the polymer yield in run 2 when the polymerization temperature is 30°C. These facts indicate the polymer radical can not survive at as high a temperature as 100°C. but survives at a low temperature (30°C.).

TABLE I
Effect of Temperature on the Polymer Increase in Period II^a

Run	Period I (Dose rate = 25,000 rad/hr.)				Period II (dose rate = 300 rad/hr.)			
	Ethylene pressure, kg./cm. ²	Temperature, °C.	Time, hr.	Yield, g.	Ethylene pressure, kg./cm. ²	Temperature, °C.	Time, hr.	Yield, g.
1	400	30	0.5	0.140				
2					150	30	4.0	0.026
3 ^b	400	30	0.5	—	150	30	4.0	0.351
4	400	100	1.0	0.155				
5 ^b	400	100	1.0	—	150	30	4.0	0.176

^a Reaction volume = 100 ml.

^b Polymerization in period I continued to period II.

On the other hand, the molecular weight of polymer formed increases with reaction time in both periods I and II. The relation between molecular weight and the amount of polymer formed is shown in Figure 2, where the polymer yield and molecular weight in period II have been corrected by eliminating the effect of the polymer which is formed at a dose rate of 300 rad/hr. (shown in Fig. 1D). In the polymerization at high dose rate, 2.5×10^4 rad/hr., a convex curve is obtained, while in period II subsequent to period I, a straight line is obtained.

The ratio of the amount of polymer formed to molecular weight (M_p/\bar{M}_n) equals the number of moles of polymer chain or the number of radicals. From Figure 2, it can be seen that the number of polymer chains increases in

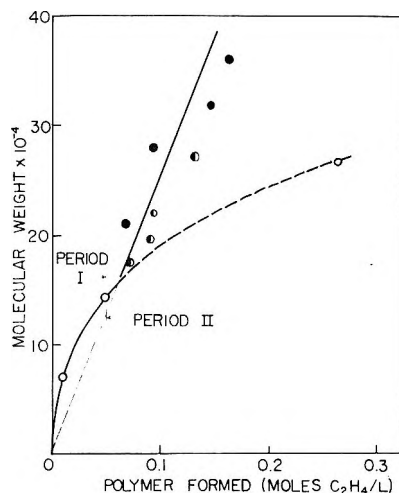


Fig. 2. Molecular weight vs. amount of polymer formed: (O) (period I) dose rate 2.5×10^4 rad/hr., pressure 400 kg./cm.², temperature 30°C.; (●) dose rate 300 rad/hr., pressure 400 kg./cm.², temperature 30°C.; (⊙) dose rate 300 rad/hr., pressure 200 kg./cm.², temperature 30°C.

period I, but remains constant in period II. In other words, both initiation and propagation reactions occur in period I with a high dose rate, while in period II, at a low dose rate, the initiation reaction does not take place but the propagation reaction occurs. Since post-polymerization was not observed, it is presumed that monomer or growing chain excitation is necessary for the propagation reaction.

It is interesting that a considerable amount of polymer is obtained with extremely small doses in period II, and the G value (number of molecules of ethylene polymerized per 100 e.v. absorbed by monomer and polymer) can reach as much as 10^5 – 10^6 .

More detailed data and discussion of these experiments will be reported in a subsequent paper.

Reference

1. Machi, S., M. Hagiwara, M. Gotoda, and T. Kagiya, *J. Polymer Sci.*, **B2**, 765 (1964).

Résumé

Lors de la polymérisation en bloc de l'éthylène à pression élevée, induite par les radiations γ , on montre que le radical polymérique en croissance possède une longue durée de vie à la température de 30°C . Il est possible d'isoler la réaction de propagation des autres réactions élémentaires. Pendant la période de propagation, le poids moléculaire du polymère augmente proportionnellement avec le rendement en polymères lors de l'irradiation à des vitesses de dose extrêmement faibles. À une température de 100°C , la durée de vie du radical polymérique en croissance n'est pas longue mais est normale.

Zusammenfassung

Bei der γ -Strahlungs-induzierten Polymerisation von Äthylen in Substanz unter hohem Druck besitzt das wachsende Polymerradikal bei der niedrigen Temperatur von 30°C eine lange Lebensdauer. Eine Isolierung der Wachstumsreaktion von den anderen Reaktionen ist möglich. In der Wachstumsperiode nimmt das Molekulargewicht des Polymeren bei Bestrahlung mit extrem niedriger Dosisleistung proportional zur Polymerausbeute zu. Bei der erhöhten Temperatur von 100°C ist die Lebensdauer des wachsenden Polymerradikals nicht mehr lang sondern normal.

Received September 21, 1964

Revised January 22, 1965

Prod. No. 4651A

Effect of Thiourea on the Radical Polymerization of Vinyl Monomers. Part I. Polymerization of Acrylonitrile with the Hydrogen Peroxide—Thiourea Catalyst System

TAKA AKI SUGIMURA, NOBORU YASUMOTO, and YUJI MINOURA, *Atomic Energy Research Institute, Osaka City University, Osaka, Japan*

Synopsis

The polymerization of acrylonitrile (AN) was studied in aqueous solution with hydrogen peroxide (H_2O_2) as catalyst and thiourea (TU) as cocatalyst at $30^\circ C$. Since the polymerization was carried out at a relatively low temperature, AN was not polymerized by hydrogen peroxide alone. Upon addition of TU to the reaction system, polymerization occurred immediately, and the rate of polymerization increased with increasing TU concentration. In order to obtain the overall polymerization equation, the dependence of polymerization rate on H_2O_2 and AN concentration was studied kinetically. It was found that the overall polymerization rate R_p was represented by the equation: $R_p = K[TU]^{1/2}[H_2O_2]^{1/2}[AN]$, where K is the rate constant. The acceleration in the presence of TU might be attributed to a redox reaction between H_2O_2 and TU which would produce free radicals rapidly. The effect of substituents was investigated by use of various *N*-substituted derivatives of TU. The polymerization rate increased linearly with the σ^* constants of the substituents as electron-withdrawing substituents were added. The polymerization mechanism is discussed on the basis of the results.

INTRODUCTION

Since polymerization of vinyl monomers by peroxides, both organic and inorganic, is greatly accelerated by the addition of small quantities of reducing agents, this reaction has been investigated for many initiating systems, usually referred to as redox system.

There are various well known initiating systems of this type containing two components, a reducing agent (e.g., metal ion, reducing sugar, tertiary amine, or sulfinic acid) and a peroxide, such as hydrogen peroxide, potassium persulfate, or an organic peroxide. In these cases, the production of free radicals was shown to be due to a one-electron transfer with concomitant cleavage of the —O—O— bond.

In the present study an attempt was made to find new initiating systems.

It was shown in a few patents^{1,2} that the addition of a thiocarbonyl compound to the hydrogen peroxide initiating polymerization of vinyl monomer considerably accelerated the rate of polymerization, but no

details were given. The polymerization of acrylonitrile (AN) by hydrogen peroxide was, therefore, carried out in aqueous media, thiourea (TU) added to this reaction system as cocatalyst, and the effect of thiourea on the polymerization was investigated.

As the polymerization was carried out at relatively low temperature, polymerization did not occur with hydrogen peroxide alone. However, on addition of thiourea, polyacrylonitrile was produced immediately.

No polymerization occurred in the presence of urea and guanidine instead of thiourea as cocatalysts. Kinetic results showed the overall polymerization was proportional to $[TU]^{1/2}$, $[H_2O_2]^{1/2}$, and $[AN]$.

The effect of substituents was studied from the polymerization rate measurements on various *N*-substituted thioureas. The polymerization rate increased as with increasing electron-withdrawing character of the substituents.

EXPERIMENTAL

Reagents

Acrylonitrile was a commercial product and was dried with sodium carbonate and distilled under N_2 atmosphere under reduced pressure. The middle fraction was used (b.p. 77.5–77.8°C.). Hydrogen peroxide (ca. 30% aqueous solution) was diluted with ion-free water to 100 times, and this solution kept diluted at room temperature. The concentration of this solution was determined iodometrically prior to use. Thiourea, diethylthiourea, and ethylenethiourea were commercial products and were recrystallized from aqueous solution twice. The melting points of these purified reagents were 176–178°C., 77°C., and 195–197°C., respectively. Monoacetyl- and diacetylthiourea were prepared according to the method described by Kohman.³ Diacetylthiourea consisted of yellowish crystals, m.p. 151–152°C.

ANAL. Calcd. for $C_5H_8O_2N_2S$: C, 37.5%; H, 5.0%; N, 17.5%. Found: C, 38.3%; H, 5.3%; N, 17.8%.

Monoacetylthiourea was a colorless crystalline material, m.p. 166–168°C.

ANAL. Calcd. for $C_8H_8ON_2S$: C, 30.0%; H, 6.7%; N, 23.3%. Found: C, 30.7%; H, 7.2%; N, 24.0%.

Polymerization Procedure

In order to determine the effectiveness of the various redox systems, acrylonitrile was polymerized by a number of two-component catalyst systems, of which one component was a peroxide and the other was thiourea (TU), guanidine, or mercaptobenzothiazole. These compounds were dissolved in 10 ml. of acrylonitrile and allowed to stand for 12 hr. at room temperature.

All polymerizations, except in the qualitative experiments, were carried out in 100 ml. Erlenmeyer flasks at $30 \pm 0.05^\circ\text{C}$. in a thermostatted bath for the desired length of time.

The rate of polymerization was calculated from the time of polymerization and the per cent conversion to polymer obtained on precipitating the contents of the flask in a large excess of methanol, collecting it on a sintered glass filter, and weighing after drying at 50°C . in a vacuum oven to constant weight.

Molecular Weight Determination

The degree of polymerization \bar{P}_n was obtained from the intrinsic viscosity of the polymers, as measured with an Ubbelohde viscometer in dimethylformamide at 25°C ., by use of the relation:⁴

$$[\eta] = 1.66 \times 10^{-4} \bar{M}_n^{0.81} \quad (1)$$

RESULTS

Polymerization with Various Catalyst Systems

The results of polymerization of acrylonitrile by various systems are summarized in Table I. Hydrogen peroxide–thiourea, organic hydroperoxide–thiourea, and perester–thiourea catalyst systems were all effective accelerating catalyst systems. With dialkyl, diacyl, and diaralkyl peroxides as initiator and thiourea as catalyst, however, polymerization was not observed. With guanidine or urea instead of thiourea, no effective accelerating catalyst systems were found.

TABLE I
Polymerization of Acrylonitrile by Various Combined Catalyst Systems at 30°C .
(Bulk)^{a,b}

Cocatalyst	Peroxide ^c								
	PMHP	DCP	CHP	t-BP	t-BPBz	BPO	t-BHP	H ₂ O ₂	KPS
None	N	N	N	N	N	N	N	N	N
Thiourea and derivatives ^d	VR	N	R	N	R	N	R	VR	VR
Urea	N	N	N	N	N	N	N	N	N
Diphenylguanidine	N	N	—	N	—	—	N	N	N
Mercaptobenzothiazole	—	N	—	N	—	—	—	N	—

^a Conditions: [Peroxides] = 12×10^{-3} mole/l., [Additives] = 4×10^{-3} mole/l., [AN] = 6×10^{-1} mole/l.

^b N = no polymerization observed even after 12 hr., R = polymerization accelerated; VR = polymerization occurred very rapidly.

^c PMHP = *p*-menthane hydroperoxide; DCP = dicumyl peroxide; CHP = cumene hydroperoxide; t-BP = *tert*-butyl peroxide; t-BPBz = *tert*-butyl perbenzoate; BPO = benzoyl peroxide; t-BHP = *tert*-butyl hydroperoxide; KPS = potassium persulfate.

^d Thiourea derivatives used were: *N,N'*-diphenyl-, ethylene-, diacetyl-, monoacetyl-, and diethylthiourea.

Effect of Hydrogen Peroxide-Thiourea System on Polymerization

The polymerization of acrylonitrile by hydrogen peroxide-thiourea system was studied kinetically.

Under the experimental conditions used, no polyacrylonitrile was obtained even after 12 hr. with hydrogen peroxide alone, but when thiourea was added to the reaction systems, polymerization occurred immediately. It was observed that thiourea markedly affected the polymerization of acrylonitrile initiated by hydrogen peroxide. The time-conversion curves at various thiourea concentrations ($4\text{--}12 \times 10^{-3}$ mole/l.) at constant hydrogen peroxide concentration (4×10^{-3} mole/l.) are shown in Figure 1. The relationship between the rate of polymerization (which was calculated from Fig. 1), and thiourea concentration is shown in Figure 2.

The rate of polymerization was proportional to the square root of thiourea concentration. Because polymerization was carried out in the presence of atmospheric oxygen and at relatively low temperature, a short induction period was found. With addition of thiourea to the reaction system, the rate of polymerization increased with increasing thiourea concentration; the induction period also became shorter with increasing thiourea concentration.

The influence of H_2O_2 and monomer concentration on the polymerization was examined in order to establish the overall polymerization rate equation. Similar to the case of polymerization by means of other two-component catalyst systems, e.g., Fenton's reagent,⁵ the rate of polymerization was one-half order with respect to H_2O_2 concentration (Fig. 3), and first-order

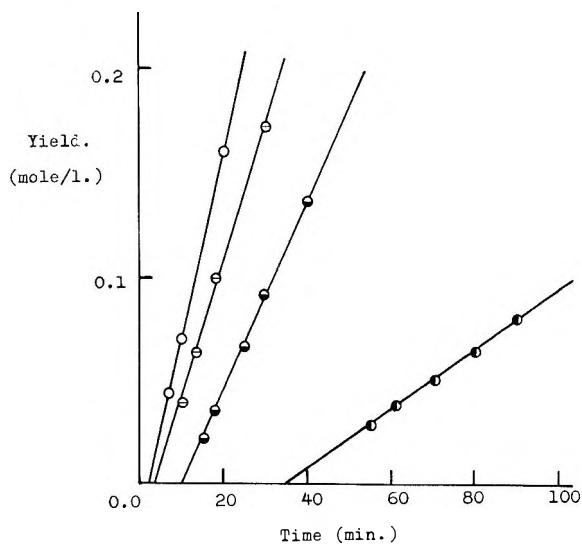


Fig. 1. Weight of monomer polymerized as a function of time at various TU concentrations: (●) 3.96×10^{-3} mole/l.; (●) 5.96×10^{-3} mole/l.; (⊙) 7.93×10^{-3} mole/l.; (○) 11.89×10^{-3} mole/l. $[\text{AN}] = 6.08 \times 10^{-1}$ mole/l.; $[\text{H}_2\text{O}_2] = 3.96 \times 10^{-3}$ mole/l.

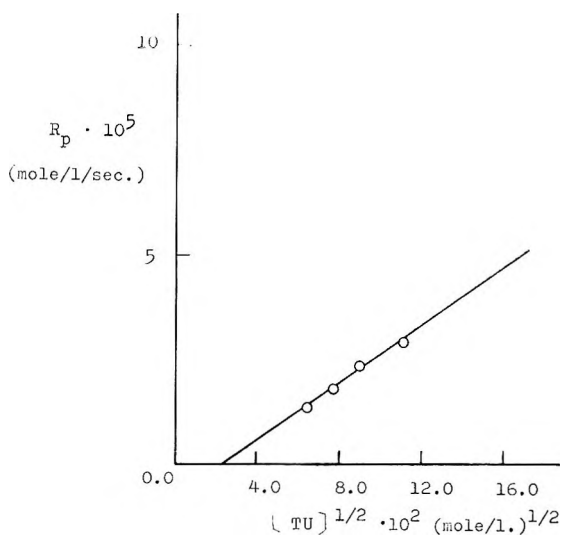


Fig. 2. Rate of polymerization vs. thiourea concentration. $[H_2O_2] = 4.01 \times 10^{-3}$ mole/l.; $[AN] = 6.08 \times 10^{-1}$ mole/l.

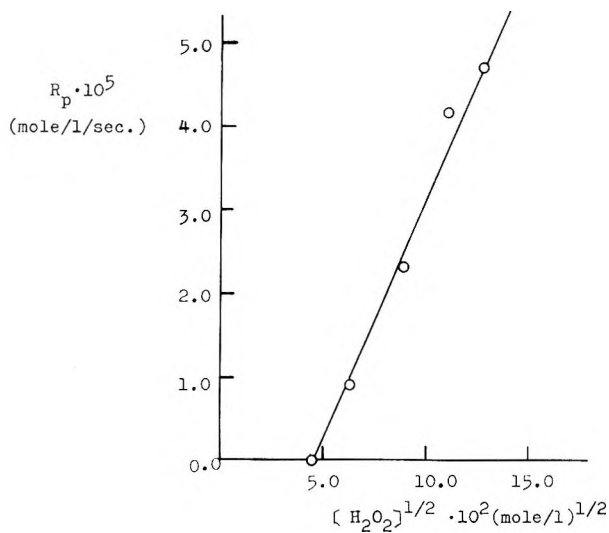


Fig. 3. Rate of polymerization vs. H_2O_2 concentration. $[AN] = 6.1 \times 10^{-1}$ mole/l.; $[TU] = 4.0 \times 10^{-3}$ mole/l.

to monomer concentration (Fig. 4). These results gave for the overall rate of polymerization the equation:

$$R_p = K[AN][H_2O_2]^{1/2}[TU]^{1/2} \quad (2)$$

where K is the rate constant.

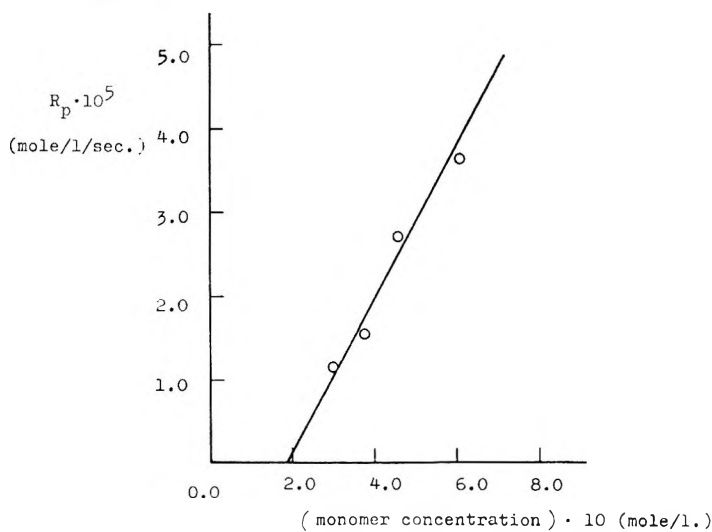


Fig. 4. Rate of polymerization vs. monomer concentration. $[H_2O_2] = 12.2 \times 10^{-3}$ mole/l.; $[TU] = 4.0 \times 10^{-3}$ mole/l.

Effect of Substituents on Thiourea

The effect of substituents was investigated for the polymerization of acrylonitrile initiated by hydrogen peroxide–thiourea catalyst systems by using various derivatives of thiourea. The thiourea derivatives used were:

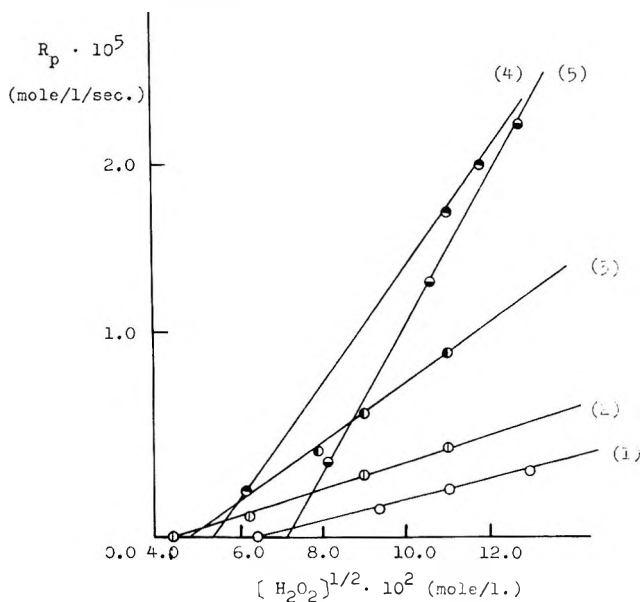


Fig. 5. Effect of substituents on the polymerization rate: (1) diethylthiourea; (2) thiourea; (3) ethylenethiourea; (4) monoacetylthiourea; (5) diacetylthiourea. The concentration of TU and its derivatives was 4.0×10^{-3} mole/l. in all cases.

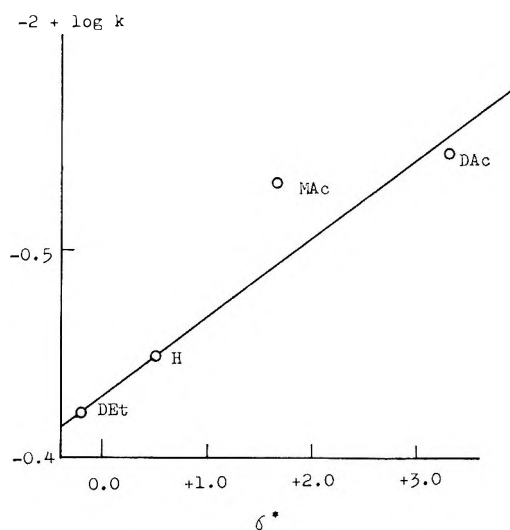


Fig. 6. Relation between Hammett σ^* value and polymerization rate constants: (*DEt*) diethylthiourea; (*H*) thiourea; (*MAc*) monoacetylthiourea; (*DAc*) diacetylthiourea.

N-acetyl-, *N,N'*-diacetyl-, *N,N'*-diethyl-, and ethylene-thiourea. The relation between the rate of polymerization and H_2O_2 concentration at constant thiourea concentration with various thiourea derivatives was found (Fig. 5). There was a linear relationship between the polymerization rate constant K , which was calculated from eq. (2) and Figure 5, and the value of the σ^* constant of the substituents. (Fig. 6). In this case the Hammett-Taft substituent constant σ^* , which should be applied for aliphatic compounds, was used as the summed up value.

Molecular Weight

The reciprocal of degree of polymerization, which was calculated from intrinsic viscosity, was proportional to $[\text{H}_2\text{O}_2]^{1/2}$ and $[\text{TU}]^{1/2}$ (Fig. 7).

DISCUSSION

It was found that the polymerization of acrylonitrile was greatly affected by the addition of TU even at relatively low temperature (30°C), whereas no effect was observed when urea or guanidine was used instead of TU. The rate of polymerization was proportional to $[\text{TU}]^{1/2}$, and the polymerization rate increased as with the electron-withdrawing capacity of substituents at the nitrogens of thiourea, as shown in Figure 6.

These results indicate that the increase of the rate of polymerization may be due to the acceleration of homolytic decomposition of hydrogen peroxide by the addition of thiourea. In this case, the following two initiation mechanisms might be considered: (1) sulfinic acid produced by the reaction between hydrogen peroxide and thiourea initiates acrylonitrile polymeriza-

tion immediately; (2) $\cdot\text{OH}$ radical production is accelerated by the redox reaction between H_2O_2 and thiourea as is the case with Fenton's reagent⁵ or the benzoyl peroxide-dimethylaniline system.⁶⁻⁸ Sulfinic acid has been reported to be an effective radical initiator of vinyl monomers.⁹⁻¹¹ It was reported that aliphatic sulfinic acids are less stable than aromatic sulfinic acids, and the shorter-chain aliphatic acids are less stable than the longer-chain acids. Sulfinic acids are known, in general, for their tendency to decompose.¹²

Formamidine sulfinic acid, however, was isolated after the reaction of H_2O_2 and thiourea at low temperature (0°C .) in aqueous solution.¹³

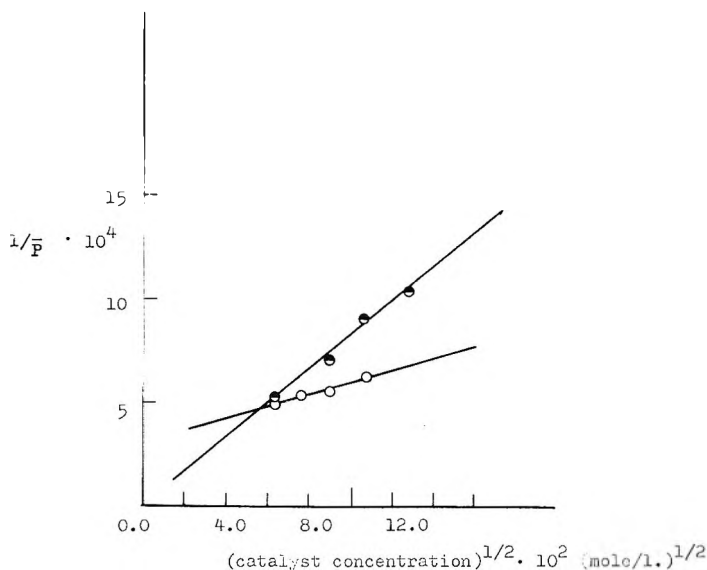


Fig. 7. Dependence of degree of polymerization on TU and H_2O_2 concentration: (●) $1/\bar{P}$ vs. $[\text{H}_2\text{O}_2]$ at constant $[\text{TU}] = 4.01 \times 10^{-3}$ mole/l.; (○) $1/\bar{P}$ vs. $[\text{TU}]$ at constant $[\text{H}_2\text{O}_2] = 3.90 \times 10^{-3}$ mole/l.

Therefore, it must be considered in our case as well that sulfinic acid is formed, and that the acid initiates the polymerization of acrylonitrile. However, the experimental conditions of the present study were very different from those of Barnett,¹³ that is, reaction temperature was relatively high and the reaction medium was very dilute with respect to H_2O_2 and thiourea concentration.

If sulfinic acid was produced, therefore, it should be decomposed to the sulfonic acid and disulfoxide,^{14,15} and it seems likely that these compounds have no activity as initiators for polymerization of acrylonitrile. In fact, formamidine sulfinic acid which was prepared according to Barnett's method was found to have a weak initiating ability for polymerization of acrylonitrile under the same experimental conditions. However there still remains some doubt about this point.

Here $I\cdot$, $S\cdot$, $P\cdot$ represent H_2O_2 , thiourea, and polymer radical, respectively. From the steady-state assumption, the overall polymerization rate R_p is as given in eq. (11)

$$R_p = k_p(2k_d/k_t)^{1/2}[TU]^{1/2}[H_2O_2]^{1/2}[AN] \quad (11)$$

and the degree of polymerization \overline{P}_n is

$$1/\overline{P}_n = R_t/R_p = (2k_t k_i/k_p)^{1/2}[TU]^{1/2}[H_2O_2]^{1/2}[AN] \quad (12)$$

Equations (11) and (12) are in good agreement with the experimental results. The initiation reaction should be studied in more detail, but it seems likely that above polymerization scheme is appropriate.

References

1. Brit. Pat. 715,382 (1951).
2. Japan. Pat. 3840 (1953).
3. Kohman, E. F., *J. Am. Chem. Soc.*, **37**, 2130 (1951).
4. Besshoges, J., *J. Polymer Sci.*, **17**, 81 (1955).
5. Boxendale, J. H., M. G. Evans, et al., *Trans. Faraday Soc.*, **42**, 668 (1946).
6. Horner, L., and K. Scherf, *Ann.*, **573**, 35 (1951); *ibid.*, **574**, 202 (1951); *J. Polymer Sci.*, **18**, 438 (1955).
7. Imoto, M., et al., *J. Polymer Sci.*, **22**, 137 (1956).
8. Tobolsky, A. V., and K. F. O'Driscoll, *J. Colloid Sci.*, **11**, 244 (1956).
9. Hagger, O., *Helv. Chim. Acta.*, **31**, 822 (1948).
10. Ynfiensta, J. L., *Collection Czech. Chem. Commun.*, **13**, 592 (1948).
11. Overberger, C. G., and J. J. Godfrey, *J. Polymer Sci.*, **40**, 179 (1959).
12. Marvel, C. S., and R. S. Johnson, *J. Org. Chem.*, **13**, 822 (1948).
13. Barnett, E. B., *J. Chem. Soc.*, **97**, 63 (1910).
14. Kice, J. L., and K. W. Bowers, *J. Am. Chem. Soc.*, **84**, 605 (1962).
15. Otto, R., *Ann.*, **145**, 13, 317 (1868); *Ber.*, **10**, 2182 (1877).
16. Schroder, D. C., *Chem. Revs.*, **55**, 181 (1955).

Résumé

On a étudié la polymérisation de l'acrylonitrile (AN) à 30°C en solution aqueuse avec du peroxyde d'hydrogène (H_2O_2) comme catalyseur et de la thiourée (TU) comme co-catalyseur. Comme la polymérisation a été effectuée à une température relativement basse, l'acrylonitrile ne polymérise pas avec le peroxyde d'hydrogène seul. Lorsqu'on ajoute de la thiourée au système réactionnel, la polymérisation a lieu immédiatement et la vitesse de polymérisation augmente avec la concentration en thiourée. En vue d'obtenir l'équation globale de la polymérisation, on a étudié cinétiquement la dépendance de la vitesse de polymérisation vis-à-vis de la concentration en H_2O_2 et AN respectivement. On a trouvé que la vitesse globale de polymérisation (R_p) peut être représentée par l'équation suivante: $R_p = K[TU]^{1/2}[H_2O_2]^{1/2}[AN]$, où K est la constante de vitesse. L'effet d'accélération peut être attribué à la réaction "Redox" entre H_2O_2 et TU produisant rapidement des radicaux libres. On a étudié l'influence des substituants en employant des dérivés substitués à l'azote de la thiourée. La vitesse de polymérisation augmente linéairement avec les constantes des substituants, lorsqu'on ajoute des substituants électrocapteurs à la position-N de la thiourée. Sur la base de ces résultats, on discute du mécanisme de la polymérisation.

Zusammenfassung

Die Polymerisation von Acrylnitril (AN) wurde in wässriger Lösung mit Wasserstoffperoxyd (H_2O_2) als Katalysator und Thioharnstoff (TU) als Kokatalysator bei 30°C untersucht. Da die Polymerisation bei verhältnismässig niedriger Temperatur ausgeführt wurde, bewirkte Wasserstoffperoxyd allein keine Polymerisation von AN. Bei Zusatz von TU zum Reaktionssystem trat unmittelbar Polymerisation ein und die Polymerisationsgeschwindigkeit nahm mit steigender TU-Konzentration zu. Um eine Beziehung für die Bruttopolymerisationsgeschwindigkeit zu erhalten, wurde die Abhängigkeit der Polymerisationsgeschwindigkeit von der H_2O_2 - und AN-Konzentration untersucht. Für die Bruttopolymerisationsgeschwindigkeit R_p gilt folgende Gleichung $R_p = K[\text{TU}]^{1/2}[\text{H}_2\text{O}_2]^{1/2}[\text{AN}]$ wo K die Geschwindigkeitskonstante ist. Der Beschleunigungseffekt kann wahrscheinlich der zur raschen Erzeugung freier Radikale führenden "Redox"-Reaktion zwischen H_2O_2 und TU zugeschrieben werden. An N -Derivaten von TU wurde der Substituenteneinfluss untersucht. Mit elektronenentziehenden Substituenten an der N -Stellung von TU trat in linearer Abhängigkeit von den Substituentenkonstanten eine Erhöhung der Polymerisationsgeschwindigkeit auf. Auf der Grundlage der Ergebnisse wurde der Polymerisationsmechanismus diskutiert.

Received September 21, 1964

Revised February 9, 1965

Prod. No. 4650A

Flow Behavior of Polydimethylsiloxane

TADAO KATAOKA and SHIGEYUKI UEDA, *Textile Research Institute of the Japanese Government, Kanagawaku, Yokohama, Japan*

Synopsis

Viscosities of polydimethylsiloxane were measured over a wide range of shear rates and molecular weights to clarify the flow behavior of bulk polymers. It was observed that each flow curve for high molecular weight samples had an inflection point, and at high shear rates all curves tended to converge. The relationship between viscosities and molecular weights at various shear rates showed the following features: no sharp inflection in the zero shear relation and non-Newtonian properties below M_c . It is suggested that viscosities of high molecular weight samples become almost the same, irrespective of molecular weight, at very high shear rates.

INTRODUCTION

The flow behavior of bulk polymers and polymer solutions has been studied theoretically¹ and experimentally² by many investigators, and useful results have been accumulated.³

Polydimethylsiloxane has a glass temperature well below room temperature and is convenient, experimentally, for bulk polymer flow studies. Nevertheless, only a few data have been published over wide ranges of flow parameters.⁴⁻⁸ For example, Bagley discussed the viscosity-molecular weight relation at various shear rates⁶ and the power law relation between shear stress and shear rate,⁷ but his investigation covered only narrow ranges of shear rates and molecular weights.^{9,10}

This study was carried out to clarify flow behavior of polydimethylsiloxane over wide ranges of shear rates and molecular weights.

EXPERIMENTAL

Twelve samples of polydimethylsiloxane having the viscosity-average molecular weights shown in Table I were used. The molecular weights were calculated from intrinsic viscosities of toluene solutions at 25°C. by eq. (1):¹¹

$$[\eta] = 2.15 \times 10^{-4} \bar{M}_v^{0.65} \quad (1)$$

The bulk viscosity was measured in the lower shear rate region by a cone-plate viscometer and in the high shear rate region by two capillary viscometers. For samples A, B, G, and I capillary viscometers were not used. Measurements can be carried out at constant shear stress with the conc-

TABLE I
Samples Used

Sample designation	Nominal viscosity, cstokes	Molecular weight $\bar{M}_v \times 10^{-3}$	Maximum Reynolds number
A	30	2.7	—
B	100	4.7	—
C	300	10.3	0.2
D	1,000	22.0	40
E	3,000	33.4	29
F	10,000	57.0	27
G	30,000	80.5	—
H	100,000	105	22
I	300,000	140	—
J	500,000	179	21
K	1,000,000	206	20
L	—	482	3.7

plate viscometer by the aid of weights hung to a pulley. In capillary viscometers, samples are extruded either by nitrogen pressure (N_2 pressure-extrusion type) or by weights (Melt Indexer). In the N_2 pressure extrusion, any pressure below 150 kg./cm.² can be applied. In the Melt Indexer, various weights up to 21.5 kg. can be used. Friction between the piston and the cylinder was found to be negligible according to the procedure suggested by Marker et al.¹² Dimensions of the cones and dies are listed in Table II. A large-angle cone was used for high viscosity samples

TABLE II
Cones and Dies Used

Cones			Dies			
No.	r , cm.	Angle	No.	R , mm.	L , mm.	L/R
1	3.0	0.5°	1	1.05	12.6	12
2	3.0	2.0°	2	1.05	18.9	18
			3	0.50	2.0	4
			4	0.25	1.0	4
			5	0.25	2.0	8
			6	0.25	3.0	12
			7	0.25	4.5	18

and a small-angle cone for low viscosity samples. Large radius dies were used at relatively low shear rates and small radius dies at high shear rates.

For the cone-plate viscometer data, the shear stress τ and the shear rate $\dot{\gamma}$ were calculated from the torque M applied and the angular velocity of rotation of the plate Ω by using eqs. (2) and (3):

$$\tau = 3M/2\pi r^3 \quad (2)$$

$$\dot{\gamma} = \Omega/\theta \quad (3)$$

where r is the radius of the cone and θ is the angle between the cone and the plate.

In the capillary method, τ and $\dot{\gamma}$ were calculated by eqs. (4) and (5)

$$\tau = Rp_c/2L \quad (4)$$

$$p_c = p_t - m\rho v^2$$

$$\dot{\gamma} = 4Q/\pi R^3 \quad (5)$$

where R and L are the radius and length of the die, respectively, Q is the volume rate of the extrudate emerging from the die, and p_c the pressure held in equilibrium inside the die, p_t the total applied pressure, $m\rho v^2$ the kinetic energy correction term, m is a constant, ρ is the density of the liquid and v is the linear velocity of the extrudate at the exit of the capillary. To evaluate the kinetic energy term, a value of m of 1.12 was taken,¹³ and the density was presumed invariable during the extrusion process. In the low molecular weight samples, there were some cases where this term was large, and the measurement was restricted to the shear rate range in which these terms were below 20% of applied pressure.

In case of the viscoelastic liquid the shear stress was corrected for elastic energy by the use of the total end correction e :^{14,15}

$$\tau_c = p_c/2 [L/R + e] \quad (6)$$

e contains the Couette correction term which is necessary for pure liquids. The experimental evaluation of e has been reported by Bagley¹⁴ and Arai.¹⁵ Further, the shear rate must be corrected for non-Newtonian flow in the following way:¹⁶

$$\dot{\gamma}_c = \dot{\gamma} [3/4 + 1/4 (d \log \dot{\gamma}/d \log \tau_c)] \quad (7)$$

Viscosity measurements were first carried out at a temperature fixed near 7°C., and all the data were reduced to the value at 7°C. by the use of shift factors.

At a high shear rate, heat is generated, and this may cause viscosity reduction. The maximum temperature increase ΔT during the extrusion process was measured roughly by placing a thermometer in the stream of the extrudate emerging from the die. For sample J with die 4, ΔT was 4–5°C. at the pressure of 100 kg./cm.², which corresponds to a shear stress of about 1×10^7 dynes/cm.² (not corrected for end effect), while it was less than 1°C. at the shear stress of about 7×10^6 dynes/cm.² Therefore the data obtained at higher shear stress should be corrected for ΔT . However, in this study this heat effect was neglected, since accurate measurements had not been carried out over the whole shear stress range.

RESULTS AND DISCUSSION

Sample J was taken to show the typical results in Figure 1. Here, all data are represented; these include original data obtained with dies with L/R various ratios as well as the data obtained with the cone-plate vis-

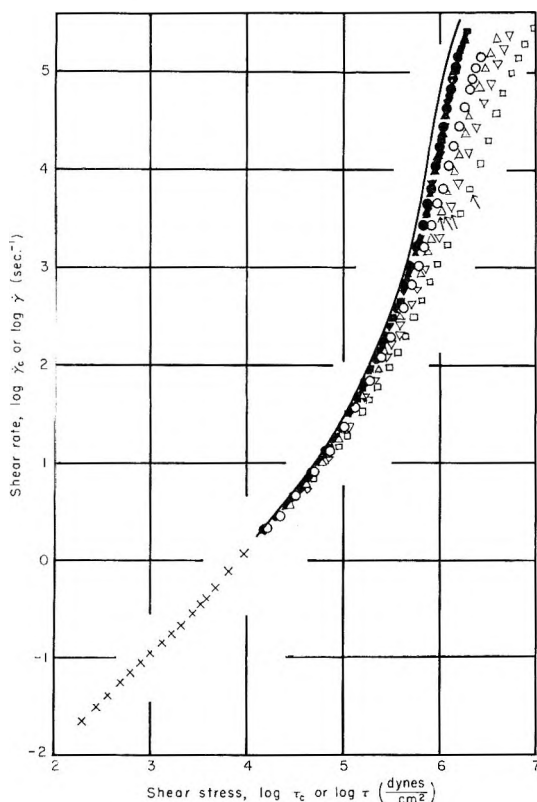


Fig. 1. Relation between shear stress and shear rate for sample J: (\times) cone-plate data; (O , \bullet) capillary, $L/R = 18$; (Δ , \blacktriangle) capillary, $L/R = 12$; (∇ , \blacktriangledown) capillary, $L/R = 8$; (\square , \blacksquare) capillary, $L/R = 4$. Open symbols indicate experimental values; filled symbols denote corrected values.

cometer, a master curve corrected for the total end effect by eq. (6), and a true flow curve corrected for non-Newtonian flow by eq. (7). The last curve is well superimposed on the cone-plate viscometer data. The arrows in Figure 1 represent points above which melt fracture seems to occur. The fracture starts at almost the same shear rate irrespective of die dimensions. Maximum Reynolds numbers of all runs are listed in Table I. The data imply that all flows are laminar in the classical sense even though irregular flow does occur. When the disturbance occurs only at the inlet and does not affect flow in the capillary, eqs. (5) and (6) can be applied.

As described in the experimental section, two dies with different radii and the same L/R ratio were used to draw a single curve. For example, plots for $L/R = 4.0$ were obtained by the die 3 in the shear rate region 2–270 sec.^{-1} and with die 4 in the $102\text{--}3 \times 10^5 \text{ sec.}^{-1}$ region. The fact that plots by different dies were well superimposed in the overlapping shear rate range suggests that no slippage occurs, at least in the shear rate range of about 100–300 sec.^{-1} . It is not certain whether slippage occurs in the other shear

rate ranges or not, but in this study the absence of slippage is assumed in the entire shear rate range studied.

When extrudate which had been extruded at the highest shear rate was again extruded at a lower shear rate, the observed value fell on the initial curve. Therefore, the absence of shear degradation was proved in the shear rate range examined. This was ascertained for all samples.

It can be seen in Figure 1 that the flow curve covers the shear rate range of 10^{-2} – 3×10^5 sec.⁻¹. The slope at the lower shear rate region is unity, thus showing Newtonian flow. The slope increases to a maximum with

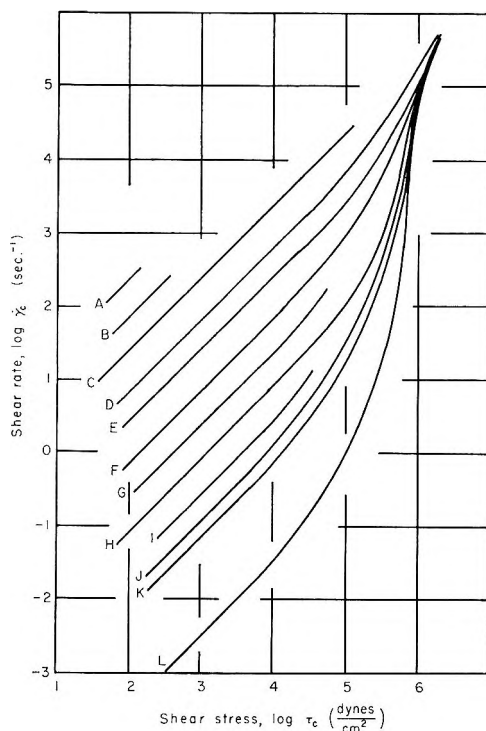


Fig. 2. Flow curves for all samples.

increasing shear rate and then decreases. The existence of an inflection point in the flow curve for bulk polymer has not been reported very often.¹⁷

Figure 2 shows flow curves of all samples. As described in the experimental section, samples A, B, G, and I were not measured by the capillary viscometer, and the flow curves were obtained only for the relatively low shear rates. All samples with molecular weights above 22,000 showed non-Newtonian behavior. All flow curves, except for sample D, had an inflection point. Although none of the samples showed the second Newtonian region, the slopes of the curves tended to approach unity at high shear rates. Very interesting behavior is observed in the high shear rate region, in that flow curves of all samples tend to converge.

As described in the experimental section, $\Delta T = 4\text{--}5^\circ\text{C.}$ was observed at high shear rates. The temperature dependency of viscosity of polydimethylsiloxane is very small: at 7°C. an increase of 5°C. causes a 15% decrease in viscosity. Such a small variation of viscosity does not alter seriously the relative relation obtained in Figure 2, but the fact that the curve for sample L, the highest molecular weight sample, intersects curves for samples J and K seems strange and must be examined further.

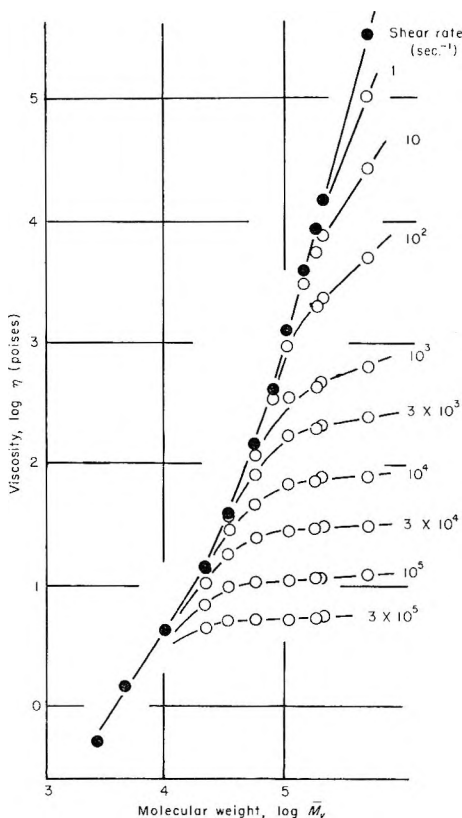


Fig. 3. Viscosity-molecular weight relation at (O) various shear rates and (●) zero shear viscosity.

Figure 3 shows the relations between viscosities at various shear rates and molecular weights. In the zero shear relation no sharp inflection was observed. Even in case of the molecular weight below M_c , non-Newtonian properties were observed. Viscosities of high molecular weight samples decreased enormously with the increase of the shear rate and attained almost the same value, irrespective of molecular weights, at very high shear rates.

Generally, the zero shear viscosity-molecular weight relation is represented by two lines, except at the lowest molecular weights, and a sharp inflection at the intersection of these two lines corresponds to M_c . The

results shown in Figure 3, differ from the general case, although there are some doubts about the use of viscosity-average molecular weights and a few plots in the low molecular weight region. Recently Teramoto et al.¹⁸ reported that no sharp inflection was observed in this relation; also, Bagley⁶ reports no sharp inflection in his study of polydimethylsiloxane. At any rate, more precise experiments are necessary. The M_c value of about 36,000 obtained from Figure 3 (although not as a sharp inflection) is in good agreement with the data previously reported.^{6,8}

It is generally said that non-Newtonian phenomena are observed for molecular weights above M_c , which is about twice the molecular weight between entanglement points. However, Figure 3 shows non-Newtonian behavior even below M_c . Recently, there was some controversy¹⁹ over the question of whether non-Newtonian phenomena would be observed in low molecular weight samples. This problem must be examined further in conjunction with the effect of chain entanglements.

The fact that the viscosities level off at almost the same value regardless of the molecular weights is very important to the discussion of flow mechanism of bulk polymers at high shear rates. Almost complete orientation of long chains may cause this behavior. Some information on the elastic properties of the melt in capillary flow can be obtained from the total end correction e ,¹³ but it is difficult to explain the above-mentioned behavior without making other direct measurements of the flow orientation and elasticity at high shear rates.

References

1. Bueche, F., *J. Chem. Phys.*, **20**, 1959 (1952); *ibid.*, **21**, 1950 (1953).
2. Fox, T. G., and P. J. Flory, *J. Am. Chem. Soc.*, **70**, 2384 (1948); R. S. Spencer and R. E. Dillon, *J. Colloid Sci.*, **3**, 163 (1948); *ibid.*, **4**, 241 (1949).
3. Fox, T. G., S. Gratch, and S. Loshaek, in *Rheology*, F. Eirich, ed., Vol. 1, Academic Press, New York, 1956, p. 431.
4. Currie, C. C., and B. F. Smith, *Ind. Eng. Chem.*, **42**, 2457 (1950).
5. Barry, A. J., *J. Appl. Phys.*, **17**, 1020 (1946).
6. Bagley, E. B., and D. C. West, *J. Appl. Phys.*, **29**, 1511 (1958).
7. Bagley, E. B., *J. Appl. Phys.*, **30**, 597 (1959).
8. Arai, T., and K. Sekido, *Repts. Progr. Polymer Phys. Japan*, **7**, 159 (1964).
9. Schreiber, H., E. B. Bagley, and D. C. West, *Polymer*, **4**, 355 (1963).
10. Schreiber, H. P., *Polymer*, **4**, 365 (1963).
11. Kolorelov, A., K. A. Andrianov, L. S. Uchecheva, and T. E. Vuegenskaya, *Dokl. Akad. Nauk SSSR*, **89**, 65 (1959).
12. Marker, L., R. Early, and S. L. Aggarwal, *J. Polymer Sci.*, **38**, 381 (1959).
13. Philippoff, W., and F. H. Gaskins, *Trans. Soc. Rheol.*, **2**, 263 (1958).
14. Bagley, E. B., *J. Appl. Phys.*, **28**, 624 (1957).
15. Arai, T., *J. Soc. Rubber Ind. Japan*, **30**, 993 (1957).
16. Krieger, I. M., and S. H. Maron, *J. Appl. Phys.*, **23**, 147 (1952).
17. Ballmann, R. L., *Nature*, **202**, 288 (1964).
18. Teramoto, A., H. Tanaka, and H. Fujita, paper presented at 12th Symposium on High Polymer in Japan, Nagoya, Japan, November 1963.
19. Bagley, E. B., A. Rudin, and H. P. Schreiber, *Nature*, **203**, 175 (1964); J. F. Hutton, *Nature*, **203**, 177 (1964).

Résumé

On a mesuré les viscosités du polydiméthylsiloxane dans un large domaine de vitesses de cisaillement et de poids moléculaires en vue d'éclaircir le comportement à l'écoulement de polymères en bloc. On a observé que chaque courbe d'écoulement pour les échantillons de poids moléculaires élevés possède un point d'inflexion et qu'à des vitesses de cisaillement élevées toutes les courbes tendent à converger. La relation entre les viscosités et les poids moléculaires à différentes vitesses de cisaillement présente les caractéristiques suivantes: pas de discontinuité brusque pour une vitesse de cisaillement nulle, propriétés non-Newtoniennes au-dessous de M_c et la suggestion que les viscosités des échantillons de poids moléculaires élevés deviennent presque les mêmes quels que soient les poids moléculaires pour des vitesses de cisaillement très élevées.

Zusammenfassung

Zur Aufklärung des Fließverhaltens von Polymeren in Substanz wurde die Viskosität von Polydimethylsiloxan in einem grossen Schubgeschwindigkeits- und Molekulargewichtsbereich gemessen. Es zeigte sich, dass bei hochmolekularen Proben jede Fließkurve einen Wendepunkt besitzt und dass bei hoher Schubgeschwindigkeit alle Kurven eine Neigung zur Konvergenz zeigen. Die Beziehung zwischen Viskosität und Molekulargewicht zeigt bei variiertem Schubgeschwindigkeit folgendes Bild: Kein scharfer Knick bei der Beziehung für Schub Null, nicht Newton-Verhalten unterhalb M_c sowie der Hinweis, dass die Viskosität hochmolekularer Proben unabhängig vom Molekulargewicht bei sehr hoher Schubgeschwindigkeit fast identisch ist.

Received September 3, 1964

Revised November 20, 1964

Prod. No. 4652A

Epoxide-Alcohol Reaction Catalyzed by Boron Trifluoride. Part I. Phenyl Glycidyl Ether-Alcohol Reaction in Dioxane*

LIENG-HUANG LEE, JOHN W. PANKEY, and J. P. HEESCHEN,
*Polymer and Chemicals Research Laboratory, Analytical Laboratories, and
Chemical Physics Research Laboratory, The Dow Chemical Company,
Midland, Michigan*

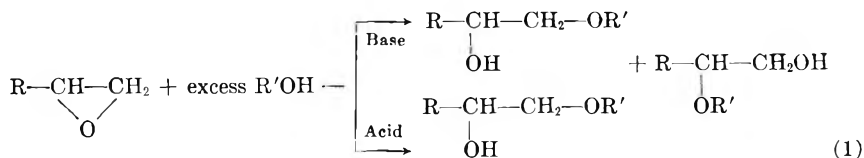
Synopsis

Phenyl glycidyl ether, a model compound for bisphenol-A type epoxy resins, was reacted with alcohols in dioxane in the presence of boron trifluoride etherate. For isobutyl, *sec*-butyl, and *n*-butyl alcohols the reaction paths were similar and found to be: (1) epoxide-alcohol 1:1 addition, (2) epoxide-alcohol-dioxane addition, and (3) homopolymerization of the epoxide. With excess alcohol, homopolymerization could be minimized. In all cases, the predominant 1:1 adduct was shown to be 1-butoxy-3-phenoxy-2-propanol. There was indication that a small amount of the 1:1 adduct containing primary hydroxyl group was formed also. With *tert*-butyl alcohol, 3-phenoxy-1,2-propanediol was obtained as well. With phenol, the main reaction was homopolymerization of phenyl glycidyl ether.

INTRODUCTION

Phenyl glycidyl ether, 1,2-epoxy-3-phenoxy propane, has been used as a model compound for studying the curing mechanism of epoxy resins from bisphenol A, 2,2-bis[*p*-(2,3-epoxypropoxy)phenyl]-propane. The purpose of the present study was to determine the effect of the type of alcohol on the products obtained when phenyl glycidyl ether reacts with alcohol in the presence of boron trifluoride etherate.

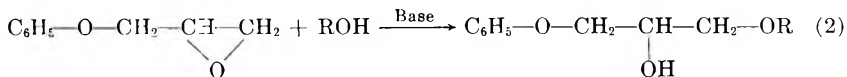
Petrov¹ summarizes the reaction between aliphatic epoxides and alcohols as:



Chitwood and Freure² obtained a similar result from the reaction between propylene oxide and alcohols catalyzed by boron trifluoride etherate.

* Paper presented at the 143rd Meeting, American Chemical Society, New York, September 1962.

Shechter and Wynstra^{3,4} studied the reactions between phenyl glycidyl ether and alcohols in the presence of basic catalysts. The products were not identified, but it was assumed that opening of the epoxide ring would give primary ether with secondary hydroxyl:



They found also that the SnCl_4 -catalyzed reaction between phenyl glycidyl ether and isopropyl alcohol was rather specific, but did not identify the product.

For the present study dioxane was chosen as the solvent with the assumption that it would not enter into the reaction. Interestingly, we found that a small amount of the dioxane reacted and became incorporated into the addition products. This participation by a solvent such as dioxane should give some insight into the contradictory mechanisms regarding this type of reaction. Further discussion regarding mechanism will be published at a future date.

EXPERIMENTAL

Reagent grade phenyl glycidyl ether was redistilled (b.p. 124°C./15 mm.). Reagent grade boron trifluoride etherate (48% BF_3 , Baker) was used without further treatment. Isobutyl alcohol (b.p. 107–107.5°C.), *sec*-butyl alcohol (b.p. 99°C.), *n*-butyl alcohol (b.p. 117°C.), and *tert*-butyl alcohol (b.p. 81°C.) were distilled over calcium oxide. Phenol (Dow, b.p. 121°C./100 mm.) and dioxane (b.p. 101°C.) were distilled in the same manner. The water content of each reagent was determined by Karl Fischer titration. The results were: dioxane, 0.03%; isobutyl alcohol, 0.04%; *sec*-butyl alcohol, 0.05%; *tert*-butyl alcohol, 0.04%; *n*-butyl alcohol, 0.04%; phenyl glycidyl ether, 0.02%; and phenol, 0.04% water.

In a typical preparative experiment, 250 ml. of alcohol (10*M* in dioxane) and 250 ml. of phenyl glycidyl ether (2*M* in dioxane) were mixed in a flask. To this mixture was added a 25-ml. portion of boron trifluoride etherate (0.4*M* in dioxane). The mixture (alcohol:epoxide: BF_3 = 4.762:0.9524:0.0191) was allowed to remain at room temperature for 3 days and then fractionally distilled.

Analyses of the distillation fractions are given in Table I. The per cent recovery is based on initial weight of epoxide plus equimolar amount of alcohol. The empirical formulas of the apparently pure fractions are based on mass spectrum results and elemental analyses for C and H. The residue fractions were assigned as homopolymers of phenyl glycidyl ether, based on molecular weight determination.

All butanol adducts were oxidized with a chromic acid mixture, giving 20–50% yields. The major products were found by infrared spectroscopy to be ketones with high carbonyl frequency (1747 cm^{-1}) as a result of the inductive effect of the alkoxy and phenoxy groups. Infrared spectra

TABLE I
Results of Product Analysis (Alcohol:Epoxide:BF₃ = 4.762:0.9524:0.0191M)

Alcohol	Recov- ery, %	Frac- tion	Wt. %	Boiling point, °C. (3 mm.)	[η] ²⁵ _B	d_4^{25}	Mol. wt.		C, %		H, %		Empirical formula (and molecular weight)
							B.p. Elev. spec.	Mass spec.	Calcd.	Found	Calcd.	Found	
Isobutyl alcohol	93.2	I	76.2	138-143	1.4950	1.0202	224	224	69.64	69.36	8.92	9.02	C ₁₃ H ₂₆ O ₃ (224)
		II	7.8	147-202	1.4960	1.0224	—	—	—	—	—	—	—
		III	6.0	202	1.4915	1.0508	307	312	65.38	65.23	8.94	8.68	C ₁₇ H ₂₈ O ₃ (312)
		IV	10.0	Residue	—	1.0939	805	—	—	—	—	—	—
<i>sec</i> -Butyl alcohol	90.1	I	73.2	138-139	1.4970	1.0251	224	224	69.64	69.80	8.92	9.15	C ₁₃ H ₂₆ O ₃ (224)
		II	4.5	140-190	1.5180	1.0435	228	—	—	—	—	—	—
		III	10.9	200-201	1.4955	1.0574	317	312	65.38	65.38	8.94	7.46	C ₁₇ H ₂₈ O ₃ (312)
		IV	11.4	Residue	—	1.1133	661	—	—	—	—	—	—
<i>n</i> -Butyl alcohol	91.1	I	83.6	146-147	1.4990	1.0280	228	224	69.64	69.69	8.92	9.32	C ₁₃ H ₂₆ O ₃ (224)
		II	2.3	167-205	1.5150	—	230	—	—	—	—	—	—
		III	5.7	205-206	1.4955	1.0581	298	312	65.38	65.25	8.94	8.90	C ₁₇ H ₂₈ O ₃ (312)
		IV	8.4	Residue	—	1.1060	537	—	—	—	—	—	—
<i>tert</i> -Butyl alcohol	82.3	I	53.8	132-138	1.4950	1.0184	221	224	69.64	70.64	8.92	9.53	C ₁₃ H ₂₆ O ₃ (224)
		II	5.6	148-155	—	—	197	—	—	—	—	—	—
		III	15.4	156-158 ^a	—	—	169	168	64.22	64.80	7.14	7.05	C ₉ H ₁₈ O ₃ (168)
		IV	3.6	173-196	—	—	217	—	—	—	—	—	—
Phenol	78.5	V	9.9	200-207	1.5096	1.0946	316	311	—	64.75	—	6.90	—
		VI	11.7	Residue	—	—	400	—	—	—	—	—	—
		I	14.7	187-199	1.5820	—	252	244	—	75.08	—	6.01	—
		II	12.2	200-220	—	—	312	—	—	—	—	—	—
	III	8.7	221-246	—	—	332	332	68.67	67.47	7.23	7.19	C ₁₉ H ₂₂ O ₃ (332)	
	IV	64.4	Residue	1.5480	—	740	—	—	—	—	—	—	

^a M.p. 56-59°C.

showed no carboxyl OH, and NMR spectra of the *tert*-butyl and *n*-butyl adducts showed no aldehyde proton. This evidence indicates the major adducts contain secondary hydroxyl and little or no primary hydroxyl.

Proton nuclear magnetic resonance (NMR) spectra were run at 20% (w/v) concentration in CCl_4 and in pyridine. All butanol adducts, except the epoxide-*tert*-butyl alcohol-dioxane adduct, were observed also as 10% solutions in acetone at -65 to -72°C . Chemical shifts are reported as parts per million shielding relative to tetramethylsilane (TMS) as internal standard at 0 ppm. All spectra were obtained at 60M cycles/sec. with a Varian Associates Model A-60 analytical NMR spectrometer equipped with V-5037 variable temperature system.

RESULTS

Adducts with Normal-, Secondary-, and Isobutanol

Phenyl Glycidyl Ether-Butanol Adducts. Elemental, mass spectra, and NMR analyses of fractions I showed them to be relatively pure single isomers of the one-to-one adducts of phenyl glycidyl ether and butanol, 1-butoxy-3-phenoxy-2-propanol, $\text{C}_6\text{H}_5\text{OCH}_2\text{CH}(\text{OH})\text{CH}_2\text{OC}_6\text{H}_5$. No further purification was performed.

NMR spectra of the isobutyl alcohol adduct in CCl_4 and in pyridine are shown in Figure 1, with assignments. Absorption due to protons *b* and *c* is very complex and tends to collapse because the chemical shifts among these protons are of the order of or less than the couplings among themselves, and there is significant coupling among protons *c* and *d*. Note the strong deshielding of the glyceryl methyne proton relative to others upon

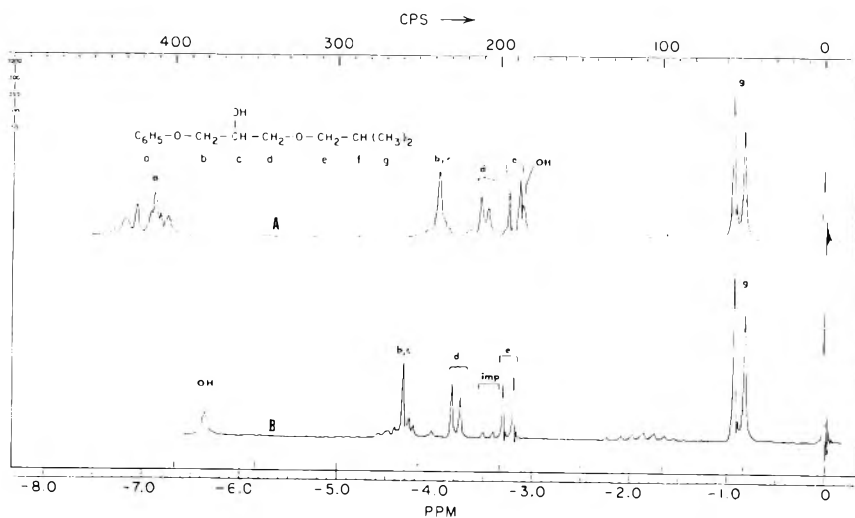


Fig. 1. 60 Mcycle proton NMR spectrum of phenyl glycidyl ether-isobutyl alcohol adduct: (A) 20% w/v in CCl_4 ; (B) 20% w/v in pyridine. Internal reference TMS at 0 ppm.

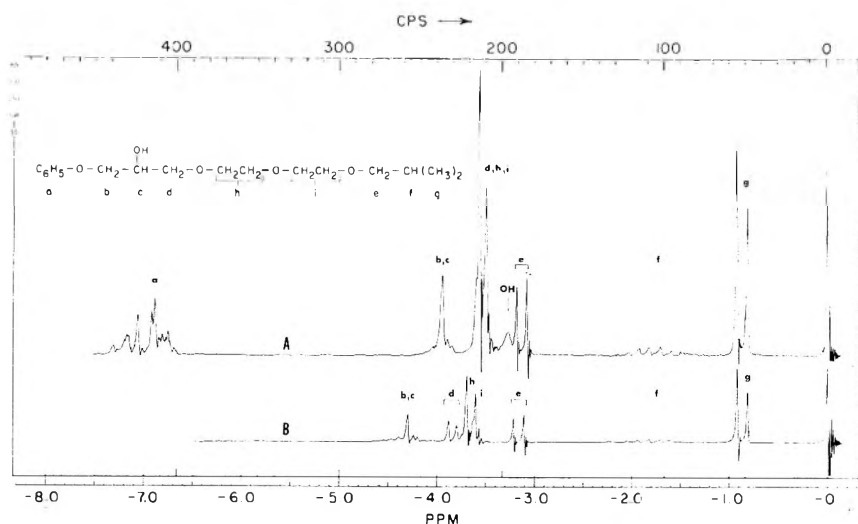


Fig. 2. 60 Mcycle proton NMR spectrum of phenyl glycidyl ether-dioxane-isobutyl alcohol adduct: (A) 20% w/v in CCl_4 ; (B) 20% w/v in pyridine. Internal reference TMS at 0 ppm.

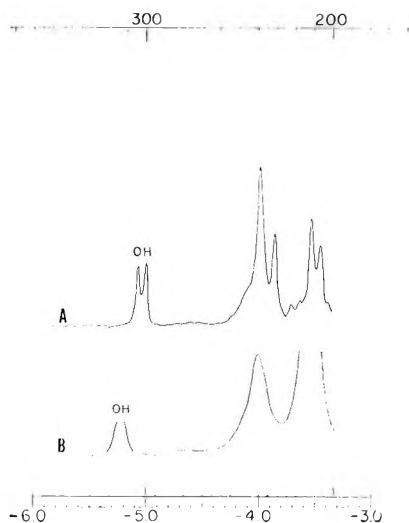


Fig. 3. Hydroxyl proton NMR spectra at 60 Mcycle of: (A) phenyl glycidyl ether-isobutyl alcohol adduct, 10% w/v in acetone at -72°C .; (B) phenyl glycidyl ether-dioxane-isobutyl alcohol, 10% w/v in acetone at -66°C . Internal reference TMS at 0 ppm.

going from CCl_4 to pyridine as solvent. This would indicate that the methyne proton lies nearest to solvated pyridine, therefore, that the sample has secondary hydroxyl, rather than primary. Assignment as secondary hydroxyl is established definitely by the low-temperature (-72°C .) NMR spectrum in acetone solution, (Fig. 3A). Here, hydroxyl proton ex-

change is slow and the OH spectrum is a doublet, $J \sim 4.5$ cycles/sec., showing that the carbon to which it is attached bears just one proton (two α protons would have caused the hydroxyl absorption to be a $\sim 1:2:1$ triplet).

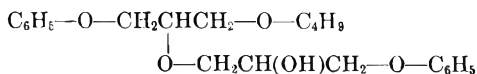
The corresponding *n*- and *sec*-butyl adducts give identical NMR spectra for the phenyl and glyceryl protons, and have appropriate butoxy spectra. Hydroxyl doublets in the NMR spectra in acetone at low temperature establish these compounds as having secondary hydroxyl also.

There is some evidence for formation of 10–15% 2-isobutoxy-3-phenoxy-1-propanol. A doublet marked "imp" in Figure 1B, the pyridine solution of the isobutoxy adduct, suggests a second kind of isobutoxy group in this sample. In acetone at -72°C ., a broad absorption at -4.5 ppm could be the corresponding OH. Similar features were not seen in the NMR spectra of the normal and secondary butanol adducts.

Phenyl Glycidyl Ether-Dioxane-Butanol Adducts. Elemental, mass spectrum, and NMR analyses of fractions III showed them to be predominantly 1-phenoxy-3-[2-(2-butoxyethoxy)-ethoxy]-2-propanol, $\text{C}_6\text{H}_5\text{—O—CH}_2\text{CH(OH)CH}_2\text{—O—CH}_2\text{CH}_2\text{OCH}_2\text{CH}_2\text{—O—C}_4\text{H}_9$.

Details of the structural assignment are based on the following observations in the NMR spectra (typical assigned spectra are those of the isobutanol adduct, Fig. 2). (1) There are approximately equimolar amounts of phenoxy, butoxy, glyceryl skeleton, OH, and structure attributable to dioxane residue. (2) Hydroxyl absorption is a doublet at -65 to -70°C . in acetone, indicating predominantly secondary alcohol. This is shown in Figure 3B for the isobutanol adduct. (3) The dioxane unit shows two different sets of $\text{—OCE}_2\text{CH}_2\text{O—}$ groupings, indicating the dioxane ring is opened and unsymmetrically terminated. (4) Upon going from CCl_4 to pyridine solution the glyceryl chain protons are strongly deshielded, while the butoxy and dioxane residue protons are affected relatively little. This gives strong support to placement of the hydroxyl on the glyceryl chain.

Mass spectroscopy results showed two impurity peaks in fractions III of all samples, at m/e of 224 and 374. The mass 224 material presumably is the 1:1 adduct of phenyl glycidyl ether and alcohol. The mass 374 impurity is assigned tentatively as the 2:1 adduct:



Products with *tert*-Butanol

Fraction I was characterized in the same manner as the other butoxy adduct and found to be predominantly 1-*tert*-butoxy-3-phenoxy-2-propanol. Purity as 1:1 adduct was less than found for the other butyl alcohols.

A second *tert*-butyl line in the NMR spectrum of fraction I accounted for ca. 15% of all *tert*-butyl groups. Part of the sample was fractionated further and the lesser component was found to have $m/e = 280$ by mass spectrometry. This could be phenoxy-di-*tert*-butoxypropane.

Fraction III was identified as predominantly 3-phenoxy-1,2-propanediol, $\text{HOCH}_2\text{CH}(\text{OH})\text{CH}_2\text{OC}_6\text{H}_5$, on the basis of its C and H analyses and its melting point. (Reported melting points are $53\text{--}54^\circ\text{C}$.⁵ and $55\text{--}57^\circ\text{C}$.⁶).

Fraction V, which presumably would have been the phenyl glycidyl ether-dioxane-alcohol adduct, was found to contain many components. NMR examination of Fraction V showed that this sample contained 0.37 *tert*-butyl groups and 0.73 opened dioxane units per phenoxy group, by integration. Seven different *tert*-butyl peaks were seen in pyridine solution, indicating seven or more different *tert*-butyl groups were present. About half of the *tert*-butyl absorption lay in one line, and could be due to one major *tert*-butyl-containing component. Spectral structure assigned to the dioxane residue was not entirely the same as that seen in the other butoxy-dioxane adducts.

Mass spectroscopy results for fraction V showed the expected mass (m/e) 312 and the two impurity peaks at masses of 374 and 224, as seen with the other butanols. Additional impurity peaks were found at masses (m/e) 256, 267, and 299.

Products with Phenol

Fraction I, which presumably would be the 1:1 phenyl glycidyl ether-phenol adduct, was shown to be very impure, on the basis of the very complex NMR spectrum.

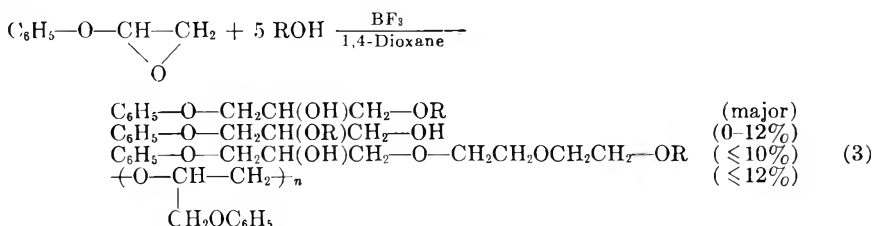
Fractions III appear to contain the phenyl glycidyl ether-dioxane-phenol adduct by mass spectrometry.

The bulk of the sample was residue, assigned as homopolymer of phenyl glycidyl ether.

CONCLUSION

We have examined the products of the reaction of fivefold quantities of the butanols and phenol with phenyl glycidyl ether, in dioxane solution, in the presence of boron trifluoride etherate.

With the butanols the major reactions were:



The *tert*-butanol gave significantly lower yields of these adducts, and many other products were found, as well.

With phenol under similar conditions the major product was the homopolymer. Although there is evidence for the types of adducts shown in eq. (3) above, a large number of other products was found as well.

Zusammenfassung

Phenylglycidyläther, eine Modellverbindung für Epoxyharze vom Bisphenol-A-Typ wurde in Dioxan in Gegenwart von Bortrifluorid-Ätherat mit Alkohol zur Reaktion gebracht. Bei Isobutyl-, *sec*-Butyl-, und *n*-Butylalkohol bestanden ähnliche Reaktionswege und zwar: (1) Epoxyd-Alkoholaddition eins zu eins, (2) Epoxyd-Alkohol-Dioxanaddition und (3) Homopolymerisation des Epoxyds. Mit überschüssigem Alkohol konnte die Homopolymerisation auf ein Minimum gebracht werden. In allen Fällen war das vorherrschende Eins-zu-eins-Addukt 1-Butoxy-3-phenoxy-2-propanol. Es bestehen Anzeichen, dass auch kleine Menge des Eins-zu-eins-Addukts mit einer primären Hydroxylgruppe gebildet wurde. Mit *tert*-Butylalkohol wurde auch 3-Phenoxy-1,2-propanediol erhalten. Mit Phenol bestand die Hauptreaktion in einer Homopolymerisation des Phenylglycidyläthers.

Received December 21, 1964

Prod. No. 4657A

Effect of Reaction Medium on Copolymerization of Acrylonitrile and Sodium Allyl Sulfonate

ZENZI IZUMI, HIROSHI KIUCHI, and MASAMOTO WATANABE,
Central Research Laboratories, Toyo Rayon Company, Otsu, Japan

Synopsis

The copolymerization of acrylonitrile (AN) with sodium allyl sulfonate (SAS) in dimethyl sulfoxide (DMSO) at pH 7, aqueous DMSO solution (6% H₂O), DMSO at pH 1.5, and aqueous solution at pH 7 has been investigated. Monomer reactivity ratios at 45°C. for AN and SAS are found to be $r_1 = 1.00 \pm 0.01$, $r_2 = 0.38 \pm 0.02$ in DMSO at pH 7; $r_1 = 1.25 \pm 0.01$, $r_2 = 0.28 \pm 0.02$ in aqueous DMSO; $r_1 = 1.85 \pm 0.01$, $r_2 = 0.43 \pm 0.01$ in DMSO at pH 1.5. From these values Price Q and e values, respectively, calculated for SAS were 0.19 and 0.22 in DMSO at pH 7, 0.14 and 0.18 in aqueous DMSO, and 0.18 and 0.70 in DMSO at pH 1.5. The large differences in reactivity of SAS may be attributed to the different electron distributions in SAS in each solvent which are caused by the poor solvating power of dimethyl sulfoxide and by the addition of protons. In copolymerization in aqueous solution, the physical condition depends upon the content of SAS in the monomer feed, and SAS is copolymerized to only a small extent in the range of heterogeneous systems, whereas SAS is copolymerized rather well in the range of homogeneous systems. Homopolymerization of SAS shows a first-order dependence on initiator concentration and a three-halves-order dependence on monomer concentration; this is attributed to degradative chain transfer of SAS. Rates of copolymerization of AN and SAS decrease with increasing SAS content.

INTRODUCTION

Monomer reactivity ratios for copolymerization by radical mechanisms have not been observed to be influenced by the nature of the medium, except in the case of heterogeneous polymerization, where the ratio of monomer concentration in the locus of polymerization is different from the feed ratio¹⁻⁶ or in the case of acidic or basic water-soluble monomers in aqueous solution at different pH.⁷⁻¹⁰ Recently, the authors found that the reactivity ratios of sodium *p*-styrenesulfonate are greatly influenced by the reaction medium, not only in aqueous solution at different pH but also in dimethyl sulfoxide (DMSO) solution, both in homogeneous systems.¹¹ To confirm these phenomena, which may be characteristic of electrolyte monomers, sodium allyl sulfonate (SAS) was investigated more extensively. While this work was in progress, Miyamichi reported¹² that the reactivity ratios of copolymerization of acrylonitrile (AN) and SAS are different in the two solvents, aqueous solution and DMSO solution, owing to the heterogeneity in the former case.

In the present study, the reactivity ratios of copolymerization of AN and SAS in four solvents; DMSO at pH 7, DMSO at pH 1.5, DMSO + H₂O (94:6), and aqueous solution at pH 7 were studied. The reactivity ratios are found to be different in all four solvents, and factors causing this are discussed. Homopolymerization rates of SAS and rates of copolymerization of AN and SAS are also given; these show the degradative chain transfer characteristic of allylic monomers.

EXPERIMENTAL

Materials

SAS (supplied by Wako Chemical Co.) was purified by recrystallization from 90% ethanol twice. The purity of this monomer was determined to be 98.07% by the mercury acetate addition method. Polymer grade AN (supplied by Nitto Chemical Co.) was purified by the method of Bamford.¹³ DMSO (supplied by Crown Zellerbach Co.) was dried with sodium carbonate and then vacuum-distilled under 4 mm. nitrogen pressure twice. The fraction boiling in the range $65.0 \pm 0.2^\circ\text{C}$. was collected. Azobisisobutyronitrile (AIBN) (supplied by Otsuka Chemical Co.) was purified by recrystallization from anhydrous methanol. The recrystallized product was refrigerated to minimize thermal decomposition. Ammonium persulfate (APS) (supplied by Wako Chemical Co.) was purified by recrystallization from water, and then the solution, of which the concentration was determined iodometrically was stored in a refrigerator to minimize thermal decomposition. Other reagents were considered to be extremely pure and used without further treatment.

Polymerization Technique

Homopolymerization of SAS in DMSO was carried out in a sealed tube *in vacuo* at 45°C . The conversion was determined by the measurement of double bonds by the mercury acetate addition method.

Copolymers for the determination of the monomer reactivity ratios were prepared in a sealed tube *in vacuo*, the pH of the reaction mixtures being adjusted to 1.5 or 7 by addition of hydrochloric acid or sodium hydroxide, respectively.

Rates of copolymerization in DMSO at pH 7 were obtained from the observed rates of volume contraction in the dilatometer shown in Figure 1. The total mole fraction α consumed in the reaction was obtained from eq. (1) as expressed previously.¹⁴

$$\alpha = (1000/V)(Ah/M_1 + M_2)(R + 1/\Delta_1 R + \Delta_2) \quad (1)$$

where h is the observed change in the height of the liquid in a dilatometer capillary at time t , A is the cross-sectional area of the capillary, V is the volume of the dilatometer bulb $[M_1]$ and $[M_2]$ are the initial concentrations of AN and SAS monomer, respectively, in the feed in moles/l., Δ_1 and

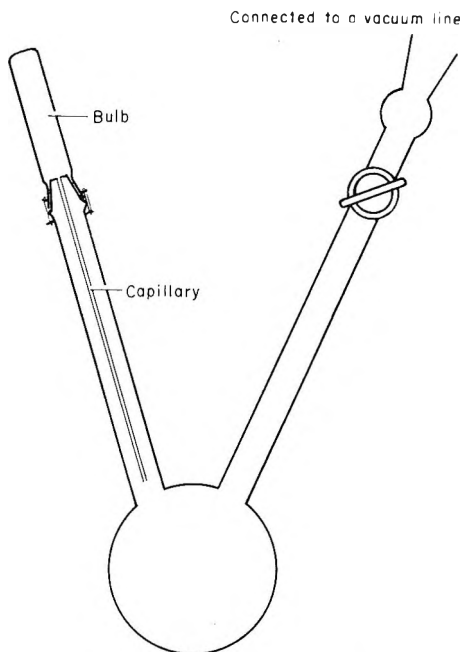


Fig. 1. Dilatometer used.

Δ_2 are the changes in volume caused by complete polymerization of 1 mole of the respective monomers to the polymers, and R is the AN/SAS molar ratio in the initial copolymer.

The numerical values used here at 45°C. are $V = 9.28 \text{ cm.}^3$, $M_1 + M_2 = 1.0 \text{ mole/l.}$ in aqueous solution and 2.0 mole/l. in DMSO, $\Delta_1 = 14.21 \text{ cm.}^3/\text{mole}$ in aqueous solution and $20.52 \text{ cm.}^3/\text{mole}$ in DMSO, $\Delta_2 = 15.90 \text{ cm.}^3/\text{mole}$ in aqueous solution and $16.21 \text{ cm.}^3/\text{mole}$ in DMSO, and $A = 9.347 \times 10^{-3} \text{ cm.}^2$. On substituting these values in eq. (1), eqs. (2) and (3) are obtained for DMSO solution and aqueous solution, respectively:

$$\alpha = [0.508(R + 1)/(20.52R + 16.21)]h \quad (2)$$

$$\alpha = [1.016(R + 1)/(14.21R + 15.90)]h \quad (3)$$

where R is the AN/SAS molar ratio in the initial copolymer. Initial rates of copolymerization were obtained from tangents to the curve of α versus time t at low conversion.

The copolymers were quantitatively precipitated with alkaline ethanol and washed with hot 90% ethanol using a centrifugal separator.

The compositions of AN-SAS copolymers containing over 10 mole-% SAS were determined from nitrogen contents obtained by the Kjeldahl method. The copolymers with SAS contents less than 10 mole-% were analyzed by the infrared absorption method by using a mixture of AN-SAS (SAS 9.99 mole-%) copolymer and polyacrylonitrile as standards; here it was assumed that the absorbance index of the copolymer follows Beer's

law. The spectra were recorded with a Perkin-Elmer Model 21 double beam spectrophotometer equipped with a sodium chloride prism. As characteristic absorptions, the one at 2237 cm.^{-1} for AN and another at 1047 cm.^{-1} for SAS were chosen.

RESULTS AND DISCUSSION

Homopolymerization of SAS in DMSO

Plots of conversion against time are given in Figure 2, and the rates of polymerization of SAS in DMSO are found to be as low as 1/100 of the rate of polymerization of AN in DMSO.¹¹ The effect of initiator concentration on polymerization rate at 45°C. is shown in Figure 3, and the experimental points are well represented by a straight line of slope 1. The effect of monomer concentration on polymerization rate is shown in Figure 4, and the experimental points are well represented by a straight line of slope

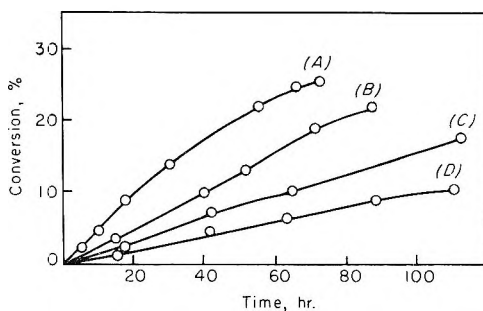


Fig. 2. Conversion-time curve for polymerization of SAS in DMSO at 45°C. at $[\text{SAS}]$ 2 mole/l. and varying azobisisobutyronitrile concentrations: (A) 0.06 mole/l.; (B) 0.03 mole/l.; (C) 0.02 mole/l.; (D) 0.01 mole/l.

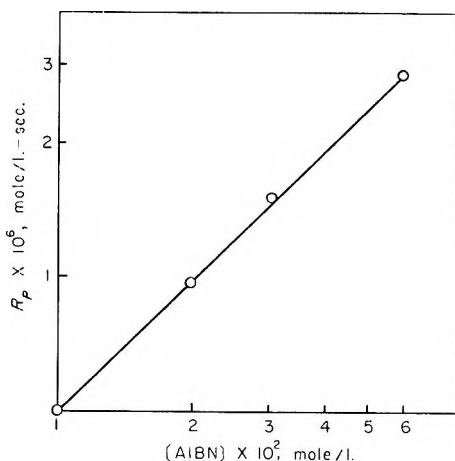


Fig. 3. Dependence of rate of polymerization of SAS on catalyst concentration at 45°C.

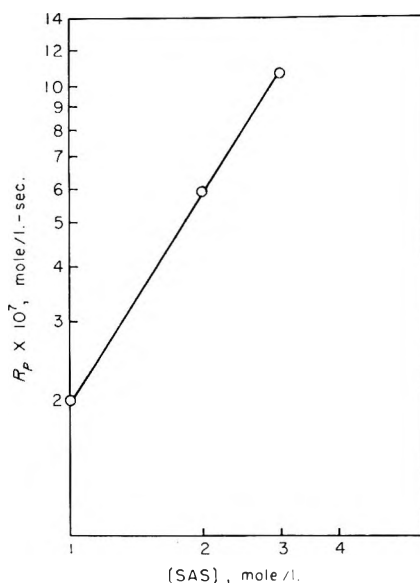


Fig. 4. Dependence of rate of polymerization of SAS on monomer concentration at 0.03 mole/l. [AIBN] at 45°C.

1.5. From the above experiments, the polymerization rate is shown to follow eq. (4).

$$-d[\text{SAS}]/dt = k[\text{AIBN}][\text{SAS}]^{3/2} \quad (4)$$

The first-order dependence on initiator concentration and three-halves-order dependence on monomer concentration of the rate of polymerization of SAS may be explained by the contribution of degradative chain transfer^{15,16} which is characteristic of the allylic monomers, such as allyl alcohol, allyl chloride, and allyl acetate.

Copolymerization

Monomer Reactivity Ratios. The data for calculating monomer reactivity ratios in the four solvents used are listed in Tables I-IV. The concentration of SAS in the copolymer against the mole per cent SAS in the monomer feed is plotted in Figure 5, and there can be seen large differences between reactivity ratios in each solvent. Monomer reactivity ratios were determined graphically by the method of Mayo and Lewis, and the ratios are listed in Table V, except for the case of aqueous solution. From these reactivity ratios and the Q and e values for AN ($Q_1 = 0.60$, $e_1 = 1.2$), Price Q and e values for SAS were calculated; these are also shown in Table V.

In the case of copolymerization in aqueous medium, the physical condition depends upon the content of SAS in the monomer feed. The copolymer produced with a SAS monomer feed of less than 40 mole-% is precipitated, whereas the copolymerization with a SAS concentration in the

TABLE I
 Copolymerization of AN and SAS in DMSO at pH 7^a

SAS in the monomer feed M_2 , mole-%	Monomer reacted, wt.-%	SAS in the copolymer m_2 , mole-%
1.0	9.19	0.99
2.0	8.08	1.91
10.0	6.90	9.99
20.0	6.79	17.5
35.0	9.50	28.0
60.0	6.06	50.0

^a Copolymerization conditions: 2.0 mole/l. monomer, 0.03 mole/l. AIBN as initiator at 45°C.

 TABLE II
 Copolymerization of AN and SAS in DMSO + H₂O (94:6)^a

SAS in the monomer feed M_2 , mole-%	Monomer reacted, wt.-%	SAS in the copolymer m_2 , mole-%
2.0	4.16	1.58
5.0	5.90	3.84
10.0	7.93	8.04
20.0	9.20	14.8
35.0	7.30	24.7
50.0	6.55	35.8
60.0	5.58	45.0

^a Copolymerization conditions: 2.0 mole/l. monomer, 0.03 mole/l. AIBN as initiator at 45°C.

 TABLE III
 Copolymerization of AN and SAS in DMSO at pH 1.5^a

SAS in the monomer feed M_2 , mole-%	Monomer reacted, wt.-%	SAS in the copolymer m_2 , mole-%
2.0	8.32	1.04
5.0	5.15	2.87
10.0	9.76	6.32
20.0	7.70	11.2
50.0	6.03	35.8
60.0	6.51	40.3

^a Copolymerization conditions: 2.0 mole/l. monomer, 0.03 mole/l. AIBN as initiator at 45°C.

monomer feed of more than 50 mole-% occurs in homogeneous system, and there is large difference in the reactivity of SAS between these two regions. Figure 5 shows that copolymerization of SAS is slight in the heterogeneous system, whereas SAS is copolymerized rather well in the homogeneous system. This phenomenon, which is attributed to the strong water

TABLE IV
Copolymerization of AN and SAS in H₂O at pH 7^a

SAS in the monomer feed M_2 , mole-%	Monomer reacted, wt.-%	SAS in the copolymer m_2 , mole-%
5.0	6.51	0.78
10.0	6.10	1.84
20.0	6.01	3.42
50.0	6.05	18.03
80.0	6.01	59.0
90.0	4.45	75.5

^a Copolymerization conditions: 1.0 mole/l. monomer, 0.01 mole/l. APS as initiator at 45°C.

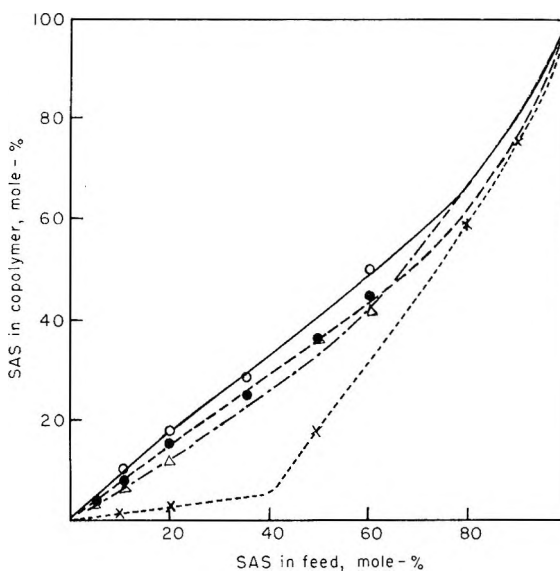


Fig. 5. Plot of SAS content in the copolymer (m_2) vs. SAS in the monomer feed (M_2): (O) experimental points in DMSO at pH 7 and (—) calculated for $r_1 = 1.00$ and $r_2 = 0.38$; (●) experimental points in DMSO + H₂O (94:6) and (---) calculated for $r_1 = 1.25$ and $r_2 = 0.28$; (Δ) experimental points in DMSO at pH 1.5 and (- - -) calculated for $r_1 = 1.85$ and $r_2 = 0.43$; (X) experimental points in aqueous solution at pH 7 and (---) line for experimental points.

TABLE V
Copolymerization Parameters for AN and SAS in Different Solvents at 45°C.

Copolymerization medium	r_1 (AN)	r_2 (SAS)	Q_2 (SAS)	e_2 (SAS)
DMSO solution at pH 7	1.00 ± 0.01	0.38 ± 0.02	0.19	0.22
DMSO + H ₂ O solution	1.25 ± 0.01	0.28 ± 0.02	0.14	0.18
DMSO solution at pH 1.5	1.85 ± 0.01	0.43 ± 0.01	0.18	0.70

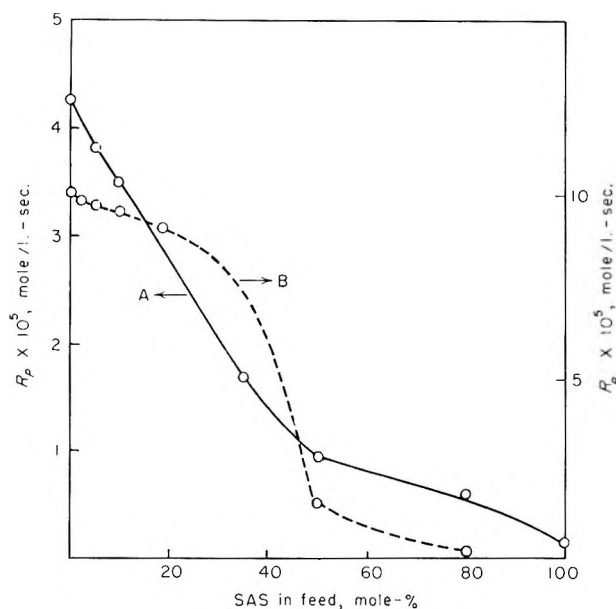


Fig. 6. Plot of initial rate of copolymerization R_p against SAS content in the monomer feed: (A) DMSO at pH 7; (B) H_2O at pH 7.

solubility of SAS, is similar to that found by Fordyce⁵ in the case of styrene and itaconic acid in emulsion system, that is, the difference is due to the adsorption of the monomers onto the precipitating particles. Therefore, the exact values of monomer reactivity ratios cannot be determined.

In other solvents, polymerization occurs in a homogeneous system, and the difference of reactivity may be attributed to a chemical effect. Considering the difference in the properties of the three solvents: DMSO at pH 7, DMSO + H_2O (94:6), and DMSO at pH 1.5, the following difference in the form of SAS may exist in each solvent. DMSO is a dipolar aprotic solvent, and the solvating power of DMSO may be weak compared to water; thus DMSO may not have sufficient solvating power to free the ions from each other. As a result therefore, SAS may exist in the form of an ion pair $CH_2=CH-CH_2SO_3^- \cdots Na^+$. The solvating power of DMSO may be increased by the addition of water, and therefore, the power of attraction between SO_3^- and Na^+ may be weakened or a part of SAS may exist as anion $CH_2=CH-CH_2SO_3^-$. In DMSO at pH 1.5, by the addition of sufficient protons, SAS may exist in the form, $CH_2=CH-CH_2SO_3H \cdots$ DMSO. Comparing Price Q and e for SAS in three solvents, Q is almost constant, but e increases in the order DMSO- H_2O (94:6) < DMSO, pH 7 < DMSO, pH 1.5. Thus, as the degree of dissociation of the polar group decreases, the electron-withdrawing power increases, giving the double bond a positive character. The above explanation may be in accord with the experimental results and coincides with data for other electrolytic monomers in aqueous solution.⁷⁻¹⁰

Copolymerization Rates. The initial rates of copolymerization R_p , at 45°C. in DMSO solution at pH 7 and in aqueous solution at pH 7 are shown in Figure 6. There can be seen a sharp decrease in copolymerization rate with increasing SAS content, which may be due to the degradative chain transfer of SAS. The decrease of rate in aqueous solutions containing less than 20 mole-% SAS in the monomer feed is rather small, which may be attributed to the heterogeneous condition. The phenomenon of sharp rise in the copolymerization rate in the transition phase from heterogeneous to homogeneous, which was observed in the case of AN-sodium-*p*-styrenesulfonate,¹⁴ cannot be seen in this case. The effect of degradative chain transfer may be larger than the effect of physical condition.

The authors wish to express their sincere gratitude to Dr. Kobayashi, the Director of our Research Department, for his help and permission to publish the results.

References

1. Fordyce, R. G., and E. C. Chaplin, *J. Am. Chem. Soc.*, **69**, 581 (1947).
2. Smith, W. V., *J. Am. Chem. Soc.*, **70**, 2177 (1948).
3. Fordyce, R. G., and G. E. Ham, *J. Polymer Sci.*, **3**, 891 (1948).
4. Fordyce, R. G., and G. E. Ham, *J. Am. Chem. Soc.*, **69**, 695 (1947).
5. Brandrup, J., *Faserforsch. Textiltech.*, **12**, 133, 208 (1961).
6. Drougas, J., and R. L. Guile, *J. Polymer Sci.*, **55**, 297 (1961).
7. Chapin, E. C., G. E. Ham, and C. R. Mills, *J. Polymer Sci.*, **4**, 597 (1949).
8. Alfrey, T., C. G. Overberg, and S. H. Pinner, *J. Am. Chem. Soc.*, **75**, 4221 (1953).
9. Suzuki, S., and H. Ito, *Kogyo Kagaku Zasshi*, **58**, 627 (1955).
10. Imoto, M., and T. Otsu, *Kobunshi Kagaku*, **16**, 324 (1959).
11. Izumi, Z., H. Kiuchi, M. Watanabe, and H. Uchiyama, *J. Polymer Sci.*, in press.
12. Miyamichi, K., A. Suzuki, T. Harada, and M. Katayama, *Kobunshi Kagaku*, **21**, 79 (1964).
13. Bamford, C. H., and A. D. Jenkins, *Proc. Roy. Soc. (London)*, **A216**, 517 (1953).
14. Izumi, Z., H. Kiuchi, and M. Watanabe, *J. Polymer Sci.*, **A1**, 705 (1963).
15. Flory, P. J., *Principles of Polymer Chemistry*, Cornell Univ. Press, Ithaca, N. Y., 1953.
16. Bartlett, P. D., and R. Altschul, *J. Am. Chem. Soc.*, **67**, 812, 816 (1945).

Résumé

On a étudié la copolymérisation de l'acrylonitrile (AN) avec l'allyle sulfonate de sodium (SAS) (1) en solution dans le diméthylsulfoxyde à pH 7, (2) en solution dans le diméthylsulfoxyde avec de l'eau (H₂O 6%), (3) en solution dans le diméthylsulfoxyde à pH 1.5, et (4) en solution aqueuse à pH 7. Les rapports de réactivité des monomères à 45°C. pour AN et SAS sont $r_1 = 1.00 \pm 0.01$, $r_2 = 0.83 \pm 0.02$ dans le solvant (1), $r_1 = 1.25 \pm 0.01$, $r_2 = 0.28 \pm 0.02$ dans le solvant (2), et $r_1 = 1.85 \pm 0.01$, $r_2 = 0.43 \pm 0.01$ dans le solvant (3). À partir de ces données, on a calculé les valeurs Q et e de Price pour SAS et on trouve 0.19 et 0.70 dans le solvant (3). Les grandes différences de réactivité de SAS peuvent être attribuées aux distributions différentes des électrons dans SAS pour chaque solvant, provoquées par le faible pouvoir de solvation du diméthylsulfoxyde et par l'addition d'un proton. Dans le solvant (4), la condition physique dépend de la teneur en SAS dans le mélange monomérique, et SAS copolymérise difficilement dans les systèmes hétérogènes, tandis qu'il copolymérise plutôt bien en système homogène. L'homopolymérisation de SAS est du premier ordre par rapport à la concentration en initiateur et d'ordre trois-demi par rapport à la concentration en monomère, ce qui

est attribué au transfert de chaîne dégradant de SAS. Les vitesses de copolymérisation de AN et de SAS diminuent avec une augmentation de la teneur en SAS.

Zusammenfassung

Die Copolymerisation von Acrylnitril (AN) mit Natriumallylsulfonat (SAS) wurde in (1) Dimethylsulfoxydlösung bei pH 7, (2) wässriger Dimethylsulfoxydlösung (H_2O 6%), (3) Dimethylsulfoxydlösung bei pH 1,5, und (4) wässriger Lösung bei pH 7 untersucht. Die Monomerreaktivitätsverhältnisse betragen für AN und SAS bei 45°C $r_1 = 1,00 \pm 0,01$, $r_2 = 0,38 \pm 0,02$ in Lösungsmittel (1), $r_1 = 1,25 \pm 0,01$, $r_2 = 0,28 \pm 0,02$ in Lösungsmittel (2), und $r_1 = 1,85 \pm 0,01$, $r_2 = 0,43 \pm 0,01$ in Lösungsmittel (3), woraus Q und e -Werte für SAS nach Price in Lösungsmittel (1) zu 0,19 und 0,22, in Lösungsmittel (2) zu 0,14 und 0,18 und in Lösungsmittel (3) zu 0,18 und 0,70 berechnet werden. Die grossen Reaktivitätsunterschiede bei SAS können auf die Unterschiede in der Elektronenverteilung von SAS in jedem Lösungsmittel zurückgeführt werden, welche durch die geringe Solvatisierungsfähigkeit von Dimethylsulfoxyd und durch die Addition eines Protons verursacht werden. Im Lösungsmittel (4) hängen die physikalischen Bedingungen vom SAS-Gehalt der Monomermischung ab: im Bereich heterogener Systeme tritt kaum eine Copolymerisation von SAS auf, während SAS im homogenen Bereich recht gutco-polymerisiert. Die Homopolymerisation von SAS ist in bezug auf die Starterkonzentration von erster Ordnung und in bezug auf die Monomerkonzentration von der Ordnung $3/2$, was auf eine verzögernde Kettenübertragung durch SAS zurückgeführt wird. Die Copolymerisationsgeschwindigkeit von AN/SAS nimmt mit steigendem SAS-Gehalt ab.

Received October 28, 1964

Revised February 4, 1965

Prod. No. 4659A

Poly(vinylene fluoride), Synthesis and Properties*

W. S. DURRELL,† G. WESTMORELAND, and M. G. MOSHONAS,‡
Peninsular ChemResearch, Inc., Gainesville, Florida

Synopsis

A new synthesis of vinylene fluoride by means of the dehalogenation of 1,2-dichloro-1,2-difluoroethane is reported. Both the pure *cis* and pure *trans* isomers of vinylene fluoride were found to polymerize quite readily. This polymer differs from the known polyfluoroolefins in having little crystallinity and fair solubility in a number of common solvents. While it is not markedly unstable thermally, it is the least stable of the polyfluoroethylenes in this respect. Several copolymers were prepared to further elucidate the polymerization behavior of vinylene fluoride, and some of the properties of these copolymers were examined.

As part of a program aimed at learning more about the low temperature properties of polymers derived from fluoroolefins it became desirable to augment the information available concerning the thermal properties of polymers with the $-\text{CHF}-$ grouping. A published report of the very low brittle temperature, $< -130^\circ\text{C}$., of poly(vinyl fluoride) film was intriguing,¹ but contrasted with the relatively high reported value of its glass transition temperature, 45°C .² Nothing has been reported on the low-temperature transitions of trifluoroethylene. 1-Chloro-1,2-difluoroethylene is reported in the patent literature as an amorphous plastic which softens at 130°C .³ Kolesnikov reported on the polymerization of compounds of the type $\text{CHF}=\text{CX}_2$, where $\text{X} = \text{Cl}$ or Br .^{4,5} Lack of detail, in addition to the fact that the studies were carried out with low molecular weight polymers, makes his data difficult to evaluate.

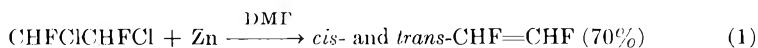
The most direct means of observing the effect of $-\text{CHF}-$ in a polymer chain would be to study poly-1,2-difluoroethylene, poly(vinylene fluoride), itself. While the monomer has been reported,⁶⁻⁸ there was no information available on homopolymers of the *cis* and *trans* isomers of 1,2-difluoroethylene nor on copolymers with other olefins. As a prelude to studies on the polymerizability of 1,2-difluoroethylene it was considered advisable to examine another potential synthetic route, since the reported method was cumbersome.⁷

* Presented at the 148th National Meeting of the American Chemical Society, Chicago, Ill. Aug. 30-Sept. 4, 1964. This work was supported by the George C. Marshall Space Flight Center, Huntsville, Alabama, under Contract NAS 8-5352. Mr. John T. Schell acted as the technical representative.

† Present address: Burke Research Company, Pompano Beach, Florida.

‡ Present address: U.S. Department of Agriculture, Winter Haven, Florida.

The dehalogenation of a 1,2-dihalo-1,2-difluoroethane seemed like an excellent route potentially. The synthesis of 1,2-dichloro-1,2-difluoroethane through the reaction of *cis*-dichloroethylene with cobaltic trifluoride was recently reported by Rausch⁹ to proceed in good yields. This compound had become available in our laboratories through another program, and the reaction with zinc occurred as anticipated in dimethylformamide (DMF), although it did not occur at an appreciable rate in refluxing dioxane [eq. (1)].



The *trans*:*cis* ratio was 0.3, or about that expected on a thermodynamic basis.⁸

Both the pure *cis* and the pure *trans* olefins, as well as a 31:69 *cis*:*trans* mixture, polymerized readily. Initiator systems which were used were of the emulsion and redox types. For the most part, however, these experiments as well as the copolymerizations discussed below, utilized the irradiation from a Co⁶⁰ γ -ray source. This latter method was used extensively for the sake of convenience.

No differences were noted in the infrared spectra of the polymers obtained from the various isomer mixtures but only a minimum of initiator systems were examined and the polymers were not studied by use of nuclear magnetic resonance spectroscopy. This latter technique might be expected to detect the subtle differences between the various stereoisomers which might be obtainable under certain conditions from the *cis* and *trans* isomers.

Only the expected minor differences in reactivities of the two olefins due to the slight difference in thermodynamic stability were observed.

Copolymerization experiments afforded additional qualitative information as to the polymerization reactivity of 1,2-difluoroethylene as well as the desired knowledge of the properties of such polymers. For example, approximately equimolar polymers were formed from equimolar mixtures with the monomers: CF₂=CFCl, CFH=CFCl, CF₂=CFOCH₂CF₃, and CH₂=CHOAc. Thus, the expected approximately equal reactivity of these olefins, none of which are resonance-stabilized, is observed. In contrast, smaller amounts of less reactive olefins were incorporated. In this category were CF₂=CFCF₃, CF₂=CFOCF₃, and CF₂=CFH. Also as expected, acrylonitrile and methyl methacrylate were much more reactive than 1,2-difluoroethylene, and consequently only minor amounts could be incorporated in copolymers with these resonance stabilized olefins. The essential details of these experiments are summarized in Table I.

The copolymer formed with CF₃NO was rather interesting. It was, as are all reported nitroso polymers,¹⁰ a 1:1 copolymer presumably of the perfectly alternating structure:



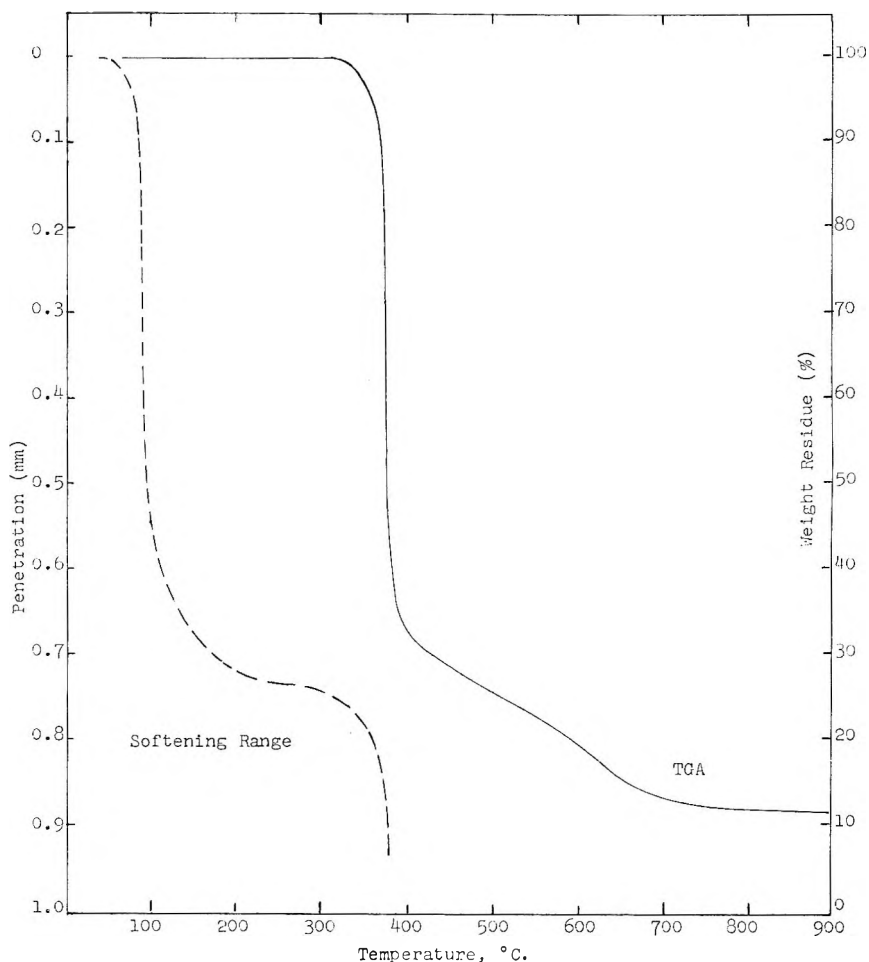


Fig. 1. Thermal behavior of poly(vinylene fluoride).

Polymers of vinylene fluoride differ markedly from the polymers of the other fluoroethylenes. These others are all highly crystalline and insoluble in most solvents. Poly(vinylidene fluoride) is only slightly soluble in acetone and in dimethylformamide.¹¹ In contrast, poly(vinylene fluoride) is soluble in both of these, as well as methyl isobutyl ketone. The copolymer with chlorotrifluoroethylene is also quite soluble in the polar solvents but is unaffected by benzene or carbon tetrachloride.

This increase in solubility is probably due, to a major extent, to the decreased crystallinity of poly(vinylene fluoride) compared to poly(vinylidene fluoride).

Another property of poly(vinylene fluoride) which differs markedly from poly(vinylidene fluoride) is its glass transition temperature, T_g . The glass temperature of $(\text{CH}_2\text{CF}_2)_n$, -50°C .,¹² is much lower than that of $(\text{CHF}-\text{CHF})_n$, which is about 50°C . as estimated from the softening behavior in

Figure 1. This difference may be largely explained by its increased lateral disymmetry along the polymer backbone¹³ with respect to poly(vinylidene fluoride). The higher value of T_g for $(\text{CHFCHF})_n$ over $(\text{CH}_2\text{-CF}_2)_n$ causes its amorphous copolymer with CF_2CFCl to be a hard transparent plastic rather than a rubber, such as Kel-F elastomer, the corresponding CH_2CF_2 copolymer.

It has been variously predicted that $(\text{CHFCHF})_n$ when synthesized, would be thermally unstable.^{7,14} The loss of weight of a sample of poly(vinylene fluoride) upon heating is illustrated in Figure 1. These data are of interest in showing that poly(vinylene fluoride) does not begin to decompose seriously until above 300°C. Qualitatively, it would appear to be less stable than poly(vinyl fluoride) which reportedly is, in turn less stable than polyethylene, polytrifluoroethylene, poly(vinylidene fluoride), and polytetrafluoroethylene.¹⁴ Thus, the lower stability of polyvinylene fluoride is a matter of degree rather than kind, as might have been expected from the implications of earlier investigators.

From the carbonaceous residue it can be concluded that the splitting out of HF is an important decomposition process, but of the original carbon only about $\frac{1}{3}$ remains, indicating that chain fragmentation occurs concomitantly. Thus, the thermal degradation behavior is intermediate between that of the other fluoroethylenes and poly- α -fluorostyrene, which stoichiometrically loses HF at 225 and 235°C. to give a polyacetylene derivative.¹⁵

In summary we might say that poly(vinylene fluoride) is of interest because of its contrasting properties with respect to the other fluoroethylene polymers. Thus, its decreased lateral symmetry compared to poly(vinylidene fluoride) results in a higher glass transition temperature (all else equal) and decreased crystallinity. This latter factor is probably primarily responsible for increased solubility of polymers and copolymers of vinylene fluoride.

EXPERIMENTAL

Gas-liquid chromatographic (GLC) analyses were performed with a standard instrument with a thermal conductivity cell. An 8-ft. column containing about 20% of dioctyl phthalate on Chromosorb effectively separated the *cis* and *trans* isomers of 1,2-difluoroethylene. Either this column or one of Kel-F Acid 8114 (Minnesota Mining & Manufacturing Co.) on Chromosorb was used to both confirm the purity and check the compositions of starting and recovered monomers and monomer mixtures in this work. The other monomers were fractionated to at least 99% purity as determined in the above fashion. Polymerization reactions were carried out either in sealed Carius tubes of appropriate wall thickness or in Fischer-Porter aerosol compatibility tubes equipped with pressure gauges and needle valves. The latter were either magnetically stirred in a bath at the desired temperature or agitated in a heated 1.4-liter autoclave rocker modified to hold several such tubes simultaneously. The Co^{60} γ -irradi-

tions were carried out with the cooperation of Dr. R. J. Hanrahan of the University of Florida, Gainesville, Florida. The radiation flux was approximately 7×10^3 r/hr. The degree of crystallinity of the polymer samples was estimated by R. W. Gould of the University of Florida from the x-ray diffraction powder patterns. The Vicat-type penetration apparatus used for the determination of the heat distortion temperature applies a load of 1000 ± 23 g. to a steel rod with a 1 mm. cross-sectional area which rests on the sample. The temperature of the sample was raised at a rate of 150°C./hr. and the penetration of rod automatically and continuously recorded as a function of temperature. This work, in addition to the thermogravimetric analysis, was carried out under the supervision of Dr. G. F. L. Ehlers of the Air Force Materials Laboratory, Wright-Patterson Air Force Base, Ohio.

Synthesis of 1,2-Difluoroethylene

1,2-Dichloro-1,2-difluoroethane (290 g., 2.0 moles based on 90% purity) was added over an 8-hr. period to a well stirred, refluxing mixture of 300 g. (4.5 g.-atom) of zinc dust, which had been activated by addition of a few drops of HBr, in 500 ml. of dimethylformamide. The mixture was stirred and refluxed for an additional 8-hr. period and the material which had evolved into a Dry Ice-acetone-cooled trap, protected by a liquid air-cooled trap, was carefully fractionated in a 12 cm. I.D., 60 cm. long silvered column, filled with extruded nickel packing. The fractions taken are listed in Table II.

TABLE II

Boiling point, $^\circ\text{C.}$	Fraction wt., g.	Composition (determined by GLC)
-42 to -40	26	99.9% <i>trans</i> -CHF=CHF
-40 to -25	11	17% <i>trans</i> -, 83% <i>cis</i> -CHF=CHF
-25 to -20	56	99.1% <i>cis</i> -, 0.4% <i>trans</i> -CHF=CHF, 0.5% unidentified compound
Residue	43	25% <i>cis</i> -CHF=CHF, 75% a mixture of 2 unidentified compounds

The *cis* and *trans* isomers were identified by comparison of their infrared spectra with the spectra of the pure compounds reported by Craig and Entemann.⁸ It should be noted that the boiling points are somewhat different from those previously reported for the *cis* and *trans* isomers of 1,2-difluoroethylene (-53.1°C. reported vs. -42 to -40°C. and -26.0°C. vs. -25 to -20°C. in this work). This discrepancy is probably a result of a lack of sufficient insulation around our variable take-off rate low-temperature head. The *trans*:*cis* ratio was about 0.3.

Homopolymerization of 1,2-Difluoroethylene

The results of various homopolymerization experiments are summarized in Table III.

TABLE III

Isomer	Initiator	Time, hr.	Temp., °C.	Yield, %	Remarks
69% <i>trans</i> + 31% <i>cis</i>	{ Emulsion ^a Redox ^c	21 24	60 25	60 37	[η] = 5.2 ^b [η] = 1.2 ^d
<i>trans</i> <i>cis</i>	Emulsion Emulsion	72 72	60 60	30 24	Spectra identical
<i>trans</i> <i>cis</i>	Co ⁶⁰ Co ⁶⁰	15 15	25 25	97 97	

^a K₂S₂O₈, 0.75 parts; K₂HPO₄, 2 parts; Cl(CF₂CFCl)₃CF₂CO₂NH₄, 3 parts; water, 200 parts; monomer, 100 parts.

^b 1% in acetone.

^c (NH₄)₂S₂O₈, 1 part; Na₂S₂O₃, 0.4 parts; FeSO₄, 0.1 part; Cl(CF₂CFCl)₃CF₂CO₂NH₄, 3 parts; water, 200 parts; monomer, 100 parts.

^d 0.5% in acetone.

The infrared spectra of the polymers showed peaks at 9.2(s), 9.7(s), 10.5(m), 10.9(m), and 12.6(m) μ .

Copolymerizations of 1,2-Difluoroethylene

Pertinent information is given in Table I.

Mr. Van A. May was responsible for the chromatographic analyses and Mr. Edward Iglehart for several of the experiments reported herein.

References

1. Kalb, G. H., D. C. Coffman, T. A. Ford, and F. L. Johnston, *J. Appl. Polymer Sci.*, **4**, 55 (1960).
2. Schmieder, K., and K. Wolf, *Kolloid-Z.*, **134**, 149 (1953).
3. Ruh, R. P., and M. R. Rector, U.S. Pat. 2,716,109 (Aug. 23, 1955).
4. Kolesnikov, G. S., and M. G. Avetyan, *Izvest. Akad. Nauk Arm. SSR, Khim. Nauki*, **11**, 201 (1958).
5. Kolesnikov, G. S., and M. G. Avetyan, *Izvest. Akad. Nauk SSSR, Otdel. Khim. Nauk*, **1959**, 331.
6. Stone, F. G. A., and W. A. G. Graham, *Chem. Ind. (London)*, **1955**, 1181.
7. Haszeldine, R. N., and B. R. Steele, *J. Chem. Soc.*, **1957**, 2800.
8. Craig, N. C., and E. A. Entemann, *J. Am. Chem. Soc.*, **83**, 3047 (1961).
9. Rausch, D. A., R. A. Davis, and D. W. Osborne, *J. Org. Chem.*, **28**, 494 (1963).
10. Crawford, G. H., D. E. Rice, and B. F. Landrum, *J. Polymer Sci.*, **A1**, 565 (1963).
11. *Kynar*, Pennsalt Chemicals Corp., Philadelphia, Pa., Data Sheet VF 2R-62a.
12. Mandelkern, L., G. M. Martin, and F. H. Quinn, Jr., *J. Res. Natl. Bur. Std.*, **58**, 137 (1957).
13. Mackenzie, J. D., Ed., *Modern Aspects of the Vitreous State*, Vol. 1, Butterworths, London, 1960.
14. Madorsky, S. L., V. E. Hart, S. Straus, and V. A. Sedlak, *J. Res. Natl. Bur. Std.*, **51**, 327 (1953).
15. Matsuda, K., J. A. Sedlak, J. S. Noland, and G. C. Gleckler, *J. Org. Chem.*, **27**, 4015 (1962).

Résumé

On a décrit une nouvelle synthèse de fluorure de vinyène par déshalogénéation du 1,2-dichloro-1,2-difluoroéthane. On a trouvé que les isomères *cis* purs et *trans* purs du fluorure de vinyène pouvaient polymériser facilement. Ce polymère diffère des polyfluoroléfines connues par le fait qu'il possède une faible cristallinité et une bonne solubilité dans un certains nombres de solvants habituels. Alors qu'il n'est pas très instable thermiquement, il est à ce point de vue le moins stable des polyfluoréthylènes. On a préparé plusieurs copolymères en vue d'élucider le comportement du fluorure de vinyène et on a examiné certaines propriétés de ces copolymères.

Zusammenfassung

Eine neue Synthese von Vinylenfluorid durch Dehalogenierung von 1,2-Dichlor-1,2-difluoräthan wird mitgeteilt. Sowohl reines *cis*- als auch reines *trans*-Isomeres von Vinylenfluorid polymerisieren leicht. Das Polymere unterscheidet sich von den bekannten Poly-(fluorolefinen) durch seine geringe Kristallinität und seine gute Löslichkeit in einer Anzahl gebräuchlicher Lösungsmittel. Es ist zwar thermisch stabil, aber doch das am wenigsten stabile unter den Poly(fluoräthylenen). Zur weiteren Aufklärung des Polymerisationsverhaltens von Vinylenfluorid wurden einige Kopolymere dargestellt und gewisse Eigenschaften dieser Kopolymeren untersucht.

Received November 20, 1964

Revised February 19, 1965

Prod. No. 4662A

Coupling of Xylylene Dihalides with Divalent Chromium. Aspects of Copolymerization and Mechanism

H. E. LUNK and E. A. YOUNGMAN, *Shell Development Company, Emeryville, California*

Synopsis

Copolymers of *p*- and *m*-xylylene have been prepared by coupling of the corresponding dihalides with chromous chloride. A stepwise mechanism is proposed for the formation of polyxylylenes, and evidence is given for the occurrence of free radicals in the decomposition of the intermediate organochromium complex.

INTRODUCTION

In 1957 Anet and Leblanc¹ reported the synthesis and isolation (in solution) of a rather stable benzyl-chromium complex, $C_6H_5CH_2Cr^{++}$, from the reduction of benzyl halides with aqueous chromous perchlorate. The species was formulated as a complex of Cr(III) with the benzyl anion. The complex decomposes slowly at room temperature or more rapidly on heating to give bibenzyl or, in the presence of oxygen, benzaldehyde. Under other conditions, toluene is the major product. It was suggested that the chromic complex had a tendency to dissociate homolytically to give benzyl radical and chromous ion. Alternatively, the composition may be regarded as a complex of Cr(II) with the benzyl radical. The free radical character of the complex was directly demonstrated in these laboratories by Kochi and Rust² by its synthesis from the reaction of phenyl-*tert*-butyl hydroperoxide and chromous sulfate. Workers here³ and elsewhere⁴⁻⁶ have studied the metal ion (especially chromous) reduction of organic halides in considerable detail. Conditions favoring reduction to hydrocarbons or to coupled products have been delineated, and several mechanisms have been proposed. The degree of separation between radical and chromium ion and the lifetime of the separated species are unanswered questions of special interest.

It occurred to us that application of the chromous ion coupling reaction to difunctional halides might provide a convenient and versatile method for synthesizing polyxylylene-type polymers. An especially attractive prospect was that the method might provide substituted polyxylylenes and copolymers not accessible by other methods. The obvious practical incentives were to produce, by copolymerization or structural modifications

of the monomers, tractable, processable polymers which retained the high thermal stability of known xylylene polymers. A second attractive prospect was that polymerization chemistry might make some unique contributions to understanding the mechanism of reaction between benzyl halides and chromous ion.

Essentially all of our work to apply this reaction to the synthesis of variously structured xylylene-type homopolymers has been anticipated in the recent paper of Hoyt et al.⁷ In this report, therefore, we will confine our attention largely to xylylene copolymers derived from *m*- and *p*-xylylene dihalides and to some mechanistic aspects of the reaction.

RESULTS AND DISCUSSION

Homopolymers and Copolymers of *m*- and *p*-Xylylene Dibromide

Chromous chloride coupling reactions were carried out with *m*- and *p*-xylylene dibromides, separately and in 1:1 or 3:1 *p/m* ratios. The polymerization products and their characterization* are presented in Table I.

TABLE I
Homopolymers and Copolymers from *m*- and *p*-Xylylene Dibromides

Feed composition, mole-% of <i>p</i> -isomer	Yield, %	Polymer composition, % <i>p</i> -isomer ^a		η_{inh}^b	Melting point, °C.	T_g , °C.	Crystallinity
		A	B				
0	77	0	—	0.12	80	9	Weak
50	92	48	49	0.19	165	30	Intermediate
75	69	75	78	0.16	310	48	High
100	83	—	100	—	440	58 ^c	High

^a A = fraction soluble in reaction medium (THF); B = fraction insoluble in THF but soluble in boiling diphenyl ether (or benzyl benzoate).

^b Determined in diphenyl ether at 150°C.

^c Extrapolated by use of the Fox equation $1/T_g = (X_A/T_{gA}) + (X_B/T_{gB})$.

The products obtained from the reaction of chromous salts with *p*- and *m*-xylylene dibromide are true random copolymers. They are free of homopolymer fractions, fractions of significantly different composition than the monomer feed, and fractions containing long runs or blocks of either structural unit.

These conclusions are derived from the following facts. (1) Torsional damping curves ($\tan \delta$ versus temperature) each exhibit only a single maximum rather than two peaks typical of binary homopolymer mixtures or -AAA-BBB- block compositions. The maxima shift to higher temperatures with increasing content of *p*-isomer. (2) Soluble and insoluble fractions have nearly the same composition. Poly-*m*-xylylene and poly-*p*-xylylene differ greatly in their solubilities; mixed homopolymers or frac-

* See experimental part for details of the procedures and methods.

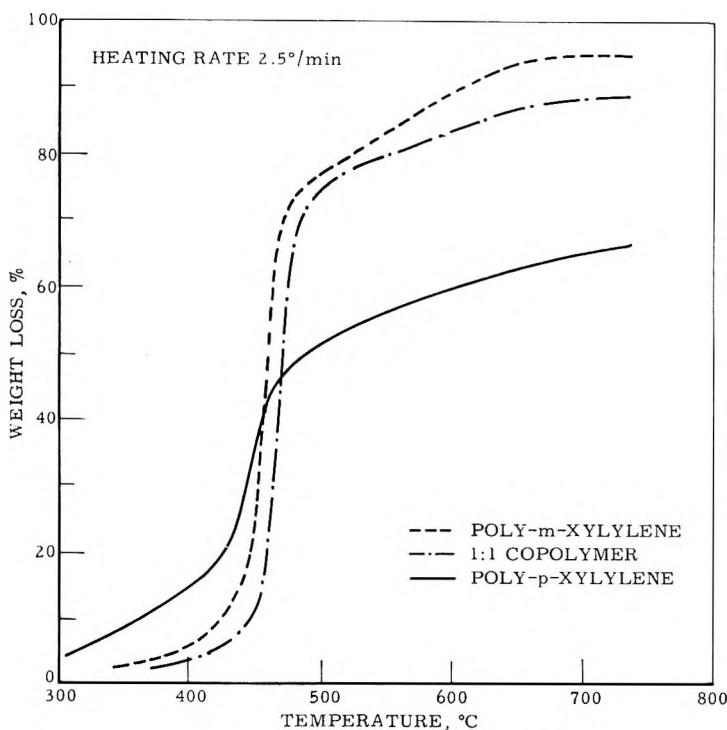


Fig. 1. Thermal stability of polyxylylenes.

tions differing significantly in composition, therefore, would be readily separable. (3) The copolymer compositions closely correspond to the feed compositions. This argument is weakened somewhat by our rather high conversions, but it has force when considered together with (1) and (2). Depletion of either monomer at high conversion must lead to a significant amount of either a soluble fraction rich in *m*-xylylene units or a very much less soluble fraction rich in *p*-xylylene units.

The melting points of the copolymers are intermediate between those of the homopolymers. The 3:1 copolymer is quite crystalline, as indicated by the x-ray diffraction pattern. The spacings at 5.26, 3.93, and 2.78 Å. correspond very closely to those of the α form of poly-*p*-xylylene.⁸ On heating to temperatures above 250°C., the copolymer changes into a different crystalline form having x-ray spacings of poly-*p*-xylylene in the β modification (4.4 Å.).⁸ We conclude that the *m*-units cannot co-crystallize, but act to depress the melting point according to theory.⁹ Further support for this contention is derived from the 1:1 copolymer, which has a lower melting point and a considerably lower degree of crystallinity.

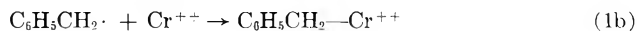
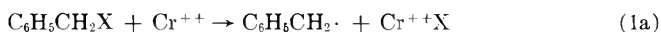
The thermal stability of the copolymers is comparable to that of poly-*p*-xylylene and poly-*m*-xylylene as shown in Figure 1. It is possible, therefore, to prepare tractable polymers with good thermal stability by copolymerization. However, all copolymers prepared in this work were very

brittle. In spite of numerous attempts using different reaction conditions, solvents, and highly purified reagents, we were not able to obtain polymers with inherent viscosities greater than 0.3 dl./g. This corresponds to a molecular weight obviously insufficient to give good mechanical properties.

We have also prepared copolymers of *p*-xylylene and 2,3,5,6-tetramethyl-*p*-xylylene by chromous chloride coupling of the corresponding dibromides. Although neither homopolymer can be fused, the 1:1 copolymer had a melting point of 350°C. and was soluble in hot diphenylmethane. As in the case of the *p/m* xylylene copolymers, molecular weights were not high enough for good mechanical properties.

Mechanism

The formation of the benzyl-chromium complex proceeds in two steps as shown by Kochi and Davis:⁶



Since the complex decomposes to give bibenzyl in good yields, it has been postulated that it dissociates homolytically to Cr^{++} and benzyl radical,¹ which is the reverse of reaction (1b).

We have now been able to demonstrate that free radicals are indeed present in solutions of the benzyl-chromium complex by showing that it initiates the homo- and copolymerization of styrene and methyl methacrylate.* The composition of the styrene-methyl methacrylate copolymer was that expected for a free-radical copolymerization. The methyl methacrylate polymer had the microtacticity, determined by NMR, corresponding to the product of a free-radical polymerization, showing not only that the reaction is initiated by free radicals, but also that it proceeds without interference by the chromium ion.†

The combination of two radicals or, more likely, the reaction of a radical with the complex as proposed by Castro and Kray⁵ would give bibenzyl according to eq. (2).



Slaugh and Raley³ suggest an alternate mechanism [eq. (3)] involving the



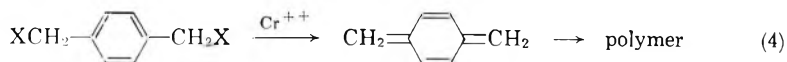
reaction of the benzyl-chromium complex with benzyl halide.

* Kochi and Davis' attempts to trap the radical⁶ with acrylonitrile or butadiene were inconclusive. Similarly, Slaugh and Raley³ were unable to increase the yield of diphenylmethane by addition of the very efficient transfer agent, ethyl thioglycolate, to diphenylmethyl-chromous complex.

† The relative population of syndiotactic, isotactic, and heterotactic triads measured according to the method of Bovey and Tiers¹⁰ is extremely sensitive to changes in the transition state of the propagation reaction. Bamford et al.¹¹ report that free-radical polymerization of MMA with transition metal carbonyls results in a distribution of triads different from that obtained in ordinary free-radical polymerizations of MMA.

Their data amply support this mechanism. Although it cannot account for the formation of bibenzyl from preformed benzyl-chromium complex, which presumably occurs via the reverse of eq. (1b) combined with eq. (2), it appears to be the most important route to bibenzyl when unreacted benzyl halides are present.

The formation of polyxylylenes must be explained by a stepwise reaction of the bifunctional xylylene dihalides. Hoyt et al.⁷ have postulated a quinonedimethane intermediate [eq. (4)] in the case of *p*-xylylene dibromide and 2,5-dimethoxy-*p*-xylylene dibromide to explain the relatively high molecular weight polymers obtained from these two monomers.



Films of poly-*p*-xylylene deposited in the condenser are cited as evidence. Our copolymerization experiments showed equal reactivity ratios for the *p*- and *m*-xylylene dibromides. The quinonedimethane reaction path [eq. (4)], therefore, cannot be a major one since it is not feasible for the *m*-isomer. It is extremely unlikely that there should be a different reaction path for the *m*-isomer which would proceed with exactly the same rate as path (4) for the *p*-isomer. The deposits of polyxylylene film must originate from a minor side reaction. We are unable to support alternate possibilities for the large differences in molecular weight obtainable with different monomers as observed by Hoyt et al.⁷ It is significant, perhaps, that not all monomers capable of forming quinonedimethane intermediates (e.g., poly- $\alpha,\alpha',\alpha',\alpha'$ -tetramethyl-*p*-xylylene and poly-2,5-di-*n*-butoxy-*p*-xylylene) yield high molecular weight polymers.⁷

EXPERIMENTAL

Starting Materials

Tetrahydrofuran was refluxed with and distilled from sodium hydroxide, then refluxed with and distilled from LiAlH_4 through a 36-in. column under nitrogen.

Chromous chloride was obtained from Fisher Scientific Company and used as received.

α,α' -Dibromo-*p*-xylene, obtained from Eastman, was recrystallized from toluene; melting point, 144.5–145°C.

α,α' -Dibromo-*m*-xylene, from Eastman, was recrystallized from toluene; melting point 76.5–77°C.

Polymer Preparation

Preparation of Poly-*m*-xylylene with CrCl_2 . Into a 500-ml. flask with reflux condenser and magnetic stirrer were placed 300 ml. of purified tetrahydrofuran, 26.4 g. (0.1 mole) of α,α' -dibromo-*m*-xylene, and 27 g. (0.22 mole) of chromous chloride. The latter was handled under nitrogen. The mixture was then refluxed with stirring.

Chromous chloride is slightly soluble in THF under formation of a pale green complex, $\text{CrCl}_2 \cdot 2\text{THF}$.¹² As the reaction proceeds, the mixture turns from green to blue, with formation of the complex $\text{CrCl}_3 \cdot 3\text{THF}$.¹²

After 48 hr. of refluxing the mixture was allowed to cool to room temperature and filtered from the chromium salts. An excess of water was added to the filtrate, and the fine precipitate was separated by centrifugation. It was dried and redissolved in 150 ml. hot benzene. On standing overnight, a fraction of the polymer had precipitated in a gelatinous form. Filtration gave 2.79 g. of product, having a melting point of 80°C. and a molecular weight (\bar{M}_n) of 5700.

To the filtrate was added an equal volume of methanol, which precipitated another 4.30 g. of polymer, with a melting point of 65°C. and a molecular weight (\bar{M}_n) of 3800.

Evaporation of the filtrate from this fraction left 0.92 g. of rather sticky material, $\bar{M}_n = 960$; total yield, 8.01 g. = 77%.

Preparation of a 1 : 1 Copolymer of *p*- and *m*-Xylylene. A mixture of 300 ml. purified THF, 8.0 g. (0.03 mole) each of α, α' -dibromo-*m*- and -*p*-xylylene and 18.5 g. (0.15 mole) of CrCl_2 was refluxed for 72 hr. The chromium salts were filtered off, and from the filtrate by addition of an excess of methanol was precipitated 5.46 g. of crude product which had a greenish color. The material was soluble in hot toluene but precipitated on cooling. Centrifugation of the hot toluene solution removed most of the green color.

The filter cake was washed with water to remove the bulk of the chromium salts; the water-insoluble residue was then extracted with boiling diphenylmethane, yielding another 0.35 g. of material. The total yield was 5.79 g. (92%). Infrared analysis showed the first fraction to contain 48% *p*-units and the second fraction 49% *p*-units, both of them very close to the ratio of the charge (50% *p*).

Preparation of 3 : 1 Copolymer of *p*- and *m*-Xylylene. Preparation was similar to that described for the 1:1 copolymer, except on a smaller scale and, of course, with a different *p/m* ratio. From the THF solution was obtained 3.27 g. of polymer containing 75% *p*-units (as determined by infrared analysis). Extraction of the THF insolubles with hot diphenylmethane gave another 1.08 g. of polymer, containing 78% *p*-units (by infrared analysis). The total yield was 4.35 g. (69%). An additional 1.6 g. was obtained by evaporation of the methanol-THF solution.

Polymer Characterization

Infrared Analysis of Copolymers of *p*- and *m*-Xylylene. The method is based on the absorption peaks at 6.65 μ (poly-*p*-xylylene) and 14.35 μ (poly-*m*-xylylene). A calibration curve was prepared by blending the appropriate amounts of poly-*p*-xylylene and poly-*m*-xylylene and pressing KBr pellets. It is assumed that blends of the homopolymers will have the same infrared absorption as copolymers of identical overall composition. The precision of the method is estimated to be $\pm 5\%$.

Measurement of Glass Transition Temperatures. A torsion pendulum with a Beckman time interval meter and digital recorder was used for the dynamic mechanical measurements.* The samples were prepared by blending 25–30% of the polymer into polystyrene which was molded into a test specimen approximately $0.65 \times 0.17 \times 7.5$ cm. The frequency of oscillation was about 1 cycle/sec. Measurements were made over the whole damping region and the loss tangents ($\tan \delta$) calculated. The peak of the $\tan \delta$ versus temperature plot was taken as the glass transition temperature.

Melting Point. Melting points were determined on a Leitz polarizing microscope with hot stage. Disappearance of birefringence was taken as the melting point.

Polymerization of Styrene With Benzyl–Chromium

To a solution of 3 ml. of Triton X 100 in 100 ml. of distilled deaerated water was added 10 ml. of 0.64*M* chromous perchlorate solution³ and 0.8 ml. (0.0032 mole) of benzyl bromide. The mixture was agitated to form the benzyl–chromium complex; then 36 g. of distilled styrene was added. A quantitative yield of polystyrene, $\eta_{inh} = 0.44$, was obtained after 22 hr. of reaction at room temperature.

Copolymerization of Styrene and Methyl Methacrylate

The same procedure as above was used, except the monomer composition was 20 g. (0.192 mole) of styrene and 20 g. (0.198 mole) of methyl methacrylate. After 16 hr. at room temperature there was obtained 17.9 g. of copolymer containing 58% styrene.

Polymerization of Methyl Methacrylate With Benzyl–Chromium

Reaction conditions were as described in the two previous examples. The yield of polymer after 22 hr. at room temperature was 15.9 g. According to NMR analysis the polymer contained 5% isotactic, 32% heterotactic, and 63% syndiotactic triads, which is very close to the values reported in the literature for free-radical polymerization.^{10,11}

We would like to thank Mr. J. L. Jungnickel for the NMR measurements and Mr. T. C. Yao for the x-ray diagrams.

References

1. Anet, F., and E. Leblanc, *J. Am. Chem. Soc.*, **79**, 2649 (1957).
2. Kochi, J., and F. F. Rust, *J. Am. Chem. Soc.*, **83**, 2017 (1961).
3. Slauch, L. H., and J. H. Raley, *Tetrahedron*, **20**, 1005 (1964).
4. Castro, C. E., *J. Am. Chem. Soc.*, **83**, 3262 (1961).
5. Castro, C. E., and W. C. Kray, Jr., *J. Am. Chem. Soc.*, **85**, 2768 (1963).
6. Kochi, J. K., and D. Davis, *J. Am. Chem. Soc.*, **86**, 5264 (1964). We thank Dr. Kochi for a preprint of this paper.

* For description of apparatus, see Weir.¹³

7. Hoyt, J. M., K. Koch, C. A. Sprang, S. Stregovsky, and C. E. Frank, paper presented to Division of Polymer Chemistry at 148th Meeting, American Chemical Society; *Polymer Preprints*, **5**, 380 (1964).
8. Brown, C. J., and A. S. Farthing, *J. Chem. Soc.*, **1953**, 3270.
9. Flory, P. J., *Trans. Faraday Soc.*, **51**, 848 (1955).
10. Bovey, F. A., and G. V. D. Tiers, *J. Polymer Sci.*, **44**, 173 (1960).
11. Bamford, C. H., M. S. Blackie, and C. A. Finch, *Chem. Ind. (London)*, **1962**, 1763.
12. Kern, R. J., *J. Inorg. Nuclear Chem.*, **24**, 1105 (1962).
13. Weir, F. E., *SPE Trans.*, **2**, 302 (1962).

Résumé

On a préparé des copolymères du *p*- et du *m*-xylylène par combinaison des dihalogénures correspondants avec le chlorure chromeux. On propose un mécanisme à plusieurs étapes pour la formation des polyxylylènes, et on met en évidence l'existence de radicaux libres dans la décomposition du complexe intermédiaire organo-chrome.

Zusammenfassung

Copolymere von *p*- und *m*-Xylylen wurden durch Kopplung der entsprechenden Dihalogenide mit Chromchlorid dargestellt. Für die Bildung von Polyxylylenen wird ein schrittweiser Mechanismus angenommen; das Auftreten freier Radikale bei der Zersetzung des intermediären Organochromkomplexes wird nachgewiesen.

Received January 19, 1965

Revised February 25, 1965

Prod. No. 4674A

Preparation and Polymerization of Vinyl Esters of Chloro- and Hydroxystearic and Eicosanoic Acids*

C. S. MARVEL, J. H. GRIFFITH, and J. L. COMP,† *Department of Chemistry, University of Arizona, Tucson, Arizona,*
and T. H. APPLEWHITE and L. A. GOLDBLATT,‡ *Western Utilization Research and Development Division, U. S. Department of Agriculture, Albany, California*

Synopsis

Homopolymers and copolymers with vinyl acetate and vinyl chloride have been prepared from the vinyl esters of 9-chlorostearic acid, 12-chlorostearic acid, 14-chloroeicosanoic acid, 9-hydroxystearic acid, 9,10-dihydroxystearic acid, 14-hydroxyeicosanoic acid, and 8-(1,3-dioxylone-2-yl) octanoic acid.

Previous work¹⁻⁴ has shown that the number, type, and location of the polar or nonpolar substituents in the fatty acid portion of vinyl esters influence the properties of their vinyl chloride copolymers. To determine further the effect of the substituent position on the ester side chain, the mono-, chloro- and hydroxystearates and -eicosanoates were prepared. Various homopolymers and copolymers with vinyl acetate and vinyl chloride were prepared and are described below.

RESULTS AND DISCUSSION

Ester Synthesis

Vinyl 9- and 12-hydroxystearates and vinyl 14-hydroxyeicosanoate were prepared from the hydroxy acids, vinyl acetate, and mercuric sulfate by slight modification of the method of Adelman⁵ used by Shono and Marvel in the original study on vinyl 12-hydroxystearate.⁴ The vinyl 9- and 12-chlorostearates and vinyl 14-chloroeicosanoate were prepared from the vinyl hydroxy esters by a modification of the method⁶ for converting alcohols to chlorides with thionyl chloride and pyridine. This method has been

* This is a partial report of work done under contract with four Utilization and Development Divisions, Agricultural Research Service, U. S. Department of Agriculture, and authorized by the Research and Marketing Act. The contract was supervised by Dr. J. C. Cowan of the Northern Division.

† Present address: Southwest Texas State College, San Marcos, Texas.

‡ Present address: Southern Utilization Research and Development Division, New Orleans, Louisiana.

noted⁶ to yield considerable olefin when applied to secondary alcohols. Under the conditions employed here, 10–15% olefin was obtained (infrared, nuclear magnetic resonance, gas-liquid chromatography, and elemental analysis). Because of limited quantities of starting materials, no attempt was made to remove these impurities; thus the polymerization studies were carried out on the chlorine-containing monomers of about 85–90% purity. This factor perhaps accounted for some of the problems encountered. The hydroxy acid starting materials were obtained by hydrogenation of dimorphecolic acid⁷ (9-hydroxy-*trans*, *trans*-10,12-octadecadienoic acid), ricinoleic acid (12-hydroxy-*cis*-9-octadecenoic acid), and lesquerolic acid⁸ (14-hydroxy-*cis*-11-eicosenoic acid).

The vinyl 9,10-dihydroxystearate was obtained by hydrolysis of vinyl 9,10-epoxystearate with fluoboric acid. Vinyl 8-(1,3-dioxylone-2-yl) octanoate (the ethylene glycol acetal of vinyl azelaaldehyde) was prepared by the method of Pryde, Moore, and Cowan.⁹

Polymerization

Homopolymers of the vinyl esters (Table I) were easily obtained in benzene, but the chloro derivatives homopolymerized very slowly in an emulsion system.

Solid, colorless products were obtained when the vinyl esters were copolymerized with vinyl acetate (Table II) or vinyl chloride (Table III). The vinyl chloride copolymers of the acetal vinyl esters were completely insoluble in tetrahydrofuran, dimethylformamide, dimethyl sulfoxide, acetone, and benzene. A semifluid gel is obtained in tetrahydrofuran, but the supernatant liquid contained no polymer after low-speed centrifugation for 1 min.

The vinyl acetate copolymers were soft materials and readily adhered to glass or metal surfaces. Until the solvent was removed, the copolymers were very tacky.

EXPERIMENTAL

Preparation of Vinyl Esters

Vinyl 9-Hydroxystearate. Copper resinate (80 mg.) and mercuric acetate (960 mg.) were dissolved in 320 ml. of vinyl acetate (Eastman) and 0.48 g. of concentrated sulfuric acid was added with ice cooling and stirring. The solution was allowed to attain ambient temperature and 40 g. of 9-hydroxystearic acid (m.p. 83.5–84.5°C.) was dissolved therein at ca. 50°C. The solution, protected from light, was allowed to stand at room temperature for 3–4 days. The solution was filtered, washed with two portions of ice water (1600 and 300 ml.), and sodium acetate trihydrate (0.75 g.) was added with gentle mixing. Brine (10 ml. of a 20% solution) was added to promote phase separation. The organic phase was separated and evaporated under reduced pressure below 40°C. bath temperature to remove most

of the vinyl acetate. The residue was taken up in 300 ml. of ether, washed with three portions (500, 250, and 250 ml.) of 20% aqueous sodium chloride, 400 ml. of 0.05*N* sodium carbonate solution, and water until washings were neutral. The ether solution, dried over sodium sulfate, was passed through a 50 g. column of activated alumina and evaporated. The dark brown residue (35–40 g.) was dissolved in 10 volumes of hot petroleum ether (b.p. 60–70°C.), decolorized with charcoal, and stored at 45°C. Colorless crystals (30–35 g., m.p. 50–53°C.) were obtained. Recrystallization from hexane gave 25–30 g. of pure vinyl 9-hydroxystearate (m.p. 53.5–54.8°C.). This material showed a single spot when examined by thin layer chromatography (TLC) on silica gel with 7:3 pentane–ether solvent.

ANAL. Calcd. for $C_{20}H_{38}O_3$: C, 73.6%; H, 11.7%. Found: C, 73.7%; H, 11.7%.

Vinyl 12-Hydroxystearate.⁴ This compound prepared as above from 12-hydroxystearic acid had m.p. 57–58°C. (lit. value⁴ 55–56°C.) and showed a single spot when analyzed by TLC.

ANAL. Calcd. for $C_{20}H_{30}O_3$: C, 73.6%; H, 11.7%. Found: C, 73.7%; H, 11.4%.

Vinyl 14-Hydroxyeicosanoate. This compound, prepared as above in similar yields from 14-hydroxyeicosanoic acid (m.p. 83.5–84.5°C.), had m.p. 63.0–64.5°C. and showed a single spot by TLC.

ANAL. Calcd. for $C_{22}H_{42}O_3$: C, 74.5%; H, 11.9%. Found: C, 74.6%; H, 11.9%.

Vinyl 14-Chloroeicosanoate. Vinyl 14-hydroxyeicosanoate (25 g., 0.07 mole) in 150 ml. of carbon tetrachloride was cooled in ice and 10 ml. of distilled thionyl chloride in 50 ml. of carbon tetrachloride was added slowly. The mixture was allowed to warm to room temperature, was treated with 11.4 ml. of pyridine, and heated on a steam bath for 2 hr. After filtration the solvent was removed under reduced pressure. The residue in 300 ml. of ether was washed four times with 50 ml. portions of water, four times with 50 ml. portions of 0.02*N* sodium carbonate solution, and with water until washings were neutral. The ether layer was dried over magnesium sulfate, decolorized with charcoal, and filtered through a cake of activated alumina. On evaporation of the solvent a colorless oil (22.5 g.) remained which had n_D^{25} 1.4609, showed one major and one minor spot on TLC (CCl_4 developing solvent) and contained approximately 12% olefin impurity as assessed by NMR proton count.

ANAL. Calcd. for $C_{22}H_{41}O_2Cl$: C, 70.8%; H, 11.1%; Cl, 9.5%. Found: C, 71.5%; H, 11.1%; Cl, 7.5%.

Vinyl 9,10-Dihydroxystearate. Vinyl 9,10-epoxystearate was prepared from the vinyl ester of Emersol and 40% peracetic acid by the procedure of Swern.¹⁰ It showed n_D^{30} 1.4530, acid value <1, iodine value 76.6, and oxirane oxygen 4.6%. A solution of 18.5 g. of vinyl 9,10-epoxystearate in 15 ml. of benzene was added dropwise to 10 g. of 25% fluoboric acid at 35°C. The addition to the vigorously agitated fluoboric acid solution was complete in 15 min., and the mixture was stirred further for 1 hr. at 35°C. The

oily layer was diluted with ether and washed with a saturated sodium bicarbonate solution and then with water until the water was neutral. The solution was dried over anhydrous sodium sulfate. The solvent was stripped under reduced pressure and the vinyl 9, 10-dihydroxystearate was recrystallized from acetone in 50% yield [m.p. 62.5–64°C., acid value <1, iodine value 74.4 (calcd. 74)]. Thin layer chromatography on silicic acid with a 4/6 ratio of chloroform to ethyl acetate gave only one spot.

ANAL. Calcd. for $C_{20}H_{38}O_4$: C, 70.13%; H, 11.18%; OH, 9.9%. Found: C, 70.22%; H, 11.29%; OH, 9.3%.

Vinyl 9-Chlorostearate. The crude product was prepared in a manner similar to that used above. The preparation had n_D^{25} 1.4601, showed a major and minor spot on TLC, but contained about 14% of an unsaturated impurity (GLC and NMR) from dehydrohalogenation.

ANAL. Calcd. for $C_{20}H_{37}O_2Cl$: C, 69.6%; H, 10.8%; Cl, 10.3%. Found: C, 70.2%; H, 10.7%; Cl, 8.5%.

Vinyl 12-Chlorostearate. This compound was prepared three times by the above method and showed n_D^{25} of 1.4595, 1.4598, and 1.4603.

The sample with highest refractive index was analyzed but still contained a 12% unsaturated impurity assessed by TLC, GLC, and NMR.

ANAL. Calcd. for $C_{20}H_{37}$: C, 69.6%; H, 10.8%; Cl, 10.3%. Found: C, 70.3%; H, 10.9%; Cl, 8.6%.

Analyses

GLC analyses were carried out with diethylene glycol succinate as stationary phase; TLC was on Silica Gel G, and NMR in CCl_4 with tetramethylsilane as the internal standard.

Polymerization of the Vinyl Esters

Solution Homopolymerization of the Vinyl Esters. A tube formed from a 24/40 standard taper joint and a stopcock (see Fig. 1) were used for the solution homopolymerization of the following vinyl esters: vinyl 9-chlorostearate, vinyl 12-chlorostearate, vinyl 9-hydroxystearate, vinyl 9,10-dihydroxystearate, vinyl 14-chloroeicosanoate, vinyl 14-hydroxyeicosanoate and vinyl 8-(1,3-dioxylone-2-yl) octanoate. Table I contains the data for each polymerization. The general procedure described below was used for all of the solution polymerizations.

A stream of dry nitrogen was bubbled through a benzene solution (6 ml.) of 1.53 g. of the vinyl ester and 0.025 g. of 2,2'-azobisisobutyronitrile in a polymerization tube. After passing nitrogen through the solution for 10 min. to remove oxygen, the tube was capped and the solution was frozen in a Dry Ice-acetone bath. The tube was evacuated to a pressure of 0.1 mm. and the stopcock closed. The polymerization tube was allowed to warm to room temperature and placed in a Fisher Isotemp oven at 65°C. After 20–70 hr., a viscous oil or solid was obtained when the benzene solution



Fig. 1. Polymerization tube.

was poured into 50 ml. of methanol. The polymer separated out as a viscous oil or semisolid on the side and bottom of the beaker. The polymer was redissolved in 5 ml. of tetrahydrofuran and reprecipitated by dropwise addition to 50 ml. of methanol. After four reprecipitations, the polymer was dried under reduced pressure to remove residual solvent. Inherent viscosity, softening range and elemental analysis were determined and are shown in Table I.

Emulsion Homopolymerization of the Vinyl Esters. The vinyl ester homopolymerization in an emulsion system is illustrated in the following manner. A 1.0 g. sample of the vinyl ester, 0.1 g. of potassium persulfate and 5 ml. of water were placed in a 50 ml. (1 in. O.D. \times 7 in.) pressure bottle (Ace glass T1506). After a stream of nitrogen was bubbled through the mixture for 20 min., 0.25 g. of Triton X-301 emulsifier was added. The bottle was flushed with nitrogen and sealed with a crown-type bottle cap. The polymerization bottle was tumbled for 60–70 hr. in a 60°C. water bath. The polymer emulsion was poured into 250 ml. of a saturated salt solution. A gummy or solid polymer was separated, and the salt solution was de-

TABLE I
Solution and Emulsion Homopolymerization of the Vinyl Esters^a

Vinyl ester, sample number (polymerization system)	Wt. ester, g.	Reac- tion time, hr.	Con- ver- sion, %	Inherent viscosity ^b	Softening range, °C.	Reprecipitation		Anal. calcd.			Anal. found				
						Solvent	Nonsolvent	C, %	H, %	Cl, %	C, %	H, %	Cl, %		
Vinyl 9-chlorostearate, C ₂₀ H ₃₇ O ₂ Cl								69.63	10.81	10.28					
I-148-1 (solution)		20	36	0.101 ^c	25	Benzene	Methanol				69.58	10.93	9.85		
I-149-15 (emulsion)		155	25	0.155	25	THF	Water				70.48	8.83	9.42		
Vinyl 12-chlorostearate, C ₂₀ H ₃₅ O ₂ Cl								69.63	10.81	10.28					
I-148-2 (solution)		70	60	0.142	25	THF	Methanol				70.13	10.69	10.05		
I-149-16 (emulsion)		155	40	0.157	25	THF	Water				70.12	10.93	10.05		
Vinyl 14-chloroeicosanoate, C ₂₂ H ₄₁ O ₂ Cl								70.88	11.08	9.50					
I-148-4 (solution)		40	20	0.112 ^c	25	Benzene	Methanol				70.95	11.56	9.30 ^d		

TABLE II
 Solution Copolymerization of the Vinyl Esters with Vinyl Acetate (Molar Ratio 1:9)^a

Vinyl ester (sample number) ^b	Conver- sion, % ^c	Inherent viscosity ^d	Softening range, °C.	Reaction time, hr.	Anal. calcd.			Anal. found		
					C, %	H, %	Cl, %	C, %	H, %	Cl, %
Vinyl 9-chlorostearate (I-148-6)	36	1.47	25	63	60.07	8.19	3.16	59.40	8.24	3.32
Vinyl 12-chlorostearate (I-148-9)	55	0.362	25	30	60.07	8.19	3.16	61.00	8.60	3.86
Vinyl 9-hydroxystearate (I-148-10)	74	0.38	25	63	61.07	8.42	3.00	61.73	8.68	
Vinyl 14-chloroeicosanoate (I-149-13)	54	0.318	25	40.5	60.64	8.42	3.00	61.84	8.73	3.68
Vinyl 14-hydroxyeicosanoate (I-149-14)	82	0.328	25	63	61.63	8.65		61.58	8.70	

^a At 65°C. in a Fisher Isotemp oven.

^b Each polymerization batch contained about 5 g. of monomers (0.393 mole VAC and 0.00435 mole vinyl ester).

^c Conversion measured after four reprecipitations from a tetrahydrofuran solution into 50:50 water:methanol.

^d Inherent viscosity of a tetrahydrofuran solution (0.4 g. of polymer/100 ml. of solvent) measured at 30°C. in a number 50 Cannon-Fenske viscometer.

TABLE III
 Emulsion Copolymerization of the Vinyl Esters with Vinyl Chloride^a

Vinyl ester (polymerization batch)	Wt. ester, g.	Wt. VCl, g.	Conversion, % ^b	Melting point, °C.	Inherent viscosity ^c	Anal. found			VCl/V _E ^d
						C, %	H, %	Cl, %	
Vinyl 9-chlorostearate									
92-1	2.0	8.0	69	160-180	1.21	45.14	5.99	44.82	13.9/1
92-2	3.0	7.0	63	155-170	1.11	47.00	6.19	41.80	10.2/1
Vinyl 14-chlorostearate									
92-3	2.0	8.0	52	<45	0.72	45.23	5.99	44.67	14.1/1
92-4	3.0	7.0	45	<45	0.69	47.14	6.15	41.98	9.9/1
Vinyl 9-hydroxystearate									
90-1	2.0	8.0	65	145-165	0.79	45.47	6.16	44.87	19.6/1
90-2	2.5	7.5	68	180-200	0.83	47.29	6.48	42.48	15.5/1
90-3	3.0	7.0	54	185-195	0.87	47.31	6.47	42.66	15.8/1
Vinyl 9,10-dihydroxystearate									
90-4	2.0	8.0	50	155-165	1.05	44.01	5.79	46.42	23.9/1
90-5	2.5	7.5	65	165-180	0.93	45.71	6.39	44.40	19.4/1
90-6	3.0	7.0	45	180-190	2.16	45.73	6.10	44.41	19.0/1
Vinyl 14-hydroxyicosanoate									
90-7	2.0	8.0	63	165-175	0.80	44.30	5.83	46.55	25.8/1
90-8	2.5	7.5	65	170-185	1.60	44.35	5.96	46.65	26.1/1
90-9	3.0	7.0	55	183-210	0.87	46.19	6.83	44.42	19.5/1
Vinyl 8-(1,3-dioxylone-2-yl) octanoate									
86-1	2.0	8.0	30	>360	Insol.	43.86	5.56	46.16	16.8/1
86-2	2.5	7.5	53	>360	Insol.	43.79	5.69	46.02	16.5/1
86-3	3.0	7.0	68	>360	Insol.	44.17	5.75	45.22	15.1/1

^a Polymerization batches were tumbled in a constant temperature bath at 60°C. for 72 hr.

^b Conversion after nine reprecipitations from tetrahydrofuran into water and three reprecipitations into methanol.

^c Inherent viscosity of a tetrahydrofuran solution (0.4 g. of polymer/100 ml. of solvent) measured at 30°C. in a number 50 Cannon-Fenske viscometer.

^d Molar ratio of monomer units (vinyl chloride/vinyl ester) calculated on basis of chlorine analysis.

canted. The emulsifier was removed from the polymer by four to six reprecipitations from tetrahydrofuran into water. The polymers were dried under vacuum to remove residual solvent. The vinyl 9- and vinyl 12-chlorostearate polymerization batches had an additional 0.05 g. of potassium persulfate added after 70 hr. and were returned to the tumbler for another 85 hr. Table I contains the data for each polymerization. The inherent viscosity was determined in tetrahydrofuran solution.

Solution Copolymerization of the Vinyl Esters with Vinyl Acetate.

Copolymers containing 10 mole-% vinyl ester and 90 mole-% vinyl acetate were prepared in a benzene solution with 2,2'-azobisisobutyronitrile as an initiator. Table II contains the pertinent data for the vinyl ester-vinyl acetate copolymers. The general procedure is described below and some slight differences are noted.

Approximately 0.0393 mole of vinyl acetate, 0.00435 mole of vinyl ester, 0.030 g. of 2,2'-azobisisobutyronitrile, and 10 ml. of benzene were placed in a tube (see Fig. 1). After bubbling nitrogen through the benzene solution for 10 min., the top was placed on the tube. The tube was frozen in a Dry Ice-acetone bath and evacuated to a pressure of 0.1 mm. After the stopcock was closed and the tube warmed to room temperature, the tubes were placed in a Fisher Isotemp oven at 65 or 68°C. for 30-63 hr.

After cooling the polymerization tube to room temperature, the vinyl 9-chlorostearate-vinyl acetate copolymer was precipitated by adding the benzene solution to 60 ml. of methanol and reprecipitated four times from 10 ml. of tetrahydrofuran into 60 ml. of methanol. A cloudy solution was obtained when the other vinyl ester-vinyl acetate copolymer solutions were poured into methanol. These copolymers precipitated when water was added to the methanol-benzene solution and were reprecipitated four times from a solution of about 10 ml. of tetrahydrofuran into about 100 ml. of a 50:50 methanol-water mixture. The copolymers were dried under reduced pressure to remove residual solvent. The inherent viscosities were determined on tetrahydrofuran solutions of the polymers (0.4 g. of polymer/100 ml. of solvent).

Emulsion Copolymerization of the Vinyl Esters with Vinyl Chloride.

Vinyl chloride copolymers containing 20, 25, and 30 wt.-% starting charge of the vinyl ester were prepared in an emulsion system. Table III contains the data for these copolymers prepared in the following manner.

A 110-ml. polymerization tube (Ace glass T1506, 1.5 in. O.D. \times 7 in.) was charged with the appropriate amount of the vinyl ester, 3.0 g. of Triton X-301 emulsifier, 4.0 ml. of 2.5% potassium persulfate, and 40 ml. of deoxygenated pH 7.0 buffer solution. The tube was cooled in a Dry Ice-acetone bath and a slight excess of vinyl chloride was added. After the excess vinyl chloride vaporized, the tube was capped. The tube, containing 10 g. of monomer, was tumbled at 60°C. for 72 hr. and the polymer coagulated by pouring the emulsion into a saturated salt solution. After washing three times with water and methanol, the precipitated polymer was dissolved in tetrahydrofuran and reprecipitated a total of nine times into water

and three times into methanol. The polymer was dried under reduced pressure to remove residual solvent. The softening ranges were determined on a Kofler hot stage and the inherent viscosities were determined on 0.2% tetrahydrofuran solutions.

The authors are indebted to Mr. J. L. O'Donnell, United States Department of Agriculture, Agricultural Research Service, Northern Utilization Research and Development Division, Peoria, Illinois, for the preparation of vinyl 9,10-dihydroxystearate and to Mr. D. J. Moore of the same laboratory for the preparation of vinyl 8-(1,3-dioxylone-2-yl) octanoate.

They also gratefully acknowledge technical assistance in the preparation of the other chloro and hydroxy compounds from Mrs. G. Piersee of the Western Utilization Research and Development Division, Albany, California.

References

1. Port, W. S., E. F. Jordan, Jr., W. E. Palm, P. L. Witnauer, J. E. Hansen, and D. Swern, *Ind. Eng. Chem.*, **47**, 472 (1955).
2. Marvel, C. S., J. C. Hill, J. C. Cowan, J. P. Friedrich, and J. L. O'Donnell, *J. Polymer Sci.*, **A2**, 2523 (1964).
3. Marvel, C. S., T. K. Dykstra, and F. C. Magne, *J. Polymer Sci.*, **62**, 369 (1962).
4. Shono, T., and C. S. Marvel, *J. Polymer Sci.*, **A1**, 2067 (1963).
5. Adelman, R. L., *J. Org. Chem.*, **14**, 1057 (1949).
6. Frazer, M. J., W. Gerrard, G. Machell, and B. D. Shepherd, *Chem. Ind. (London)* **1954**, 931.
7. Smith, C. R., Jr., T. L. Wilson, E. H. Melvin, and I. A. Wolff, *J. Am. Chem. Soc.*, **82**, 1417 (1960).
8. Smith, C. R., Jr., T. L. Wilson, T. K. Miwa, H. Zobel, R. L. Lohmar, and I. A. Wolff, *J. Org. Chem.*, **26**, 2903 (1961).
9. Pryde, E. H., D. J. Moore, and J. C. Cowan, *J. Am. Oil Chemists' Soc.*, in press.
10. Swern, D., U. S. Pat. 3,020,292 (February 6, 1962).

Résumé

On a préparé des homopolymères et des copolymères avec l'acetate de vinyle et le chlorure de vinyle à partir des esters vinyliques de l'acide 9-chlorostéarique, de l'acide 12-chlorostéarique, de l'acide 14-chloroeicosanoïque, de l'acide 9-hydroxystéarique, de l'acide 9,10-dihydroxystéarique, de l'acide 14-hydroxeicosanoïque et de l'acide 8-(1,3-dioxylone-2-yl) octanoïque.

Zusammenfassung

Homopolymere und Vinylacetat- sowie Vinylchloridcopolymer wurden aus Vinyl-estern von 9-Chlorstearinsäure, 12-Chlorstearinsäure, 14-Chloreicosansäure, 9-Hydroxystearinsäure, 9,10-Dihydroxystearinsäure, 14-Hydroxeicosansäure und 8-(1,3-Dioxylon-2-yl)octansäure dargestellt.

Received February 5, 1965
Prod No. 4681A

Molecular Motions of Polymers Having Helical Conformation. I. Poly(ethylene Glycol) and Polyoxymethylene

KUNIO HIKICHI and JIRO FURUICHI, *Department of Polymer Science, Faculty of Science, Hokkaido University, Sapporo, Japan*

Synopsis

In order to study molecular motion characteristic of a helical polymer, proton magnetic resonance spectra and the complex dielectric constants ϵ^* for a wide frequency range have been measured in the temperature region between 90°K. and the melting point for poly(ethylene glycol), which is thought to be helical in the solid state. The molecular weights of the samples are 4000, 1000, and 400. These results suggest that a molecular motion such as rotation or oscillation is able to occur even in crystalline regions well below the melting point. The temperature at which this type of molecular motion begins seems to be independent of the molecular weight of the samples, although the melting point is found to depend markedly on molecular weight. X-ray and dilatometric measurements were carried out for the same samples and indicate the absence of a crystalline phase transition (first-order transformation) at the temperature region where the narrowing of the NMR line width of PEG is observed. The results for another helical polymer, polyoxymethylene, are also presented.

Introduction

In recent years, there has been an increasing awareness of the wide-spread occurrence of helical polymer molecules. For example, polytetrafluoroethylene,^{1,2} polyoxymethylene (POM),^{3,4} poly(ethylene glycol) (PEG),^{4,5} polypeptides,^{6,7} etc., are all known to be helical in structure. Polytetrafluoroethylene, which is a typical example of a helical polymer molecule (13_6 helix), is known to undergo rotation about the helical axis in crystalline regions at room temperature.^{8,9} Such a type of molecular motion is thought to be characteristic of the helix. It would be desirable to study the molecular motions of other helical polymer molecules carefully in order to examine the occurrence of such a type of molecular motion characteristic of the helix.

An investigation of molecular motion of poly(ethylene glycol) was made by Slichter¹⁰ using the nuclear magnetic resonance (NMR) method. He reported that the resonance line consists of a narrow component and a broad component at room temperature and that the broad component of the resonance line becomes narrow at a comparatively lower temperature than the melting point of this polymer.

Recently, Read¹¹ has studied molecular motions of this polymer by means of mechanical measurements and has suggested the existence of a mechanical relaxation due to a crystalline mechanism at about 250°K. In a previous brief report of NMR measurements,¹² we have suggested that molecules in crystalline regions may begin to undergo rotational motions above 270°K.

The purpose of the present work is to study the above phenomena of PEG in detail by comparing the results of NMR measurements with other experimental results, that is, dielectric, x-ray, and thermal expansion measurements. Possibilities of the existence of a crystalline phase transition such as seen in polytetrafluoroethylene are also examined for PEG.

Results of the NMR measurements of another helical polymer molecule, polyoxymethylene (POM), are also presented and are discussed with respect to the molecular structure.

Experimental

Specimens used in this work were commercial poly(ethylene glycol) samples having molecular weights of 4000, 1000, and 400 which were obtained from Wako Pure Chemical Industry Co., Ltd. (Japan). Average molecular weights and melting points T_m of these specimens are listed in Table I together with the NMR narrowing temperature T_n and the total molecule length. The polyoxymethylene sample used in the NMR experiments was Delrin acetal resin (du Pont).

Proton magnetic resonance spectra were observed by means of a Pound-Watkins type spectrometer¹³ (Japan Electron Optics Laboratory Co., Ltd.) over a temperature range from 90°K. to the melting point of each specimen. The main static field was kept at about 3000 gauss. Each specimen used in the NMR experiments was packed in a glass tube and sealed off after evacuating above the melting point for the PEG specimens and at about 400°K. for POM to eliminate small amount of water absorbed in the polymer.

TABLE I
Characteristic of Specimens

Specimen	M.W.	T_m , °K.	T_n , °K.	Total length, A.
Carbowax 20 M	12,000	336		840
Carbowax 6000	6,000			415
PEG 4000	4,000	323	273	280
PEG 1000	1,000	308	273	70
PEG 400	400	273	(273)	28

The real and imaginary components of the dielectric constants, ϵ' and ϵ'' , were measured over a frequency range from 30 cycles/sec. to 1 M-cycle/sec. and in a temperature range from 220 to 320°K. The specimen for this measurement was a molded sheet of PEG 4000. Owing to an

ambiguity in the dimension of our specimen, relative values of ϵ' and ϵ'' were obtained in this case.

X-ray measurements were carried out by a diffractometer for a powdered specimen of PEG 4000 from 80°K. up to the melting point. Bragg d values of several diffraction peaks were measured as a function of temperature. No attempt was made to index each diffraction peak or to determine the crystal structure of this polymer, because the purpose of this experiment was to determine the existence of a phase transition.

Thermal expansion measurements were also carried out by means of a dilatometer over a temperature range of 200°K. to the melting point for the specimen of PEG 4000.

Results

The results of the proton magnetic resonance for PEG indicate that the resonance line consists of only one broad component at the lowest temperature. With increasing temperature, the resonance line becomes complex and splits into two components, broad and narrow.

Figure 1 shows the line widths as a function of temperature for PEG 4000, 1000, and 400. The line width was taken as the separation of the maximum and minimum of the derivative absorption curve in gauss.

A rather rapid narrowing of the broad component is found in the temperature range from 270°K. to just below the melting point for PEG 4000. The variation of the line width for PEG 1000 is similar to that for PEG

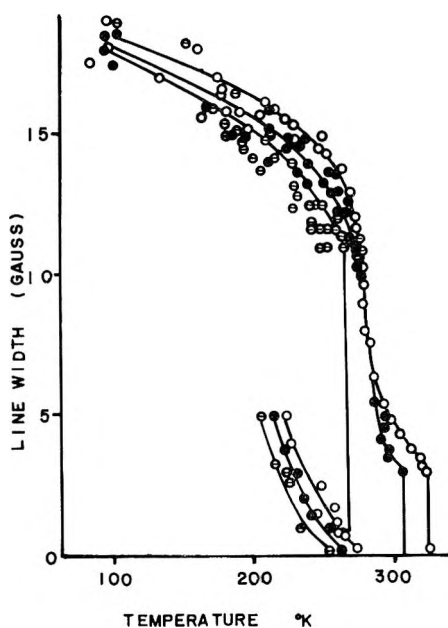


Fig. 1. Line width vs. temperature for poly(ethylene glycol): (O) PEG 4000; (●) PEG 1000; (⊙) PEG 400.

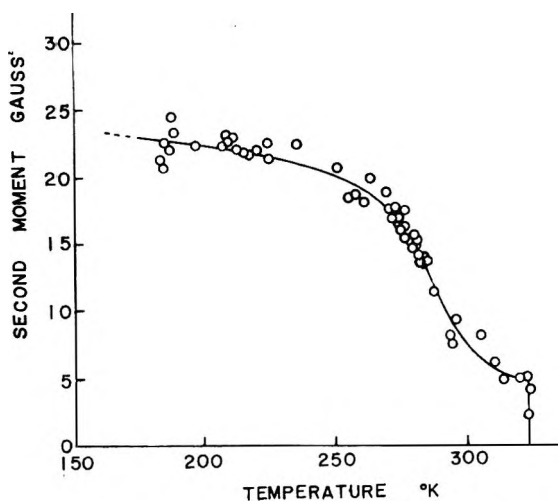


Fig. 2. Second moment vs. temperature for PEG 4000.

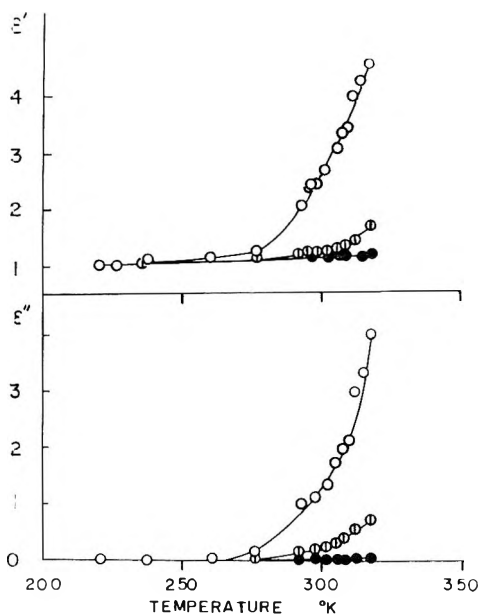


Fig. 3. Dielectric constant ϵ' and loss factor ϵ'' at various frequencies vs. temperature for PEG 4000 (arbitrary scale): (O) 30 cycles/sec.; (⊙) 1 Kcycle/sec.; (●) 100 Kcycles/sec.

4000, except that the melting point of PEG 1000 is lower. A rapid narrowing of the broad component found in PEG 4000 also occurs at 270°K. in PEG 1000. However, PEG 400 shows a marked difference at higher temperatures, though at lower temperatures it shows behavior similar to that of PEG 4000 and 1000. The melting point is lowered to 273°K., and

the abrupt narrowing region which appeared at 270°K. in PEG 4000 and 1000 is not observed. The temperature range where the narrow component appears is progressively lowered a little in the sequence PEG 4000, 1000, and 400.

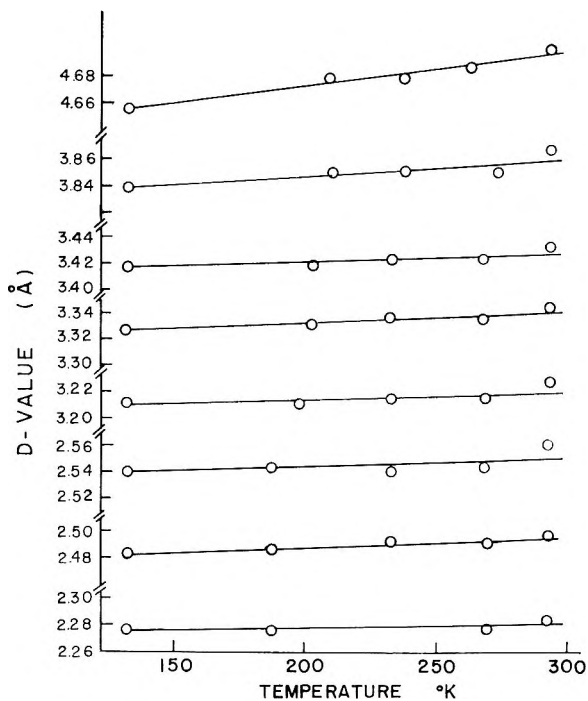


Fig. 4. d values vs. temperature for PEG 4000.

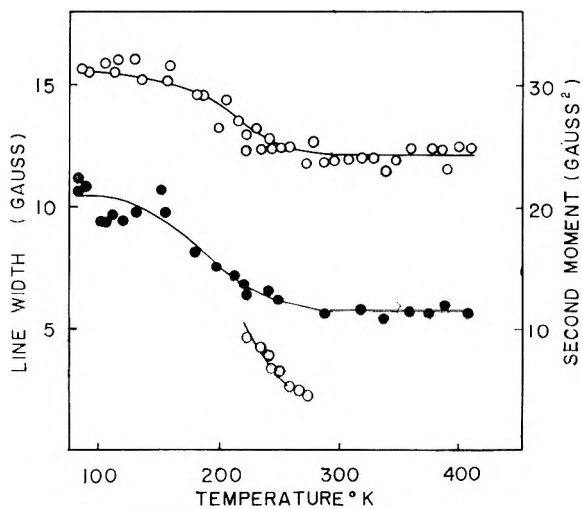


Fig. 5. Plots of (O) line width and (●) second moment vs. temperature for polyoxymethylene.

Experimental second moment values are plotted against temperature for PEG 4000 in Figure 2. The second moment plots are similar to the line width-temperature curve described above.

Dielectric constants ϵ' and loss factors ϵ'' (arbitrary scale) are plotted against temperature at three fixed frequencies for PEG 4000 in Figure 3. At 30 cycles/sec., both ϵ' and ϵ'' begin to increase from 270°K. On the other hand, they appear to be nearly constant over the whole temperature range studied at frequency of 100 kcycles/sec. However, in more detailed measurement, a small maximum of the loss factor is found in the ϵ'' -temperature plots at lower temperatures. This loss peak is located at about 230°K. and shifts to higher temperature with increasing frequency.

Thermal expansion measurements show that the volume increases linearly with increasing temperature up to about 265°K., where a deviation from linearity is seen. At 325°K., an abrupt change of the volume occurs, which is associated with the melting process. Density is found to be 1.212 g./cc. at 23°C.

d values of several x-ray diffraction peaks for PEG 4000 are shown in Figure 4 as a function of temperature. The figure shows that all d values increase with increasing temperature.

Figure 5 shows the line width and the second moment values as a function of temperature for polyoxymethylene. The line width is found to be 16 gauss at the lowest temperature, and to be 12 gauss at the highest temperature. An appreciable decrease, from 16 to 12 gauss, is found in the temperature region of 180–220°K., where a narrow component appears. The variation of the second moment is similar to that of the line width. The second moment value is 20 gauss² at the lowest temperature and is 12 gauss² at the highest temperature.

Discussion

It seems reasonable to assign the broad component of the resonance line to the contribution of crystalline regions and the narrow component to disordered regions.^{14,15} According to the above consideration, it seems reasonable that the narrowing of the broad component in the range of 260°K. to the melting point is related to some kind of movement of molecules in the crystalline regions.

A recent study of molecular structure shows that the PEG molecule in the crystal has a helical structure at room temperature.^{4,5} On the basis of this fact, the NMR results indicate that the molecules in crystalline regions must move without destruction of the helical structure. Such movement may be, presumably, rotational or oscillational motions about the helical axis.

Tadokoro has found that the infrared spectra of PEG, two absorption bands at 947 and 844 cm.⁻¹ show a fine structure at 125°K. but do not at room temperature, and he has suggested that this behavior of infrared spectra may be explained by the variation of the molecular interaction which is affected by molecular motions.¹⁶

According to the results of the mechanical properties of poly(ethylene glycols), Read¹¹ has suggested the existence of mechanical dispersion due to crystalline regions at 260°K. This temperature region may be supposed to correlate with the NMR line narrowing at 270°K.

The PEG molecule has the chemical structure $(-\text{CH}_2\text{CH}_2\text{O}-)_n$, and this repeating unit has a dipole moment. Therefore, molecular motions occurring in this polymer can be investigated experimentally through dielectric methods. As seen in Figure 3, no dielectric dispersion could be observed in the temperature range where the NMR broad component narrows. Results of dielectric measurements show that the molecular motions at 270°K. must be those having no influence on dielectric dispersion. It seems to be possible that the above-mentioned rotational or oscillational motion about the helical axis of the molecule in crystalline regions does not change the resultant dipole moment of the molecules and has little effect on dielectric phenomena.

The dielectric dispersion observed at lower temperatures may be the same one observed in Carbowax 4000 by Connor et al.¹⁷ This dispersion is reasonably thought to be related to motions in disordered regions, because the temperature range is near the narrowing regions of the NMR narrow component. This conclusion is in agreement with that of Connor et al.¹⁷

In order to obtain information on molecular motions occurring in polymers, the observed second moments of NMR spectra are usually compared with those calculated for the rigid state and for the cases in which special types of motion of certain groups take place.^{18,19}

Unfortunately, since precise crystal structure data which are necessary for the exact calculation of the second moment are not available, a detailed comparison can not be made.

If the origin of the NMR line narrowing at about 270°K. is due to crystalline regions, there may be some possibility that a crystal phase transition is observed, as for polytetrafluoroethylene, which has a helical structure⁴ like PEG and which is known to show a first-order transition at room temperature, where the NMR line narrowing is observed.^{8,9} For polytetrafluoroethylene, changes in the x-ray diffraction pattern,¹ the λ transition in heat capacity,^{20,21} and the dynamic mechanical damping peak^{22,23} were observed at room temperature. It is desirable to obtain information about thermodynamic properties of PEG in the region of temperature where NMR line narrowing occurs in order to determine the origin.

As described in the Results section, the volume increases linearly with increasing temperature. Although a slight deviation from a straight line appears from 260°K., no abrupt change of the volume can be observed. This fact shows that no first-order thermodynamic transition accompanies the NMR line narrowing at about 270°K. This conclusion is also supported by x-ray data (Fig. 4), as the several lattice spacings change continuously with temperature. The fact that a first-order transition is not observed does not always deny the possibility of a higher-order transi-

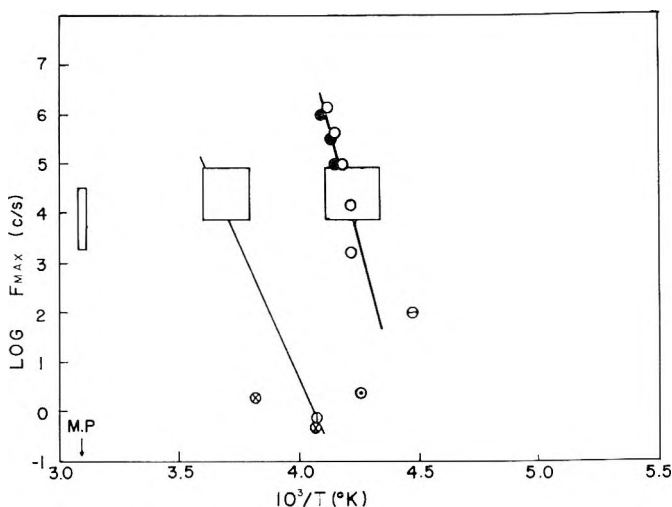


Fig. 6. Logarithm of maximum loss frequency vs. reciprocal of temperature for poly(ethylene glycol): (○) data of McCrum²⁶ (Mechanical); (⊖) data of Connor et al.¹⁷ (Dielectric); (○) data of Ishida et al.²⁷ (Dielectric); (●) present work (Dielectric); (□) present work (NMR); (⊗) data of Read¹¹ (Mechanical) Connor et al.¹⁷ for Carbowax 4000; (⊙) data of Read¹¹ and Connor et al.¹⁷ (Mechanical) for Carbowax 20 M, annealed and unannealed.

tion. Differential thermal analysis (DTA) in our laboratory indicates an abnormal behavior for PEG 4000.²⁴ In the comparison of polytetrafluoroethylene and PEG, it should be noted that the polytetrafluoroethylene chain is rigid, while the PEG chain is thought to be more flexible.

It is of interest to note that the temperature region where the NMR broad component in PEG 1000 and 4000 is independent of molecular weight though the melting point depends markedly on molecular weight, as seen in Table I. This result may suggest that the molecular mechanism responsible for the NMR narrowing process is due to motion of a small portion of the chain. PEG 400 does not show this narrowing region, as seen in Figure 1. It may be considered that this region for PEG 400 is smeared out by the abrupt narrowing due to the melting process since the melting temperature for PEG 400 is lowered to this region. A condition for the appearance of the narrowing process may be that the polymer must have molecular weight higher than 400. The *c* axis of the PEG crystal is reported to be 19.5 Å,²⁵ and PEG chain is considered to be a 7_2 helix.⁵ If low molecular weight PEG has the same structure as the higher molecular weight material, and if entire molecule is in a perfect helical structure, the total length of a helical molecule can be calculated as shown in the fifth column of Table I. It may be assumed that the unit of molecular motion is of the order of the unit cell of which the resultant dipole moment vanishes. The behavior of PEG 400 is supposed to coincide with this assumption.

Figure 6 shows a plot of the logarithm of frequency versus reciprocal temperature, the so-called relaxation map. This figure includes our NMR

and dielectric data for PEG 4000 together with the previous observations, the mechanical data for Carbowax 4000 of Read,¹¹ and those for Carbowax 20 M obtained by McCrum²⁶ as well as the dielectric results of Ishida et al.²⁷ and Connor et al.¹⁷ In Figure 6, our data (the square symbols) show the region of NMR line narrowing located at 10–100 Kcycles/sec. At lower temperatures, the dielectric results of the authors and Ishida et al.²⁷ are in fairly good agreement with the narrowing of the NMR narrow component. The activation energy of this mechanism can be deduced from the straight line in this figure as a value of ca. 80 kcal./mole, which is larger than the value reported by Read¹¹ (35 kcal./mole). The reason for this disparity is unknown.

Mechanical results of Read¹¹ for Carbowax 4000 and those of McCrum²⁶ for Carbowax 20 M fail to fit the straight line of the low temperature mechanism. It is difficult to determine the mechanism to which these mechanical phenomena are attributable. In this connection, Read's remark that the relaxation mechanism observed in PEG is markedly influenced by molecular weight and by the thermal history of the specimen should be noted. Moreover, Read has suggested that the relaxation process of Carbowax 20 M lies in the temperature region where the crystalline mechanism might be operative. If the relaxation process of this mechanical behavior is due to both disordered and crystalline regions, the mechanical data may be correlated to some extent with the NMR line narrowing region at 270°K. Rough estimation of the activation energy of this crystalline mechanism may give a value above 40 kcal./mole in Figure 6, although comparisons among measurements made by different methods and with different compounds seem unsatisfactory. However, there is no other evidence that justifies this value.

Recent results of T_1 measurements for PEG^{17,28} in a wide range of molecular weight show that minimum values of T_1 are located at temperatures below the melting point for the polymers having molecular weights in the range 600–20,000. This suggests that a relaxation mechanism within the ordered crystalline regions may be operative. This idea may be supported by the present work as discussed above.

Polyoxymethylene is known to assume a helical structure in crystalline regions (9_5 helix).^{3,4} It may be expected that POM undergoes molecular motion characteristic of the helix. Figure 5 shows that a considerable amount of molecular motion occurs in the temperature region of 180–220°K. Since a mechanical relaxation peak is reported in this temperature range which is attributed to disordered regions, the decrease of the line width and the second moment in Figure 5 may be mainly due to molecular motions in disordered regions.

The second moment of the rigid state of POM can be calculated theoretically because the crystal structure of this polymer is known. On taking into account contributions of all protons within 10 Å., the calculation of the second moment was carried out by using an electronic computer; this yielded a value of 20.0 gauss². In the calculation, it is assumed that the

crystal is hexagonal ($a = 4.46 \text{ \AA}$, $c = 17.30 \text{ \AA}$),²⁹ and the helical parameters given in literature^{3,30} were used. This value of the second moment is in good agreement with the observed value at the lowest temperature. This fact suggests that POM is essentially in a rigid state at the lowest temperature. At the highest temperature, the observed second moment was $11.5 \pm 1.0 \text{ gauss}^2$. The difference between the second moments observed at two extreme temperature regions may be, for the most part, due to molecular motions in disordered regions. If contribution from protons in disordered regions to the observed second moments is negligible at higher temperature owing to violent molecular motions, and if protons in ordered regions are in the rigid state, the expected value of the second moment at higher temperatures may be 15 gauss^2 , taking into account the crystallinity of this material (75%). This value may be somewhat larger than the observed value by a factor greater than the experimental error. The disagreement may suggest that the POM helix undergoes motion such as seen in PEG in ordered crystalline parts at higher temperatures. Recent results of x-ray measurements of POM carried out in this laboratory³¹ suggest that the POM helix may undergo a rotational or oscillational motion in crystalline regions.

The authors wish to express their gratitude to Professor M. Kaneko for encouragement and discussion during the course of the present study. Thanks are also due to Dr. H. Futama for his assistance in dilatometric measurements and Mr. A. Chiba for operating the x-ray apparatus. This work was partly supported by the Scientific Research Fund of the Ministry of Education, Japan.

References

1. Rigby, H. A., and C. W. Bunn, *Nature*, **164**, 583 (1949).
2. Bunn, C. W., and E. R. Howells, *Nature*, **174**, 549 (1954).
3. Tadokoro, H., T. Yasumoto, S. Murahashi, and I. Nitta, *J. Polymer Sci.*, **44**, 266 (1960).
4. Miyazawa, T., *J. Chem. Phys.*, **35**, 693 (1961).
5. Miyazawa, T., K. Fukushima, and Y. Ideguchi, *J. Chem. Phys.*, **37**, 2764 (1962).
6. Pauling, L., R. B. Corey, and H. R. Branson, *Proc. Natl. Acad. Sci. U.S.A.*, **37**, 205 (1951).
7. Bamford, C. H., A. Elliott, and W. E. Hanby, *Synthetic Polypeptides*, Academic Press, New York, 1956.
8. Hyndman, D., and G. F. Origlio, *J. Appl. Phys.*, **31**, 1849 (1960).
9. Yamagata, K., and S. Hirota, *J. Appl. Phys. Japan*, **29**, 866 (1960).
10. Slichter, W. P., *Makromol. Chem.*, **34**, 67 (1959).
11. Read, B. E., *Polymer*, **3**, 529 (1962).
12. Hikichi, K., and J. Furuichi, *J. Phys. Soc. Japan*, **18**, 742 (1963).
13. Pound, R. V., *Prog. Nucl. Phys.*, **2**, 21 (1952).
14. Wilson, C. W., and G. E. Pake, *J. Chem. Phys.*, **27**, 115 (1957).
15. Powles, J. G., *Polymer*, **1**, 219 (1960).
16. Yoshihara, T., H. Tadokoro, and S. Murakashi, *J. Chem. Phys.*, **41**, 2902 (1964).
17. Connor, T. M., B. E. Read, and G. Williams, paper presented at Conference on Advance in Polymer Science and Technology, London, May 1963; *J. Appl. Chem.*, **14**, 74 (1964).
18. Gutowsky, H. S., and G. E. Pake, *J. Chem. Phys.*, **18**, 162 (1950).
19. Slichter, W. P., *Fortschr. Hochpolymer. Forsch.*, **1**, 35 (1958).

20. Furukawa, G. T., R. E. McCoskey, and G. J. King, *J. Research, Natl. Bur. Std.*, **49**, 273 (1952).
21. Kuroda, T., and H. Sakami, *Repts. Govt. Ind. Res. Inst., Nagoya, Japan*, **7**, 1 (1958).
22. McCrum, N. G., *J. Polymer Sci.*, **34**, 355 (1959).
23. Woodward, A. E., and J. A. Sauer, *Fortschr. Hochpolymer. Forsch.*, **1**, 114 (1958); J. A. Sauer and A. E. Woodward, *Rev. Mod. Phys.*, **32**, 88 (1960).
24. Chiba, A., K. Hikichi, H. Futama, and J. Furuichi, paper presented at Annual Meeting of the Physical Society of Japan, Nagoya, October 1964.
25. Price, F. P., and R. W. Kilb, *J. Polymer Sci.*, **57**, 395 (1962).
26. McCrum, N. G., *J. Polymer Sci.*, **54**, 561 (1961).
27. Matsuo, M., Y. Ishida, K. Yamafuji, and M. Takayanagi, paper presented at Annual Meeting of the Society of Polymer Science, Japan, Nagoya, April 1962.
28. Allen, G., T. M. Connor, and H. Pursey, *Trans. Faraday Soc.*, **59**, 1525 (1963).
29. Hammer, C. F., T. A. Koch, and J. F. Whithney, *J. Appl. Polymer Sci.*, **1**, 169 (1961).
30. Miyazawa, T., *J. Polymer Sci.*, **55**, 215 (1961).
31. A. Hasegawa, K. Hikichi, and J. Furuichi, *J. Phys. Soc. Japan*, to be published

Résumé

En vue d'étudier les mouvements moléculaires caractéristiques d'un polymère hélicoïdal, on a mesuré les spectres de résonance magnétique protonique et les constantes diélectriques complexes ϵ^* dans un large domaine de fréquences, dans la région de 90°K jusqu'au point de fusion du polyéthylène-glycol (que l'on pense être hélicoïdal à état solide). Les poids moléculaires des échantillons sont 4000, 1000 et 400. Ces résultats suggèrent qu'un mouvement moléculaire tel qu'une rotation ou une oscillation est capable d'exister dans les régions cristallines bien en dessous du point de fusion. La température à laquelle ce type de mouvement commence, semble être indépendante du poids moléculaire des échantillons bien qu'on ait trouvé que le point de fusion dépendait fortement du poids moléculaire. Des mesures dilatométriques et aux rayons-X ont été effectuées sur les mêmes échantillons et montrent l'absence d'une transition cristalline de phase (transformation du premier ordre) dans la région de température où on observe le rétrécissement de la largeur de bande NMR du polyéthylène glycol. On présente également les résultats pour un autre polymère hélicoïdal, le polyoxyméthylène.

Zusammenfassung

Um die für ein helixförmiges Polymeres charakteristische Molekülbewegung zu untersuchen, wurden protonmagnetische Resonanzspektren sowie die komplexe Dielektrizitätskonstante ϵ^* für einen weiten Frequenzbereich bei Temperaturen von 90°K bis zum Schmelzpunkt an Polyäthylenglycol gemessen, für welches im festen Zustand eine Helix angenommen wird. Die Molekulargewichte der Proben sind 4000, 1000, und 400. Die Ergebnisse legen den Schluss nahe, dass auch in kristallinen Bereichen weit unterhalb des Schmelzpunkts eine Molekülbewegung wie Rotation oder Oszillation auftreten kann. Die Temperatur, bei welcher dieser Typ von Molekülbewegung einsetzt, scheint vom Molekulargewicht der Proben unabhängig zu sein, obgleich sich der Schmelzpunkt als merklich molekulargewichtstabhängig erweist. Röntgenuntersuchungen und dilatometrische Messungen wurden an den Proben durchgeführt und zeigen das Fehlen einer kristallinen Phasenumwandlung (Umwandlung erster Art) im Temperaturbereich, in welchem Verengung der NMR-Linienbreite von PEG beobachtet wird. Ergebnisse für ein weiteres helixförmiges Polymeres, Polyoxymethylen, werden vorgelegt.

Received September 14, 1964

Revised December 29, 1964

Prod No. 4684A

Thermostatted Cell for a Brice-Phoenix Light-Scattering Photometer

C. SMART, *Unilever Research Laboratory, Port Sunlight,
Cheshire, England*

Synopsis

A thermostat jacket is described for a Brice-Phoenix light-scattering photometer which allows accurate temperature control of the scattering medium over a wide range of temperatures. Modifications to the electronic system of the photometer have increased its sensitivity so that more accurate measurements can be made for low Rayleigh ratios. By using a circulating liquid of the same refractive index as the Pyrex glass cell, stray light within the cell has been reduced to a very low level. Some results for the Rayleigh ratios of water and benzene are presented.

Introduction

A number of modifications have been described in the literature to enable light-scattering measurements to be carried out over a wide range of temperatures by means of a Brice-Phoenix light-scattering photometer. Generally the methods of thermostating fall into three types, namely: (1) thermostating the entire light compartment of the photometer;^{1,2} (2) surrounding the light-scattering cell by a double-walled metal jacket through which liquid can be circulated,³⁻⁹ (3) immersing the light-scattering cell in a liquid which is maintained at the desired temperature.¹⁰⁻¹²

Method (1) suffers from the disadvantage that it is difficult to work at very high temperatures because of the necessity of cooling the photomultiplier tube in order to keep the noise level at a workable level. It is also rather inflexible if one desires to work at a number of temperatures. Methods (2) and (3) each have several desirable features, and this paper describes the design of a thermostat jacket which combines the desirable features of both methods.

The light-scattering cell (a 24 × 24 mm. all-Pyrex semioctagonal cell) is immersed in a liquid which is circulated through a glass jacket surrounding the cell and which is kept at a constant temperature by means of heat-exchanger coils in a constant temperature bath. The design described here could be modified to take a small 24 mm. cylindrical cell. This method of thermostating allows a temperature range of 0-70°C. to be achieved without difficulty and the temperature of the liquid within the cell can be maintained to within ±0.2°C.

An immediate disadvantage of this system however lies in the use of a small semioctagonal cell which requires the use of the narrow 4-mm. diaphragms in the incident beam. The narrow diaphragms cause a threefold decrease in the amount of light falling on the receiver at 90° which makes the accurate measurement of the Rayleigh ratio $R_{(-90)}$ of dilute aqueous solutions extremely difficult, particularly if one wishes to measure depolarizations by means of a polaroid analyzer.

Modification of the Photometer Output Circuit

In order to overcome the disadvantage of a reduced light intensity we have modified the output circuit of the photometer so that in conjunction with the Phoenix potentiometric strip chart recorder the sensitivity of the system can be increased a maximum of 25 times, while maintaining a signal-to-noise ratio of about 100:1. It must be mentioned, however, that our photomultiplier tube appears to have a noise level which is somewhat lower than average.

The potentiometric recorder, which is based on a Honeywell-Brown instrument, has a very high input impedance, and we have utilized this fact to increase the sensitivity of the system. Under normal operation when the recorder circuit is used, the output signal from the photomultiplier cathode is measured as the potential drop across a fixed 15-k Ω resistor which is in series with a 1-M Ω resistor forming the cathode load of the photomultiplier. This is shown in Figure 1, which shows a simplified diagram of the normal output circuit. Because of the very high input impedance of the recorder it is possible to increase the output signal by measuring the potential dropped across a larger proportion of the cathode load resistance. This was achieved with only a slight increase in the response time of the system; for example, the response time changes from 2.5 sec. to 3 sec. for a sensitivity of 13 times normal. Figure 2 shows the modified output circuit which we employ. Three fixed tapping points along the cathode load can be selected by means of a switch giving normal sensitivity, 13 times normal sensitivity, and 25 times normal sensitivity.

Another modification which was found to be necessary is the inclusion of a 2- μ F. capacitor across the output terminals of the photometer in order

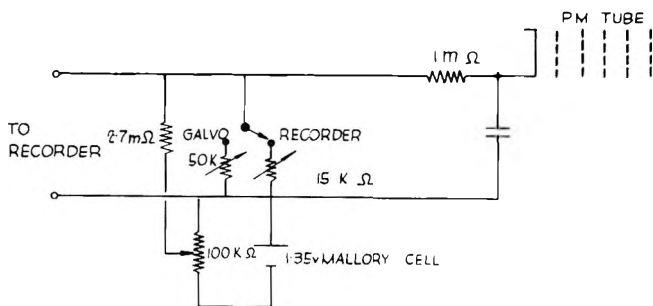


Fig. 1. Circuit diagram of unmodified Brice-Phoenix output circuit.

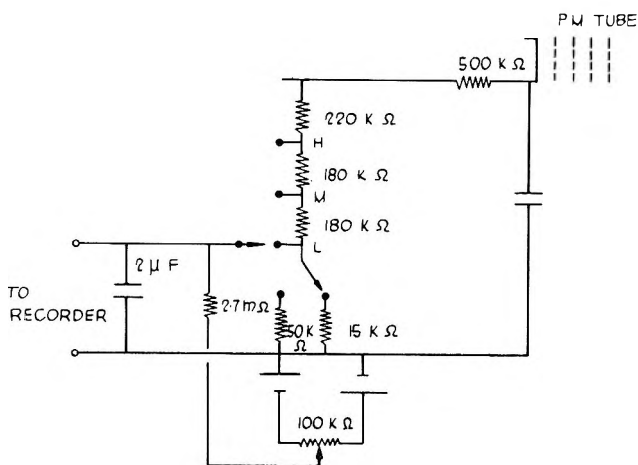


Fig. 2. Circuit diagram of Brice-Phoenix output circuit modified as described in this paper.

to reduce a.c. mains pick up, which causes a serious increase in the recorder dead band. Lastly, a second Mallory cell was introduced in the dark current backing-off circuit to give greater flexibility to the zero control on the higher sensitivity ranges.

No similarly simple modifications appear to be possible to increase the sensitivity of the system for galvanometer operation, and a more sensitive galvanometer than the normal one supplied by the Phoenix Precision Instrument Company is required for use with the thermostat system.

Description of the Thermostat Jacket

The thermostat jacket containing the small semioctagonal cell is shown in the photograph (Fig. 3).

The main body of the jacket consists of a short section of a standard, all-Pyrex 40×40 mm. semioctagonal light-scattering cell supplied by the Phoenix Precision Instrument Company, the ends of which were ground and polished to a plane perpendicular to the optical surfaces. The glass tube so formed is clamped between two machined flanges by means of four 2-in. 6 BA screws, the front screws being placed at the octagonal corners of the section to avoid interfering with the optical system. Liquid-tight seals between the glass and each flange were obtained by means of silicone rubber gaskets which also allow for the differential thermal expansion of the brass screws and the glass.

The lower flange has a locating shoulder at the back to permit the accurate alignment of the glass relative to the optical axis of the system. The lower flange also has an internal machined recess to position the light-scattering cell, and externally it is machined to fit the recess in the cell table of the instrument. Because of the thickness of the lower flange we found that with the cored cell table supplied with the instrument the inci-

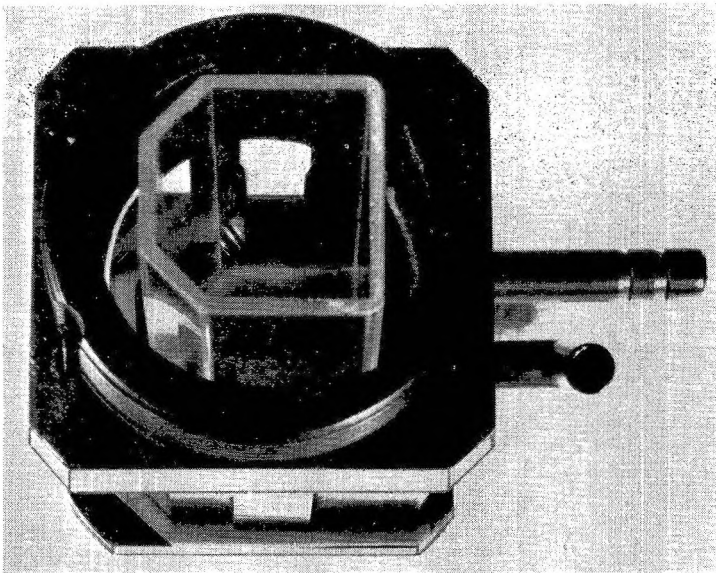


Fig. 3. Photograph of the thermostat jacket without the lid having the semi-octagonal light-scattering cell in position.

dent light beam was striking the bottom of the cell. We therefore found it necessary to make a new cell table which located the cell at a lower level. Also attached to the lower flange, between the entrance window of the jacket and the light-scattering cell, are two baffles which prevent any light scattered by imperfections in the glass wall of the jacket from interfering with the light-scattering measurements, but which still allow circulation of the liquid in the jacket. The flanges and baffles are sprayed with black paint in order to reduce reflection from their surfaces. The exterior walls of the jacket not involved in any light-scattering measurement were also sprayed with several coats of black paint.

A neutral density filter of dimensions 2.5×1 cm. of about 10% transmission is attached to the exit window of the jacket with Araldite. This filter reduces the intensity of the light falling on the photomultiplier when the incident intensity is being measured; this is necessary because we have increased the sensitivity of the instrument to such an extent that without it the recorder deflection is too great at zero degrees when the working standard and all of the filters provided are in place. In addition the filter absorbs most of the light reflected at the exit window of the jacket which would otherwise return through the cell and present a possible extra source of stray light.

Circulating liquid enters the space between the light-scattering cell and the jacket through a pipe in the lower flange and leaves by a pipe in the upper flange. The upper flange has a screwed collar to take a screw cap. When in position, the top of the light-scattering cell projects about $1/2$ in. above the top of the upper flange so that it can easily be placed in position

and removed. The screw cap is recessed to allow for this with a minimum of clearance and has a silicone rubber gasket to provide an air-tight seal at the top of the jacket. The dead volume above the outlet pipe is made as small as possible to prevent the circulating liquid from rising above the level of the outlet pipe and into the light-scattering cell when under pressure from the pump.

The thermostating liquid is contained in a totally enclosed system and is pumped through the jacket by means of a small gear pump. After passing through the jacket, the liquid passes through glass heat-exchanger coils in a large thermostated oil bath which can be maintained at any temperature between -5 and 100°C . After the heat-exchanger coils the liquid enters a small reservoir which can be inverted in order to prime the pump. All flexible pipes are made of poly(vinyl chloride). The tubing enters the photometer through the holes provided at the rear of the instrument and it is painted black both inside the instrument and for a considerable distance outside in order to eliminate "light pipe" effects.

We have found that it is necessary to filter the circulating liquid continuously immediately before it enters the jacket in order to keep it free from large dust particles. For this purpose we use a Millipore filter clamped at the edges between two silicone rubber gaskets which prevent side leakage.

A temperature difference of up to 5°C . exists between the oil bath and the liquid in the jacket when the oil bath is at very high or very low temperatures. The temperature of the liquid in the jacket is therefore measured by a calibrated copper-constantan thermocouple, the leads of which pass along the outlet pipe and through a seal in the wall of the tubing. Experiments show that equilibrium between the liquid in the light-scattering cell and the circulating liquid in the jacket is established within less than ten minutes even at the extreme temperatures. Therefore after allowing equilibrium to be reached we take the temperature of the liquid in the cell to be that of the circulating liquid in the jacket as measured by the thermocouple.

Circulating Liquid

We find that in order to reduce unwanted reflections within the thermostat jacket to a minimum and to obtain reliable values for the Rayleigh ratio of dilute aqueous solutions it is necessary to use a circulating liquid which has a refractive index close to that of the Pyrex glass light-scattering cell. A liquid of refractive index equal to that of the liquid within the cell, as used in other designs,¹⁰⁻¹² was found to be generally much less satisfactory. The refractive index of the glass is 1.474 at a wavelength of $589\text{ m}\mu$ and an ideal liquid was found to be liquid paraffin (Nujol). The only drawbacks which we have found with Nujol are its high viscosity and the fact that it is a solvent for Parafilm, with which we enclose the top of the light-scattering cell. However, by using a $10\text{-}\mu$ pore diameter Millipore filter to remove dust from the circulating liquid we can achieve an

acceptable flow rate to maintain efficient temperature control, although the filter has to be replaced every few days. Since the top of the light-scattering cell is well above the level of the Nujol, with care we can prevent the Nujol from coming into contact with the Parafilm.

Using Nujol we are able to obtain $45^\circ/135^\circ$ dissymmetries for water and dilute aqueous solutions of between 0.9 and 1.0 tending to 1.0 as the Rayleigh ratio of the solution approaches 10^{-5} cm.⁻¹. The low dissymmetries arise from stray light reflected in the backward direction, since the $45^\circ/90^\circ$ intensity ratio is close to that expected for a Rayleigh scatterer of the observed depolarization. We have not been able to locate the source of this stray light, but we think that it may arise from reflections at the scattering solution-cell wall interface.

Calculation of Rayleigh Ratios

Since we do not use the standard optical system for the instrument, the usual Brice equation requires certain modifications. For the standard optical system and with the use of the working standard method of calibration, the formula for the Rayleigh ratio given by Tomimatsu and Palmer¹⁴ is:

$$R_{(-90)} = [n^2TD/\pi h(1.049)](R_w/R_c)aG_{(-90)}/G_w \quad (1)$$

where $G_{(-90)}/G_w$ is the ratio of the galvanometer deflections at 90° and 0° when viewed through the working standard taking into account the filter factors. The other quantities are defined by Tomimatsu and Palmer.¹⁴

The refractive index of the solution has two effects on the measured intensity: one is to cause a spreading of the solid angle subtended by the receiver and the other is to foreshorten the distance between the scatterer and the receiver. The correction for the spreading of the solid angle appears as the factor n^2 in eq. (1). When this method of calibration is used, the foreshortening correction cancels out and so does not appear in the equation. Although in our system the light generally passes through two regions of different refractive index before leaving the jacket, the formula remains unaltered, since the spreading of the solid angle is the same as before and the foreshortening factor again cancels out. Changes in eq. (1) are required for our system which result from the removal of reflected light within the cell. By blackening the outside surfaces of the jacket we have removed an amount of light equal to the scattered intensity at 90° times the reflectivity of the glass-air interface, we therefore require a factor of 1.037 to compensate for this loss.¹⁴ Also in the usual system 3.7% of the incident light is reflected back into the cell from the exit window and is then scattered, but with a reversed envelope. In the case of a solution having a dissymmetry greater than unity this reflected and scattered light has a marked effect on the measured dissymmetry.^{15,16} By using the 10% neutral density filter on the exit window of the jacket we have reduced this reflected light to about 1% of its value when it re-enters the cell; hence

our equation must include an additional factor of 1.037 and our measured dissymmetries need no correction.

Since the 4-mm. apertures are used instead of the usual 1.2-cm. ones, an experimentally determined slit width factor r/r' must be included in the equation. This quantity is determined by measuring the intensity of the light scattered at 90° from a fairly dilute suspension of Rayleigh scatterers in the large semi-octagonal cell with normal apertures and then measuring the intensity of the light scattered from the same suspension in the small semi-octagonal cell with the reduced apertures. The ratio of these measurements is the required quantity r/r' , and the values we obtained are close to 1.5 for light of wavelength 436 and 546 $m\mu$. Although r/r' should depend on the refractive index of the scattering liquid we find that for aqueous solutions the variation is too small to measure.

The equation for calculating the Rayleigh ratio therefore becomes:

$$R_{(-90)} = [n^2TD/\pi h(1.049)](1.037)^2(r/r')(R_w/R_c)at(G_{-90}/G_w) \quad (2)$$

where t is the transmission of the filter attached to the exit window of the cell. If there is no depolarization of the light scattered at 90° the expression for the turbidity τ of the system is:

$$\tau = [16n^2TD/3h(1.049)](1.037)^2(r/r')(R_w/R_c)at(G_{-90}/G_w) \quad (3)$$

We use the values of T and D supplied by the Phoenix Instrument Company; h is 1.2 cm.; the values of t were measured on a Cary 14 spectrophotometer at wavelengths 436 and 546 $m\mu$. R_w/R_c is taken to be 1.02 for all solutions, and the quantities a and r/r' are determined experimentally at least once each day.

With our apparatus we find that the values of a and r/r' vary by a few per cent from day to day, probably due to changes in the illumination pattern of the lamp. In view of this behavior it is preferable to check the values of a and r/r' several times during the day if the highest accuracy is to be achieved. This, however, is a rather laborious procedure, and we therefore check the value of the product of a and r/r' by means of an intermediate standard after each measurement of a Rayleigh ratio. A block of Perspex was machined to the same dimensions and shape as the small semi-octagonal cell, and its surfaces were polished to a good optical quality. The values of a and r/r' were determined in the usual way and the Rayleigh ratio of the Perspex measured immediately afterwards. This was repeated several times so that an average value for the Rayleigh ratio of the Perspex was obtained. By measuring the scattered intensity from the Perspex block we can therefore determine the product ar/r' quickly and easily.

Conclusion

We have increased the sensitivity of the Brice-Phoenix light-scattering photometer by a considerable factor and we are able to measure the light scattering of dilute aqueous solutions over a wide range of temperatures with considerable accuracy. At the present time we are using this appa-

ratus to investigate the effect of temperature on the light-scattering properties of a number of systems, and the results will be published in due course. Because of the increased sensitivity and the reduction in the amount of stray light in the light-scattering cell we have found that the cell described here is capable of giving more reliable results than the standard Brice-Phoenix instrument. We have used this cell without circulating the Nujol through the jacket to measure the light scattering at room temperature of aqueous solutions of several simple electrolytes which have extremely low Rayleigh ratios, and we find excellent agreement between our results and those calculated from activity data.¹³

The values we obtain for the Rayleigh ratio of water at 90° are $1.08 \times 10^{-6} \text{ cm.}^{-1}$ for wavelength 546 m μ and $2.54 \times 10^{-6} \text{ cm.}^{-1}$ for wavelength 436 m μ . These results are in good agreement with those found by other workers for wavelength 546 m μ ,¹⁷⁻²¹ but are slightly lower than the results reported for wavelength 436 m μ .¹⁹⁻²¹

The values of the Rayleigh ratio at 90° for redistilled benzene obtained with our apparatus are $1.56 \pm 0.02 \times 10^{-5} \text{ cm.}^{-1}$ for wavelength 546 m μ and $4.69 \pm 0.05 \times 10^{-5} \text{ cm.}^{-1}$ for wavelength 436 m μ . The depolarization of the 90° scattered light is 0.407 for wavelength 546 m μ and 0.415 for wavelength 436 m μ . These results for benzene agree well with the values found by many workers given in the review by Kratochvil et al.²²

References

1. Tung, L. H., *J. Polymer Sci.*, **36**, 287 (1959).
2. Jaycock, M. J., and G. D. Parfitt, *Trans. Faraday Soc.*, **57**, 791 (1961).
3. Boedtker, H., and P. Doty, *J. Phys. Chem.*, **58**, 968 (1954).
4. Trementozzi, Q. A., *J. Polymer Sci.*, **23**, 887 (1957).
5. Chiang, J., *J. Polymer Sci.*, **36**, 91 (1959).
6. Henry, P. M., *J. Polymer Sci.*, **36**, 3 (1959).
7. Kinsinger, J. B., and R. E. Hughes, *J. Phys. Chem.*, **63**, 2002 (1959).
8. Strauss, U. P., and P. Ander, *J. Phys. Chem.*, **66**, 2235 (1962).
9. Orofino, T. A., and F. Wenger, *J. Phys. Chem.*, **67**, 566 (1963).
10. Casassa, E. F., and S. Katz, *J. Polymer Sci.*, **14**, 385 (1954).
11. Moore, L. D., *J. Polymer Sci.*, **20**, 137 (1956).
12. Kobayashi, T., A. Chitale, and H. P. Frank, *J. Polymer Sci.*, **24**, 156 (1957).
13. Pethica, B. A., and C. Smart, *Trans. Faraday Soc.*, to be published.
14. Tomimatsu, Y., and K. J. Palmer, *J. Phys. Chem.*, **67**, 1720 (1963).
15. Oth, A., J. Oth, and V. Desreux, *J. Polymer Sci.*, **10**, 551 (1953).
16. Sedláček, B., *Chem. Listy*, **47**, 1113 (1953).
17. Goring, D. A. I., and P. G. Napier, *J. Chem. Phys.*, **22**, 147 (1954).
18. Fessenden, R. W., and R. S. Stein, *J. Chem. Phys.*, **22**, 1778 (1954).
19. Kraut, J., and W. B. Dandliker, *J. Chem. Phys.*, **23**, 1544 (1955).
20. Mysels, K. J., and L. H. Prince, *J. Phys. Chem.*, **63**, 1699 (1959).
21. Kratochvil, J. P., private communication.
22. Kratochvil, J. P., G. Deželič, M. Kerker, and E. Matijević, *J. Polymer Sci.*, **57**, 59 (1962).

Résumé

On décrit un manchon thermostatisé pour l'appareil de diffusion lumineuse de Brice-Phoenix permettant un contrôle précis de la température du milieu diffusant sur

une large gamme de températures. Des modifications au système électronique du photomètre ont augmenté sa sensibilité afin de pouvoir faire des mesures plus précises pour de faibles rapports de Rayleigh. En employant un liquide de circulation du même indice de réfraction que la cellule en verre Pyrex, les faibles dispersions à l'intérieur de la cellule ont été réduites à un niveau très bas. On présente certains résultats pour les rapports de Rayleigh de l'eau et du benzène.

Zusammenfassung

Eine Thermostatisierungseinrichtung für das Brice-Phoenix-Lichtstreuungsphotometer wird beschrieben, welche eine genaue Temperaturkontrolle des streuenden Mediums über einen weiten Temperaturbereich gestattet. Modifizierung des elektronischen Systems des Photometers erhöht seine Empfindlichkeit, sodass genauere Messungen bei niedrigem Rayleigh-Verhältnis ausgeführt werden können. Durch Verwendung einer zirkulierenden Flüssigkeit mit gleichem Brechungsindex wie die Pyrexglaszelle wurden Lichtverluste innerhalb der Zelle auf ein sehr niedriges Ausmass herabgesetzt. Einige Ergebnisse für das Rayleigh-Verhältnis von Wasser und Benzol werden vorgelegt.

Received February 22, 1965

Prod. No. 4683A

NOTES

**Multicomponent Copolymer Calculations. II.
Optimizing Monomer Distribution Uniformity**

In batch-free radical vinyl polymerization where all monomeric materials are included in the initial charge, drastic variations in distributional uniformity are attainable depending upon selection of monomers. Presented here are several methods whereby uniformity can be optimized for systems which contain a predetermined number of constraint conditions.

This author's previously published equation¹

$$m_i = \frac{M_i Q_i \sum_{i=1}^n M_i Q_i \exp\{-e_i e_i\}}{\sum_{i=1}^n \sum_{j=1}^n M_i Q_i M_j Q_j \exp\{-e_i e_j\}} \quad (1)$$

where m_i and M_i are the mole fractions i in polymer and monomer, respectively, and where Q_i and e_i are the general reactivity constant and general polarity constant, respectively of i , relates instantaneous monomer and polymer composition during vinyl polymerization of an n component system. Under the batch, "one-shot" conditions described above, perfect uniformity of distribution would require that $m_i = M_i$. Since the denominator of eq. (1) is the same for every component (call denominator of eq. 1, D), in the perfectly uniform case

$$D = Q_j \sum_{i=1}^n M_i Q_i \exp\{-e_j e_i\} \quad (j = 1, 2, 3 \dots n) \quad (2)$$

Since for multicomponent polymers, perfect uniformity is generally unattainable under batch "one-shot" conditions, eq. (2) can be used as a measure of uniformity. An expression for discrepancy of any particular monomer would be

$$d_j = \left| D - Q_j \sum_{i=1}^n M_i Q_i \exp\{-e_j e_i\} \right| \quad (3)$$

A summation weighted discrepancy factor would be

$$d_M = \sum_{j=1}^n M_j d_j \quad (4)$$

where d_M is the sum of weighted discrepancy factors and d_j is the discrepancy of monomer j . In the case where weighting based on mole fraction is of lesser importance than other factors, i.e., stressing uniformity of a component present at low levels, either a special weighing factor for monomer j , factor S_j can be inserted, or no factor used at all. This last case reduces to

$$d = \sum_{i=1}^n d_i \quad (5)$$

where d is the sum of unweighted discrepancy factors, which measures divergence from perfect uniformity, weighting all components equally, whether they are major or minor constituents.

As an example of the usefulness attainable from these factors, a mixture of 10.0 wt.-% acrylamide, 2.5 wt.-% acrylic acid, 65.0 wt.-% styrene, and 22.5 wt.-% monomer 4 which has an assigned molecular weight of 100 and Q and e values of Q_4 and e_4 , yields a matrix of d values dependent upon Q_4 and e_4 .

Figure 1 is a conformal plot of Q_4 versus e_4 for this system, at constant d . This plot was obtained from eq. (5) using the substitution of eq. (3) and the actual Q and e values for monomers 1-3. Data processing involved a Fortran program and a Remington Rand Univac III computer.

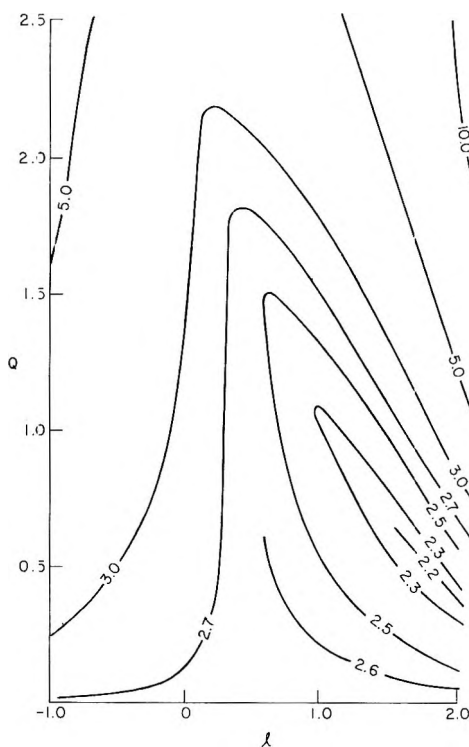


Fig. 1. Conformal diagram shows d versus Q and e .

When the conditional constraints involved modify the problem by reducing it to merely varying the levels of a finite set of monomers to optimize uniformity, the techniques described here are again usable. An example of this case would be a mixture of 10.0 wt.-% acrylamide and 2.5 wt.-% acrylic acid with the remaining 87.5 wt.-% to be divided among styrene and methyl methacrylate so as to optimize uniformity.

Calculations similar to those used in the first example yielded data shown in Figure 2. From this graph it can be seen that if uniformity were the sole criteria, the remaining 87.5% would be divided into 33.0 wt.-% styrene and 54.5 wt.-% methyl methacrylate.

Utilizing material balance equations from eq. (1)

$$C_1 = \sum_{i=0}^{\alpha} (m_i)/(\alpha + 1) \quad (6)$$

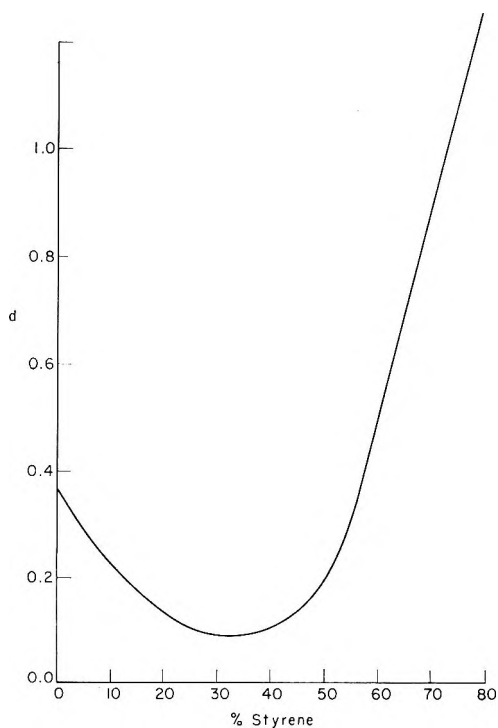


Fig. 2. % Styrene plotted against d .

and

$$M_1 = (M_1^0 - C_1\alpha)/1 - \alpha \quad (7)$$

where M_i^0 is the initial mole fraction of i in monomer, C_i is the mole fraction of i in accumulated polymer, and α is the conversion (cumulative moles polymer/total moles in final polymer), permits one to calculate an overall d_0 for an entire polymerization. Such a d_0 could be expressed mathematically as

$$d_0 = \sum_{i=1}^n \sum_{\alpha=1}^{100} d_i/100 \quad (8)$$

where d_0 is the overall discrepancy factor.

Equation (8) can be used for optimization calculations of the types shown in the two examples given, however, over the entire process from monomer to polymer at complete conversion.

For certain types of calculations, or for comparative purposes where non-related materials are being compared as to relative uniformity of distribution, eq. (3) can be transposed to the form

$$P_j = \left| 1 - \frac{Q_j \sum_{i=1}^n M_i Q_i \exp\{-e_i e_j\}}{D} \right| \quad (j = 1, 2, 3, \dots, n) \quad (9)$$

where P_j is the base line discrepancy of monomer j .

In this form discrepancy is presented with a firm base value that can be compared regardless of the monomer system. Here a value of 0 indicates complete distributional

uniformity. Equation (9) can be converted to weighted factors in much the same way as eq. (3). Equation (10) is an example of this type conversion:

$$P_M = \sum_{j=1}^n M_j P_j \quad (10)$$

where P_M is the sum of weighted base line discrepancy factors.

The significance of polymer distribution factors is considered to be a relatively unexplored area. It is hoped that with the use of discrepancy factors as presented here, correlation of another facet of copolymerization products will be possible, and that property optimization will be closer to the realm of mathematical calculation.

Reference

1. Seiner, J. A., *J. Polymer Sci.*, **A3**, 2401 (1965).

JEROME A. SEINER

Pittsburgh Plate Glass Company
Springdale, Pennsylvania

Received October 28, 1964

Revised January 25, 1965

Specific Influence of Temperature on γ -Ray Radiation Induced Polymerization of Ethylene

As described in a previous paper,¹ the rate of polymerization and molecular weight of the ethylene polymer increases continuously with reaction time during polymerization of ethylene induced by γ -radiation at 20–30°C. From this fact, we have assumed that the life of a polymer radical is quite long under irradiation and that the stationary hypothesis is not realized during the polymerization.

In this note, specific effects of reaction temperature on the life of the polymer radical, its molecular weight, and the rate of polymerization are presented. In contrast to the results at lower temperature from 20 to 45°C., the rate of polymerization and molecular

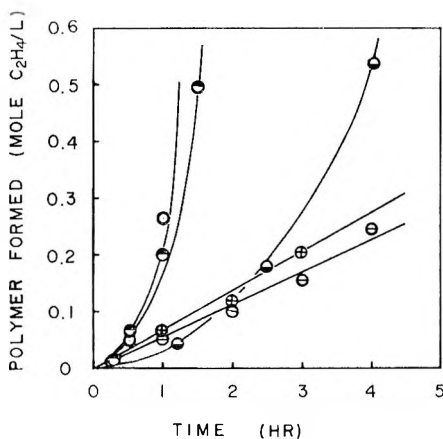


Fig. 1. Polymer yield versus reaction time. Dose-rate: 2.5×10^4 rad/hr.; Temperature and pressure: (O) 30°C., 400 kg./cm.²; (●) 30°C., 200 kg./cm.²; (●) 45°C., 400 kg./cm.²; (⊖) 100°C., 390 kg./cm.²; (⊕) 140°C., 400 kg./cm.².

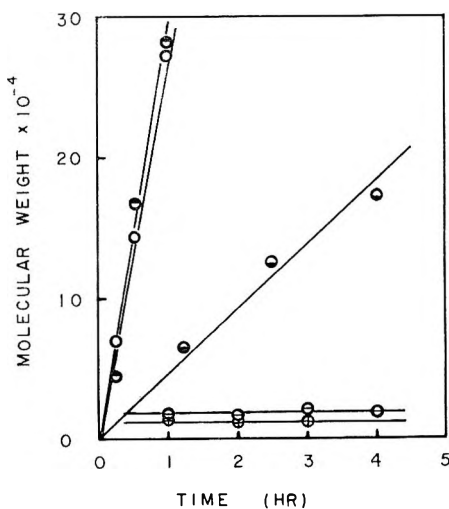


Fig. 2. The molecular weight versus reaction time. Notes and reaction conditions are the same as shown in Figure 1.

weight are independent of reaction time at elevated reaction temperature of 100 and 140°C. This difference is due to the increase in the rate of termination with reaction temperature.

Experimental

All runs were carried out using the batch system. The reaction temperature was regulated by an automatic controller and recorder with an alumel-chromel thermocouple. Other experimental methods and procedures were the same as described in the earlier paper.¹ Since the conversion was very low, the pressure of the monomer was essentially constant during the course of the reaction.

Results and Discussion

The polymer yields are plotted against reaction time at various temperatures in Figure 1.

The experiments were carried out at temperatures ranging from 30 to 140°C. with a dose-rate of 2.5×10^4 rad/hr., and at pressure of 200 and 400 kg./cm.². It can be seen that there is a great difference between the polymerizations at higher temperatures and those lower temperatures. When the polymerizations are carried out at 30 and 40°C., auto-acceleration of the rate is clearly observed. In contrast to this, the rate is not accelerated but remains almost constant during the course of the reaction at higher temperatures of 100 and 140°C.

The effect of the reaction temperature on the molecular weight of the amount of polymer formed is shown in Figure 2. The molecular weight of polymer formed at lower temperatures increases proportionally with the reaction time and can easily reach over 10^5 . In the polymerization at 100 and 140°C., the molecular weight is independent of reaction time and is much lower than that of the polymer formed at lower temperatures.

The polymerization at 30 and 45°C. is characterized by the increase in molecular weight with the reaction time. This characteristic feature can be explained by assuming the elimination of the termination and transfer reaction. The life of the polymer, in this case, is quite long and the assumption of stationary state is not true. In contrast to this, the rate and molecular weight are independent of reaction time in the polymerization at elevated temperature. This indicates that the rate of termination increases with the reaction temperature and attains a value comparable to that of initiation at 100 and 140°C. The life of the polymer radical is, therefore, normal and the stationary state hypothesis, which proposes that the rate of initiation is equal to that of termination, is almost realized.

Further study on the polymerization at lower temperatures will be reported later.

Reference

1. Machi, S., Hagiwara, M., Gotoda, M., and Kagiya, T., *J. Polymer Sci.*, **B2**, 765 (1964).

SUEO MACHI
MIYUKI HAGIWARA
MASAO GOTODA
TSUTOMU KAGIYA

Japan Atomic Energy Research Institute
Takasaki Radiation Chemistry Research Establishment
Gunma-mura, Gunma, Japan.

Received September 21, 1964

Fractionation of Poly(ethylenimine) by Curtain Electrophoresis

Poly(ethylenimine) is a reactive polymer which we are studying as a carrier molecule for the preparation of therapeutically useful macromolecules. In order to evaluate its substitution reactions we have first examined the fractionation of PEI itself by means of curtain electrophoresis. The purpose of this note is to present the data which we have obtained to date on this fractionation procedure.

Materials and Methods

PEI was obtained as a 50% aqueous solution from the Chemirad Corp., East Brunswick, New Jersey. C and N analyses indicated that the polymer concentration was 49.6% $(C_2H_5N)_x$. (It is not feasible to get true dry weights on PEI because it decomposes and gels on heating.)

For curtain electrophoresis, the polymer was diluted to 3% with 1N acetic acid and fractionated on the Beckman-Spinco curtain electrophoresis apparatus. This device, which combined horizontal paper electrophoresis with descending paper chromatography, produces vector flows with the vector angles determined by the electrophoretic and R_F flow components, so that various fractions can be collected from the 32 serrations across the bottom of the curtain (adjacent fractions were subsequently combined to yield 16 fractions). Operating conditions, including the numerical settings of the instrument dials were as follows:

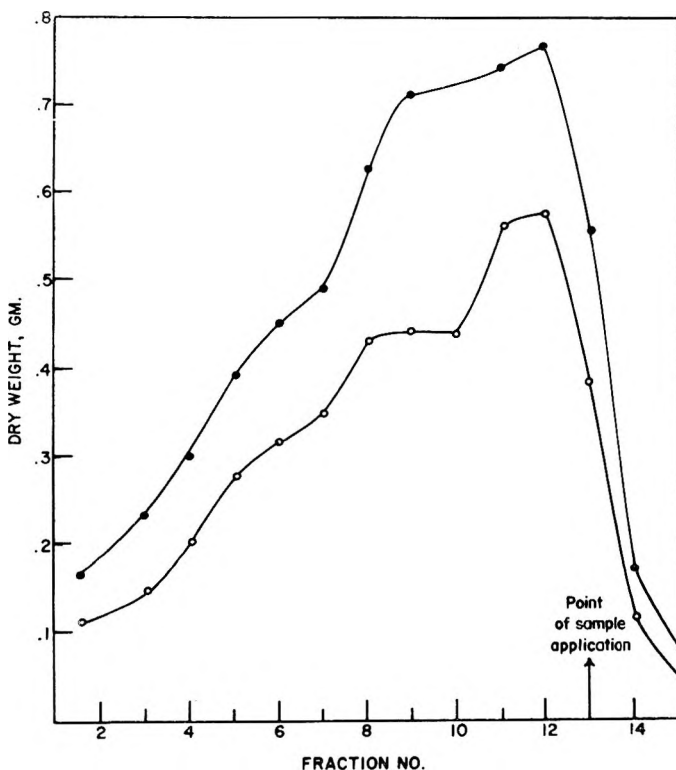


Fig. 1. Dry weights of PEI fractions before (●) and after (○) dialysis.

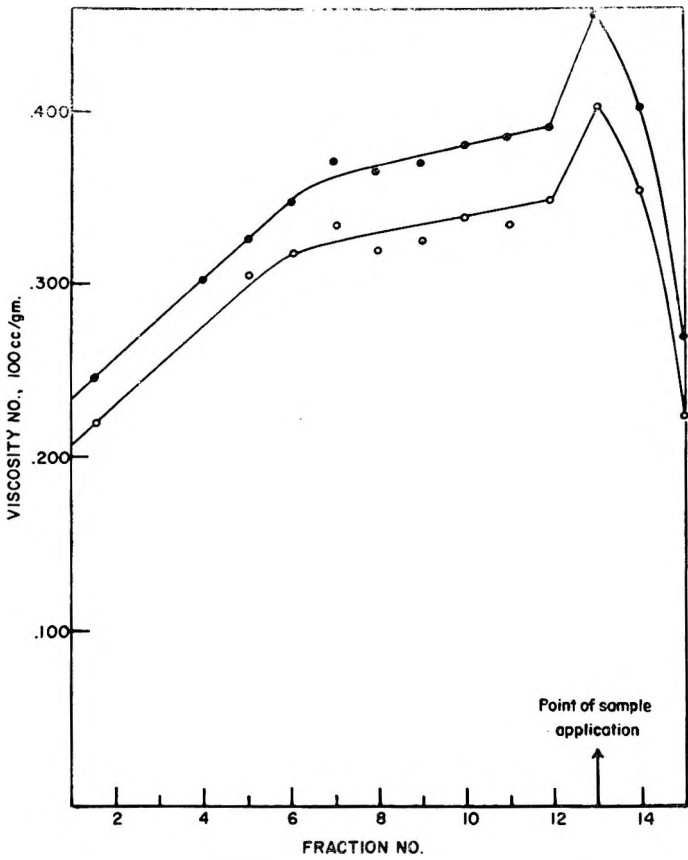


Fig. 2. Viscosity numbers of PEI fractions in water at pH 6, at 1/2% (●) and 1% (○) concentrations.

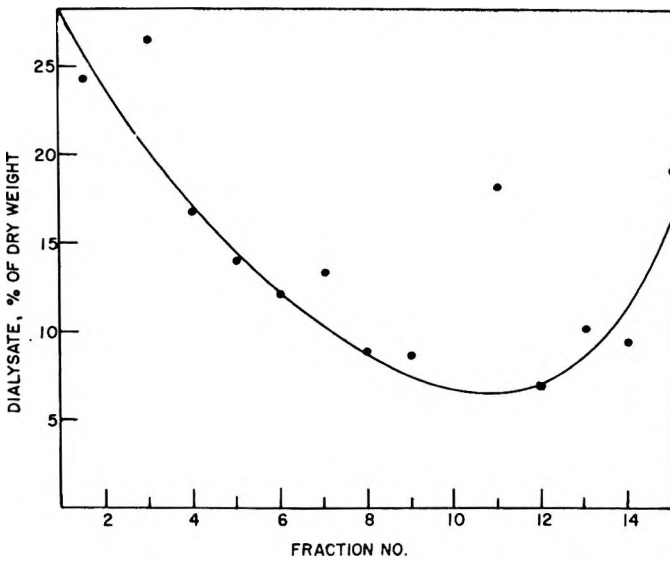


Fig. 3. Dry weights of dialysates of PEI fractions as % of dry weight of total fraction

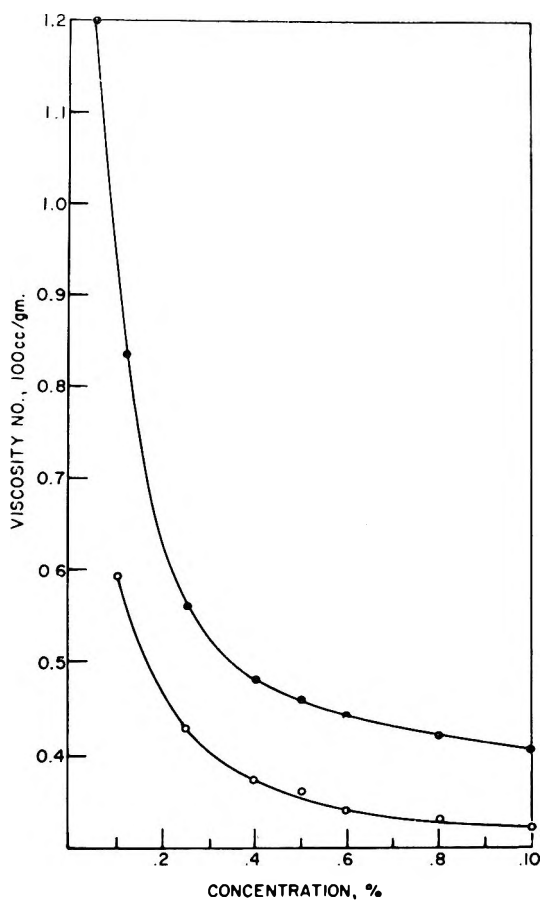


Fig. 4. Concentration dependence of the viscosity numbers of PEI fractions 6 (O) and 13 (●) in water at pH 6.

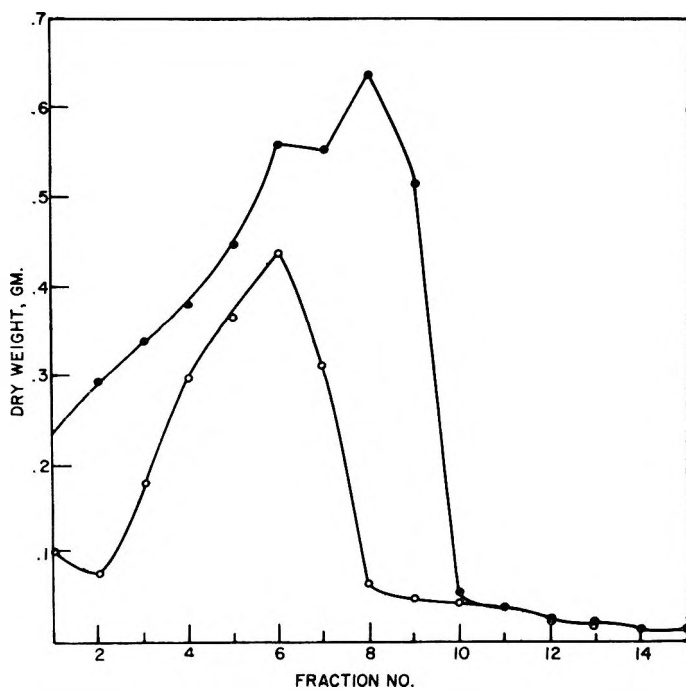


Fig. 5. Dry weights of fractions of PEI fractions 10 (●) and 13 (O) refracted.

Electrolyte, 1*N* acetic acid; feed rate 2 ml./hr.; electrolyte to flow setting, 10; wick flow setting, 5.5; current, constant at 40 ma.

After a suitable amount of material had been collected, the pH of each sample was roughly measured with indicator paper. Then each was evaporated to dryness on the

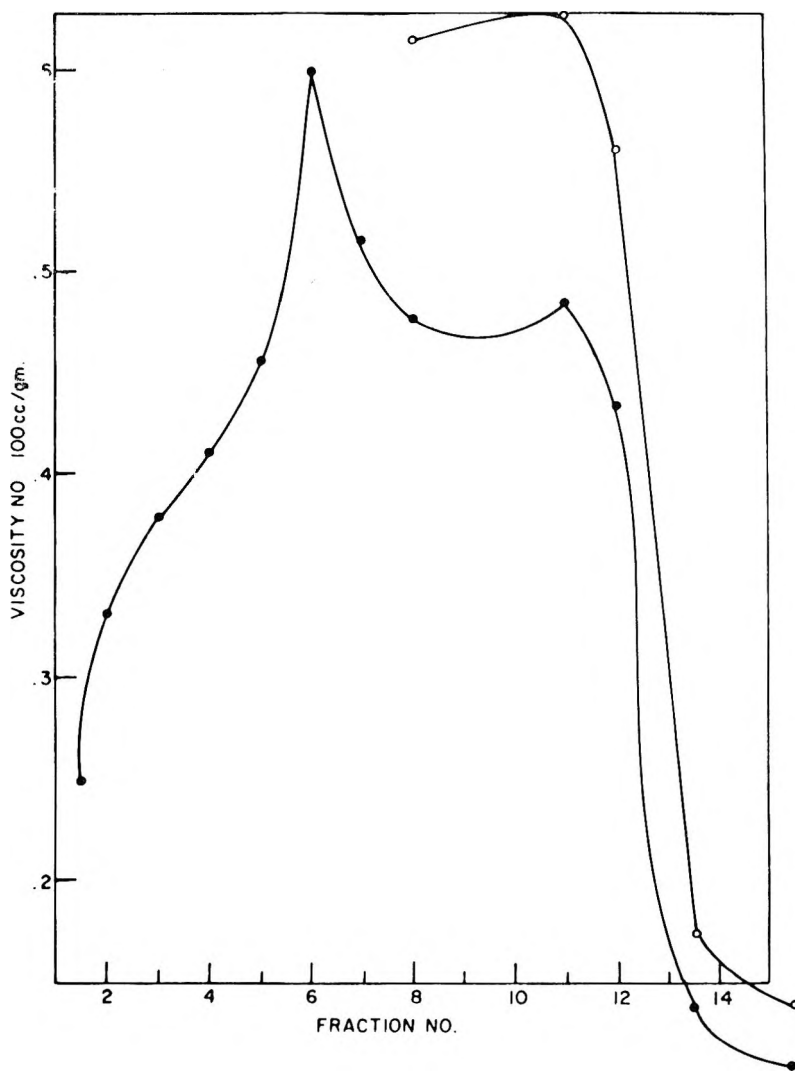


Fig. 6. Viscosity numbers of fractions of PEI fraction 13 refractionated at concentrations of 1/4% (●) and 1% (○).

rotary evaporator, diluted to 100 ml., an aliquot lyophilized, the remainder dialyzed against distilled H₂O and lyophilized. One per cent solutions of the resultant fractions had a pH of approximately 6, as measured with indicator paper, and were used for viscosity determinations.

Results

Figures 1-8 show the results of analyses performed on the PEI fractions.

Discussion

The data presented here leave little doubt that fractionation has been accomplished. The weight distribution of Fraction 13 looks fairly good, although the viscosity data definitely indicates that further fractionation is required to get material which approaches homogeneity.

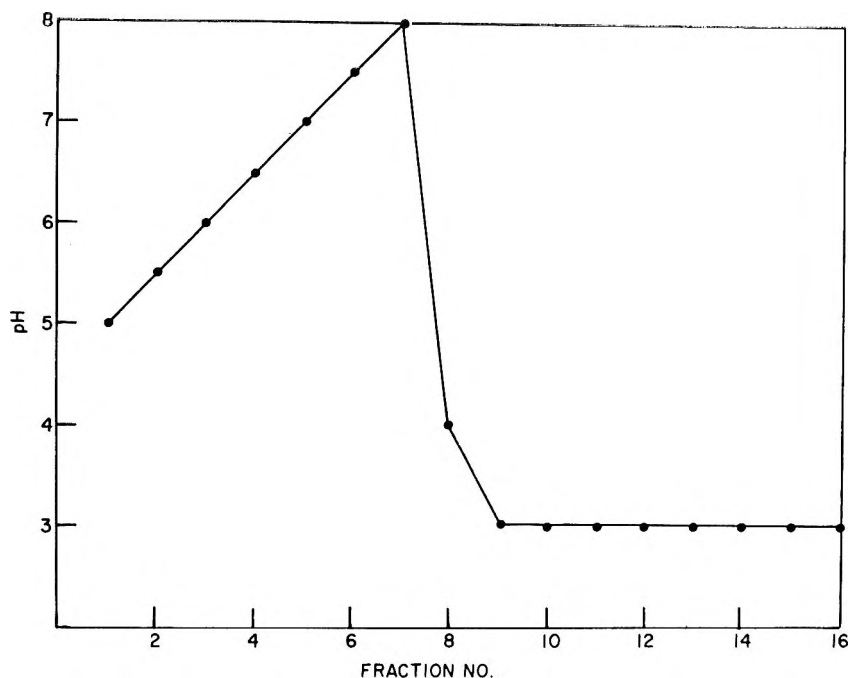


Fig. 7. pH of PEI fractions as collected from the curtain.

The basis of the fractionation is not clear. While there is a substantial enhancement of the viscosity in some fractions and diminution in others, there is a possibility that the shape of the molecule, i.e., the degree of branching¹⁻⁵ rather than the molecular weight, may be the determining factor. An acidic electrolyte was deliberately chosen to expand the polymer and to enhance any variations in molecular shape. Perhaps refractionation at various pH values or salt concentrations would improve separation. Unfortunately, the process is time consuming, and we have found that the fractionated polymer is light sensitive and tends to discolor after a short time. This makes the accumulation of enough material for serial fractionations rather difficult. In subsequent papers we hope to present data which will shed more light on the branching of PEI.

Microanalyses were performed by Byron Baer, Paula M. Parissius, and Evelyn Peake under the direction of W. C. Alford, Chief of the Laboratory's Analytical section. We wish to express the most profound thanks to the personnel of the Research Triangle Institute, where we were guest workers at their Camille Dreyfus Laboratory during the

course of much of this investigation. Especially helpful was the advice and encouragement given us by Drs. Peterlin, Stennett, and Clark, which represented a major asset to our research.

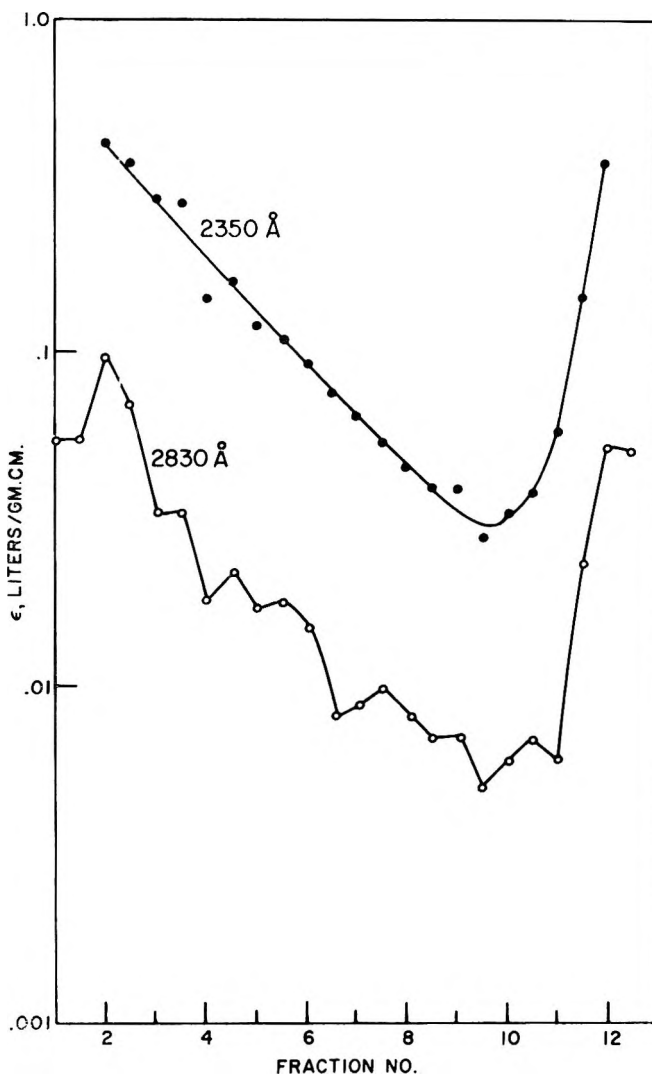


Fig. 8. Extinction coefficient ϵ (l./g. cm.) of PEI fractions at 2350 Å.(●) and 2830 Å.(○) plotted on a log scale.

References

1. Barb, W. G., *J. Chem. Soc.*, **1955**, 2564, 2577.
2. Leibnitz, E., H.-G. Kännecke, and G. Gawalek, *J. Prakt. Chem.*, **6**, 289 (1958).
3. Kännecke, H.-G., and M. Heise, *J. Prakt. Chem.*, **9**, 282 (1959).

4. Jones, G. D., A. Langsjoen, M. Neumann, and J. Zomlefer, *J. Org. Chem.*, **9**, 125 (1944).
5. Kern, W., and E. Brenneisen, *J. Prakt. Chem.*, **159**, 193 (1941).

T. D. PERRINE
PATRICK F. GOOLSBY*

National Institute of Arthritis and Metabolic Diseases
National Institutes of Health
Bethesda, Maryland

Received January 15, 1965
Revised March 4, 1965

* Present address: Chrysler Space Division, Huntsville, Alabama.

Anomalous Effects of Catalyst Mole Ratio on Molecular Weight of Ziegler Polyethylene

Molecular weight control by varying the catalyst ratio was originally disclosed by Ziegler.¹ The ratio of the metal alkyl to the transition metal halide affords a close control of the average molecular weight of the polymer obtained. Further, many workers¹⁻⁷ have shown that for a catalyst system composed of either an aluminum trialkyl or an aluminum dialkyl chloride as co-catalyst with either titanium trichloride or titanium tetrachloride, the average molecular weight of the polymer obtained increases sharply and then remains relatively steady as the Al/Ti mole ratio increases, even to catalyst ratios as high as 26.

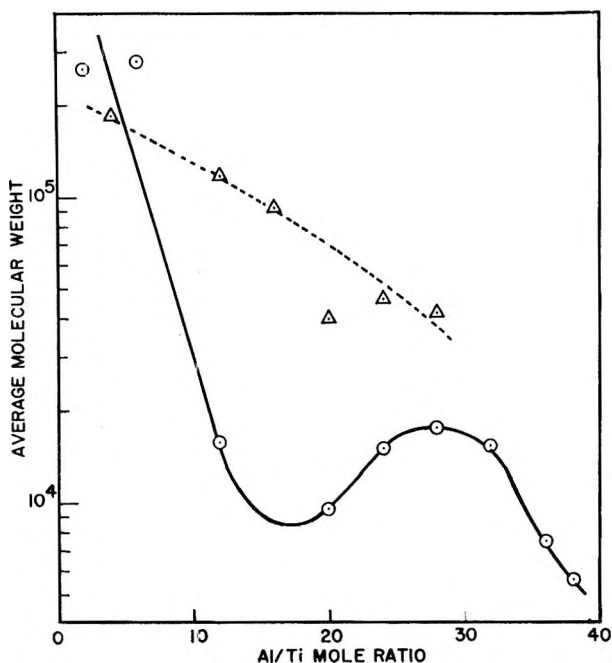


Fig. 1. Variation of average molecular weight with catalyst mole ratio. Titanium tetrachloride-ethyl aluminum sesquichloride (Δ); titanium tetrachloride-isobutyl aluminum dichloride (\circ).

A detailed study of the catalyst systems composed of ethyl aluminum sesquichloride and isobutyl aluminum dichloride as co-catalysts with titanium tetrachloride, undertaken in these laboratories, shows that the Al/Ti mole ratio provides a close control of average molecular weight in these systems also. Unexpectedly, however, there is a large molecular weight decrease as the Al/Ti mole ratio increases (Fig. 1). This is surprising in the light of previous work.¹⁻⁷

The curve for the titanium tetrachloride-isobutyl aluminum dichloride catalyst system (Fig. 1) has a distinct minimum at an Al/Ti mole ratio of 17 from which one may infer that at least two different catalyst species are present. With the titanium tetrachloride-ethyl aluminum sesquichloride catalyst system this effect is not nearly as pronounced, and the slightly curved line relationship appears more reasonable than the depiction of a minimum.

These catalyst systems both afforded maximum yields, based on titanium tetrachloride, at Al/Ti mole ratios greater than 20. The polymers obtained from both systems ex-

hibited highly non-Newtonian flow behavior, indicating broad distributions. Density and infrared data indicated a very high degree of crystallinity.

The molecular weight distributions of some of these polymers have been examined.⁸ Fractionation data showed that besides being extremely broad, each distribution showed bimodal characteristics, again indicating the possible presence of two types of catalyst site.

Experimental

Polymerizations were carried out in a 1/2 gal. stainless steel stirred reactor at 100 psig. and a temperature of $\sim 155^{\circ}\text{C}$. The preformed catalyst containing 1.0 mmole titanium was transferred to the reactor, containing 1 l. of a mixture of isoparaffinic hydrocarbons (having a boiling range of $157\text{--}177^{\circ}\text{C}$.) at $\sim 135^{\circ}\text{C}$. and atmospheric pressure, under a nitrogen blanket. Ethylene was added immediately and the reaction vessel pressurized to, and maintained at, 100 psi.

After 60 min. the ethylene feed was stopped, the catalyst residues removed by extraction with ethylene glycol at 150°C ., the precipitated polymer washed free of solvent and dried in a vacuum oven at 90°C .

Inherent viscosity, $\{\eta\}$, was determined at 130°C . in tetralin; the molecular weight, \bar{M}_v , was calculated using the expression:⁹

$$\{\eta\} = 5.10 \times 10^{-4} \bar{M}_v^{0.725}$$

References

1. Ziegler, K., Belg. Pat. 540,459 (1959).
2. Ziegler, K., Can. Pat. 674,609 (1963).
3. Fukui, K., T. Kagiya, S. Machi, T. Shimidzu, and S. Yuasa, *Bull. Chem. Soc. Japan*, **35**, 303 (1962).
4. Fukui, K., T. Kagiya, S. Machi, T. Shimidzu, and S. Yuasa, *Bull. Chem. Soc. Japan*, **35**, 306 (1962).
5. Kodama, S., T. Kagiya, S. Machi, T. Shimidzu, S. Yuasa, and K. Fukui, *J. Appl. Polymer Sci.*, **3**, 20 (1960).
6. Friedlander, H. N., and K. Oita, *Ind. Eng. Chem.*, **49**, 1885 (1957).
7. Berger, M. N., and T. H. Boulthbee, *J. Appl. Chem.*, **9**, 490 (1959).
8. Cottam, B. J., *J. Appl. Polymer Sci.*, **9**, 1853 (1965).
9. Tung, L. H., *J. Polymer Sci.*, **24**, 333 (1957).

R. A. ROTHENBURY

Research and Development Laboratory
Dow Chemical of Canada, Limited
Sarnia, Ontario, Canada

Received March 10, 1965